Embassy of the Arab Republic of Egypt
The Egyptian Cultural & Educational Bureau
London

Development of Novel Acute Myeloid Leukaemia Therapy: Targeting the Leukaemic Bone Marrow Protective Niche Secretome to Enhance Chemotherapy Sensitivity

Dr Ahmed Bahaaeldin Nabih Elmarghany

MBChB, MSc

Submitted in fulfilment of the requirements for the degree

of Doctor of Philosophy

School of Cancer Sciences

College of Medical, Veterinary and Life Sciences

University of Glasgow

April 2025

Abstract

Acute myeloid leukaemia (AML) is a heterogeneous and complex disease that is rapidly proliferative with a high rate of relapse. The bone marrow microenvironment (BMME) is known to be important in chemoresistance in AML, but the exact mechanism is not fully explored. Studies have shown that interleukin-6 (IL-6) contributes to AML survival. Our previously published data showed that AML blasts are protected from chemotherapy by interaction with the BMME. Investigating cytokines produced by bone marrow stromal cell (BMSC) using a co-culture (CC) system showed that IL-6 is present at a significantly higher concentration in CC compared to both liquid culture (LC) and BMSC cultured alone, showing that the interaction of the AML blasts and BMSC produce higher levels of IL-6 than they would in monocultures.

IL-6 is recognised as one of the key cytokines released by BMSC. Numerous studies are investigating its role in enhancing the viability of AML cells. IL-6 triggers the JAK-STAT signalling pathway, leading to the phosphorylation of STAT3, a transcription factor that regulates various genes associated with proliferation and survival. Moreover, research has identified a STAT-independent pathway involving IL-6. When IL-6 binds to its receptor and the co-receptor gp130, it not only activates the JAK-STAT pathway but also stimulates SRC family kinases.

It was hypothesised that such BMME-mediated chemoresistance is partly owing to cytokines and chemokines secreted by BMSC, the main cellular component of the BMME, such as IL-6, which can promote AML chemoresistance through stimulation of the JAK-STAT and SRC signalling. We aimed to study the prosurvival role of BMSC-secreted cytokines and signalling pathways involved in chemoprotection and how to abolish their effect to improve therapeutic outcomes. Inhibiting both pathways using ruxolitinib, a licensed JAK inhibitor, and dasatinib, a licensed SRC inhibitor, could increase AML sensitivity to standard chemotherapy.

Three core-binding factor AML cell lines (Kasumi-1 and SKNO-1 expressing t(8;21), and ME-1 expressing inv(16)), one non-core binding factor cell line (THP-1), and one human stromal cell line (HS5) were used to investigate AML cell lines and BMSC secretome. ProcartaPlex™ immunoassay with different cytokines was

performed on the supernatant of Kasumi-1, ME-1, and THP-1 cell suspension alone and CC (direct contact and transwell) with HS5 cells. Moreover, we assessed the prosurvival role of IL-6, VEGF, HGF, and SDF-1α when combined with cytosine arabinoside (Ara-C) at its EC50 on the Kasumi-1 cell line using flow cytometry for apoptosis by Annexin / DAPI staining. We found a protective effect of IL-6 treatment when cells were pre-treated with IL-6 before Ara-C treatment in the Kasumi-1 cell line regarding the percentage of late apoptotic cells (Annexin +/ DAPI +), not the percentage of surviving cells (Annexin - / DAPI -). Using Luminex® technology, from 11 cytokines analysed, there were five cytokines (GM-CSF, TNF-α, IL-2, IL-6, IL-18) present at a higher level in CC compared to Kasumi-1, ME-1, THP-1 or HS5 cells cultured alone. IL-2 and IL-6 were significantly increased in CC compared to Kasumi-1 monoculture; GM-CSF, TNF-α and IL-2 were significantly higher in ME-1 CC compared to LC. With THP-1 cells, IL-2 and IL-18 were found to be higher in CC compared to LC.

Using cell lines that showed HS5 chemoprotection, we assessed SRC signalling pathway gene expression such as *SRC*, *YAP*, and *CYR61* by qPCR in our *in vitro* CC system. Next, the concentration of dasatinib was determined by western blot. Apoptosis and cell cycle analyses elucidated the effect of CC, with and without dasatinib, on leukaemia cell viability. A significant increase in *SRC* gene expression ($p=0.015$, $n=4$) and total and phospho-SRC protein were observed when ME-1 cells were co-cultured on the HS5 cell line compared to suspension culture. A decrease in AML cell viability by apoptosis assay and an increase in subG1 in cell cycle analysis were noticed when AML cells within the CC system were treated with dasatinib (1nM) and Ara-C at its EC_{50}, in comparison to treatment with Ara-C alone. This indicated that CC conferred protection to AML cells against Ara-C, which dasatinib could partly reverse.

Next, using the Kasumi-1 cell line, JAK-STAT signalling by flow cytometry using phospho-STAT3 (Y705) in our *in vitro* co-culture (CC) system was assessed either in direct contact or via transwell with Kasumi-1 to investigate the role of cytokines secreted by HS5. Then, the concentration of ruxolitinib required to inhibit pY705 was determined. Apoptosis (Annexin / DAPI) and cell cycle analyses (Ki-67 / DAPI) elucidated the effect of CC, with and without ruxolitinib, on leukaemia cell viability.

A significant increase was observed in STAT3 pY705 when Kasumi-1 cells were co-cultured on the HS5 cell line compared to suspension culture ($p=0.001$, $n=5$). Treatment in CC with ruxolitinib (0.5μM) significantly reduced Kasumi-1 pY705 (46% inhibition of phosphorylation; $p= 0.0023$, $n=5$), proving that ruxolitinib inhibited the CC-induced JAK-STAT signalling. A significant decrease was noticed in AML cell viability by apoptosis assay ($p= 0.0026$), with a significant increase in subG1 in cell cycle analysis ($p=0.0001$) when AML cells, within the CC system, were treated with ruxolitinib (0.5μM) and Ara-C in comparison to treatment with Ara-C alone. This indicated that CC conferred protection to AML cells against Ara-C and could be partly reversed by ruxolitinib.

Overall, the BMME has an important role in providing AML chemoresistance through various cytokines secreted; we can confirm that IL-6 may provide chemoprotection for the Kasumi-1 cell line when treated with the standard chemotherapy agent, Ara-C. Targeting signalling pathways could abolish BMSC-mediated chemoresistance; ruxolitinib and dasatinib could serve as adjuvant chemotherapy to Ara-C in AML.

Table of Contents

List of Tables

List of Figures

List of Equation

List of Publications

Paper

Laing, A., **Elmarghany, A.,** Alghaith, A. A., Gouma, A., Stevens, T., Winton, A., Cassels, J., Clarke, C. J., Schwab, C., Harrison, C. J., Gibson, B., & Keeshan, K. (2025). Paediatric bone marrow mesenchymal stem cells support acute myeloid leukaemia cell survival and enhance chemoresistance via contact-independent mechanism. *British Journal of Haematology*, **206(3),** 858–863. https://doi.org/10.1111/bjh.19884

Conference Abstracts

Elmarghany, A., Laing, A., Copland, M., & Keeshan, K. (2022). Role of IL6 in developing resistance of AML cells to standard chemotherapy. *British Journal of Haematology* **197**, 221.

Elmarghany, A., Jørgensen, H., & Copland, M. (2024). Inhibition of SRC signalling reverses stromal chemoprotection in adult core binding factor acute myeloid leukaemia cell line model. *International Journal of Laboratory Hematology*, **46(S2)**, 34–35. https://doi.org/10.1111/ijlh.14396

Elmarghany, A., Keeshan, K., Jørgensen, H., & Copland, M. (2024). Targeting the leukaemic bone marrow protective niche may increase the sensitivity of acute myeloid leukaemia (AML) to standard chemotherapy, *HemaSphere*, **8(S1)**, 696-697. https://doi.org/10.1002/hem3.104

Acknowledgement

(وَفَوْقَ كُلِّ ذِي عِلْمٍ عَلِيمٌ) (يوسف؛٧٦)

(And above every man who has knowledge, there is someone more knowledgeable) 12:76

In the name of Allah, the Most Gracious, the Most Merciful. All praise and gratitude are due to Allah, for without His will and countless blessings, none of this would have been possible. I would like to express my deepest gratitude to my supervisors, Prof. Mhairi Copland and Dr. Heather Jorgensen, for their unwavering guidance, support, and encouragement throughout this journey. Their expertise and patience have been invaluable to me. I am profoundly thankful to Dr. Heather Jorgensen, who, as a PGR convenor, played a pivotal role in helping my smooth transition away from a challenging situation with my former supervisor. Her support not only restored my confidence but also reaffirmed my belief in my abilities.

A heartfelt thanks to Meaad, a fellow PhD student, who has been a pillar of support from the very beginning of my PhD journey. Her guidance, insights, and encouragement have been instrumental in navigating the complexities of this process. To my wife, my sincerest appreciation. As a fellow PhD student, she understands the challenges and sacrifices of this journey. Her unwavering support and presence during the most demanding times, even in the smallest of issues, have been my anchor. I am also grateful to Dr. Alan Hair and Jennifer Cassels for their technical assistance in the lab. Their expertise and willingness to help have made a significant difference in my research experience. To all my colleagues in the lab, thank you for the camaraderie, collaboration, and enriching discussions that have made this journey both productive and enjoyable. Lastly, to my family and friends, your constant encouragement, love, and prayers have been a source of strength and motivation throughout this journey. Your belief in me has carried me through the most challenging moments.

Thank you all for being part of this incredible journey.

Author's Declaration

I declare that, except where explicit reference is made to the contribution of others, this thesis is the result of my work and has not been submitted for any other degree at the University of Glasgow or any other institution.

Signature:

Printed Name: Ahmed Bahaaeldin Nabih Elmarghany

Date:

Definitions/Abbreviations

Most of these abbreviations are also explained in the text. However, certain abbreviations, particularly those for genes, are not included within the text to enhance reading simplicity and they are mentioned here for clarification.

°C	Degree Celsius
ABC	ATP binding cassette
Akt	AKT serine/threonine kinase
alloHSCT	Allogeneic haematopoietic stem cell transplantation
AML	Acute myeloid leukaemia
Ang-1	Angiopoietin 1
ANOVA	Analysis of Variation
Ara-C	Cytarabine / Cytosine arabinoside
ASXL1	ASXL transcriptional regulator 1
ATP5B	ATP Synthase F1 Subunit Beta
B-ALL	B cell acute lymphoblastic leukaemia
BCL-2	B-cell lymphoma 2
BCORL1	BCL-6 corepressor-like 1
BCR::ABL1	breakpoint cluster region-Abelson
BiTEs	Bispecific T-cell engagers
BM	Bone marrow
BMAT	Bone marrow adipose tissue
BMME	Bone marrow microenvironment
BMSC	Bone marrow stromal cell
bZIP	Basic Leucine Zipper Domain
C-PARP	Cleaved Poly ADP-Ribose Polymerase
C^{++}	Calcium ion
CAF	Cancer associate fibroblast
CAR	CXCL12-abundant reticular
CAR-T	Chimeric antigen receptor- T cell
CBFB	Core binding factor subunit B
CC	Co-culture
CC (C)	Co-culture with contact
CC (TW)	Co-culture with transwell
CCN1	Cellular Communication Network Factor 1
CCUS	Clonal cytopenia of undetermined significance
CD	Cluster differentiation
CEBP-α	CCAAT/enhancer binding protein alpha
CH	Clonal haematopoiesis
CHIP	Clonal haematopoiesis of indeterminate potential
CM	Complete / conditioned medium (according to the context)
CML	Chronic myeloid leukaemia
CR	Complete remission
CREBBP	CREB binding protein
CTGF	Connective Tissue Growth Factor
CTLA-4	Cytotoxic T-lymphocytes antigen-4
CTV	Cell trace violet

CXCL12	C-X-C motif chemokine ligand 12 (SDF-1α)
CXCR4	C-X-C motif chemokine receptor 4
CYP450	Cytochrome P450
CYR61	cysteine-rich angiogenic inducer 61
DAPI	4',6-diamidino-2-phenylindole
Das	Dasatinib
DCs	Dendritic cells
ddPCR	Digital droplet PCR
DKK1	Dickkopf-1
DMEM	Dulbecco's Modified Eagle Medium
DMSO	Dimethysulfoxide
DNMT3A	DNA methyltransferase 3 alpha
DNR	Daunorubicin
ECM	Extracellular matrix
EDTA	Ethylenediaminetetraacetic acid
ELN	European LeukemiaNet
EZH2	Enhancer of Zeste Homolog 2
FAB	French-American-British
FBS	Fetal bovine serum
FDA	Food and drug administration
FISH	Fluorescence in situ hybridization
FLT-3	fms-like tyrosine kinase 3
GAPDH	Glyceraldehyde-3-Phosphate Dehydrogenase
GDF15	Growth differentiation factor 15
GDSC	Genomics of Drug Sensitivity in Cancer
GM	Geometric mean
GM-CSF	Granulocyte-Monocyte colony stimulating factor
GNAS	Guanine Nucleotide binding protein, Alpha Stimulating activity polypeptide
GO	Gene ontology / Gemtuzumab Ozogamicin (according to the context)
gp130	Glycoprotein 130
GPS	Galinpepimut-S
GSEA	Gene set enrichment analysis
HBSS	Hanks-buffered saline solution
HGF	Hepatocyte growth factor
HO1	Heme oxygenase 1
HS5	Human stromal cell line
HSC	Haematopoietic stem cell
HSCT	Haematopoietic stem cell transplantation
ICI	immune checkpoint inhibitors
IDH	isocitrate dehydrogenase
IDO1	Indoleamine 2,3-dioxygenase 1
IFN-g	Interferon gamma
IGF-1	Insulin like growth factor-1
IL	Interleukin
ILR	Interleukin receptor
Inv(16)	Inversion in chromosome 16
ITD	Internal tandem duplication
IκB	NF-κB inhibitor
JAK	Janus kinase

KAT6A	Lysine Acetyltransferase 6A
KMT2A	Lysine Methyltransferase 2A
LAAs	Leukaemia associated antigens
LC	Liquid culture
LDAC	Low dose Ara-C
LepR	Leptin receptor
LSC	Leukaemia stem cell
MCL-1	Myeloid cell leukaemia-1
MDS	Myelodysplastic syndrome
MECOM	MDS1 and EVI1 complex locus
MFC	Multiparameter flow cytometry
Mins	Minutes
MLLT3	Mixed linage leukaemia translocated to 3
MMPs	matrix metalloproteinases
MPL	myeloproliferative leukaemia virus oncogene
MPN	Myeloproliferative neoplasm
MRD	Measurable/minimal residual disease
MRTFA	Myocardin Related Transcription Factor A
MSCs	Mesenchymal Stem/stromal cells
MUC1	Mucin 1 protein
MVD	Microvessel density
MYH11	Myosin heavy chain 11
NaCl	Sodium Chloride
Na-Deoxy	Sodium Deoxycholate
NaOH	Sodium Hydroxide
NF-κB	Nuclear factor kappa B
NK	Natural killer
NOS	Not otherwise specified
NOS2	Nitric oxide synthase 2
NPM1	Nucleophosmin
NUP98	Nucleoporin 98
OPN	Osteopontin
OS	Overall survival
OXPHOS	Oxidative phosphorylation
PBS	Phosphate-buffered saline
PD-1/PD-L1	Programmed death receptor/legend-1
PDGFRb	Platelet derived growth factor b
PGE2	Prostaglandin E2
PDX	patient-derived xenograft
PI3K	Phosphatidylinositol 3-Kinase
pMSC	Paediatric mesenchymal stromal cell
PPM1D	Protein Phosphatase, Mg2+/Mn2+ Dependent 1D
PR3	Proteinase3
pS	Serine Phosphorylation
PS	Phosphatidylserine
PTPN11	protein tyrosine phosphate non-receptor type 11
pY	Tyrosine phosphorylation
qPCR	Quantitative polymerase chain reaction
RARA-γ	Retinoic acid receptor gamma
Rb	Retinoblastoma
RBM15	RNA binding motif protein 15

RHAMM	Receptor for hyaluronic acid-mediated motility
ROS	Reactive oxygen species
RPMI	Roswell Park Memorial Institute
RUNX1	Runt-related transcription factor 1
RUNX1T1	RUNX1 partner transcriptional co-repressor 1
Rux	Ruxolitinib
S.D	Standard deviation
SBDS	Shwachman–Bodian–Diamond syndrome
SCF	Stem cell factor
SDF-1α	Stem/Stromal cell derived factor alpha
SF3B1	Splicing factor 3B subunit 1
SFK	SRC family kinase
SNS	Sympathetic nervous system
SRC	Sarcoma
SRSF2	Serine/Arginine-Rich Splicing Factor 2
STAG2	Stromal antigen 2
STAT	Signal Transducer and Activator of Transcription
t(9;11)	Translocation between chromosome 9 and chromosome 11
TAMs	Tumour-associated macrophages
TAZ	Transcriptional coactivator with PDZ-binding motif
TB	Trypan blue
TBP	TATA-Box Binding Protein
TCA	Tricarboxylic acid cycle
TEAD	Transcriptional Enhanced Associate Domain
TET2	Ten-eleven translocation 2
TGF-β	transforming growth factor-b
TIM-3	T-cell immunoglobulin and mucin domain
TKI	Tyrosine kinase inhibitor
TNF-α	Tumor necrosis factor alpha
TP53	Tumor protein 53
TPO	Thrombopoietin
Tregs	Regulatory T cells
U2AF1	U2 Small Nuclear RNA Auxiliary Factor 1
VAF	Variant Allele Frequency
VC	Vehicle control
VCAM-1	Vascular cell adhesion molecules
VEGF-A	Vascular endothelial growth factor-A
VEGFR	Vascular endothelial growth factor receptor
VLA	Very late antigen
WHO	World Health Organisation
WT1	Wilms' tumour 1
YAP	Yes associated protein
ZRSR2	Zinc Finger, RAN-Binding Domain Containing 2

1 Introduction

1.1 Acute myeloid leukaemia (AML)

1.1.1 AML background

Acute myeloid leukaemia (AML) is characterised by the clonal proliferation of heterogeneous malignant (blast) cells. Blasts grow uncontrollably without differentiation but with loss of sensitivity to apoptosis, causing general signs and symptoms of leukaemia such as anaemia, severe infection, and bleeding. In severe cases, some patients might develop extramedullary infiltration, including central nervous system involvement (Short et al., 2018).

AML is considered a disease of adults, representing 50% of all adult leukaemia. However, it also affects children and represents 15% of childhood malignancies. It is nonetheless a disease of the elderly where the median age of onset is 69 years (Short et al., 2018). Because elderly patients might not withstand chemotherapy with its side effects and are often not fit for allogeneic haematopoietic stem cell transplantation (alloHSCT), the overall survival (OS) in patients older than 60 years is very poor, with less than 10% surviving for 3 years or more. The mortality is caused by relapse and treatment-related toxicity (Patel et al., 2021). Clinical outcomes that are poor in AML are determined by age, remission duration, types of genetic mutation, and patient's health status and co-morbidities. Cytogenetic mutations determine the prognosis and risk stratification, referred to as the European Leukaemia Net (ELN) classification (Table 1-1) (Döhner et al., 2022). The mortality-to-incidence ratio hasn't shown a significant decrease over the last 19 years, so novel targeted therapies with less toxic effects are needed to decrease the incidence of relapse and to increase OS.

Table 1-1 2022 ELN AML risk stratification by genetic abnormalities at initial diagnosis
(Döhner et al., 2022)

Risk category	Genetic abnormality
Favourable	▪ t(8;21)(q22;q22.1)/*RUNX1::RUNX1T1* ▪ inv(16)(p13.1q22) or t(16;16)(p13.1;q22)/ *CBFB::MYH11* ▪ Mutated *NPM1* without *FLT3-ITD* ▪ bZIP in-frame mutated *CEBPA*
Intermediate	▪ Mutated *NPM* with *FLT3-ITD* ▪ Wild-type *NPM1* with *FLT3-ITD* (without adverse-risk genetic lesions) ▪ t(9;11)(p21.3;q23.3)/*MLLT3::KMT2A* ▪ Cytogenetic and/or molecular abnormalities not classified as favourable or adverse
Adverse	▪ t(6;9)(p23.3;q34.1)/*DEK::NUP214* ▪ t(v;11q23.3)/*KMT2A*-rearranged ▪ t(9;22)(q34.1;q11.2)/*BCR::ABL1* ▪ t(8;16)(p11.2;p13.3)/*KAT6A::CREBBP* ▪ inv(3)(q21.3q26.2) or t(3;3)(q21.3;q26.2)/ *GATA2*, *MECOM*(EVI1) ▪ t(3q26.2;v)/*MECOM*(EVI1)-rearranged ▪ -5 or del(5q);-7;-17/abn(17p) ▪ Complex karyotype, monosomal karyotype ▪ Mutated CXC*L1, BCOR, EZH2, RUNX1, SF3B1, SRSF2*, *STAG2, U2AF1,* and/or *ZRSR2* ▪ Mutated *TP53*

1.1.2 AML pathogenesis and diagnosis

1.1.2.1 Leukaemia Stem Cell (LSC) in AML: Dormancy, Resistance, and Niche Exploitation

LSCs are a rare subpopulation within AML that are critically implicated in treatment failure and disease relapse. Located predominantly in the $CD34^+/CD38^-$ bone marrow fraction, these cells possess the ability to self-renew and sustain long-term malignant haematopoiesis (Stelmach & Trumpp, 2023).

A hallmark trait of LSCs is their dormant or quiescent state, like normal Haematopoietic stem cells (HSCs), which allows them to evade conventional chemotherapeutic agents that primarily target rapidly dividing cells. This quiescence is maintained through intrinsic regulation and crucial support from the bone marrow microenvironment, conferring LSC with increased chemoresistance and enabling them to reinitiate disease post-treatment. Hence, LSCs are sometimes referred to as Leukaemia Initiating Cells (LICs) (Essers & Trumpp, 2010).

HSCs and LSCs share some core properties, such as self-renewal capacity and a largely quiescent state, but they differ sharply in function and behaviour. HSC maintains long-term haematopoietic potential by remaining in a tightly regulated dormant state within the bone marrow niche, entering the cell cycle only when required to regenerate normal blood lineages. In contrast, LSC exploit quiescence not for preservation, but as a survival strategy that confers resistance to chemotherapy and enables relapse (O'Reilly et al., 2021). While HSCs rely on normal niche support to sustain healthy blood production, LSCs hijack and reprogram the microenvironment to suppress normal haematopoiesis and favour leukaemic cell survival, as will be discussed later in this chapter (Urs et al., 2024). Phenotypically, LSCs are often, but not always, found in the $CD34^+/CD38^-$ compartment, whereas HSCs display standard stem cell markers. Metabolically, HSCs are predominantly glycolysis-driven, whereas LSCs depend more heavily on oxidative phosphorylation, amino acid, and fatty acid metabolism (Tabe et al., 2017). Furthermore, LSCs possess multiple resistance mechanisms beyond quiescence, including the expression of drug-efflux pumps, activation of pro-survival signalling pathways, metabolic adaptations, and enhanced niche

protection as they actively reshape the bone marrow niche, steering it toward a leukaemia-favouring environment that promotes LSC survival and suppresses normal haematopoiesis, all of which distinguish them from their healthy counterparts (Niu et al., 2022).

In summary, while HSCs are essential for normal blood regeneration and remain quiescent under tight control, LSCs corrupt these fundamental stem cell traits to survive therapy, remodel their niche, and drive AML relapse. This dual understanding not only underscores the biological divergence between HSCs and LSCs but also highlights potential therapeutic vulnerabilities like targeting metabolism or niche interactions that may selectively eliminate LSCs while sparing healthy HSCs.

1.1.2.2 Molecular pathogenesis

Clonal haematopoiesis (CH) is an abnormal expansion of one or more blood cell lineages within the haematopoietic environment caused by somatic mutations in HSC, and this is a characteristic of a pre-leukaemic state (Steensma et al., 2015). Using whole-exome sequencing and whole-genome sequencing, CH was found to be related to age, as somatic mutations were found in old ages, even without overt leukaemia, especially *DNMT3A* and *TET2* found in older women and non-leukaemic cells, respectively (Xie et al., 2014). Moreover, mutations in *DNMT3A, TET2, JAK2, ASXL1, TP53, GNAS, PPM1D, BCORL1 and SF3B,* are highly associated with myeloid malignancy development (Jaiswal et al., 2014; Xie et al., 2014).

High-sensitivity techniques enhance the detection of CH, which is found in most of the population as they age. To narrow the diagnosis of CH, the term clonal haematopoiesis of indeterminate potential (CHIP) has been introduced. Unlike CH, CHIP is characterised by a minimum variant allele frequency (VAF) of 2% and a higher risk of progression to AML (Young et al., 2019). To diagnose CHIP, somatic mutation of myeloid malignancy-associated genes should be detected without cytopenia or dysplasia. If unexplained cytopenia persists for more than four months, the condition is classified as clonal cytopenia of undetermined significance (CCUS). If a patient with CCUS meets the morphological criteria of MDS with a blast count of less than 20%, an MDS diagnosis is established. If blast counts exceed 20%, the diagnosis is AML (Hörst et al., 2024). Figure 1-1 shows the

likely progression of CH to AML, although de novo AML may still occur without this pre-leukaemic progression.

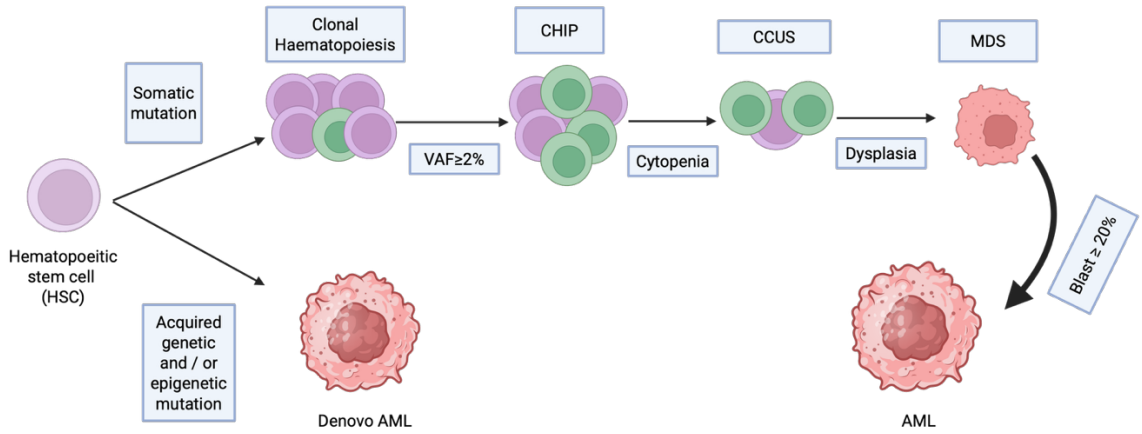

Figure 1-1 Schematic representation of the progression of CH to AML.
Somatic mutations in HSC can give rise to CH, which in some cases progresses to CHIP. Additional genetic alterations may lead to MDS or other pre-leukaemic states, and ultimately to AML. Progression is not inevitable, and many individuals with CH remain stable without developing malignancy. HSC, Haematopoietic stem cell, CHIP, clonal haematopoiesis of indeterminate potential, CCUS, Clonal cytopenia of undetermined significance, MDS, Myelodysplastic syndrome, AML, Acute myeloid leukaemia, VAF, Variant allele frequency. Purple cells, HSCs, Green cells, HSCs with somatic mutation.

Previously, there was a two-hit theory for AML pathogenesis, which depended mainly on classifying somatic gene mutations into two different groups; group 1 is responsible for HSC proliferation and survival, and group 2, which is involved in the blockage of differentiation and escaping apoptosis (Kelly & Gilliland, 2002). Later, this theory was updated to be a multi-hit theory where combined genetic mutations, e.g., *FLT3*/*TET2*, resulted in an epigenetic signature leading to distinct leukaemic disease not responding to either chemotherapy or FLT3 inhibitor referring to the role of epigenetic mutation in driving AML (Shih et al., 2015).

Recently, in the era of whole genome sequencing with a greater understanding of genetic mutation, it was clear that AML patients have 14 genetic mutations on average, most of which are leukaemia driver mutations (Papaemmanuil et al., 2016). Other mutations were found in HSC and might have a role in

leukaemogenesis, although these genes were described as passenger genes as it is believed that they do not directly cause leukaemia (Ding et al., 2012).

1.1.2.3 Morphology

Bone marrow (BM) cell morphology was the first tool for leukaemia diagnosis and classification. The outmoded French-American-British (FAB) classification (Bennett et al., 1976) aided in the diagnosis of AML with the presence of more than 30% of blast cells in the peripheral blood (PB) or BM being diagnostic of AML. This FAB classification relied mainly on the morphology of the blood cells, types and state of differentiation and maturation resulting in eight groups from M0 to M7. Indeed, cell morphology is highly subjective and may result in misdiagnosis because of different smear preparations and staining (Huang et al., 2020).

With advances in AML research and the evolution of genetic studies, the diagnosis of AML evolved to depend on recurrent genetic abnormalities and the presence of only 20% of blast cells in PB or BM samples. These advances have placed a much lesser role of morphology in leukaemia diagnosis. Indeed, the latest WHO classification excludes the role of morphology in the diagnosis of AML except for differentiating between myelodysplastic syndrome (MDS) and AML and in some AML subtypes like AML with BCR::ABL1 which still need 20% blasts for diagnosis to avoid overlap with chronic myeloid leukaemia (CML) and AML with CEBPA mutation (Khoury et al., 2022).

1.1.2.4 Immunophenotyping and measurable/minimal residual disease (MRD)

By using multiparameter flow cytometry (MFC), AML could be diagnosed based on the intracellular markers or those expressed on the surface of the cell. However, these markers are not expressed on all AML cells because of heterogeneity, so there is a need for more specific and sensitive tools for accurate diagnosis and precise classification for targeted treatment.

MFC is currently used to phenotype all leukaemia cells during diagnosis, including the LSC, which will be used for MRD detection and patient monitoring after remission (Döhner et al., 2022).

1.1.2.5 Cytogenetic analysis

Since 2002, when the first WHO classification emerged which depended on cytogenetic abnormalities, cytogenetic analysis has been the cornerstone of haematological malignancy diagnosis, classification, risk stratification, and therapeutic intervention (Vardiman et al., 2002).

Conventional cytogenetic analysis, i.e., karyotyping, is the first tool for screening the disease and searching for common AML recurrent genetic abnormalities. Although it can only detect large structural and numerical chromosomal abnormalities, it can diagnose up to 60% of AML cases. In the case of failed karyotyping or it being inconclusive, fluorescence in situ hybridisation (FISH) is the next step for accurate and specific detection of abnormalities like *RUNX1::RUNX1T1, BCR::ABL1, CBFB::MYH11,* and *KMT2A* rearrangement (Snaith et al., 2024).

Molecular genetic studies like quantitative polymerase chain reaction (qPCR) and digital droplet PCR (ddPCR) are conducted at diagnosis of AML to screen for recurrent genetic abnormalities with a specific mutation, e.g. *NPM1*, *KMT2A*, and facilitate MRD monitoring following treatment, which could be targeted based on these molecular study results (Döhner et al., 2022).

1.1.3 WHO classification of AML:

The current 5th WHO classification of AML (Table 1-2) emphasizes what was previously published in the last classification with some changes to correlate with novel findings within the last few years for more clarification of disease diagnosis and management.

AML is classified into two groups: the first is based on genetic abnormality, and the other is based on differentiation. This classification clarifies 'AML – not otherwise specified (NOS)' mentioned in the previous classification.

In the current (5th) WHO classification, the morphology cut-off of 20 % blasts was eliminated. The cut-off was 30% in the original FAB classification, lowered to 20% in the first WHO classification (Vardiman et al., 2002). Blast enumeration has many challenges, and lowering the cut-off to 10% could lead to overtreatment. So,

instead of decreasing the cut-off further, it was better to correlate genetic mutations with morphologic findings to ensure that the mutational landscape defined the pathology, irrespective of the number of blast cells. The exception is AML with *BCR::ABL1* fusion to avoid confusing the diagnosis of CML with AML, and AML with *CEBPA* mutation as there is no solid evidence to support changing the cut-off criterion. Moreover, WHO kept the 20% cut-off for delineation between AML and MDS (Khoury et al., 2022). On the other hand, the international consensus classification chooses to lower the cut-off of 20% to 10% for recurrent genetic abnormalities rather than eliminating the role of blast count except for both conditions mentioned in the WHO classification which are AML with BCR::ABL1 and AML with CEBPA kept at 20% blast cut-off (Weinberg et al., 2023).

The current classification added one subtype to the AML first group, called 'AML with other defined genetic alterations' allowing addition of any new or uncommon genetic alteration proven to be related to AML in any future classification (Khoury et al., 2022).

In conclusion, the new classification emphasises the correlation between clinical, molecular alteration and pathological aspects of the disease while eliminating the subjective role of morphology diagnosis.

Table 1-2 World Health Organisation (WHO) classification of haematolymphoid tumour 5th edition: Acute Myeloid Leukaemia entity (Khoury et al., 2022).

Acute myeloid leukaemia with defining genetic abnormalities	Acute myeloid leukaemia, defined by differentiation
APL with t(15;17)(q24.1;q21.2)/*PML::RARA* fusion	
AML with t(8;21)(q22;q22.1)/*RUNX1::RUNX1T1* fusion	
AML with inv(16)(p13.1q22) or t(16;16)(p13.1;q22)/*CBFB::MYH11* fusion	Acute myeloid leukaemia with minimal differentiation
AML with t(6;9)(p22.3;q34.1)/*DEK::NUP214* fusion	Acute myeloid leukaemia without maturation
AML with *RBM15::MRTFA* fusion	Acute myeloid leukaemia with maturation
AML with t(9;22)(q34.1;q11.2)/ *BCR::ABL1* fusion	Acute basophilic leukaemia
AML with *KMT2A* rearrangement	Acute myelomonocytic leukaemia
AML with *MECOM* rearrangement	Acute monocytic leukaemia
AML with *NUP98* rearrangement	Acute erythroid leukaemia
AML with *NPM1* mutation	Acute megakaryoblastic leukaemia
AML with *CEBPA* mutation	
AML, myelodysplasia-related	
AML with other defined genetic alterations	

1.2 Bone marrow microenvironment

1.2.1 Bone marrow microenvironment in normal haematopoiesis

Bone marrow microenvironment (BMME), which is also referred to as the BM niche, was first described by Schofield in 1978 as a group of non-haematopoietic stem cells surrounding and regulating the HSC functions such as self-renewal, proliferation, differentiation and mobilisation (Schofield, 1978).

This BMME can be physiologically categorised into haematopoietic and non-haematopoietic niches. The haematopoietic niche consists mainly of HSCs in various states, either quiescent waiting for activation signalling or active ready for self-renewal, proliferation, and mobilisation to peripheral circulation for final differentiation into different types of blood cells. The non-haematopoietic niche comprises all other cells: Mesenchymal stromal/stem cell (MSC), endothelial cells, adipocytes, and cells of the sympathetic nervous system (SNS) found around the HSCs which control the state of HSC through release of various factors (Shafat, Gnaneswaran, et al., 2017). For example, it has been observed that cytokines like IL-6 and chemokines as IL-8, CXCL12, and monocyte chemoattractant protein-1 (MCP-1) play a role in modulating HSC retention in BM (Ostanin et al., 2011).

Anatomically, the BMME can be classified into endosteal niche and perivascular niche; the endosteal niche is located near the bone cortical/trabecula and consists of cells responsible for bone formation and resorption. i.e., osteoblast and osteoclast (Calvi et al., 2003). The perivascular niche, also called the endothelial niche, which is placed near endothelial vascular sinusoids, is surrounded by various types of cells, such as bone marrow stromal cell (BMSC), as well as extracellular matrix (ECM), as shown in (Figure 1-2) (Skelding et al., 2023).

Some studies have discussed the role of the BM niche in regulating HSC state and function. HSCs are kept quiescent when located near the endosteal niche. However, when activated to proliferate and differentiate, HSC will mobilize toward the perivascular niche to be ready to enter the peripheral circulation (Heazlewood et al., 2014; Lévesque et al., 2010; Suárez-Álvarez et al., 2012). On the other hand, some studies explained the role of the endothelial cells lining the blood sinusoids in preserving the quiescent state of HSC through the adhesion

molecules expressed on the endothelium such as P-selectin, E-selectin, and vascular cell adhesion molecule-1 (VCAM-1) (Barnhouse et al., 2021; Schweitzer et al., 1996; Sipkins et al., 2005).

Although the BMME has been categorised and described as two distinct niches with controversial roles regarding HSC fate regulation, it is considered dynamic with difficulty in separation as BM arterioles enter the BM through the periosteum and blood sinusoids spread all over the BM cavity (Behrmann et al., 2018).

MSC, the main cell component within BMME, are immunophenotypically CD73+, CD90+, CD105+ and CD34−, CD31−, CD45RA−, CD14−, CD19−, and HLA-DR−. MSCs are a heterogeneous group of cells expressing various types of receptors: LepR, CXCL12 (ligand for CXCR4) on CXCL12-abundant reticular cells (CAR cells), nestin and CD146, that can differentiate into adipocytes, chondrocytes, and osteocytes. BMME cells expressed different types of molecules, such as CXCL12, stem cell factor (SCF, binds c-Kit receptor), angiopoietin 1 (Ang-1, binds Tie-2), thrombopoietin (TPO) (ligand for myeloproliferative leukaemia virus oncogene (MPL) and Osteopontin (OPN) (with αvβ1 integrin) which have a role in regulation of HSCs (Goulard et al., 2018).

Osteoblasts and osteoclasts have roles in the HSCs regulation. Osteoblasts expand HSC by increasing their number and inhibiting their differentiation through parathyroid hormone receptor stimulation (Calvi, 2006). However, osteoclasts, stimulated by receptor activator of NF-κB ligand (RANKL), increase HSC mobilisation and differentiation, dependent on decreasing SCF, CXCL12 and OPN in the endosteum and through matrix metalloproteinase (MMP-9) and CXCR4 (Kollet et al., 2006).

Bone marrow adipose tissue (BMAT) has a pivotal role in regulating HSC quiescence and activation through adiponectin secretion (Masamoto et al., 2017). On the other hand, BMAT can negatively regulate the hematopoietic microenvironment, influencing HSC function (Naveiras et al., 2009). It was suggested that BMAT rapidly compensates for cytopenia through increased haematopoiesis. Moreover, it maintains HSC regeneration through the secretion of SCF, referring to its role in HSC maintenance (B. O. Zhou et al., 2017).

SNS and Schwann cells play a key role in HSC regulation. Non-myelinated Schwann cells activate latent transforming growth factor-β (TGF-β), affecting HSC quiescence and increasing mobilization. So, denervated sympathetic cells cause loss of HSC from the BM by decreasing the number of cells secreting TGF-β (Yamazaki et al., 2011).

1.2.2 Bone marrow microenvironment within AML

The previous section made clear what BMME looks like within a normal population and how various types of non-haematopoietic cells regulate HSCs' function, maintenance, survival, mobilisation, and differentiation until they reach the peripheral circulation.

This section will discuss alteration within the BMME of AML patients to gain more knowledge on how this permissive microenvironment supports LSC proliferation and survival and to develop potential targeted therapies against leukaemia-induced BMME (Figure 1-2).

A highly vascularised BMME is a characteristic finding for tumours in general and is found to be manifested in AML (Padró et al., 2000). This is due to angiogenesis, which is the formation of new blood vessels different from normal vessels present in healthy BM. The process of angiogenesis is stimulated by the hypoxic environment found in AML. These new blood vessels support AML cells with nutrients, growth factors and oxygen to promote growth and proliferation. For a clear estimation of angiogenesis, BM microvessel density (MVD) was measured. It was found that MVD was high in haematological malignancy as well as solid tumours compared to a healthy population. A high basal MVD was found in advanced cases of AML, suggesting that it has a role in AML prognosis (Negaard et al., 2009)

The SNS creates a good environment for HSC, AML infiltration causes neuropathy in SNS, leading to disruption of BMME, which supports AML expansion (Arranz et al., 2014; Hanoun et al., 2014).

Fibroblasts, which can change to cancer-associated fibroblasts (CAF) within the AML microenvironment, play a pivotal role in increasing AML proliferation and

apoptosis inhibition. CAFs secrete growth differentiation factor 15 (GDF15), which has a role in AML chemoprotection (Zhai et al., 2016). Moreover, it was found that culturing AML cells with fibroblast cell lines resulted in increased angiogenic interleukin-8 (IL-8), enhanced AML proliferation and modulated antiapoptotic signalling (Ryningen et al., 2005). One study discussed transforming MSCs into CAFs that protected B-cell acute lymphoblastic leukaemia (B-ALL) cells from chemotherapy through mitochondrial transfer (Burt et al., 2019). Taken together, CAFs provide chemoresistance to different types of leukaemia through distinct mechanisms (Miari & Williams, 2024).

One mechanism of permissive microenvironment is to help LSC escape chemotherapy by being kept quiescent near the endosteal niche. MSCs transforming into CAR cells secrete the chemokine CXCL12 to bind to the CXCR4 receptor expressed on LSC. This CXCL12/CXCR4 axis helps LSC to reside in a protective niche, difficult for chemotherapy to penetrate (A. Wang & Zhong, 2018). Inhibiting this axis leads to the mobilisation of AML cells out of their protective niche with more exposure to chemotherapy (Zeng et al., 2009). Moreover, this axis activates many survival pathways, such as JAK-STAT, PI3K-Akt, and MEK-ERK pathways, leading to AML survival and proliferation (Ladikou et al., 2020; Yao et al., 2021). Adhesion molecules play an important role in AML progression and survival. One study found that very late antigen (VLA)-4 was highly expressed on LSC, which binds to VCAM-1 expressed on stromal cells, activating the NF-κB pathway in both AML and stromal cells, suggesting that it has a role in providing AML chemoresistance (Jacamo et al., 2014).

An important mechanism by which AML creates a protective BMME involves the suppression of immune surveillance. MSCs within the BMME contribute significantly to this immunosuppressive milieu. They secrete a range of regulatory molecules, including indoleamine 2,3-dioxygenase 1 (IDO1), heme oxygenase 1 (HO1), arginase 1 and 2, nitric oxide synthase 2 (NOS2), hepatocyte growth factor (HGF), transforming growth factor beta (TGF-β), interleukin-10 (IL-10), and prostaglandin E2 (PGE2). The secretome collectively inhibits the activation of effector lymphocytes, thereby impairing effective anti-tumour immunity (Méndez-Ferrer et al., 2020).

The immune system's ability to recognise and eliminate AML cells critically depends on the presence and functionality of T cells within the tumour microenvironment. However, AML patients often exhibit a marked reduction in both CD4+ and CD8+ T cell populations. Moreover, these T cells frequently display features of exhaustion and senescence, further compromising their cytotoxic potential (Tang et al., 2020).

Natural killer (NK) cells, components of the innate immune system, are also essential for immunosurveillance in AML and various solid tumours. One mechanism through which NK cell activity is impaired in AML involves the downregulation of IFN-γ, a cytokine crucial for dendritic cell maturation and the initiation of adaptive immune responses (Gurney & O'Dwyer, 2021).

Regulatory T cells (Tregs) also contribute to immune evasion in AML. These cells expand in response to tumour-associated antigens and immunosuppressive cytokines, particularly TGF-ß and IL-10. Their presence is associated with the inhibition of anti-tumour immune responses, thereby facilitating immune escape and disease progression (Curti et al., 2007).

Macrophages, primarily derived from circulating monocytes, are present in virtually all tissues and perform critical roles in immune defence. They can eliminate cancer cells through cytotoxicity, phagocytosis, antibody-dependent mechanisms, and by initiating both innate and adaptive immune responses. However, in the context of cancer, macrophages can adopt a tumour-promoting phenotype. These tumour-associated macrophages (TAMs) support tumour growth, induce angiogenesis, enhance metastatic potential, and suppress anti-tumour immunity, thereby contributing to disease progression (Mantovani et al., 2017).

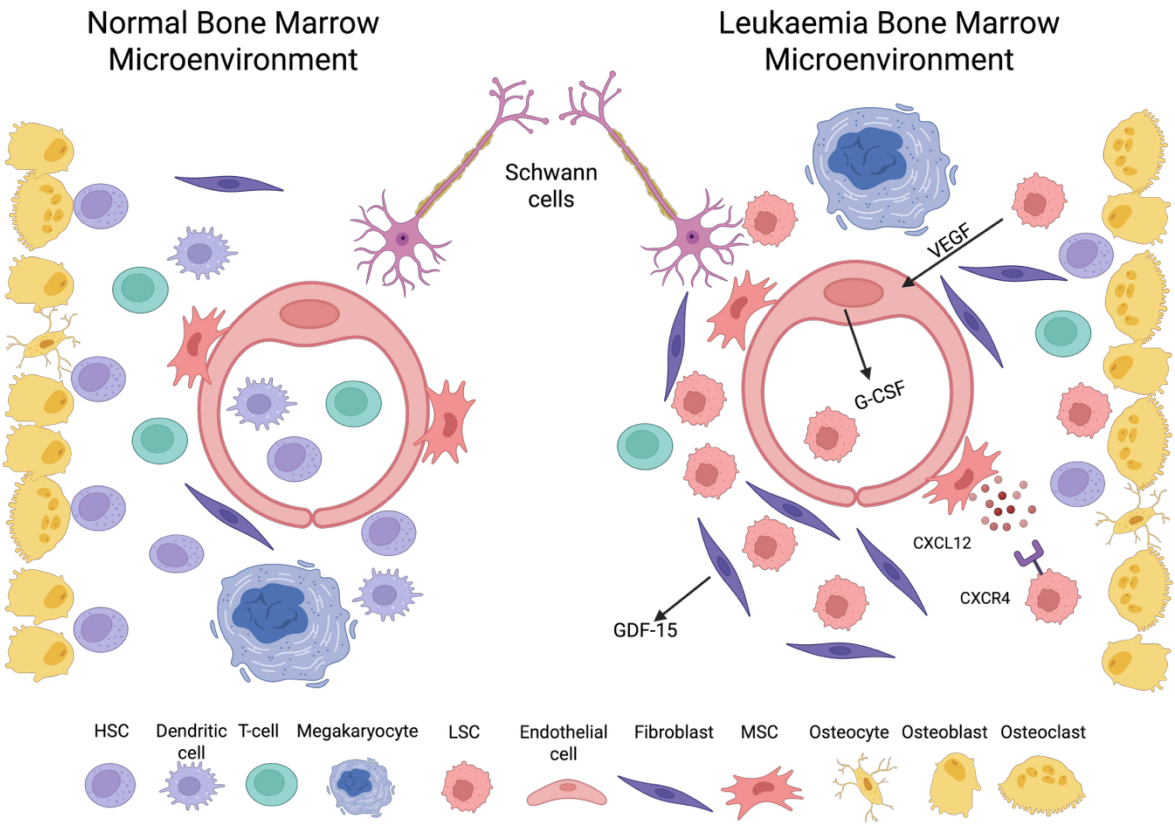

Figure 1-2 Bone marrow microenvironment components within healthy population and AML patients.
Normal bone marrow shows haematopoietic stem cells in different states: quiescent near the endosteal niche and bone-forming cells, activated near the vascular niche and mobilised inside the peripheral circulation. Moreover, normal bone marrow shows adequate fibroblasts, osteoblasts, osteoclasts and MSCs. On the other hand, the leukaemia bone marrow niche contains LSC and an increased number of osteoclast and fibroblasts, changing the bone marrow architecture to support LSC survival, growth, and proliferation. VEGF; Vascular endothelial growth factor, GDF-15; Growth differentiation factor, G-CSF; Granulocyte-colony-stimulating factor.

1.2.3 Bi-directional relationship between AML LSC and BMME

The interplay between LSC and BMME is like 'the chicken or the egg' mystery, whereby it is unclear whether a mutation in BM stromal cells causes a transformation from HSC to LSC and leukaemia initiation and progression or whether this starts with a mutation in HSC causing leukaemia, which then remodels the BMME, making it a permissive environment for LSC expansion, proliferation, survival, and chemotherapy resistance (Figure 1-3). Herein, we can discuss both theories and their supportive evidence.

1.2.3.1 Bone marrow niche as a predisposing factor for leukaemia

This hypothesis, suggesting that the BM niche might act as an initiating step of leukaemia, was built on several studies in mice that discovered a group of mutations in non-haematopoietic stem cells that eventually led to leukaemia.

These mutations, which are different from known genetic mutations found in LSC, cause myeloproliferative neoplasm (MPN)-like and MDS-like diseases that result in myeloid malignancy (Blau et al., 2007; J.-A. Kim et al., 2015; Y. Kim et al., 2015; von der Heide et al., 2017). Herein, those somatic mutations (*PTPN11, DROSHA, DICER1, SBDs*) found to be expressed in MSCs will be discussed. The role and mechanisms of how the BMME confers chemoresistance and supports AML cell survival and proliferation will be discussed in a later section.

Further important evidence that BMME has a pivotal role in initiating leukaemia is the development of leukaemia in patients after alloHSCT who developed donor-derived leukaemia. Although it is a rare example, one study worked on 12 cases that developed leukaemia after alloHSCT and categorised the cases into two groups; one group showed the transference of the malignant clone from the donor, and the other group showed the evolution of the malignant clone in the healthy donor cells once transplanted which might be related to the recipient BMME. This malignant clone transforms healthy donor HSC into LSC (Sala-Torra et al., 2006).

Several genetic mutations in non-haematopoietic cells (e.g. *Ctnnb1* in osteoblast (Kode et al., 2014)), especially MSCs were found to be involved in the progression of leukaemia. Indeed, leukaemia itself might take years to manifest, as these mutations cause CH, leading to MPN-like and MDS-like diseases that eventually progress to AML (Deininger et al., 2017).

Nuclear factor Kappa B (NF-κB) is responsible for haematopoietic cell proliferation and differentiation. It was found that mice deficient in the NF-κB inhibitor-α (IκBα), an inhibitor of NF-κB gene transcription, developed MPN-like diseases (Rupec et al., 2005).

Walkley *et al* found that the interaction between BMME and HSCs in mice with a mutant retinoblastoma protein (Rb), a cell cycle regulator in the process of haematopoiesis, has a role in MPN-like disease development (Walkley, Shea, et al., 2007). Together with a previous finding by the same research group that found that MPN-like disease was developed in mice with retinoic acid receptor (RAR)-γ deficiency, they indicated that mutations in BMME cells could initiate MPN and secondary leukaemia (Walkley, Olsen, et al., 2007).

Other factors are involved in causing MPN, such as inhibition of Notch activation, CREB-binding protein insufficiency, and protein tyrosine phosphate non-receptor type 11(*PTPN11*) mutation (Dong et al., 2016; Y.-W. Kim et al., 2008; Zimmer et al., 2011). *PTPN11* is present in young patients with Noonan syndrome and plays a role in developing MDS/MPN, which ends with juvenile myelomonocytic leukaemia (Dong et al., 2016). Moreover, patients with MDS showed abnormal expression in MSC genes encoding for RNA processing, such as *SBDS, DROSHA and DICER1*, referring to the role of MSC genetic mutation in initiating leukaemia (Santamaría et al., 2012).

Taken together, there is strong evidence suggesting that BMME, with its cell component, especially MSCs, could participate in leukaemia initiation and progression through genetic mutations affecting those cells responsible for haematopoiesis regulation, such as proliferation and differentiation. Most studies discussed were done on mice; clinical studies are needed for strong validation (Méndez-Ferrer et al., 2020).

1.2.3.2 LSC remodel the bone marrow niche to support leukaemia expansion

In the previous section, we demonstrated how the BMME could initiate leukaemogenesis through somatic mutations expressed in MSCs. Here, we will discuss the crosstalk between AML cells and different cells of BMME and how LSC could participate in remodelling the BMME, making it a shelter for AML (Figure 1-3) (Urs et al., 2024).

One of the most important factors for creating a permissive BM for leukaemia is a highly vascularised BM. Indeed, this was found within the BMME within AML, where LSC and MSC secreted vascular endothelial growth factor (VEGF). VEGF stimulates the endothelial cells to secrete GM-CSF and IL-6 to promote the process of angiogenesis (Hatfield et al., 2006). In addition to the role of VEGF in angiogenesis, VEGF-C was found to take part in apoptosis inhibition through increased anti-apoptotic B-cell lymphoma 2 (Bcl-2) expression with maintained pro-apoptotic Bax level, resulting in increasing Bcl-2/Bax ratio in two AML cell lines, favouring the growth and survival of LSC (Dias et al., 2002).

Adipose tissue plays an important role in providing energy to LSC within the AML microenvironment. Rapidly proliferating LSC reduces the available BM cavity space available for normal HSC, and causes lipase phosphorylation in the adipose tissue, leading to lipolysis and free fatty acid liberation (Shafat, Oellerich, et al., 2017). As HSC normally depends on glycolysis for respiration and LSC depends on oxidative respiration, hypoxia and free fatty acid liberation would form a suitable microenvironment for LSC survival and proliferation by providing energy to AML cells and impairing normal haematopoiesis (Tabe et al., 2017).

Interactions between LSC and BMME cells play a fundamental role in BMME remodelling. One group of mediators of this interaction are adhesion molecules, which are expressed on endothelial cells. An example is E-selectin which binds to LSC, resulting in activation of Wnt/β-catenin and hedgehog signalling pathways in AML cells, supporting their survival (Chien et al., 2013). The other way is through reactive oxygen species (ROS) produced from AML metabolism and transferred to stromal cells upon direct contact, stimulating them to secrete acetate, which is chemically converted from pyruvate. The secreted acetate is used by AML cells to nourish the tricarboxylic acid cycle (TCA) and increase lipid biosynthesis that was found to be involved in AML chemoresistance (Vilaplana-Lopera et al., 2022).

Secretion of soluble factors should be considered in the crosstalk between LSC and BMME cells. Exosome secretion from leukaemia cells establishes a fertile microenvironment for AML blast to grow and survive. Exosomes are nanovesicles secreted by leukaemia cells which contain important proteins and other molecules capable of contributing to tumour development and metastasis through different mechanisms, including MET receptor tyrosine kinase activation, exosomes enriched in microRNA for cell signalling modulation, and cytokine release and stimulation for the autocrine circuit. *In vitro* experiments showed that CML cells secrete exosomes that stimulate MSCs to produce IL-8, a cytokine that promotes leukaemia growth (Corrado et al., 2014). AML cell lines and blast cells also secrete exosomes, which enter MSC to modulate its function and support leukaemia survival (Huan et al., 2015). Furthermore, *in vivo* experiments showed that secreted exosomes from engrafted AML inhibited osteogenesis and suppressed normal haematopoiesis by inducing the expression of Dickkopf-1 (DKK1) on BM MSC, and through inhibition of HSC supporting factors such as CXCL12 and Insulin-

like growth factor-1(IGF-1), resulting in bone loss and normal haematopoiesis inhibition (B. Kumar et al., 2018).

AML cells secrete tumour necrosis factor-alpha (TNF-α) and CXCL2. These pro-inflammatory cytokines and chemokines remodel the endosteal endothelium, resulting in the degradation of endosteal niche cells, such as osteoblasts and stromal cells. Destruction of the endosteal niche will disturb normal HSC function, ending with haematopoiesis inhibition (Duarte et al., 2018).

One component of the BMME that showed remodelling within AML infiltration is the ECM; one study has shown that AML cells secrete MMPs, which degrade ECM and damage the vasculature. It was found that MMP inhibition reduces AML growth and increases AML sensitivity to chemotherapy (Pirillo et al., 2022).

AML infiltration affects all immune cells within the BMME, such as T-cells, dendritic cells, and macrophages. AML inflammation was found to be associated with atypical and dysfunctional B cells with increased regulatory T-cells. Moreover, AML cases with extensive inflammation are associated with inferior outcomes, which led Lasry *et al.*, to develop an inflammation-associated gene signature (iscore) to help classify AML patients based on the state of the immune microenvironment which might improve risk-stratification (Lasry et al., 2023).

In summary, there is a bidirectional relationship between LSC and BMME cells, both modulate each other to form a suitable microenvironment to allow leukaemia cells to grow, proliferate freely and escape immune surveillance and chemotherapeutic drugs. All these changes come at the expense of normal haematopoiesis, which leads to BM destruction and AML infiltration. A novel, targeted therapy for the crosstalk between AML and its BMME might restore chemosensitivity, decrease relapse, and increase OS.

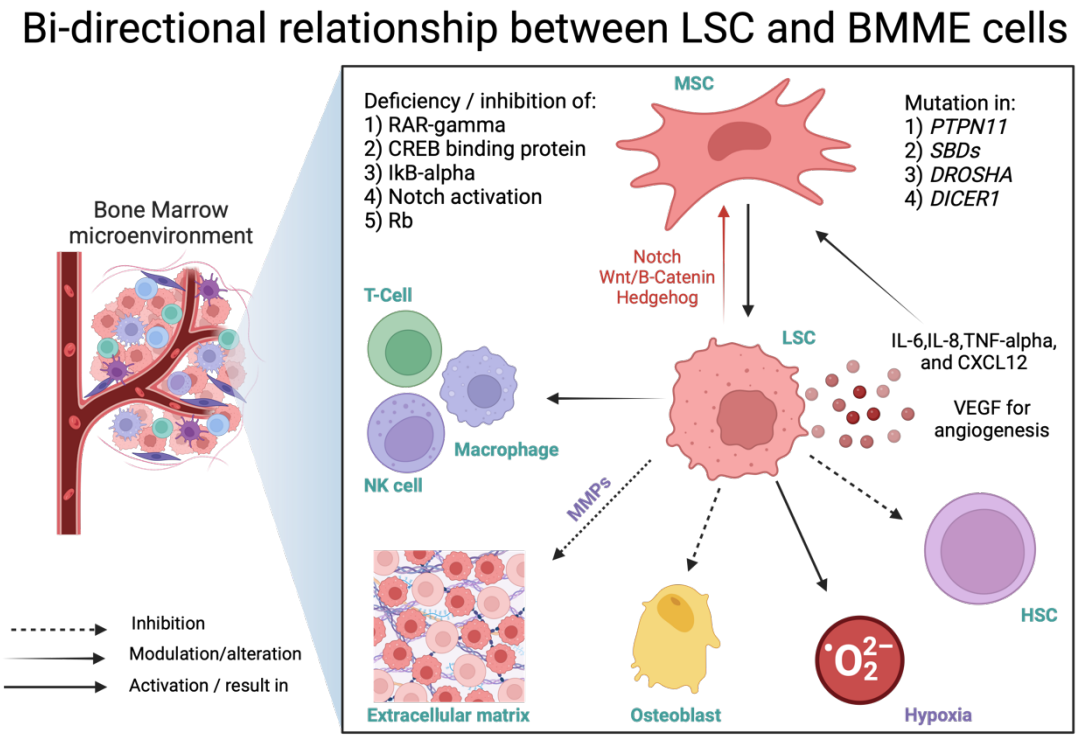

Figure 1-3 The interplay between leukaemia stem cell and bone marrow microenvironment cells.
The figure shows how LSC affect BMME and vice versa. LSC secrete different cytokines and chemokines to modulate MSC function, inhibit extracellular matrix by secreting matrix metalloproteinase, suppress HSC function and proliferation and inhibit osteoblast differentiation and bone formation through exosome secretion, modulate immune cells to escape surveillance, secrete VEGF for angiogenesis, and increase oxygen consumption and create a hypoxic environment. All these actions create a suitable microenvironment to act as a shelter to support leukaemia growth and proliferation. Furthermore, somatic gene mutations and some molecular deficiencies in MSC promote MPN-like disease and secondary AML. Rb, retinoblastoma, TNF-a, tumour necrosis factor-alpha, HSC, haematopoietic stem cell, LSC, leukaemia stem cell, NK, natural killer cell, VEGF, vascular endothelial growth factor, MSC, mesenchymal stem cell, RAR, retinoic acid receptor, MMPs, matrix metalloproteinase

1.2.4 Role of bone marrow microenvironment in AML chemoresistance and relapse

In the previous section, it was clear that either genetic mutation in stromal cell initiates leukaemia, or AML LSC remodel the BMME to create a permissive microenvironment for AML cells to grow and survive. Indeed, leukaemia needs a specific environment to grow, proliferate and expand. A recent study showed that the normal BMME secretome differs completely from AML-derived BMME (Sadovskaya et al., 2023). Culturing AML cell lines with MSCs isolated from healthy donors was able to inhibit AML proliferation and enhance apoptosis through its secretome. However, AML-derived MSC secretome protects AML cell lines from

apoptosis, suggesting that AML-derived MSCs have an altered cytokine profile from healthy BM MSCs (de Freitas et al., 2024).

MSC helps to support the AML cell from self- and drug-induced apoptosis by creating a suitable microenvironment. This can be achieved by the different secreted cytokines that affect AML proliferation, differentiation, and survival. Despite this supporting relationship, AML patients are still heterogeneous regarding the effect of cytokines produced by the MSC on the viability and proliferation of leukaemia cell. However, the overall cytokine-mediated MSC effect is increasing the growth probability and the anti-apoptotic effect on AML cell (Brenner et al., 2017) .

MSC can produce cytokines and chemokines, creating a refuge for haematopoietic cell, leukaemia cell, and tumour cell from chemotherapeutic drugs. It has been shown that leukaemia cells can also affect BMSC without direct cellular contact. This happens because leukaemia cells can produce soluble factors that can upregulate and downregulate BMSC gene expression, leading to changes in the BMSC cytokine profile with a more pro-inflammatory signature (Civini et al., 2013).

Studies have shown that the human BMSC line, HS5 protects AML cell against self- and drug-induced apoptosis (Garrido et al., 2001). This protection is derived through cell-to-cell contact, which is significantly more than non-contact conditions provided by cytokines and growth factors secreted by stromal cell. This apoptosis inhibition was independent of Bcl-2 protein expression in AML (Garrido et al., 2001). HS5 cell secrete little IL-3 and SCF, however, both are considered myeloid survival growth factors (Roecklein & Torok-Storb, 1995). Despite this, HS5 cell still confer protection against apoptosis, suggesting that other mechanisms have a vital role in this apoptosis inhibition, such as the secretion of other cytokines or the contact condition related to adhesion molecules (Garrido et al., 2001).

Although lots of studies have shown the important role of BMSC in conferring chemoprotection to AML blast, the mechanism of how protection is provided is still not elucidated. One study showed that BMSC-mediated chemoprotection is through the activation of ATP-binding cassette (ABC) transporters which can efflux

several molecules including chemotherapeutic drugs and induce an AML blast 'new population' that became more quiescent and chemoresistent (Boutin et al., 2020). Another study showed that specific BMSC increase AML survival, e.g., nestin+ BMSC, through increased activity of the TCA cycle and oxidative phosphorylation (OXPHOS) and simultaneously help LSC with antioxidant defence, which is important to compensate for increased ROS levels during leukaemogenesis and chemotherapy (Forte et al., 2020). It was found that stroma can confer resistance to mitoxantrone through a matricellular protein called CYR61 which is upregulated in AML cells by HS5 and HS-27A cell lines (Long et al., 2015).

Other studies have shown that the molecular mechanism of BMSC-mediated chemoresistance is partly related to cytokines secretion; IL-6 is considered one of the main cytokines secreted by BMSC (Kyurkchiev, 2014). Many studies are exploring how IL-6 can increase AML cell viability. IL-6 activates the Janus-activated Kinase-Signal transducer and activator of transcription (JAK-STAT) signalling pathway which phosphorylates STAT3, a transcription factor responsible for the regulation of many proliferative and survival genes (Sansone & Bromberg, 2012).

Serine phosphorylated STAT3 (pS-STAT3) was shown to alter mitochondrial OXPHOS, resulting in AML chemoresistance (Hou et al., 2020). Small, intracellular, calcium-sensing molecules, S100A8 and S100A9 which can modulate some cellular processes such as cell proliferation and differentiation, were found to be upregulated in AML cocultured with BMSC through IL-6/JAK-STAT signalling activation. IL-6 was found to promote chemoresistance by upregulation of fatty acid uptake. Through STAT3 activation, IL-6 can enhance CD36 expression at both genetic and protein levels, which promotes lipid metabolism, causing chemoresistance. It was found that CD36 antibody exhibit a synergistic effect with Ara-C against AML chemoresistance (Y. Zhang et al., 2022).

Returning to calcium-sensing molecules of the S100 family, one study showed that BMSC-derived exosomes provide chemoresistance and support AML cell proliferation and invasion through S100A4 upregulation (Lyu et al., 2021). It was found that stromal cell-mediated chemoresistance can occur through upregulation of the PI3K/Akt signalling pathway which is activated by IL-6 (P. Chen et al., 2016).

All these different mechanisms of how BMSC confer chemoprotection to AML cells are illustrated in (Figure 1-4).

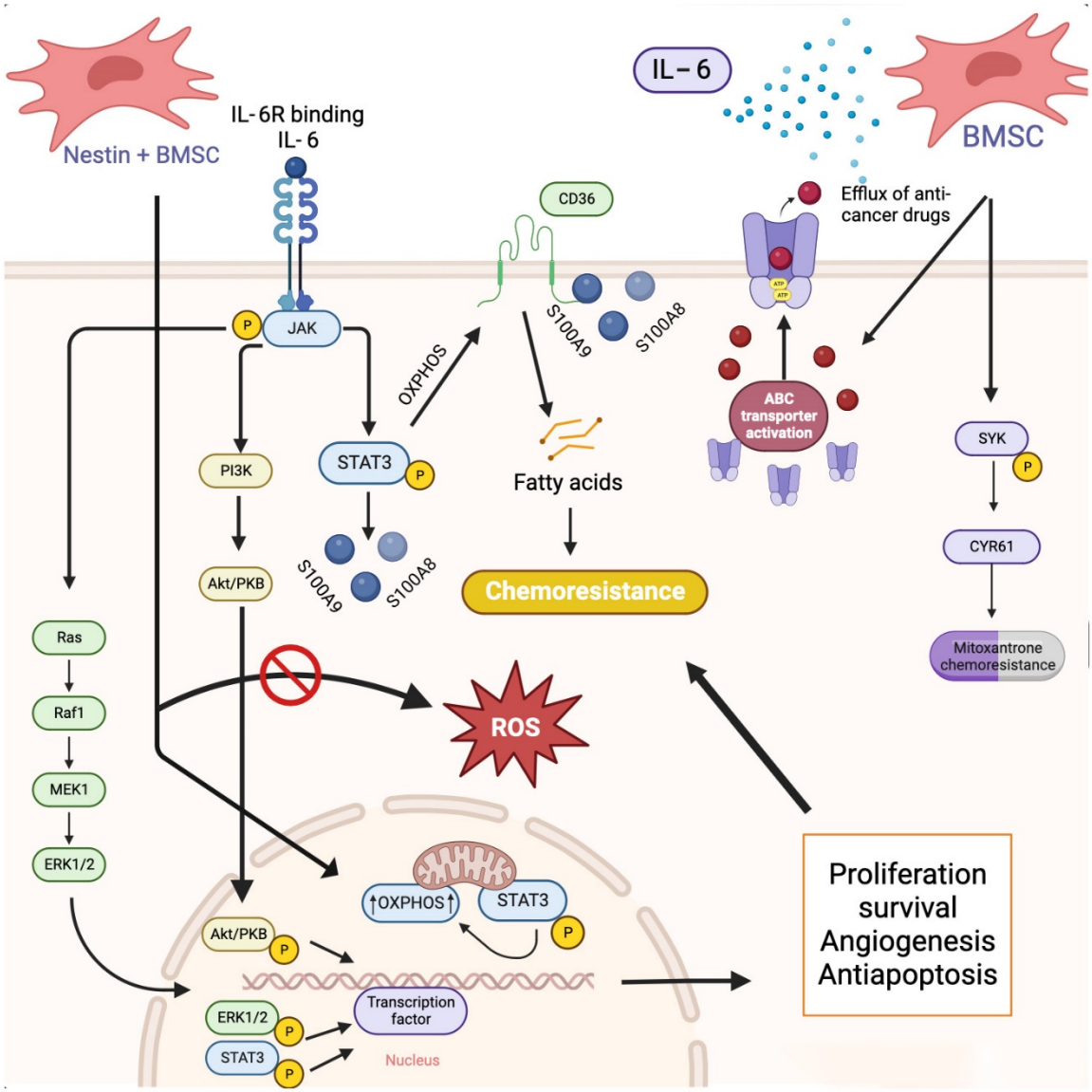

Figure 1-4 Different mechanisms of mesenchymal stromal cell-mediated chemoresistance in AML.
Protection is provided either through the BMSC secretome (e.g., IL-6) or direct cell-cell contact. IL-6 activates many pathways, such as JAK/STAT, that lead finally to proliferation, survival and anti-apoptotic effects. However, direct contact can activate the ABC transporter or phosphorylation of some proteins, e.g., SYK, leading to chemoresistance. BMSC, bone marrow stromal cell; IL-6, Interleukin-6; OXPHOS, oxidative phosphorylation. ROS, reactive oxygen species. SYK, SRC tyrosine kinase.

1.3 AML Treatment

1.3.1 Principles of AML therapy

The current standard AML treatment regimen has a backbone of chemotherapeutic agents e.g., cytarabine (Ara-C) and daunorubicin (DNR) (Rowe, 2022). Although AML patients show a good response to chemotherapy leading to remission, the prognosis is still poor because of drug resistance and high relapse rates. Thus, innovative targeted therapies or strategies are sought to overcome chemotherapy resistance and relapse in AML (Sendker et al., 2021).

Although some factors (patient age, co-morbidity, risk stratification of the disease, etc.) can affect AML treatment regarding the choice of chemotherapy or the dose of the drug, the main aim of the treatment is to achieve complete remission (CR) and prevent relapse through remission-induction therapy and post-remission consolidation therapy. Induction therapy is accomplished using chemotherapeutic drugs or hypomethylating drugs with or without targeted therapy, and consolidation therapy using either further cycles of cytotoxic chemotherapeutic drugs such as high-dose Ara-C or alloHSCT (Pelcovits & Niroula, 2020).

1.3.2 Conventional chemotherapy

Standard chemotherapy that consists mainly of an induction phase and post-remission phase was developed in 1970 with an induction phase consisting of a 7 plus 3 protocol that involves Ara-C given for 7 days by continuous infusion of 200mg/m^2 and 45-60 mg/m^2 of DNR for 3 days (Rai et al., 1981). Regarding the post-remission phase (consolidation therapy) that follows directly after the induction phase, this depends on the cytogenetic abnormalities and molecular abnormalities of the disease. With cases of CR that have a low-risk disease, chemotherapy should be completed. However, either partial remission or high-risk stratification diseases such as monosomy 7 are considered an indication for alloHSCT after achieving remission (Taga et al., 2016).

1.3.3 FDA-approved novel therapy for AML

Treatment of AML has been dependent on standard chemotherapy for over 40 years. In 2017, a novel drug revolution happened when FDA were able to approve new targeted therapies (small molecule). This approval was based on recent data about the molecular ontogeny of AML. AML pathways were studied which led to the successful development of these novel drugs (Table 1-3) (Mukherjee & Sekeres, 2019).

These novel chemotherapies depend on different mechanisms of attacking AML. These therapies include targeted antibodies e.g., gemtuzumab ozogamicin (GO) which acts on AML cells expressing cell surface CD33; targeted inhibitors of specific mutations such as FLT3 inhibitors and IDH1/2 inhibitors; pro-apoptotic agents such as BCL-2 (Short et al., 2020).

These novel chemotherapies changed the course of AML treatment and altered the landscape of leukaemia therapy, personalizing treatment by targeting the specific mutation the patient acquires not just the “generic” leukaemia cells. These novel therapies are better than conventional chemotherapy regarding patient adherence, specific genomic targeting, and reduced toxicities. However, patients on a single novel agent will frequently relapse, so patient selection, long-term drug efficacy, agent biosafety, level of toxicity and possibility of combination with other new therapies or standard treatment should be assessed (Mukherjee & Sekeres, 2019).

Table 1-3 FDA-approved novel targeted therapy for the treatment of AML
(Bazinet & Assouline, 2021; Winer & Stone, 2019).

Drug	**Mechanism of action**	**FDA approval year**	**Clinical trial number**	**Clinical Indications**
Olutasidenib (Rezlidhia) (Kang, 2023)	Selective IDH1 inhibitor	2022	NCT02719574	R/R AML with a susceptible *IDH1* mutation
Gemtuzumab ozogamicin (GO)	Anti CD33	2000/2017*	NCT00927498	Newly Diagnosed CD33+ adult patients. R/R adult and paediatric patients.
Ivosidenib (Tibsovo)	IDH1 inhibitor	2018	NCT02074839	*IDH1*-mutated newly diagnosed, R/R AML.
Enasidenib (Idhifa)	IDH2 inhibitor	2017	NCT01915498	*IDH2*-mutated R/R AML
Glasdegib	Hedgehog pathway inhibitors	2018	NCT01546038	Newly diagnosed AML who are ineligible for ICT taken with LDAC.

Venetoclax (Venclexta)	Bcl-2 inhibitor	2018	NCT02203773 NCT02287233 NCT02993523 NCT03069352	Newly diagnosed AML, who are ineligible for ICT given with azacitidine, decitabine, or LDAC.
Liposomal Cytarabine and Daunorubicin (CPX-351) (Vyxeos)	Same as standard Ara-C and DNR but in a liposomal encapsulation	2017	NCT01696084	Newly diagnosed t-AML or AML-MRC
Midostaurin (Rydapt)	FLT3 inhibitors	2017	NCT00651261	Newly diagnosed AML with FLT3 mutation
Gilteritinib (Xospata)		2018	NCT02421939	R/R AML with FLT3 mutation
Quizartinib (Vanflyta)(Erba et al., 2023)		2023	NCT02668653	Newly diagnosed AML with FLT3-ITD mutation

*Gemtuzumab ozogamicin (GO), was approved first in 2000, it was withdrawn from the market in 2010 till the next approval in 2017. Abbreviations: AML, acute myeloid leukaemia; AML-MRC, acute myeloid leukaemia with myelodysplasia-related changes; FDA, U.S. Food and Drug Administration; *FLT3*, fms-like tyrosine kinase 3; ICT, intensive chemotherapy; *IDH*, isocitrate dehydrogenase; R/R, relapsed/refractory; t-AML, therapy-related acute myeloid leukaemia; LDAC, Low dose Ara-C.

1.3.4 Immunotherapy as a treatment for AML

Although conventional chemotherapy is considered the cornerstone of AML treatment, and HSCT is one of the most effective treatments of AML, relapse and resistance still occur through different mechanisms, as immune escape, immunosuppression and MRD. Hence, immunotherapy emerged to overcome the challenges that cause AML relapse (Greiner et al., 2022).

Immunotherapies can overcome AML resistance in patients with relapsed and/or refractory AML. These therapies could be categorised into cancer vaccines, immune checkpoint inhibitors (ICIs), antibody-based immunotherapies, and adoptive T-cell therapies (Wu et al., 2024).

1.3.4.1 Cancer vaccines

Cancer vaccines aim to stimulate the immune system to recognise and attack leukaemia-associated antigens (LAAs) such as Wilms' tumour 1 (WT1), proteinase3 (PR3), receptor for hyaluronic acid-mediated motility (RHAMM), and mucin 1 protein (MUC1) (Barbullushi et al., 2022). Two main types are explored: peptide-based and dendritic cell vaccines.

Peptide-based vaccines like galinpepimut-S (GPS), a multivalent WT1 peptide vaccine, have shown promising immune responses in AML patients. However, clinical efficacy still requires further validation and more studies investigating combination therapy are needed (Maslak et al., 2018).

Dendritic cells (DCs) are antigen-presenting cells that can stimulate innate and adaptive immune responses. Based on these characteristic, DC-based vaccines have been developed to induce targeted immune responses and overcome immunologic escape(Hato et al., 2024) . DCs, which are used in vaccines derived from either leukaemia cells (Houtenbos et al., 2006) or monocytes (L. J. Zhou & Tedder, 1996), need to be loaded by LAA to present it to effector immune cells. DC-based vaccines are particularly effective in post-remission settings to prevent relapse. While safe and tolerable, cancer vaccines still face delivery and efficacy challenges *in vivo* (Anguille et al., 2017).

1.3.4.2 Immune Checkpoint Inhibitors

ICIs restore T-cell activity by targeting immune inhibitory pathways exploited by AML cells, primarily through programmed death receptor/Ligand-1 (PD-1/PD-L1), cytotoxic T-lymphocyte antigen-4 (CTLA-4), T-cell immunoglobulin and mucin domain (TIM-3), and CD47 pathways (Abaza & Zeidan, 2022). Nivolumab, pembrolizumab, ipilimumab, and novel drugs like sabatolimab and magrolimab have entered clinical trials, often in combination with hypomethylating agents (e.g., azacitidine). These combinations aim to overcome immune suppression and improve remission rates, especially in relapsed AML (Brunner et al., 2021). However, ICIs in AML are less effective than in solid tumours, partly due to the low mutational burden and immune evasion in AML, and their use can be complicated by immune-related adverse events (Giannopoulos, 2019).

1.3.4.3 Antibody-Based Immunotherapies

This category includes monoclonal antibodies (e.g., cusatuzumab), which mediate antibody-dependent cellular cytotoxicity via recruiting the effector immune cells, bispecific antibodies (e.g., bispecific T-cell engagers (BiTEs) like AMG330), which bind directly to antigens, leading to a link between targeted cells and effector cells, and antibody-drug conjugates (e.g., GO), which bind the drug to the antibody for direct treatment (Vago & Gojo, 2020).

Monoclonal antibodies directly target surface antigens like CD33, CD123, or CD70, but often affect normal hematopoietic cells. Bispecific antibodies engage both leukaemia cells and immune effector cells (e.g., T or NK cells), enhancing cytotoxicity (Reusing et al., 2021). Antibody-drug conjugates deliver cytotoxic agents selectively to leukaemia cells, improving specificity. These therapies have shown promising effects. However, toxicity (e.g., cytokine release syndrome) and limited targeting specificity remain major limitations (Senapati et al., 2022).

1.3.4.4 Adoptive T-Cell Therapies

Adoptive T-cell therapy, including CAR-T and TCR-T cell strategies, involves engineering T cells to recognise and eliminate leukaemia cells. CAR-T cells, particularly those targeting CD33 and CD123, have demonstrated potent anti-leukaemia activity, though on-target/off-tumour effects and cytokine release

syndrome are concerns (Daver et al., 2021). TCR-T cells are tailored to recognise intracellular antigens presented by MHC molecules, such as WT1 and NPM1. Despite promising early-phase results, broader application is hampered by toxicity, limited antigen specificity, and high production costs. Still, these therapies hold great potential, especially in refractory or high-risk AML cases (Vanhooren et al., 2023).

1.3.5 Ruxolitinib and dasatinib as a future treatment for AML

1.3.5.1 Ruxolitinib

Ruxolitinib (previously known as INCB018424) is a JAK inhibitor. It is a tyrosine kinase inhibitor (TKI), inhibiting the JAK-STAT signalling pathway by selectively inhibiting JAK1/2. When cytokine binds to the ligand binding site on the receptor, receptor conformational changes happen with JAK proteins juxtaposing to each other on the receptor intracellular domain, leading to JAK autophosphorylation. This then leads to tyrosine phosphorylation of the receptor. Receptor phosphorylation recruits STATs for binding with phosphorylated residues on the receptor, causing STAT phosphorylation, which in turn leads to STAT dimerisation and nuclear localisation, where it can promote transcription activation of survival and proliferative genes. Using ruxolitinib, competitive inhibition of the ATP-binding site occurs on the catalytic site of the kinase domain of JAK protein, leading to inhibition of JAK autophosphorylation and, in turn, inhibition of intracellular receptor and STAT phosphorylation (Figure 1-5)(Mascarenhas & Hoffman, 2012). After its approval in 2011, It has been used clinically to treat JAK2 *V617F*-positive MPNs, including intermediate or high-risk myelofibrosis and polycythaemia vera in patients who are intolerant or have hydroxyurea resistance (Bose & Verstovsek, 2017).

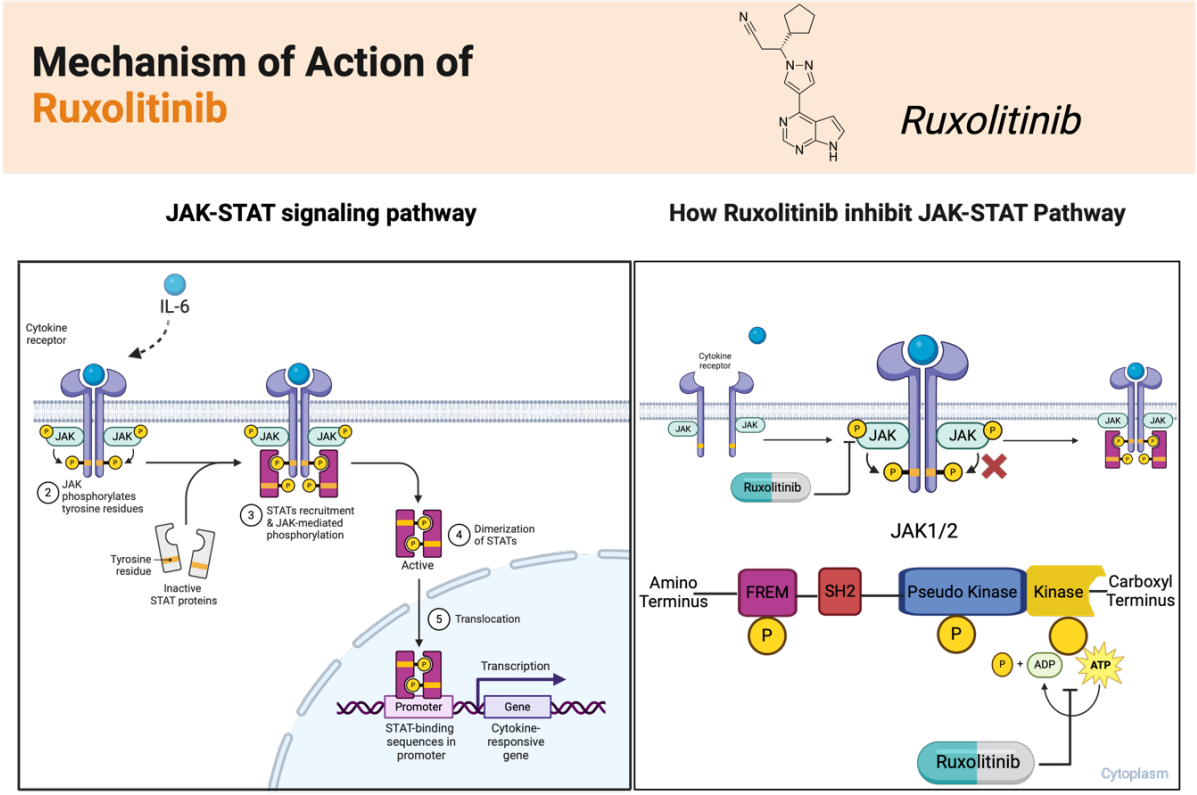

Figure 1-5 JAK-STAT signalling pathway and how ruxolitinib could inhibit it.
Upon binding of cytokine to its receptor, receptor conformational changes happen leading to JAK and STAT phosphorylation. Ruxolitinib, a JAK inhibitor, competitively inhibits ATP-binding catalytic sites on JAK1 and JAK2, causing JAK-STAT signalling pathway inhibition.

Ruxolitinib is metabolised hepatically through the cytochrome P450 (CYP450) enzymatic pathway, specifically CYP2C9 and CYP3A4, and eliminated through the kidney; any hepatic or renal insufficiency or administration of CYP3A4 inhibitors or inducers should be taken into account during treatment as it affects ruxolitinib metabolism (Appeldoorn et al., 2023).

Regarding the adverse effects of ruxolitinib, it was found during the COMFORT trial that there are both haematological and non-haematological side effects. The haematological adverse effects, including anaemia and thrombocytopenia, arise due to JAK signalling inhibition, with erythropoietin and thrombopoietin signalling being inhibited. The non-haematological adverse events include fatigue, headache and dizziness with some gastric symptoms like diarrhoea and abdominal pain (Bryan & Verstovsek, 2016).

Since 2011, when the FDA approved ruxolitinib for the treatment of myelofibrosis, studies have been conducted on its use for other diseases. In 2019, ruxolitinib was approved for the treatment of acute graft-versus-host disease after alloHSCT,

which is refractory to steroids (Przepiorka et al., 2020). Moreover, in 2021, ruxolitinib was approved and administered in cream form to treat atopic dermatitis (Eichenfield et al., 2024). Ruxolitinib was studied to treat coronavirus disease 2019 (COVID-19) during the pandemic off-label, this indication is not yet approved (Cao et al., 2020; Goker Bagca & Biray Avci, 2020). However, it is unlikely to be studied in COVID-19 as there is an increased risk of infections with ruxolitinib (Lussana et al., 2018).

Although the progression of MPNs to AML, represents a very small subtype of secondary AML, it was found that 35 to 50% of post-MPN-AML had the same *JAK2-V617F* mutation as primary myelofibrosis (Abdel-Wahab et al., 2010) which raised the awareness of using ruxolitinib in secondary AML as a single agent in patients not fit for alloHCST or concomitant with the conventional chemotherapy Ara-C in younger patients who are fit for cytotoxic therapy (McKinnell et al., 2022).

One trial study of ruxolitinib, NCT00674479, was undertaken on 38 refractory/relapsed leukaemia patients; 18 were post-MPN-AML, of which 12 had *JAK2* mutation. This study showed that 3 out of 18 had CR after using ruxolitinib, concluding that ruxolitinib might have anti-leukaemic activity, especially in post-MPN-AML with more trials needed to approve it as secondary AML treatment (Eghtedar et al., 2012).

Another trial, NCT03558607, was designed to test ruxolitinib with intensive chemotherapy on healthy young patients with post-MPN-AML that hadn't been treated with ruxolitinib. Although the designed number for this trial was 17 patients, this trial was terminated because of the low number of patients entering the study, resulting in only 2 cases recruited. Both patients achieved CR, but one died of pneumonia after developing neutropenic fever, but the other patient had not relapsed after 24 months follow-up (D. H. Kim et al., 2023). The combination of ruxolitinib and decitabine, was used in a clinical trial for blast-phase MPN treatment (NCT02076191), and showed favourable OS among patients on the trial. This combination has the potential to be considered as a therapeutic option for MPN in blast phase or post-MPN-AML (Mascarenhas et al., 2020).

Based on what was mentioned, ruxolitinib might have anti-leukaemic activity, and as an approved drug by the FDA, ruxolitinib should be entered for a clinical trial

for primary AML patients, not only for secondary AML progressing from myelofibrosis.

1.3.5.2 Dasatinib

Dasatinib, approved by the FDA for treating CML, is a small molecular compound working through competition with ATP on the binding site of the catalytic domain of tyrosine kinases. It is a multi-targeted kinase inhibitor that inhibits BCR::ABL1 (breakpoint cluster region-Abelson), SRC family, platelet-derived growth factor receptor b (PDGFRb), c-Kit and other kinases. It is used to treat newly diagnosed and imatinib-resistant CML cases (Montero et al., 2011) and resistant Ph+ ALL (Shah et al., 2004). Some studies showed that dasatinib might have a role in AML, as some AML cases have a c-Kit mutation that could be targeted by dasatinib (Heo et al., 2017; Mpakou et al., 2013).

Dasatinib is an oral drug, metabolized and eliminated through hepatic CYP450, (CYP3A4). Dasatinib is rapidly absorbed with no effect of food on its absorption, however, low gastric pH such as with antacids and proton pump inhibitors (e.g., omeprazole) decrease the drug's absorption. As metabolism and elimination depend on CYP450, any drug affecting CYP3A4 enzyme could affect dasatinib metabolism, although renal insufficiency, age and race don't perturb its pharmacokinetics (Hořínková et al., 2019; Levêque et al., 2020).

Dasatinib has general side effects like other TKI that can be divided into haematological and non-haematological toxicities. Haematological toxicities include neutropenia, anaemia and thrombocytopenia, with non-haematological ones including musculoskeletal disorders, gastric, metabolic, cardiac, and pulmonary toxicities. Although all these adverse events start mildly on initiation of dasatinib treatment and often resolve spontaneously, pulmonary toxicities are of concern as they are more dangerous, especially in high-risk patients that could lead to the stopping the drug. Pleural effusion and pulmonary arterial hypertension are the most common pulmonary toxicities that need appropriate management to improve patient prognosis and quality of life (F. Cheng et al., 2023; Nekoukar et al., 2021).

SRC family kinases (SFK), which include SRC, LCK, FYN, LYN and YES, are inhibited by dasatinib (Montero et al., 2011); SRC is a non-receptor tyrosine kinase that plays a role in cell growth, differentiation, and survival (Hsu et al., 2020). Dasatinib inhibits SRC by binding to the ATP-binding site of the kinase domain, preventing the transfer of phosphate groups to tyrosine residues on target proteins. Upon binding to the ATP-binding site, dasatinib induces conformational changes in the kinase domain of SRC. This stabilises the kinase's inactive conformation, making it less effective in phosphorylating its substrates. As SRC activation is mainly through tyrosine phosphorylation (Y416), dasatinib prevents this activation by interfering with phosphorylation (Figure 1-6). By inhibiting P-SRC, dasatinib affects multiple signalling pathways involved in cell proliferation, survival, and migration.

Researchers have investigated the role of dasatinib in AML, based on the mechanism of action of dasatinib inhibiting tyrosine kinase c-Kit. Dasatinib was tested on core binding factor AML cell lines, t(8;21) (q22;q22), bearing N822K KIT mutation; these cell lines were Kasumi-1 and SKNO-1. The result showed that dasatinib at different concentrations(10nM and 500nM), was able to induce apoptosis through caspase-3 and inhibit the proliferation of the Kasumi-1 cell line, and using 1nM, dasatinib was able to inhibit the SKNO-1 cell line growth in long term stromal culture with the presence of GM-CSF (Han et al., 2010; Heo et al., 2017; Mpakou et al., 2013).

The ability of dasatinib to induce apoptosis and inhibit cell growth in core binding factor AML cell lines carrying KIT mutation give the opportunity to test the drug as an adjuvant therapy to standard chemotherapy. Indeed, A retrospective study from a multicentre group was conducted over 10 years to study the effect of combining GO or KIT inhibitors with intensive chemotherapy and showed that there was no beneficial role of adding GO to standard chemotherapy. However, KIT inhibitors showed an increase in OS and disease-free survival in patients with core binding factor AML (Rojek et al., 2024).

A recently published letter regarding a retrospective study showed that dasatinib has anti-leukaemic activity in AML irrespective of KIT mutation status, and this might be because of dasatinib ability to sensitise blast cells to chemotherapy and induce AML differentiation (Srinivasan, 2024). This lead us in our research to

investigate dasatinib in combination with standard chemotherapy, aiming to increase AML sensitivity to chemotherapeutic drugs by inhibiting the SRC signalling pathway, which was thought to be involved in BMSC-mediated chemoresistance.

Two identified clinical trials investigated adding dasatinib to standard chemotherapy for core binding factor AML and its effect on event-free survival and OS. These two trials were the German Austrian Acute Myeloid Leukaemia Study Group 11-08 (AMLSG 11-08) (NCT00850382) and Cancer And Leukaemia Group 10801 (CALGB10801) (NCT01238211). The results for both clinical trials were similar; the 3-year OS was 74.7% in AMLSG 11-08. and 77% in CALGB10801. Phase 3 clinical trial (NCT02013648) was started to confirm the results of the previous two clinical trials and ended in February 2024. To the best of our knowledge, the result of this clinical trial have not been published yet (Marcucci et al., 2020; Paschka et al., 2018).

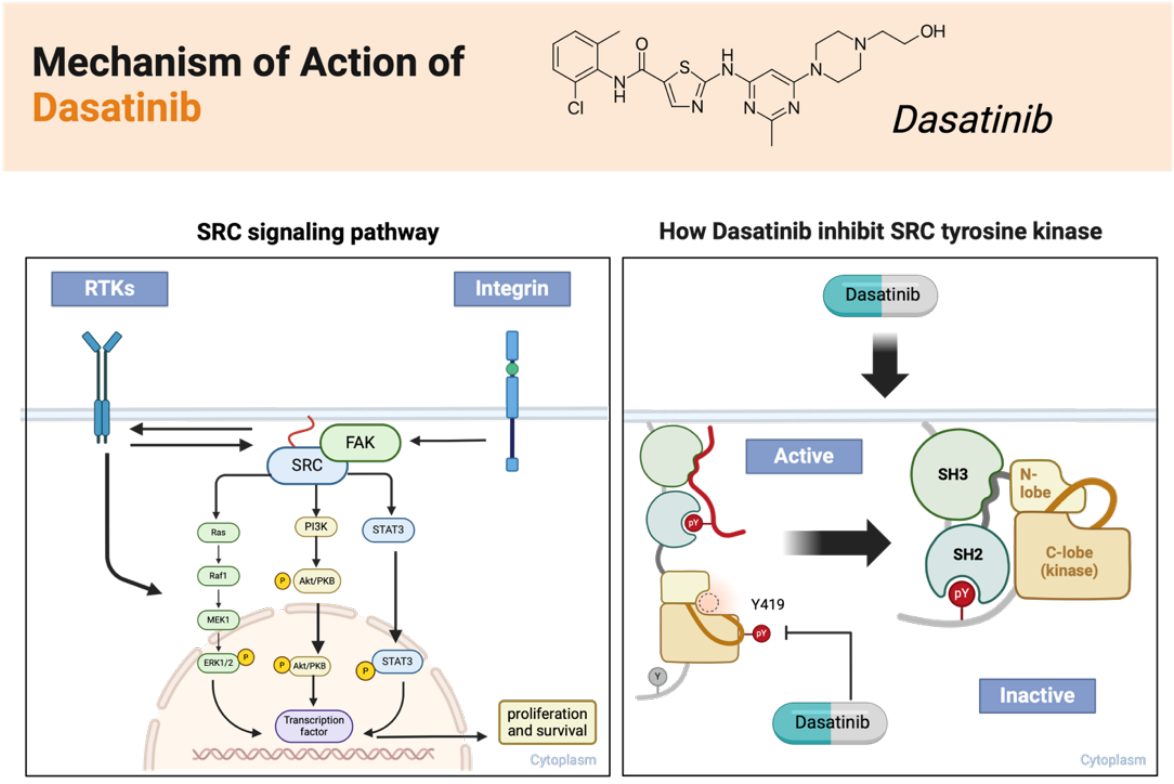

Figure 1-6 Dasatinib inhibits SRC tyrosine kinase signalling.
On the left, different SRC signalling pathways involved in cell growth, proliferation, and survival are illustrated. On the right, dasatinib competes with the ATP binding site on the active SRC tyrosine kinase, making it inactive.

1.4 Hypothesis

Given the heterogeneity of AML driven by diverse somatic mutations and the bidirectional interaction between leukaemic cells and the BMME, it is hypothesised that the BMME may significantly contribute to the development of chemoresistance, ultimately influencing patient survival and relapse rates. Although targeted therapies against specific mutations such as IDH1 and FLT3 have shown clinical benefit, there remains a critical need to develop novel, less cytotoxic therapeutic strategies that specifically disrupt the protective role of the BMME in AML, particularly its capacity to protect LSC from conventional chemotherapy.

1.4.1 Study aims:

1) Investigate the BMME secretome to add to our knowledge of cytokines and chemokines secreted from the BM niche in healthy and in AML infiltrated BM;

2) Investigate the prosurvival role of the cytokines found to be present in a higher concentration in AML-infiltrated BM;

3) Examine the signalling pathways stimulated by those defined cytokines and study how their stimulation affects AML cell survival;

4) Investigating the role of novel, targeted, and FDA-approved drugs on AML cell viability and proliferation.

2 Materials and methods

2.1 Materials

2.1.1 Suppliers

Company name	Address
Applied biosystems	Lingley House, 120 Birchwood Boulevard, Warrington, WA3 7QH, UK
BD Biosciences	1030 Eskdale Road, Winnersh Triangle, Wokingham, Berkshire, RG41
BioRad	The Junction, Station Road, Watford, Hertfordshire, WD17 1ET, UK
BioLegend UK Ltd	4B Highgate Business Centre 33 Greenwood Place London NW5 1LB United Kingdom
Cell signaling technology	Dellaertweg 9b 2316 WZ Leiden The Netherlands
Corning, Scientific Laboratory Supplies Ltd	Biocity Scotland, Bo'Ness Road, Newhouse, ML1 5UH, UK
DSMZ-German Collection of Microorganisms and Cell Cultures GmbH	Inhoffenstraße 7B 38124 Braunschweig Science Campus Braunschweig-Süd GERMANY
eBioscience, Thermo-Fisher Scientific (TFS)	Unit 3, Fountain Drive, Inchinnan, Renfrew, PA4 9RF, UK
Fisher Scientific UK	Bishop Meadow Road, Loughborough, LE11 5RG, UK
Gibco, TFS	Unit 3, Fountain Drive, Inchinnan, Renfrew, PA4 9RF, UK
Greiner Bio-One	Unit 5/Brunel Way, Stonehouse, GL10 3SX, UK
Hawksey	25 Marlborough Road, Lancing Business Park, Lancing, Sussex, BN15 8TN, UK
Honeywell, Scientific Laboratory Supplies Ltd	Biocity Scotland, Bo'Ness Road, Newhouse, ML1 5UH, UK
Integrated DNA technologies (IDT)	BVBA, Interleuvenlaan 12A, B-3001 Leuven, Belgium
Invitrogen, TFS	Unit 3, Fountain Drive, Inchinnan, Renfrew, PA4 9RF, UK
LI-COR Biosciences Uk Ltd	St John's Innovation Centre, Cowley Rd, Milton, Cambridge, CB4 0WS, UK
Lonza	Chesterford Research Park, Building 200, Little Chesterford, UK
Lorne Laboratories	1 Danehill, Earley, Reading, RG6 4UT, UK

MedChemExpress, Cambridge Bioscience Limited	2-3, Munro House, Trafalgar Way, Bar Hill, Cambridge CB23 8SQ
Merck Millipore	Fleming Road, Kirkton Campus, Livingston, EH54 7BN, UK
PeproTech EC	PeproTech House, 29 Margravine Road, London, W6 8LL, UK
PromoCell	PromoCell GmbH, Sickingenstr. 63/65, 69126, Heidelberg, Germany
Qiagen	Skeleton House, Lloyd Street North, Manchester, M15 6SH
R&D systems (Biotechne)	19 Barton Lane Abingdon Science Park Abingdon, OX14 3NB
Roche	Hexagon Place, 6 Falcon Way, Shire Park, Welwyn Garden City, AL7 1TW, UK
Santa Cruze Biotecnology, Insight Biotechnology Limited	PO Box 520. Wembley Middlesex HA9 7YN UK.
Selleckchem, Stratech Scientific Ltd	Cambridge House, St Thomas' Place, Cambridgeshire Business Park, Ely, CB7 4EX, UK
Sigma-Aldrich, Merck Life Science UK Ltd	The Old Brickyard, New Rd, Gillingham, Dorset, SP8 4XT
Stem Cell Technologies	7 rue du lac, 38120, Saint Égrève, France
VWR Chemicals	Hunter Boulevard, Magna Park, Lutterworth, Leicestershire, LE17 4XN, UK

2.1.2 Laboratory appliance

instrument type	Instrument	Suppliers
Centrifuges	3-16KL Refrigerated	SIGMA
	4K15	
	1-14 Microfuge	
Flow cytometry	BD FACSCanto II	BD Biosciences
Luminex®	MAGPIX	TFS
Microplate reader	SpectraMax® M5 Plate Reader	MDS Analytical Technologies
PCR systems	QuantStudioTM 7 Pro	TFS
Spectrophotometer	NanoDropTM 1000	LabTech
Western Blotting	Li-Cor Odyssey FC	LI-COR
	Invitrogen™ Mini Gel Tank	TFS
	Invitrogen™ Mini Blot Module	

2.1.3 Tissue culture

2.1.3.1 Tissue culture materials

Items	Supplier
Blunt ended needles	BD
Cell counting chamber (Haemocytometer)	HAWKSLEY
Cell strainers (70 and 100 µm)	Fisher Scientific
Cryovials	Greiner Bio-one
Eppendorf tubes (0.5, 1.5 mL)	Greiner Bio-one
FACS tubes	BD biosciences
Falcon Tubes (15, and 50 mL)	Greiner Bio-one
Filter tips (10,20, 100, 200, 100 µm)	Greiner Bio-one
Media vacuum filter	Sarstedt
Sterile tissue culture pipette (5, 10, 25 cm)	Greiner Bio-one
Syringes (1, 5, 10, 20, and 50 mL)	BD
Syringe filters (0.45, and 0.20 µm)	Sartorius
Thincert cell culture insert for 12 well plates, TC, sterile, translucent membrane (pet), pore diameter: 0,4 µm	Greiner Bio-one
Tissue culture flasks (25, 75, 150 cm^3)	Corning
Well plates (6.12,24,48,96)	Greiner Bio-one

2.1.3.2 Tissue Culture Reagents

Reagent/material	Supplier	Catalogue #
Accutase	Gibco, TFS	00-4555-56
Colcemid 10µg/mL	Roche	10295892001
Cytarabine (Ara-C)	Sigma	C3350000
Dasatinib 25mg	Selleckchem	BMS-354825
Dimethysulfoxide (DMSO)	TFS	D2650-100ML
Dulbecco's Modified Eagle Medium (DMEM)	Gibco, TFS	11965092
Ethanol	VWR Chemicals	20821.330
Hanks-buffered saline solution (HBSS) 10X	TFS	14065-049
Heat inactivated Fetal bovine serum (FBS)	Gibco, TFS	16140071
Isopropanol	Fisher Scientific	24137
L-glutamine	Gibco, TFS	25030081
Mesenchymal Stem Cell Growth Medium II	Promocell	C-28009
Methanol	Fisher Scientific	24229
MycoAlertTM mycoplasma detection Kit	Lonza	LT07-318
Penicillin-streptomycin (Pen/Strep)	Gibco, TFS	15140122
Phosphate-buffered saline tablets (PBS)	TFS	BR0014G

ProcartaPlex™ Human Th1/Th2 Cytokine Panel, 11plex	Invitrogen, TFS	EPX110-10810-901
ProcartaPlex™ Human Basic Kit		EPX010-10420-901
ProcartaPlex™ IL-6 Human Simplex Kit		EPX01A-10213-901
ProcartaPlex™ Panel cytokine 6-Plex (Custom Designed)		PPX-06
Recombinant Human HGF (HEK293 derived)	PeproTech	100-39H
Recombinant human IL-6		200-06
Recombinant Human SDF-1α (CXCL12)		300-28A
Recombinant Human VEGF165		100-20
Resazurin salt	Merck	R7017
Roswell Park Memorial Institute (RPMI) 1640 medium	Gibco, TFS	*11875093*
Ruxolitinib Phosphate	Selleckchem	S5243
Triton X-100	Sigma-Aldrich	9036-19-5
Trypan blue	TFS	15250061
Trypsin- Ethylenediaminetetraacetic acid (EDTA)	Gibco, TFS	25200072

2.1.3.3 Tissue culture media components

2.1.3.3.1 AML cell line culture medium

Reagent	Volume	Final concentration
RPMI	390 mL	
FBS	100 mL	20% (v/v)
L-Glutamine	5 mL	2mM
Penicillin/Streptomycin (Pen/Strep)	5 mL	1% (v/v)

2.1.3.3.2 MSC Growth Medium 2

Reagent	Volume	Final concentration (%)
MSC growth medium basal media	45 mL	
MSC growth medium supplement mix	5 mL	10% (v/v)

2.1.3.3.3 MSC culture Media

Reagent	Volume	Final concentration
DMEM	390 mL	
MSC growth medium 2	100 mL	20% (v/v)
L-Glutamine	5 mL	2mM
Pen/Strep	5 mL	1% (v/v)

2.1.3.3.4 MSC cell line (HS5) culture media

Reagent	Volume	Final concentration
DMEM	440 mL	
FBS	50 mL	10% (v/v)
L-Glutamine	5 mL	2mM
Pen/Strep	5 mL	1% (v/v)

2.1.3.3.5 Cell line freezing media

Reagent	Final concentration (%)
RPMI media for AML cell line / DMEM media for HS5	90% (v/v)
DMSO	10% (v/v)

2.1.4 Flow cytometry

2.1.4.1 Flow cytometry reagents

Reagent/material	Supplier	Catalogue #
Annexin V-FITC	BD Biosciences	556419
CellTrace Violet Cell (CTV) proliferation kit	Invitrogen, TFS	C34571
Colcemid 10µg/mL	Roche	10295892001
DAPI	Sigma	D9542-10MG
DAPI dihydrochloride	Merck	D95420-10MG
FACS clean solution	BD Biosciences	340345
FACS flow solution	BD Biosciences	336524
Fixation/Permeabilization solution kit	BD biosciences	554714
Hank's balanced salt solution (HBSS) x10 With calcium, magnesium, no phenol red	Gibco, TFS	14025092
UlteaComp eBeads Compensation beads	Invitrogen, TFS	01-2222-42

2.1.4.2 Flow cytometry antibodies (anti-human)

Antibody	Clone	Fluorochrome	Dilution	Suppliers	Type of staining
CD73	AD2	APC	(1:100)	BD Biosciences	Surface
CD90	5E10	PE	(1:100)	BD Biosciences	Surface
CD45	2D1	APC-Cy7	(1:100)	BD Biosciences	Surface
CD33	WM-53	PerCP-Cy5.5	(1:50)	BD Biosciences	Surface
Ki-67	SOLA15	PE-Cy7	(1:50)	Invitrogen, TFS	Intracellular
Annexin-V		FITC	(1:300)	BD Biosciences	Surface
Phospho -STAT3 (Tyr705)	13A3-1	PerCP-Cy5.5	(1:100)	BioLegend	Intracellular
Cleaved Caspase-3	Asp175	Alexa Fluor™ 488	(1:800)	Cell signaling	Intracellular
Cleaved PARP	ASP214	Alexa Fluor™ 488	(1:800)	Cell signaling	Intracellular
Alexa Fluor™ 488 goat anti-rabbit IgG (H+L)			(1:800)	Invitrogen, TFS	Intracellular

2.1.5 Molecular biology

2.1.5.1 Molecular biology reagents

Reagents	Suppliers	Catalogue#
High Capacity cDNA Reverse Transcription	Applied Biosystems, TFS	4368814
PowerTrack™ SYBR™ Green Master Mix	Applied Biosystems, TFS	A46109
RNeasy® Plus Mini Kit	Qiagen	74134

2.1.5.2 Primers

Gene name	Forward	Reverse
ATP5B	ATCAAACTGGACGTCCACCAC	TCCATCCTGTCAGGGACTATG
CYR61	CGCCTTGTGAAAGAAACCCG	GGTTCGGGGGATTTCTTGGT
SRC	TCCAGATTGTCAACAACACAGAG	CAGTAGGCACCTTTCGTGGT
TAZ	CCGTGTCCAATCACCAGTCCT	CTTGGTGAAGCAGATGTCTGC
TBP	AGTTCTGGGATTGTACCGCA	TGTGCACACCATTTTCCCAG
TEAD4	GCTCTGGATGTTGGAGTTCTCG	GGCTTGACTGGCTGATGTG
YAP1	GCAGTTGGGAGCTGTTTCTC	GCCATGTTGTCTGATCG

2.1.5.3 SYBR Green master mix

Reagent	Volume (µL)
2x SYBR MasterMix (blue)	5
Forward Primer (10µM)	0.4
Reverse Primer (10µM)	
Sample buffer (Yellow)	0.25
cDNA Sample	0.4
Nuclease-free water	3.95
Total per reaction	10

2.1.5.4 High Capacity cDNA Reverse Transcription master mix

Component	Volume / reaction (µL)
10x RT buffer	2
25x DNTP mix (100 mM)	0.8
10X RT Random Primers	2
MultiScribe Reverse Transcriptase	1
RNAase Inhibitor	1
(Nuclease-free water)	As required
RNA sample	500ng (up to 13.2µL)
Total per reaction	20

2.1.5.5 Qiagen RNA extraction (RNeasy plus mini kit)

Component	Volume commonly used
Buffer RLT (lysis buffer)	350µL
Buffer RW1 (Wash buffer)	700µL
Buffer RPE (Wash buffer)	500µL
RNase-Free Water	30-50µL
70% Ethanol	350µL
RNeasy Mini Spin Colum	One /sample
Collection Tubes (2mL)	

2.1.6 Western blotting

2.1.6.1 Western blotting reagents

Reagents	Supplier
Bovine Serum Albumin (BSA)	Merck
Complete protease inhibitor cocktail tablets	Roche
EDTA	Sigma
IGEPAL CA-630	Merck
Methanol	Merck
Nitrocellulose Membrane, 0.45 µm, 30 cm x 3.5 m	Invitrogen, TFS
NuPAGE Sample Reducing Agent (10X)	Invitrogen, TFS
NuPAGE™ 4 to 12%, Bis-Tris, 1.0 mm, Mini Protein Gel. (10 well / 12 well)	Invitrogen, TFS
NuPAGE™ LDS Sample Buffer (4X)	Invitrogen, TFS
NuPAGE™ MOPS SDS Running Buffer (20X)	Invitrogen, TFS
NuPAGE™ Transfer Buffer (20X)	Invitrogen, TFS
PageRuler™ Plus Prestained Protein Ladder, 10 to 250 kDa	Thermo Scientific
PhosSTOP easy pack phosphatase inhibitor cocktail tablets	Roche
Pierce™ BCA Protein Assay Kit	Thermo Scientific
Ponceau S solution	Sigma
Sodium Chloride (NaCl)	Sigma
Sodium Hydroxide (NaOH)	Fisher Scientific
Sodium Deoxycholate (Na-Deoxy)	Sigma
SuperSignal™ West Pico PLUS Chemiluminescent Substrate	Thermo Scientific
Trisma base	Sigma
Trisma HCl	Sigma
Tween 20	Sigma

2.1.6.2 Western blotting solutions

2.1.6.2.1 1M Tris-HCL

Reagents	Weight
Trisma base	121.4g
dH_2O	1000mL
HCL/NaOH	To appropriate pH

2.1.6.2.2 Blocking solution

Reagents	Volume/Weight	Final concentration
Dried skimmed milk powder	5g	5% (w/v)
TBST	100mL	

2.1.6.2.3 RIPA buffer

Reagents	Volume/Amount	Final concentration
1M Tris-HCL (PH7.4)	2.5mL	50nM
10% NP-40 (IGEPAL CA-630)	5mL	1% (v/v)
10 % (Na-Deoxy)	1.25mL	0.25% (v/v)
5M NaCl	1.5mL	150mM
250mM EDTA	200µL	1mM
dH_2O	39.55mL	
Complete protease inhibitor tablets*	1 tablet in 1mL	10% (v/v)
PhosSTOP phosphatase inhibitor tablets*	1 tablet in 1mL	10% (v/v)

*Added to required volumes of RIPA buffer immediately before use

2.1.6.2.4 Running buffer

Reagents	Volume	Final concentration
NuPAGE™ MOPS SDS Running Buffer (20X)	50mL	1X
dH_2O	950mL	

2.1.6.2.5 SDS loading buffer

Reagents	Volume/Amount	Final concentration
NuPAGE™ LDS Sample Buffer (4X)	5µL	1X
NuPAGE Sample Reducing Agent (10X)	2µL	1X
Sample	40µg (up to 13µL)	
dH_2O	As required	
Total Volume	20µL	

2.1.6.2.6 Transfer buffer

Reagents	Volume	Final concentration
NuPAGE™ Transfer Buffer (20X)	50mL	1X
Methanol	200mL	20% (v/v)
dH_2O	750mL	

2.1.6.2.7 TBS-T

Reagents	Volume	Final concentration
1M Tris (PH7.6)	20mL	20mM
5M NaCl	30mL	150mM
Tween 20	1mL	0.1% (v/v)
dH_2O	949mL	

2.1.6.3 Western blotting antibodies

Antibodies	Reactive Species	Dilution	Block	Supplier
Polyclonal goat Anti-mouse IgG, HRP-linked	Mouse	1:10000	TBST	Dako
Polyclonal goat Anti-rabbit IgG, HRP-linked	Rabbit	1:10000	TBST	Dako
Cleaved-Caspase	Rabbit	1:1000	5% BSA	Cell signaling
Cleaved-PARP	Rabbit	1:1000	5% BSA	Cell signaling
CYR61	Rabbit	1:1000	5% BSA	Cell signaling
GAPDH	Rabbit	1:1000	5% BSA	Cell signaling
IRDye®680RD Donkey-anti Mouse IgG	Mouse	1:10000	TBST	LI-COR
IRDye®800CW Donkey-anti Rabbit IgG	Rabbit	1:10000	TBST	LI-COR
Phospho-SRC Family (Tyr416) (D49G4)	Rabbit	1:1000	5% BSA	Cell signaling
P-STAT3 (Y705)	Mouse	1:1000	5% BSA	Cell signaling
Total SRC	Mouse	1:300	5% BSA	Cell signaling
Total STAT	Mouse	1:1000	5% BSA	Cell signaling
YAP	Rabbit	1:1000	5% BSA	Cell signaling

2.2 Methods

2.2.1 Drugs and reagents

2.2.1.1 Cytarabine (Ara-C)

Cytarabine vial of 150mg powder, 2.43 mg was dissolved in 1mL of water to prepare a stock solution with a final concentration of 10mM and stored at 2-8°C.

2.2.1.2 Ruxolitinib

Ruxolitinib phosphate (INCB018424, INC424) vial of 25mg powder, 5mg was dissolved in 1.2365mL of DMSO to prepare a stock solution with a final concentration of 10mM and stored in aliquots at -80°C.

2.2.1.3 Dasatinib

Dasatinib vial of 10mg powder, 1mg was dissolved in 2.0491mL of DMSO to prepare a stock solution with a final concentration of 1mM and stored in aliquots at -80°C.

2.2.1.4 Cytokines

HGF vial of 25μg, SDF-1α (CXCL12) vial of 10μg, VEGF-A vial of 10μg, and IL-6 vial of 100μg powder were initially reconstituted in water to 0.1 mg/mL as per the manufacturer's instructions and then diluted using 0.1% (w/v) BSA for a final concentration of 10μg/mL and stored in aliquots at -80°C.

2.2.2 Tissue Culture

All cell culture procedures were performed in a laminar airflow hood using aseptic technique. All cells were incubated at 37°C with 5% CO_2. The materials used for tissue culture are listed in 2.1.3.1 and 2.1.3.2. Specific growth medium and tissue culture solution compositions are detailed in 2.1.3.3.

2.2.2.1 Cell counting and viability assessment.

All cell counts were performed using a haemocytometer/ automatic cell counter and trypan blue (TB) exclusion of non-viable cells. TB penetrates the cell membrane in non-viable cells leading to blue colourization of the cells that could

be easily excluded from cell counts. A working stock solution of 0.8mM TB was made and 10µL mixed with 10µL of cell suspension to give a 1:2 dilution of the cells, before adding to the Neubauer haemocytometer with cover slip or applying it to the automatic counter. Cell counts were performed on an inverted microscope in the haemocytometer, and at least 100 viable cells were counted in 4 large squares. The total number of viable cells was divided by 4, multiplied by the 2 (TB dilution factor) and then by 10^4, to give the total number of viable cells per mL.

2.2.2.2 AML and MSC cell lines and human samples

The AML cell lines Kasumi 1, THP-1, SKNO-1, and ME-1 and stromal cell line HS5 were used for Ara-C, ruxolitinib and dasatinib drug treatments. All cell lines used had certificates of authentication from Eurofins Genomics. The paediatric cell line Kasumi-1 was used in coculture (CC) experiments with HS5 cell line and paediatric AML BMSC. The clinical information and culture conditions are summarised in (Table 2-1). All culture conditions are described by either the American Type Culture Collection (ATCC) or Deutsche Sammlung von Mikroorganismen und Zellkulturen (DSMZ). All cell lines were sub-cultured every 2-3 days and tested for mycoplasma contamination with the MycoAlert mycoplasma detection kit (Lonza). For cell line cryopreservation, $2x10^6$ cells were frozen in culturing media supplemented with 10% DMSO.

The HS5 cell line was used in CC experiments. After thawing, cells were washed in 10mL DMEM media with 10% (v/v) FBS and centrifuged at a low speed (110g) for seven minutes (mins). Pelleted cells were counted and seeded in 15mL media into culture flasks ($2.5x10^5$ cells per T75 flask) and incubated at 37°C in 5% CO_2. The media was replaced every two days until cells were greater than 70% confluent. Cells were dissociated using Trypsin and seeded for the ongoing experiment or cryopreserved in vials of $3x10^5$ cells using the freezing media supplemented with 10% DMSO. The cells were not used beyond passage 5 for experiments. The paediatric BMSC, isolated previously in our lab and frozen in liquid nitrogen, thawed by the same method, but instead of 10% (v/v) FBS that was added to DMEM media, 20% (v/v) MSC growth medium 2 was added.

Table 2-1 Cell line and isolated human MSC origin and culture conditions.

Cell line	Clinical Data	Culture Medium	Reference/Source
Kasumi-1	7yr old male t(8;21), KIT mutation N822	Complete RPMI-1640, 20% FBS	(Asou et al., 1991)
ME-1	40yr old male inv(16)(p13q22) leading to the fusion gene CBFB-MYH11	Complete RPMI-1640, 20% FBS	(Yanagisawa et al., 1991)
SKNO-1	22yr old male t(8;21) effecting RUNX1-RUNX1T1 (AML1-ETO) rearrangement	Complete RPMI-1640, 10% FBS, 5-10% conditioned medium of the cell line 5637	(Matozaki et al., 1995)
THP-1	1yr old male t(9;11)	Complete RPMI-1640, 10% FBS	(Tsuchiya et al., 1980)
HS5	30 years male, Bone marrow stroma (fibroblast)	Complete DMEM, 10% FBS	(Roecklein & Torok-Storb, 1995)
MSC isolated from pAML022	3.5yr female inv(16),	Complete DMEM, 20% MSC growth medium 2	
MSC isolated from pAML026	0.3yr female t(11q23)	Complete DMEM, 20% MSC growth medium 2	

2.2.3 Coculture (CC) experiments

The BM cell line (HS5) was seeded at a density of $2.5x10^5$ in 1mL MSC culture media in 12 well plate and left for 24 hours or until >80% confluent. Leukaemia cells were re-suspended in their specific culture media, cell counts were performed by TB exclusion, and cells were seeded at double the density of the HS5 cells onto the confluent layer of HS5 cells (CC), making the ratio of AML to HS5 2:1, or, directly into an empty well for liquid culture (LC). The AML cell lines were seeded at a density of $5x10^5$. The cells were added to the wells in 1mL of culture media. Ara-C and other drugs (ruxolitinib and dasatinib) were immediately added to the drug-treated wells or culture media to the vehicle control (VC) wells. For all cell lines, the EC50 concentration of Ara-C was used. The EC50 concentration was calculated for Kasumi 1, ME-1, SKNO-1, and THP-1 cells and those calculated concentrations were used in CC experiments (Figure 3-2). The cells were left for 48 hours unless otherwise specified. The cells were harvested from LC by transferring the cell suspension to a 15mL falcon tube and two PBS washes (1mL) of the well to collect residual cells. In the CC wells, the cell suspension was removed from the wells and added to a falcon tube, followed by a PBS wash of 1mL. In the case of cell-

cell contact, 200μL trypsin-EDTA was added to the cells and incubated for 5-10 mins at 37°C until a single-cell suspension was formed. The dissociated cells and two further PBS washes (1mL each) were added to the falcon tube. Trypsin-EDTA was also added to the LC tubes to reduce variability in the treatment of the two groups. LC and CC cells were centrifuged at 300g for 10 mins and re-suspended in 1mL of PBS. Using the transwell assay (explained in 2.2.3.1), samples were then ready to be utilised for RNA and protein extraction and flow cytometry to analyse cell surface marker expression, apoptosis, cell cycle and cell proliferation. In the case of cell-cell contact, interrogation of AML cells could only be performed after the separation of AML cells from HS5 using CD73 by flow cytometry. A schematic representation of the CC experiments is shown in (Figure 2-1).

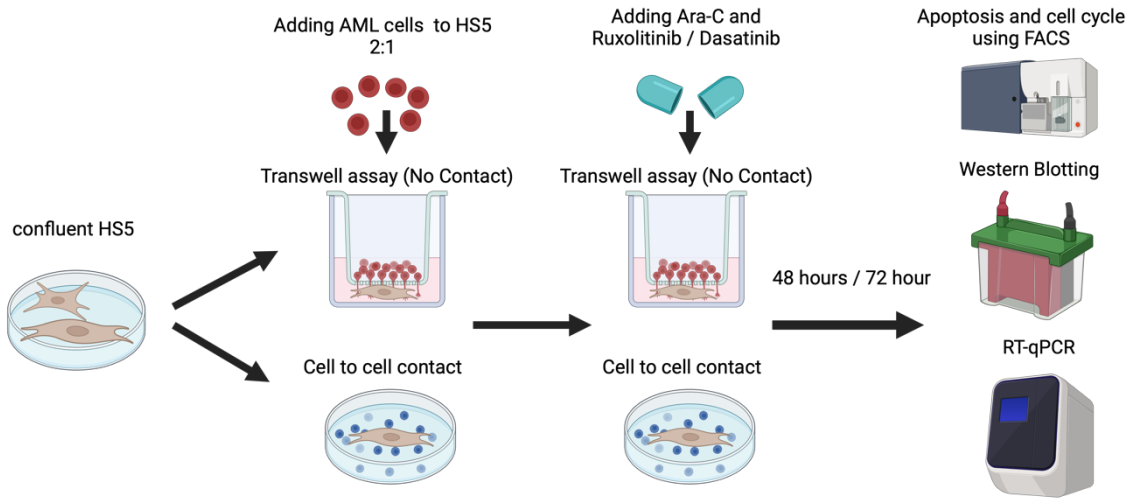

Figure 2-1 Schematic representation showing CC experiment.

2.2.3.1 Transwell assay

A transwell assay is a robust and easy technique widely used in basic research to study cell-cell interaction, migration and invasion. This assay involves a two-chamber system separated by a permeable membrane, allowing researchers to investigate how cells move or interact under various conditions.

Transwell Insert is a cylindrical chamber that fits into a well of a multi-well plate. By applying this insert to the multi-well plate, upper and lower chambers will be created. The bottom of the insert is made of a porous membrane which can vary in pore size, allowing selective passage of cells, nutrients, or other molecules.

In our experiments, HS5 cell line was seeded in the lower chamber and AML cells were added to the upper chamber allowing HS5 conditioned medium containing cytokines, chemokines and nutrients to go through the membrane avoiding cell-cell contact.

2.2.4 Flow Cytometry Protocols

Flow cytometry is a technique composed of fluidics, optic, and detection systems. The physical and chemical characteristics of cells will be analysed as the cells pass one by one through a laser beam in a fluid stream resulting in scattering light and emitting fluorescence if labelled with fluorescent markers. Detectors capture forward scatter representing cell size, side scatter representing cell complexity, and fluorescence at different wavelengths. These signals are processed to provide detailed data on cell properties, making flow cytometry useful for immunophenotyping, apoptosis detection, cell cycle analysis, cell sorting, and functional assays. It offers multiparametric analysis and quantitative data.

2.2.4.1 Surface staining

In all flow cytometry experiments, equal numbers of cells were centrifuged at 300g for 5 min at RT in tubes and one wash with 2mL PBS (HBSS if followed by apoptosis assay). Unstained cells were used to set voltages and eComp beads were used for compensation in all experiments. Single-stained and Fluorescence Minus One (FMO) controls were used as appropriate in all experiments. These controls were used to help distinguish between true positive signals and background or spillover signals. Antibody titrations were performed for each antibody on AML cell lines before an experiment to determine the optimal dilution. Cells were incubated in the dark and on ice /4°C with the antibody mix for 30 mins. After incubation, cells were centrifuged at 300g for 5 min at RT, and a further 2mL PBS wash was performed. The cell pellet was then re-suspended in 200µL PBS. Samples were protected from light and run on the BD FACS Canto II. FlowJo V10.7.1 software was used for analysis.

2.2.4.2 Intracellular staining

For phospho-epitope staining, treated and untreated cells were fixed by adding 37% (v/v) formaldehyde directly into the culture medium to obtain a final

concentration of 1.5% (v/v) formaldehyde. Cells were incubated in fixative for 10 mins at room temperature (RT) and pelleted by centrifugation at 300g for 5 min at 4°C. They were then permeabilized by resuspending with vigorous vortexing in 500 µl ice-cold methanol per 10^6 cells and incubated at 4°C for at least 10 mins. Cells were washed twice (2mL each) in staining media (PBS containing 1% (w/v) BSA) and then resuspended at 0.5-1 x 10^6 cells per 100µl. 50ng of fluorophore-specific mAbs were added and incubated for 15-30 mins at RT. The cells were washed with 2mL staining media. Finally, samples were resuspended in 100µl staining media and analysed.

2.2.4.3 Apoptosis assay

This assay is used to ascertain distinctions in cell viability and apoptosis patterns between LC and CC groups, both with and without drug treatment. Annexin-V and DAPI were utilized in this assay. In the presence of calcium, Annexin V selectively binds to phosphatidylserine (PS) exposed on the cell membrane during the initial stages of apoptosis. Meanwhile, DAPI attaches to DNA within the nucleus when the integrity of the cell membrane is compromised, indicating cells in advanced stages of apoptosis or necrosis.

In the CC experiments, HS5 should be excluded first using one stromal cell marker; CD73 was selected as it showed a good demarcation between AML and HS5 cells. Cells were first stained with surface marker CD73, as outlined in 2.2.4.1. Subsequently, an apoptosis staining cocktail was prepared using 1x HBSS solution with Annexin-V (at a dilution of 1:300) and DAPI staining (at a dilution of 1:1000). 100µL of this cocktail was added to each tube for 15 mins incubation period at RT in the absence of light, and an additional 200µL HBSS solution was added to the samples. These samples were promptly processed using the BD FACS Canto II system. Analysis was performed by gating the samples based on forward scatter/side scatter (FSC/SSC) parameters, gating on single cells using FSC-A/FSC-H, and then gating on CD73 negative cells for HS5 exclusion, after that, assessment of viable cells (Q4), those in early (Q3), late apoptosis (Q2), and necrotic or dead cells (Q1) was performed using Annexin V and DAPI staining, as illustrated in (Figure 2-2). Detailed descriptions of the specific gating strategies for apoptosis assays in each CC experiment are provided in the corresponding results chapters.

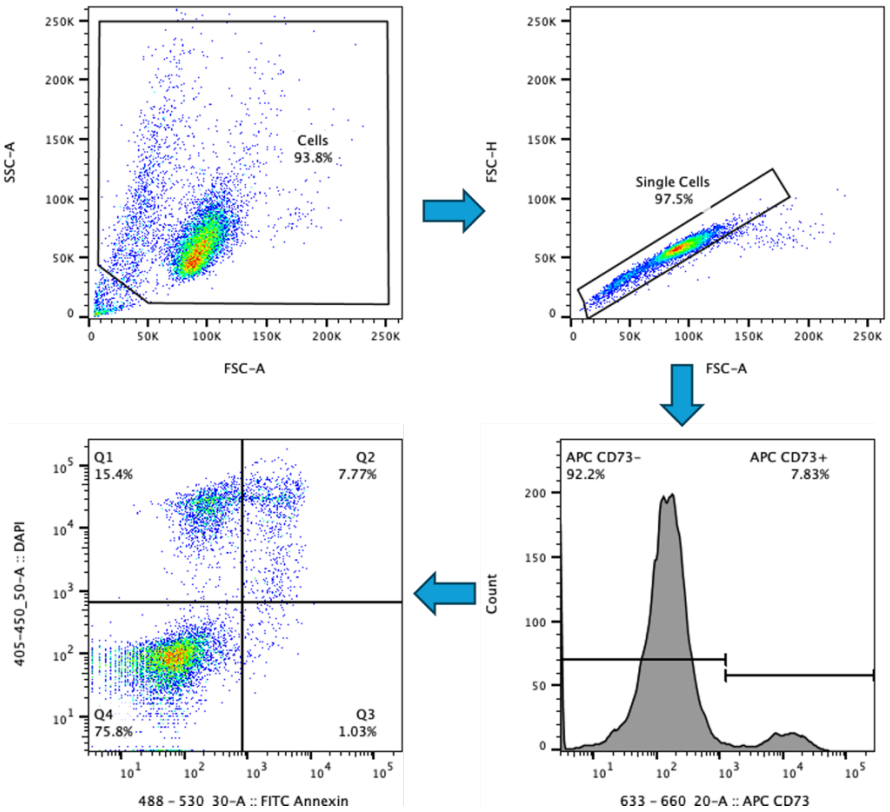

Figure 2-2 Gating strategy for detecting the different stages of apoptosis using Annexin-V and DAPI staining.
Both viable and non-viable cells are included in the initial gate using FSC-A/SSC-A. Gating on CD73+ HS5 for stromal cell exclusion and analysis for leukaemia cells for apoptosis. Viable leukaemia cell populations Annexin-V - DAPI - (Q4), early apoptosis Annexin-V + DAPI - (Q3), late apoptosis Annexin-V + DAPI + (Q2), and dead cells Annexin-V - DAPI + (Q1).

2.2.4.4 Cell cycle assay

In the CC experiments, all cells were stained for CD73, a stromal cell marker, before preparation for cell cycle. The BD Cytofix/Cytoperm Fixation and Permeabilization kit (BD Biosciences) was used to prepare cells for cell cycle analysis, before staining with Ki-67 (1:100 dilution) and DAPI (1:1000 dilution). 100 -150,000 cells were used for each tube. After centrifugation at 300g for 5 min at RT, the cell pellet was vortexed and 250µL of the fixation/permeabilization solution (containing paraformaldehyde 4.2% (v/v)) was added. After incubation at RT for 20 mins, cells were centrifuged at 250g for 10 min at RT, paraformaldehyde discarded, and the pellet washed using 500µL wash/permeabilization (wash/perm) solution. A further wash with 500µL wash/perm solution was performed, and then 50µL of 1:100 Ki-67 solution was added to the tubes and incubated for 30 mins at 2-8°C. A further wash with 500µL wash/perm solution was performed, after that, 100µL of 1:1000 DAPI solution was added to the tubes. Cells were incubated for 10 mins at RT in the absence of light and then samples were immediately run on

the BD FACS Canto II. DAPI was acquired on a linear scale. Plots were objectively analysed using the FlowJo software analysis as illustrated in (Figure 2-3).

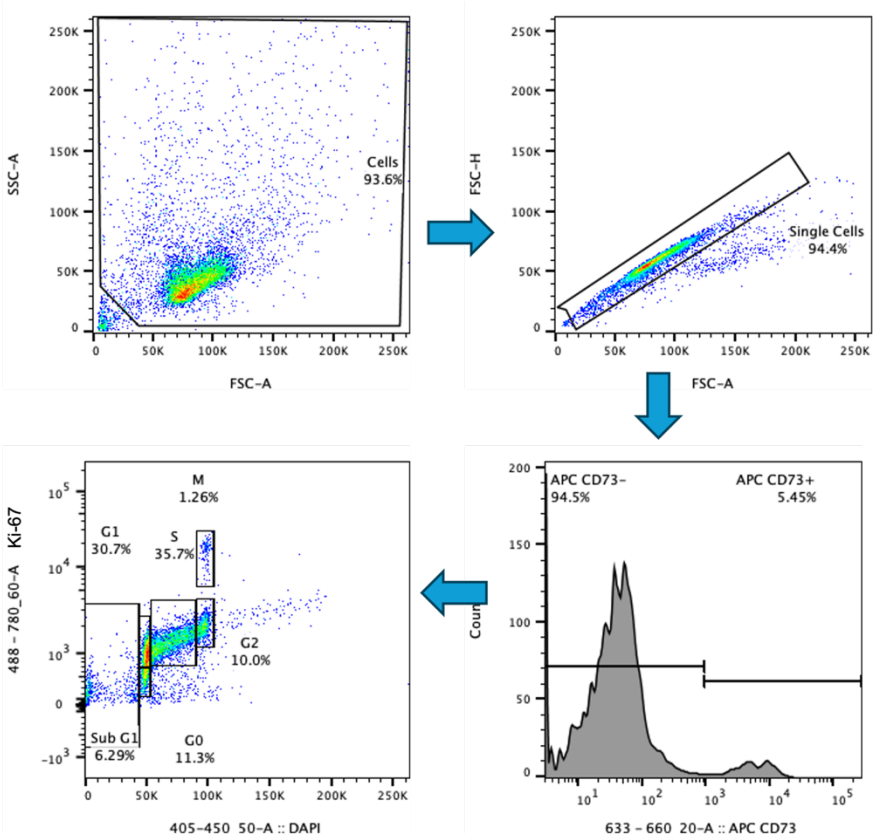

Figure 2-3 Gating strategy for detecting the different stages of cell cycle using Ki-67 and DAPI staining.

2.2.4.5 CellTrace™ Violet assay

CellTrace™ violet (CTV) is a fluorescent dye used to label cells and detect multiple generations of cells using dye dilution. It is a fluorescent cell-permeable dye that covalently binds to intracellular amine molecules. As cells divide and create new generations of cells, the intensity of the fluorescent dye reduces by half, allowing the different generations of cells (G0-G3) to be detected and cell proliferation to be assessed.

AML cells were counted. $2x10^6$ cells were centrifuged for 10 mins at 200g and resuspended in 5mL of 2% (v/v) FBS/PBS with 5µL of 5mM CTV stock solution, to make a final concentration of 5µM of CTV. The cells were then incubated at 37°C in the dark for 20 mins. Five times of 20% (v/v) FBS/PBS,25mL in our experiment, was then added to the falcon tube and incubated at RT for five mins. The cells were then centrifuged for 10 mins at 200g at RT and washed once with 4mL complete medium (CM) and then re-suspended in the CM. Cells were plated in

wells with and without pre-plated HS5 for CC experiments with Ara-C/Dasatinib/Ruxolitinib treatment. After 72 hours, cells in different conditions were collected for FACS analysis.

A day 0 sample was taken for flow analysis to allow voltages to be set for the experiment. A colcemid, colchicine structural analogue of N-deacetyl-N-methylcolchicin, control was performed by adding 10µL to 1mL of cell suspension (final concentration 100ng/mL). Colcemid causes metaphase arrest by binding tubulin and preventing spindle formation during mitosis. It therefore provides an undivided sample control (CTV^{max}).

A division index (DI) was calculated to quantify the CTV proliferation results. The DI is the total number of divisions divided by the total number of cells at the start of the culture. Using FlowJo, each generation of cell divisions was manually gated (G_d). The total number of divisions was then calculated by adding the total number of cells within each generation of cells (G_i) divided by the number of divisions (2^{G_d}) multiplied by the generation number (G_d). Next, the total number of cells present at the start of the culture was calculated by adding the total number of events in each generation (G_i) divided by the number of divisions the cell has undertaken (2^{G_d}). Using this formula we can calculate the division index.

$$DI = \frac{\sum_{\substack{i=0 \\ d=0}}^{n} \left(\frac{G_i}{2^{G_d}} x G_d\right)}{\sum_{\substack{i=0 \\ d=0}}^{n} \left(G_i / 2^{G_d}\right)}$$

Equation 1 Calculation of division index for cell proliferation analysis.

2.2.5 Multiplex immunoassay

2.2.5.1 Cell Culture Supernatant Collection

Cell culture supernatant was collected for AML cell lines (Kasumi-1, ME-1 and THP-1) in LC, CC with cell-to-cell contact, CC without cell contact using transwell assay, and from HS5 alone. To do this, 12-well plates were used with a total volume of 2mL of media. BMSCs were seeded at $5x10^4/cm^2$ (250,000 cells/well) and left for 24 hours. AML cell lines were seeded at $5x10^5$ cells/well onto the pre-

prepared BMSC layer in transwell or LC in 1mL of culture media with no cytokine supplementation. Cell culture supernatant was collected at 24 hours. The cell suspensions were collected from the wells and centrifuged at 300g for 5 mins. The cell culture supernatant was then removed, with care not to disturb the cell pellet, and stored at -80°C.

2.2.5.2 ProcartaPlex™ Multiplex Immunoassay

The ProcartaPlex™ multiplex immunoassay kits utilise antibody-based magnetic bead assays to enable the simultaneous detection and quantification of multiple cytokines within a single well. In this process, monoclonal antibodies specific to a target analyte are attached to colour-coded beads, which are fluorescently labelled with red and infrared fluorophores. The detection system recognises these distinct colours, facilitating the identification of beads corresponding to analytes. Upon binding the analyte to the antibody-coated beads, a detection antibody is introduced to form an immunocomplex. Subsequently, streptavidin-PE (SA-PE), a fluorescent detection label, is added for quantification, yielding a mean fluorescent intensity (MFI) value for each analyte (Figure 2-4). By constructing a standard curve for each analyte using the MFI of standards with known analyte concentrations, the concentration of each analyte in the test samples can be accurately determined. ProcartaPlex™ Human Th1/Th2 Cytokine Panel, 11 plex kit, a custom-designed 6-Plex ProcartaPlex™ Panel kit and IL-6 Human ProcartaPlex™ Simplex Kit were used for cytokine profiling of the cell culture supernatants. The cell culture supernatant was not diluted for use in the first two kits, but depending on the result coming from the 11 plex kit showed that IL-6 is very high in samples, so samples were diluted into 1:100 dilution for IL-6 Simplex Kit. The manufacturer's instructions were followed to prepare the 96-well plate for analysis on the MAGPIX Instrument. Samples and standards were performed in duplicate. Frozen cell supernatant samples were thawed on ice and centrifuged at 10,000g for 5 mins before use. In brief, standards were prepared using four-fold serial dilutions. The magnetic beads were added to the plate, followed by several wash steps according to kit instructions, and then the standards and samples were added to the plate. The plate was incubated at RT on a plate shaker for 2 hours. After further wash steps, the detection antibody was added followed by SA-PE. A reading buffer was added before running on the machine.

ProcartaPlex™ analyst software was used to analyse the ProcartaPlex™ multiplex immunoassay data. GraphPad was then used to perform statistical analysis.

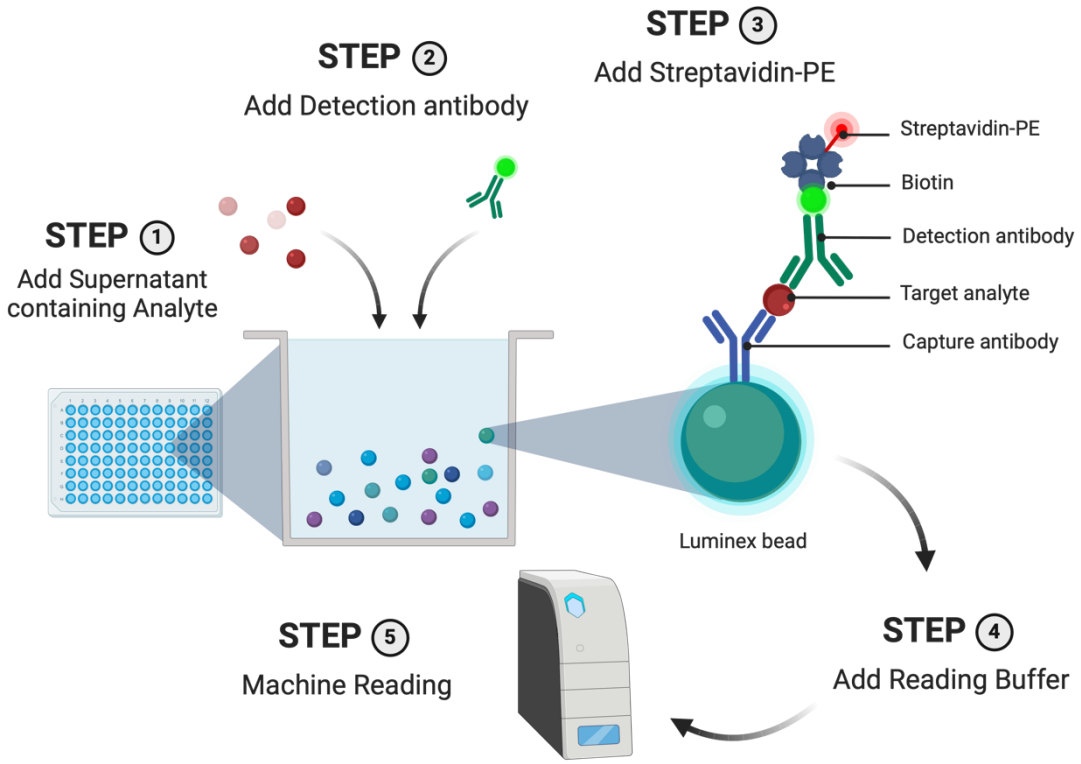

Figure 2-4 Schematic representation of the Multiplex Immunoassay principle and workflow. Magnetic capture beads, each tagged with a distinct red or infrared dye, are coated with monoclonal antibodies specific to an analyte. When the cell culture supernatant is added, the analyte, if present, binds to its corresponding monoclonal antibody. A biotinylated detection antibody, specific to the analyte, is then introduced, forming an immunocomplex (sandwich). Subsequently, fluorescent SA-PE is added to the sample, enabling the quantification of each analyte.

2.2.6 Quantitative Polymerase Chain Reaction (qPCR)

2.2.6.1 RNA extraction

RNA was extracted from cell pellets of the sample, using the Qiagen RNeasy plus mini kit according to the manufacturer's protocols. $5x10^5$ cells were used. All the samples were subjected to DNase treatment to ensure the degradation of genomic DNA. RNA samples were eluted in the RNase-free water (RNeasy® Plus Mini Kit).

2.2.6.2 Nucleic acid quantification

The concentration of extracted RNA was measured using the NanoDrop™ 1000 spectrophotometer. This method relies on the UV absorbance principle, where RNA and DNA exhibit absorption peaks at 260nm due to double conjugated bonds

in their purine and pyrimidine rings, while proteins absorb at 280nm due to tryptophan, tyrosine, and phenylalanine residues. Thus, absorbance at 260 quantifies nucleic acids (RNA and DNA), while absorption at 280nm measures protein content. The purity of RNA and DNA was assessed by the 260/280 absorbance ratio, with a ratio of ≥2 indicating pure RNA and ~1.8 indicating pure DNA. RNA samples were always kept on ice during analysis and stored at -80°C for later use.

2.2.6.3 cDNA synthesis

500ng of total RNA in a 20µL reaction volume was converted into complementary (c)DNA using the High-Capacity cDNA Reverse Transcription kit following the manufacturer's protocol. All reagents were thawed on ice for the cDNA reaction setup, and the reverse transcriptase master mix (RTMM) was prepared according to the manufacturer's instructions on ice as outlined in 2.1.5.4. A total of 6.8µL of the RTMM was added to the reaction, with the remaining 13.2µL to be filled with a mix of dH_2O and RNA. The amount of RNA added was adjusted with dH_2O based on its concentration to achieve the desired final concentration. The tubes were gently vortexed and centrifuged for 10 seconds to eliminate any air bubbles before being placed into a thermal cycler. The reactions were carried out in the thermal cycler with the following conditions: 25°C for 10 mins, 37°C for 2 hours, and 85°C for 5 mins. After completion, the reaction underwent a cooling step and was either immediately used in PCR reactions or stored at -20°C for future use.

2.2.6.4 Quantitative RT-PCR

Quantitative polymerase chain reaction (qPCR) was utilized to amplify specified genes in the given samples, employing two detection methods: SYBR Green and TaqMan. In SYBR Green PCR, which was used in my experiments, the fluorescent dye binds to double-stranded DNA, with fluorescence intensity increasing proportionally to the number of amplifying amplicons. TaqMan PCR utilizes dual-labelled probes, with a fluorophore at the 5' end and a quencher at the 3' end. When the TaqMan probe binds to complementary DNA, Taq Polymerase degrades the probe, releasing the fluorophore. Fluorescent signals were detected using QuantStudio 7 Pro Real-Time PCR. The reaction mixtures were prepared according to outline 2.1.5.3 for SYBR Green PCR, with amplification carried out over 40

cycles. Each sample underwent three technical replicates, and relative expression was determined using the $2^{-\Delta\Delta CT}$ method for all experiments (Livak & Schmittgen, 2001). *ATP* and *TBP* were employed as housekeeping genes for SYBR Green. Melting curve analysis was conducted for new primers to ensure binding to the targeted template. Data was analysed using Microsoft Excel and data was imported into GraphPad for statistical analysis.

2.2.7 Western blot

Western blotting, a technique for analysing proteins, involves isolating and separating proteins by size, transferring them onto a membrane, and detecting specific proteins using antibodies (Figure 2-5).

2.2.7.1 Cell lysate preparation

To prepare cell lysates and quantify proteins, cells were centrifuged at 300g for 5 min at RT, washed twice with 1mL cold PBS, and lysed with radio-immunoprecipitation assay (RIPA) buffer for 30 mins on ice. RIPA buffer constituents are outlined in 2.1.6.2.3. The lysate was then centrifuged at a maximum speed for 10 mins, and the supernatant was stored in -80°C or quantified using a bicinchoninic acid assay (BCA) protein assay.

2.2.7.2 Protein quantification:

The concentration of protein lysates was determined using a (BCA) protein assay kit, following the manufacturer's instructions for the microplate procedure. The absorbance was read at 595nm using a Spectramax M5 plate reader. A standard curve was generated to calculate protein concentrations using Microsoft Excel, with a standard curve concentration range of 125-2000µg/mL. The appropriate amount of protein (40µg) was mixed with SDS loading buffer as outlined in 2.1.6.2.5 and boiled at 70° C for 10 mins. After cooling, the mixture was subjected to sodium dodecyl sulphate-polyacrylamide gel electrophoresis (SDS-PAGE).

2.2.7.3 SDS-PAGE and membrane transfer

Proteins were separated using a 4-12% gel for SDS-PAGE and membrane transfer. The gels used were precast NuPAGE™ Bis-Tris Gels, loaded with samples and a 5µL

protein ladder, and run at 80 volts (V) for 15 mins then at 120V until resolution using NuPAGE™ MOPS SDS Running Buffer. Gels were then transferred onto a nitrocellulose membrane using NuPAGE™ Transfer Buffer and a Blot Module Set, followed by electrophoresis for one and a half hours at 25V.

2.2.7.4 Antibody labelling and detection

All antibody incubation and washing steps were performed on an orbital shaker. All washes were done with TBS-Tween (TBS-T). Ponceau S was used to stain the membrane to assess the efficiency of the transfer before antibody labelling. The membrane was blocked with a blocking solution (2.1.6.2.2) for at least 30 mins at RT. Three times washing of 5mL for 5 mins was applied to the membrane before primary antibody incubation in 5% (w/v) BSA overnight at 4°C. The membrane was then washed three times with 5mL for 5 mins and incubated with the secondary horse radish peroxidase (HRP) antibody in 5% (w/v) BSA for one hour at RT. The list of antibodies is provided in 2.1.6.3. The membrane was then visualised on the 600nm, 700nm, 800nm, and Chemiluminescent channel on the Li-COR Odyssey FC, using 1mL of SuperSignal™ West Pico PLUS Chemiluminescent Substrate for HRP-linked antibody.

Regarding the controls used in Western blotting, all results are normalised to an internal control, such as comparing conditions like CC versus LC, or treated versus untreated samples. The presence of a band at the expected molecular weight across different conditions indicates that the primary antibody is functional, thereby serving as a control for antibody specificity and detection. Additionally, GAPDH is employed as a loading control to assess the relative protein loading and ensure uniform sample input across lanes by comparing band intensities.

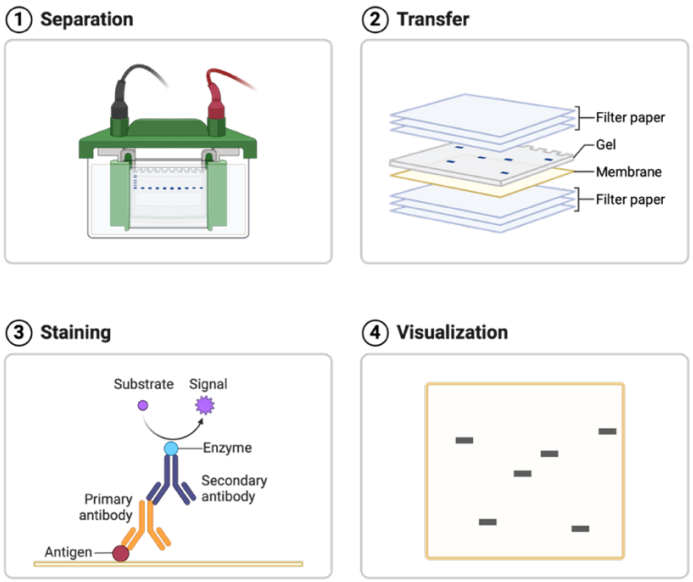

Figure 2-5 Schematic representation of Western blot workflow.

2.2.8 Ethics for human samples

Bone marrow and peripheral blood samples were obtained with written informed consent, following the declaration of Helsinki and with West of Scotland Research Ethics Committee approval (15-WS-0077), from patients or guardians of paediatric patients in the West of Scotland and patients taking part in the MyeChild01 clinical trial within the United Kingdom.

2.2.9 Statistics

2.2.9.1 Data representation and statistical tests.

Unless otherwise specified, data represents mean value +/- standard deviation (SD). For statistical analysis comparing 2 groups, a paired or unpaired, two-tailed, Student's t-test was used. For more than two independent groups, One-way Analysis of Variance (ANOVA) was used to compare the mean of each group to each other. A One-way ANOVA was used for AML cell lines when the same sample was compared in different conditions i.e. LC, CC, and LC/CC +/- Drug. A p-value of <0.05 was considered significant.

2.2.9.2 Normality Testing and Statistical Assumptions

Normality testing was performed only for experiments with five or more replicates, as tests of normality are not considered reliable for smaller sample sizes. For experiments with fewer than five replicates, statistical testing was not preceded by a formal normality assessment. In cases where statistical analysis was conducted without a normality test, data were assumed to follow a normal distribution, and parametric tests were applied based on supporting evidence from the literature for similar experimental designs and biological measurements.

2.2.9.3 Statistical analysis limitations

Some experiments, especially Western blot, showed in the second result chapter, were performed with only one / two replicates (N=1/2). Due to the small sample size, formal statistical testing was not applied, as results from such limited data cannot provide robust significance estimates. These findings should therefore be interpreted with caution, and conclusions drawn from them are considered preliminary. This limitation underscores the importance of conducting additional experiments with larger replicate numbers to confirm and strengthen these observations.

In the ProcartaPlex™ experiments, each condition was intended to include three biological and three technical replicates. However, due to technical errors, some measurements were not successfully captured by the MAGPIX instrument, resulting in only two replicates being available for those data points.

2.2.9.4 Graphs and figures

Graphs and statistical analyses were performed using GraphPad Prism version 10 and R. Biorender.com was used for the generation of schematic figures for this thesis.

3 Result 1: Impact of secreted cytokines within the CC system on AML cell viability

3.1 Introduction

3.1.1 Bone marrow niche supports AML cell survival

HSCs are the primitive cells that lead to the production of all haematopoietic cells. These cells reside in the BM and have different fates, either quiescent in the marrow near the bone trabeculae or self-renewing until fully differentiated and mobilised to the peripheral blood (Morrison & Scadden, 2014). This fate is regulated by a specific microenvironment in the BM, which is called the BM niche.

MSC helps support the AML cells from self- and drug-induced apoptosis by creating a suitable microenvironment (Goulard et al., 2018). This can be achieved by the different secreted cytokines that affect AML proliferation, differentiation, and survival. Inflammatory responses commonly found in the BM niche in different haematological malignancies are a stimulus for malignant clones to produce more subclones by provoking additional mutation in haematopoietic cells. These inflammatory responses are mainly related to cytokines secreted either by the leukaemia-initiating cells or by MSC enabling crosstalk between AML cells and BMME (Zambetti et al., 2016). Table 3-1 shows a group of cytokines that might have a role in AML chemoresistance and relapse. Furthermore, in murine AML, severe remodelling of the BM architecture is related to increased inflammatory stimulus (Duarte et al., 2018). Therefore, novel therapeutic drugs may be developed because of our understanding of the regulation of inflammatory pathways in the AML BMME (Habbel et al., 2020).

Table 3-1 Cytokines hypothesised to have a role in AML chemoresistance

Cytokines	Physiological role	Pathological role in AML
GM-CSF	Haematopoietic growth factor	GM-CSF level in AML patients could indicate a poor prognosis, although the cytokine itself could act as a proapoptotic and antiapoptotic through various mechanism of action (Faderl et al., 2003; A. Kumar et al., 2022).
TNF-α	Pro-inflammatory	It has a role in the onset and progression of leukaemia, moreover, its serum level indicates poor prognosis in AML patients (Tsimberidou et al., 2008; X. Zhou et al., 2017).
IFN-γ	Pro-inflammatory	It has a pivotal role in modulating the BMME to support AML LSC, treatment with IFN-γ lead to chemoresistance (Ciciarello et al., 2019; Corradi et al., 2022; B. Wang et al., 2024).
IL-1β	Pro-inflammatory	Within BM niche, IL-1β increases AML growth and proliferation and inhibits normal marrow expansion (Y. Wang et al., 2020).
IL-2	Promote function of regulatory T-cell	AML patients treated with immunotherapy in post consolidation phase after complete remission would benefit from combining this immunotherapy with IL-2 and histamine dihydrochloride, as leukaemia free survival was improved (Brune, 2006). However, IL-2 receptor alpha (IL-2RA) showed inhibition of AML cell apoptosis and increase of proliferation (Nguyen et al., 2020).
IL-4	Anti-inflammatory	Could be used as therapeutic cytokine as it has antileukemic action on AML through phosphorylation of STAT6 that leads to an

		induction of apoptosis and inhibition of growth and proliferation (Peña-Martínez et al., 2018).
IL-6	Pro-inflammatory	Cause AML chemoresistance through different mechanisms (Hou et al., 2020, 2023; Y. Zhang et al., 2022), and its level could predict AML prognosis (Stevens et al., 2017)
IL-18	Pro-inflammatory	Could be used as a prognostic marker in cases of AML (Saadi et al., 2021; B. Zhang et al., 2002)

3.1.2 IL-6, a component of the BMSC cytokine secretome, has a vital role in providing AML chemoprotection

BMME contains different types of cells. One important cellular component, that is responsible for providing AML cells with protection against chemotherapy, and helping AML cells to grow and proliferate, is MSC (Brenner et al., 2017). The molecular mechanism of how MSC provide chemoprotection is not fully elucidated. There are many molecular mechanisms thought to be involved in chemoresistance (Ahmed et al., 2020; Boutin et al., 2020; Brenner et al., 2017; J. Cheng et al., 2019; Forte et al., 2020; Long et al., 2015). Studies showed that the molecular mechanism of BMSC-mediated chemoresistance is partly related to cytokines secretion; IL-6 is considered one of the main cytokines secreted by BMSC (Kyurkchiev, 2014). Many studies are exploring how IL-6 can increase AML cell viability. STAT3 phosphorylation alters mitochondrial OXPHOS, resulting in AML chemoresistance (Hou et al., 2020). S100A8 and S100A9 molecules, which can modulate some cellular processes, such as cell proliferation and differentiation through fluctuation of intracellular Ca^{++} level (Bresnick et al., 2015), were found to be upregulated in AML cocultured with BMSC through IL-6/JAK-STAT signalling activation (Böttcher et al., 2022). It was found that stromal cell-mediated chemoresistance can occur through not only JAK-STAT signalling upregulation but also PI3K/Akt signalling pathway activated by IL-6 (P. Chen et al., 2016).

3.1.3 Cytokines are present in CC in a higher concentration compared to LC

Previous data from our group found four cytokines present in a high concentration when AML cells of six paediatric samples were cocultured with BMSC isolated from three paediatric AML patients for 72 hours. These cytokines, namely IL-6, VEGF-A, HGF and SDF-1α, are present at a high level in the CC condition compared to LC or BMSC alone. All cytokines show a significant difference between CC and LC. However, IL-6 is the only cytokine showing a significant difference between CC and BMSC alone (Figure 3-1) (Laing et al., 2025).

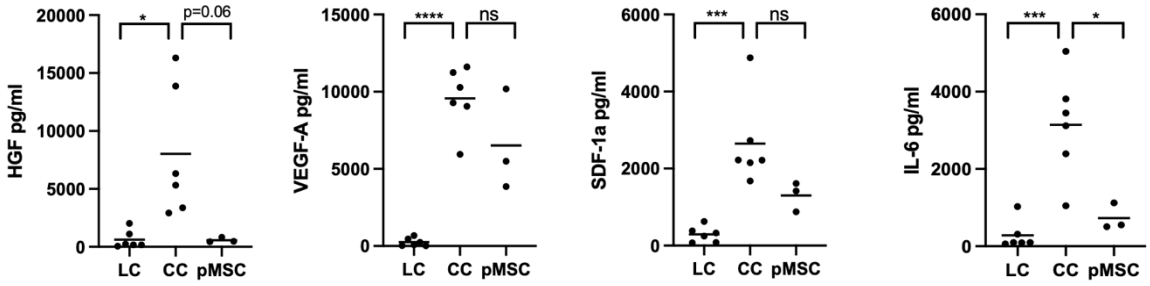

Figure 3-1 Four cytokines are present at significantly higher levels in the CC compared to LC at the 72-hours time point.
Graphs showing the 4 different cytokine concentrations of HGF, VEGF-A, SDF-1α and IL-6 at 72-hours time points for 6 paediatric-AML samples and 3 paediatric-AML BMSC samples. P values were determined using a two-sided unpaired student's t-test (* $p<0.05$, *** $p<0.001$, **** $p<0.0001$). Reproduced with permission from John Wiley & Sons – Books. License number: 1550397-1 (Laing et al., 2025)

3.2 Aims and objectives

Previously, it was shown that cytokine secretion within BMME takes part in providing AML chemoresistance, and our in-house data that there are some cytokines present at a higher concentration in CC compared to LC and BMSC alone. Therefore, the following aims were developed:

1) Confirm the protective effect provided by immortalised stromal cells, HS5 to different AML cell lines;

2) Investigate the pro-survival role of specific cytokines on AML cell viability and proliferation;

3) Screen the cytokines profile using multiplex immunoassay of adult and paediatric immortalised AML cell lines alone or cocultured with immortalised human BMSC.

3.3 Results

3.3.1 Determination of cell sensitivity by EC50 comparison for Ara-C against various human AML cell lines

The half maximal effective concentration (EC_{50}) was calculated for Ara-C in four AML cell lines (Kasumi-1, ME-1, SKNO-1, and THP-1) to determine the concentrations of Ara-C drug treatment to be used in further experiments. EC_{50} was defined as the concentration of drug responsible for a 50% reduction in cell viability in LC. Cells in the log growth phase ($1x10^5$) were added to each well of a 24-well plate in cell line culture media. Using a range of concentrations of Ara-C based on the Genomics of Drug Sensitivity in Cancer (GDSC) website (retrieved June 9, 2024, from https://www.cancerrxgene.org/). Ara-C was added to wells of Kasumi-1, ME-1 and SKNO-1 cells in triplicate in these defined concentrations: 1,10, 100, 250, 500nM); and higher concentrations for the THP-1 cell line, i.e., 1μM, 2μM and 4μM. The cells were treated with Ara-C for 72 hrs, and then an apoptosis assay was performed using Annexin-V/DAPI to provide information about cell viability. Three biological replicates were performed for each AML cell line (Figure 3-2). The EC_{50} was calculated using GraphPad Prism software (version 10).

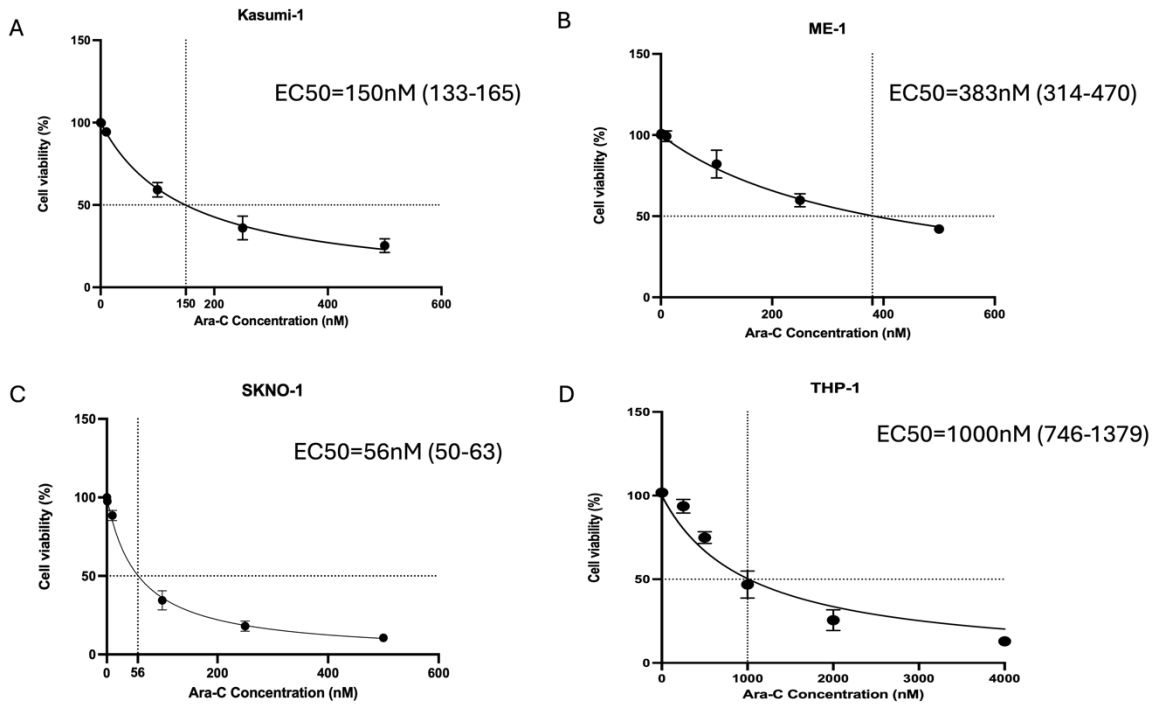

Figure 3-2 Differential sensitivity of AML cell lines to Ara-C.
(A-D) EC_{50} concentrations were calculated for Kasumi-1, ME-1, SKNO-1 and THP-1 AML cell lines using Annexin-V / DAPI apoptosis assay. Cell viability is shown as the mean ± S.D. of three independent experiments n=3.

3.3.2 IL-6 and VEGEF-A increase resistance to Ara-C in the paediatric AML cell line, Kasumi-1

3.3.2.1 IL-6 and VEFG-A maintain cell viability of Kasumi-1 cell line when challenged with Ara-C

The Kasumi-1 cell line, a core binding factor AML cell line, was chosen to investigate the prosurvival role of cytokines previously mentioned. It was selected to represent the paediatric age group. All four cytokines, IL-6, VEGF-A, HGF, and SDF-1α were added to the Kasumi-1 cell line using the following concentrations: IL-6 (10ng/mL), VEGF-A (10ng/mL), SDF-1α (5ng/mL) and HGF (10ng/mL) based on the previous Luminex® data on six paediatric AML samples. Cytokines were added on the same day as cell splitting and Ara-C was added at its EC_{50} concentration determined previously (Figure 3-2) after 24 hours of culture. Apoptosis assays were performed after 48 and 72 hours of adding Ara-C to see how the cell viability changed with and without adding cytokines to the culture.

Adding different cytokines to the Kasumi-1 cell line didn't affect cell viability. However, adding cytokines to the Kasumi-1 cell line with Ara-C resulted in changes in cell viability at both 48 and 72 hours. VEGF-A and IL-6 slightly increased Kasumi-1 cell viability compared to either the other two cytokines, HGF and SDF-1α, or the untreated sample. This difference was seen at both time points. Statistical analysis wasn't done here as this experiment was repeated only twice and acted as preliminary data for further experiments (Figure 3-3).

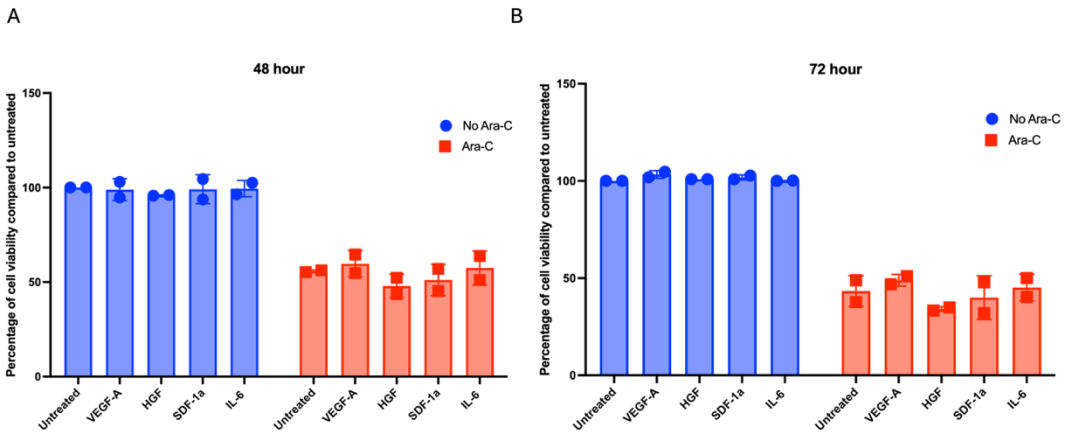

Figure 3-3 Impact of Ara-C and Cytokines on Kasumi-1 Cell Viability Over Time.
Apoptosis assay (Annexin-V / DAPI) in Kasumi-1 cell line with Ara-C at its EC_{50} and IL-6 (10ng/mL), VEGF-A (10ng/mL), HGF (10ng/mL) or of SDF-1α (5ng/mL). (A) 48-hours (B) 72-hours. The bars represent the average of n=2 experiments.

3.3.2.2 IL-6 enhances Kasumi-1 cell survival by inhibiting late apoptosis

IL-6 was chosen for further study. A 72-hours timepoint was used for the next experiment. Here, it was noticed that cell viability didn't differ between AML treated with Ara-C alone compared to Ara-C plus IL-6. Considering the analysis of late apoptosis, it was found that adding IL-6 to Ara-C significantly decreased late apoptosis in the Kasumi-1 cell line (p= 0.0185) (Figure 3-4).

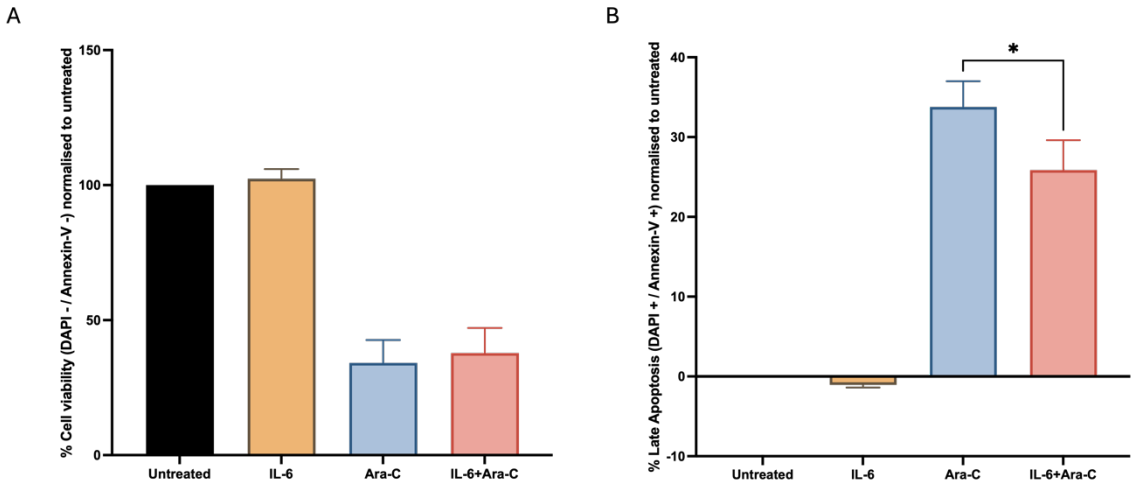

Figure 3-4 Percentage of Kasumi-1 viable and late apoptotic cells after adding IL-6 alone, with Ara-C and with Ara-C and IL-6.
Apoptosis assay (Annexin-V / DAPI) on Kasumi-1 cell line at 72 hours timepoint with and without EC50 Ara-C and 10ng/mL IL-6 normalised to untreated sample. (A) Percentage of cell viability (DAPI - / Annexin-V -) (B) Percentage of late apoptosis (DAPI + / Annexin-V +). Graphs are shown as the mean ± S.D. of three independent experiments n=3. Statistically significant differences were determined, and $*P < 0.05$ is considered statistical significance using one-way ANOVA with Tukey's multiple comparisons test.

3.3.3 HS5 provides chemoprotection for AML cell lines against Ara-C

The previous experiments were done on AML cells cultured alone without showing the role of BMSC. The next experiments were designed to mimic what happens *in vivo* by applying a 2D CC system using the immortalised stromal cell line, HS5, and AML cell lines, Kasumi-1, ME-1, THP-1 and SKNO-1. These AML cell lines were chosen to represent paediatric and adult AML. AML cell line characters are listed in (Table 2-1) in the method section.

The experiment showed that all AML cell lines had increased cell survival when cocultured with HS5 in a ratio of 2:1 (Leukaemia cells: stromal cells) and cultured with Ara-C (at 72 hours EC_{50}), specified for each cell line, for 48 hours. The level

of protection was dependent on the level of significance of the difference between LC and CC. It was noticed that Kasumi-1, ME-1 and THP-1 showed significant differences between LC and CC after adding Ara-C (p=0.004,p=0.006,p=0.008) respectively, however, SKNO-1 didn't show a significant difference in protection from apoptosis between LC and CC after adding Ara-C (p=0.222) (Figure 3-5).

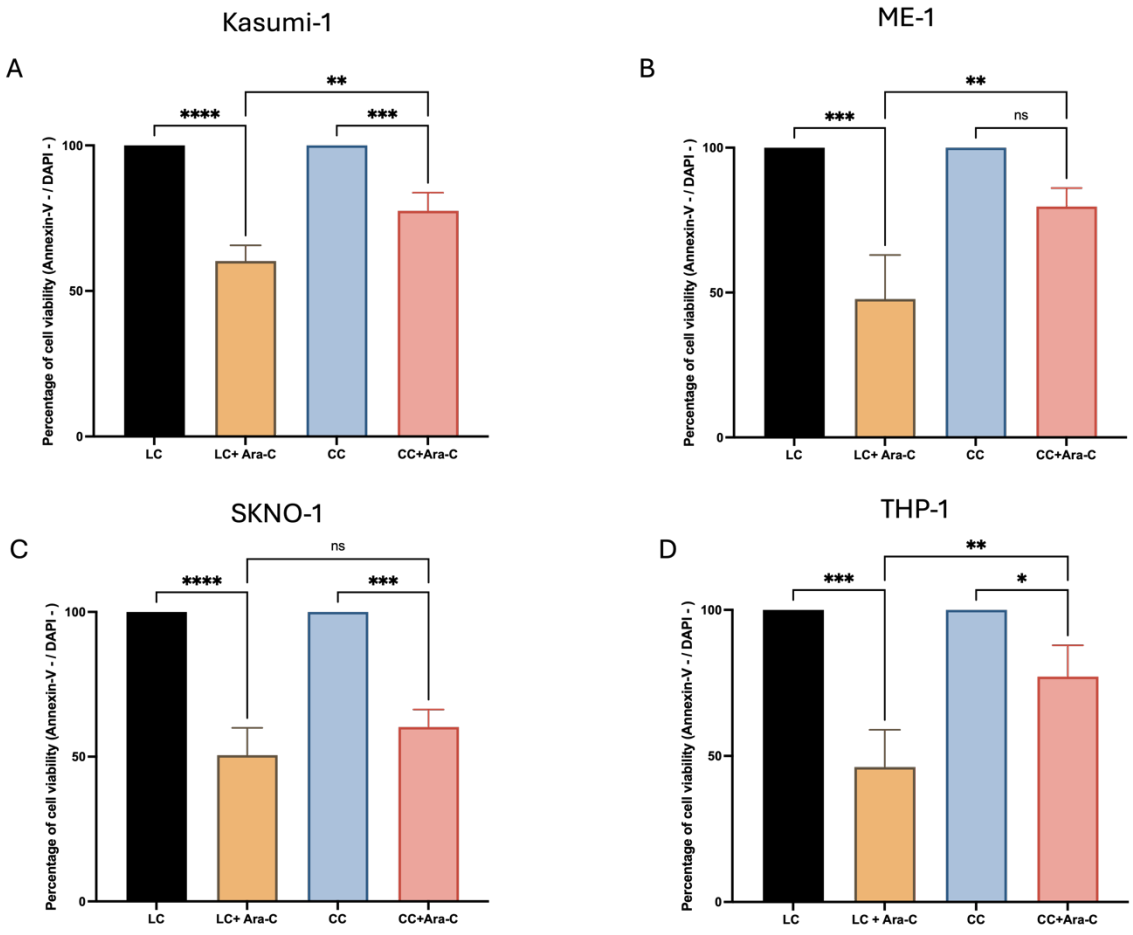

Figure 3-5 ME-1 shows the greatest resistance to Ara-C, while SKNO-1 is the most sensitive among the AML cell lines cultured with HS5.
Apoptosis assay (Annexin-V/DAPI) showing cell viability of AML cell lines in LC and CC with HS5 using EC50 Ara-C (defined for each cell line previously) after 48 hours of exposure compared to no drug control. (A) Kasumi-1 (B) ME-1 (C) SKNO-1 (D) THP-1. All data are for LC plus Ara-C and CC plus Ara-C, normalised to no drug control. Values are plotted as the mean ± S.D. of three independent experiments n=3. *P < 0.05, **P < 0.01, ***P < 0.001 ****P < 0.0001 are considered statistical significance using one-way ANOVA with Tukey's multiple comparisons test.

3.3.4 Defining the cytokine secretome in AML cell lines cocultured with HS5 compared to liquid culture and HS5 alone

3.3.4.1 Nine cytokines present at a high concentration in CC compared to LC

The previous experiments showed that the immortalised stromal cell line HS5 was responsible for stroma-mediated chemoprotection in selected AML cell lines. Moreover, cytokines such as IL-6 provide chemoresistance to the standard chemotherapy agent, Ara-C. So, the next step was to elucidate how the stromal cells provided this chemoprotection and whether this protection was linked solely to cytokines secretion or was mediated through cell-to-cell contact.

To elucidate this, a multiplex immunoassay was performed, which means the ability of the assay to measure multiple analytes simultaneously within one sample. This immunoassay was a Luminex® system, which used bead-based technology that was used to detect 11 cytokines using three AML cell lines that showed significant chemoresistance to Ara-C when cultured with the HS5 cell line. These cell lines were Kasumi-1, ME-1, and THP-1 cell lines. All cell lines were cultured alone (LC), cocultured in direct contact with HS5 (CC (C)), or in indirect contact with HS5 using a transwell for separation between AML cells and HS5 cells (CC (TW)). HS5 cells were also cultured alone for comparison to all cell line conditions; cell culture supernatant was collected after 24 hours from initiating culture.

The eleven cytokines were GM-CSF, TNF-α, IFN-γ, IL-1β, IL-2, IL-4, IL-5, IL-6, IL-12p70, IL-13, and IL-18. Most are proinflammatory cytokines, which we hypothesise have a role in providing chemoresistance (Table 3-1).

Out of the eleven cytokines, nine were detectable by immunoassay, these cytokines were GM-CSF, TNF-α, IFN-γ, IL-1b, IL-2, IL-4, IL-5, IL-6, and IL-18.

A heat map for the nine cytokines was done for the three AML cell lines to show the differences between different culturing conditions regarding cytokine expression (Figure 3-6).

With the Kasumi-1 cell line, CC (C) and CC (TW) conditions showed trends toward increased concentration of all nine cytokines compared to LC. (Figure 3-7)

However, only IL-2 showed a significant increase in concentration in CC (C), CC (TW), and HS5 alone compared to LC ($p=0.0006$, $p=0.0008$, $p=0.0023$, respectively), There was no significant change between CC (C) or CC (TW) and HS5 indicating that there was no supra-additive effect within the CC system and IL-2 was secreted from HS5 (Figure 3-7 E). IL-6 was significantly increased in CC (TW) ($p=0.0277$) compared to LC with no other significant difference noticed among other culturing conditions (Figure 3-7 H). Other than IL-2 and IL-6, there was no significant difference in cytokine concentrations between LC and CC or HS5 (Figure 3-7).

In the ME-1 cell line, five cytokines, (GM-CSF, TNF-α, IL-2, IL-4, and IL-18) were found to be significantly increased in CC (C) compared to LC. Four cytokines, (GM-CSF, TNF-α, IL-2, and IL-4) were increased in both CC (C) and CC (TW) compared to LC. There was no significant difference between LC and HS5 alone with four of them (GM-CSF, TNF-α, IL-4, and IL-18) suggesting there was a supra-additive action within the CC system, and, the increased level of cytokines was not solely related to HS5 secretion (Figure 3-8). For IL-2, there is a significant increase with HS5 alone compared to LC ($p=0.0379$) but the level of significance is less than between LC and CC (C) or CC (TW) ($p=0.0049$, $p=0.0074$) respectively (Figure 3-8 E).

In the THP-1 cell line, all cytokines assessed showed no significant difference between LC and other conditions (CC (C), CC (TW), and HS5) except IL-2 which showed a significant difference between LC and CC (TW) but with no supra-additive effect within the CC system as there was a significant difference between LC and HS5 cultured alone (Figure 3-9 E). However, there was a non-significant trend toward an increase in CC (C) and CC (TW) compared to LC for the rest of the cytokines (Figure 3-9).

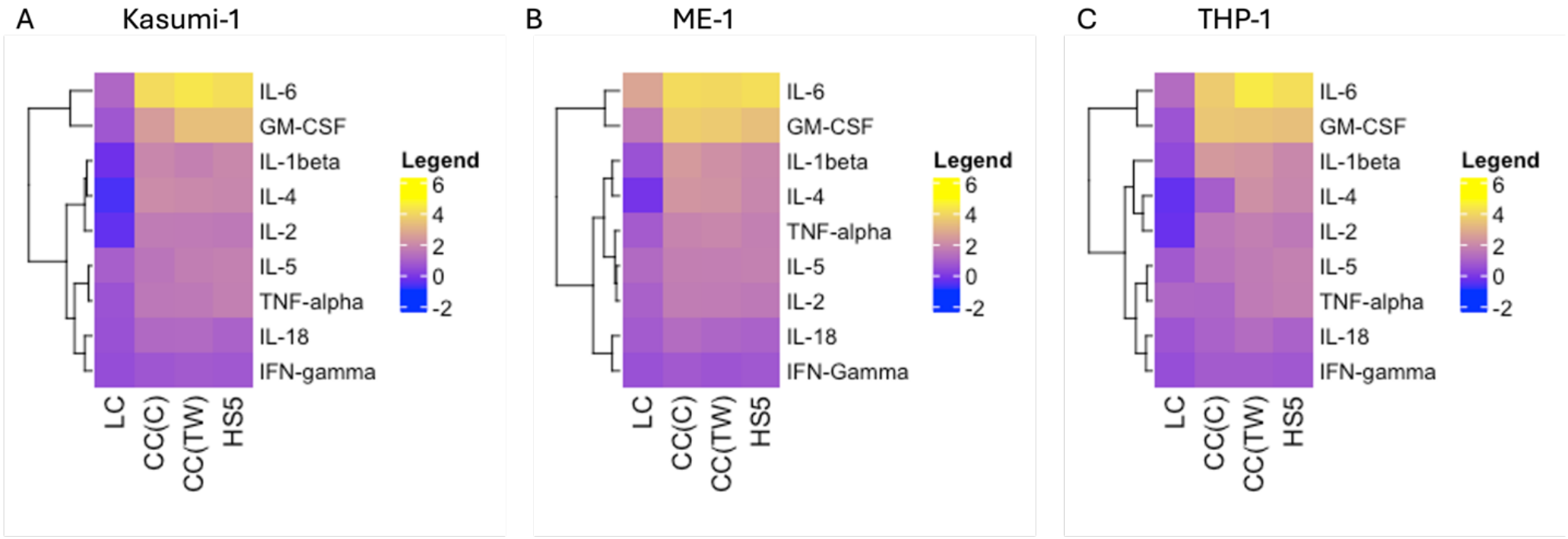

Figure 3-6 Hierarchical clustering analysis of different cytokines expression among AML cell line.
Hierarchical clustering analysis heat map showing log10-transformed concentrations for 9 cytokines (rows) for each culture condition (columns): liquid culture (LC), coculture with direct contact (CC (C)), coculture with indirect contact (CC (TW)), HS5 alone. (A) Kasumi-1 (B) ME-1 (C) THP-1. Values are plotted as the mean of three independent experiments n=3. Log10 was used in the heat map to represent cytokine concentrations as different cytokines have variable levels between cell lines, with HS5 serving as a common reference for comparison across experiments.

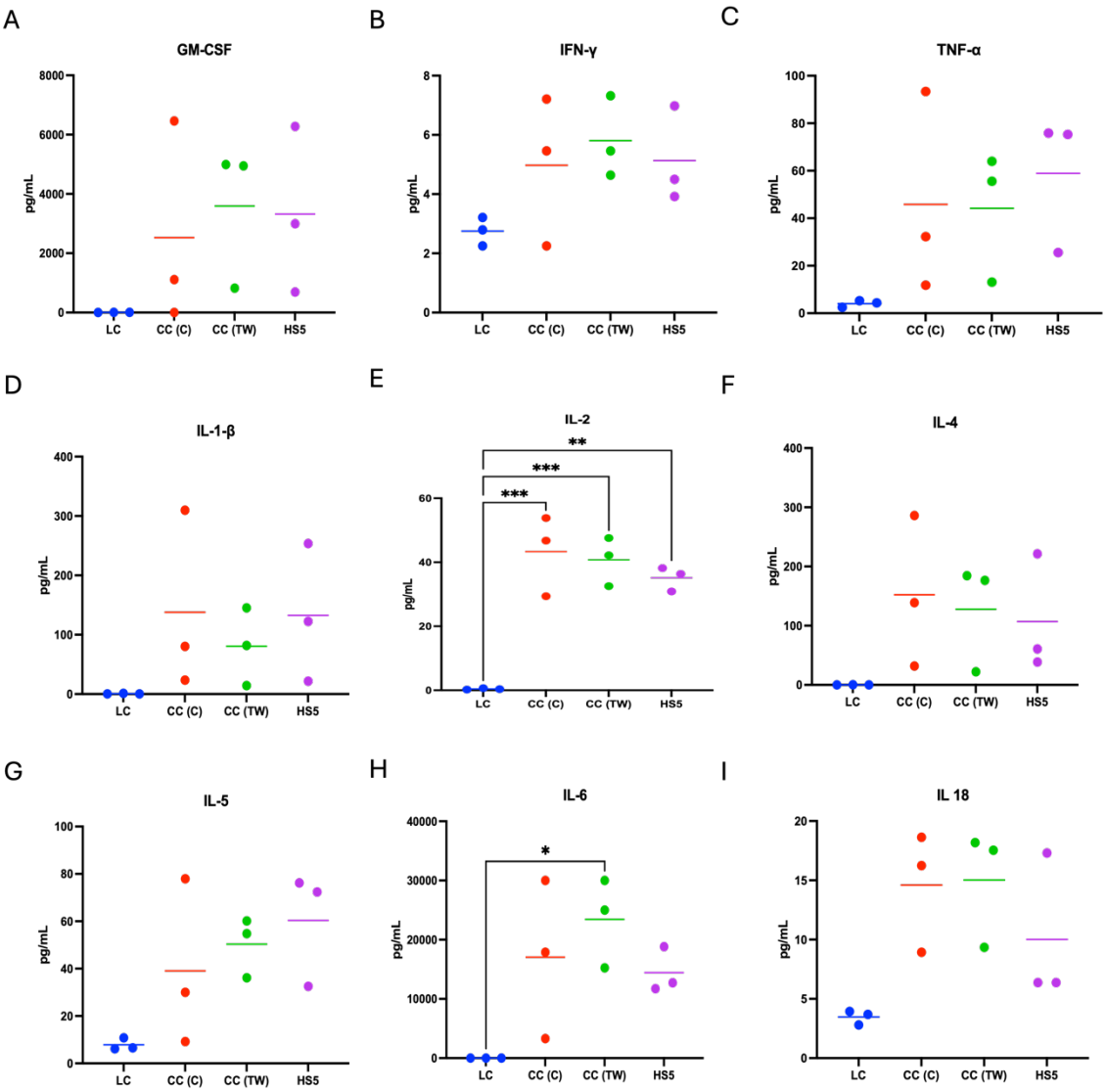

Figure 3-7 Secretome of Kasumi-1 cell line after 24 hours culture in experimental conditions. Variable cytokine concentrations (picograms/mL, pg/mL) in the Kasumi-1 cell line in different culturing conditions LC, CC (C), CC (TW) and HS5 cultured alone using multiplex immunoassay. HS5 is serving as a common reference for comparison across different cell lines. (A) GM-CSF, (B) IFN-γ, (C) TNF-α, (D) IL-1-β, (E) IL-2, (F) IL-4, (G) IL-5, (H) IL-6, (I) IL-18. Values are plotted as the mean of three independent experiments n=3. *$P < 0.05$, **$P < 0.01$, ***$P < 0.001$ are considered statistical significance using one-way ANOVA with Tukey's multiple comparisons test.

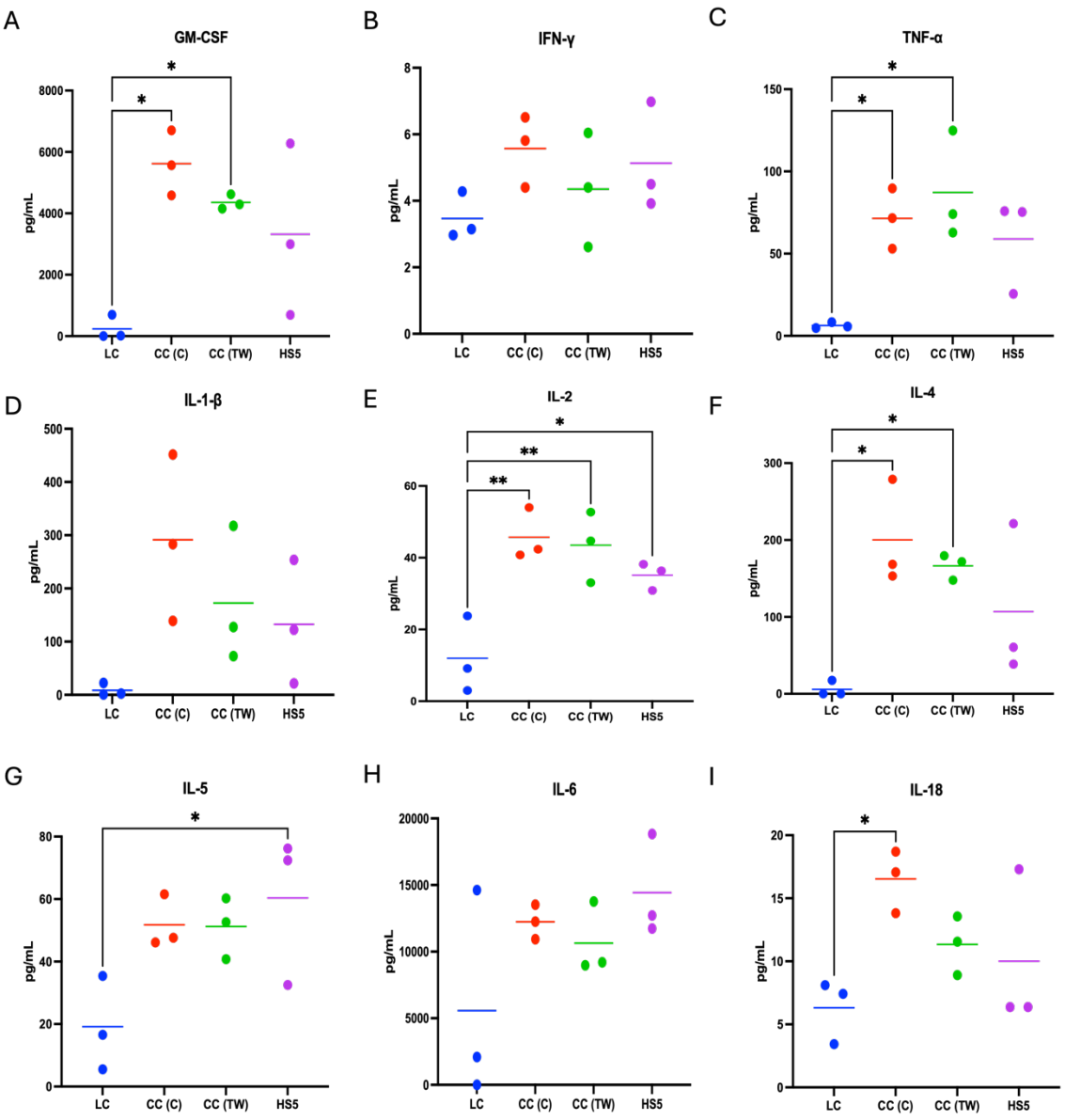

Figure 3-8 Secretome of ME-1 cell line after 24 hours culture in experimental conditions. Variable cytokine concentrations (picograms/mL, pg/mL) in the ME-1 cell line in its different culturing conditions LC, CC (C), CC (TW) and HS5 cultured alone using multiplex immunoassay. HS5 is serving as a common reference for comparison across different cell lines. (A) GM-CSF, (B) IFN-γ, (C) TNF-α, (D) IL-1-β, (E) IL-2, (F) IL-4, (G) IL-5, (H) IL-6, (I) IL-18. Values are plotted as the mean of three independent experiments n=3. *P < 0.05 and **P < 0.01 are considered statistical significance using one-way ANOVA with Tukey's multiple comparisons test.

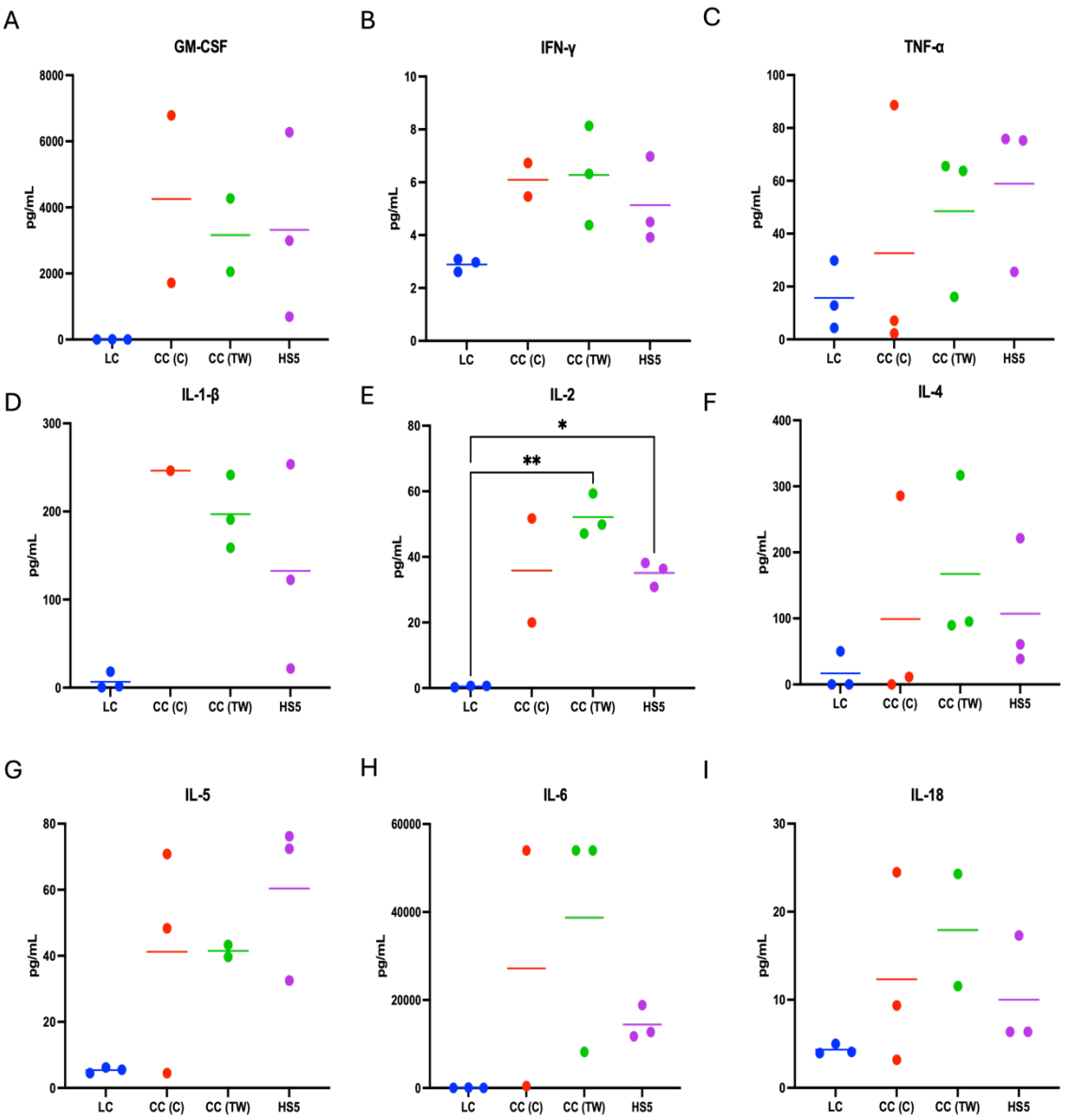

Figure 3-9 Secretome of THP-1 cell line after 24 hours culture in experimental conditions. Variable cytokine concentrations (picograms/mL, pg/mL) in the THP-1 cell line in its different culturing conditions LC, CC (C), CC (TW) and HS5 cultured alone using multiplex immunoassay. HS5 is serving as a common reference for comparison across different cell lines. (A) GM-CSF, (B) IFN-γ, (C) TNF-α, (D) IL-1-β, (E) IL-2, (F) IL-4, (G) IL-5, (H) IL-6, (I) IL-18. Values are plotted as the mean of three independent experiments n=3, although some data points only representing two biological replicates due to technical error leading to inappropriate statistical analysis. *$P < 0.05$ and **$P < 0.01$ are considered statistical significance using one-way ANOVA with Tukey's multiple comparison test.

3.3.4.2 Validation of cytokine difference among culture conditions with confirmation of IL-6 increase in CC compared to LC for the Kasumi-1 cell line

Further screening and validation of the cytokine secretome were performed on three other biological replicates of Kasumi-1, ME-1 and THP-1 cell lines to confirm the previous data showing the increase of some cytokines in the CC system compared to LC. This experiment used seven cytokines; GM-CSF, TNF-α, IL-1b, IL-2, IL-4, IL-6, and IL-18, used during the last experiment.

IFN-γ and IL-5 were omitted in the current experiment, as both cytokines showed an increased concentration within HS5 cultured alone that was higher than when AML cell lines and HS5 were cultured with each other, suggesting that there was no role of CC in secreting both cytokines and that all detected cytokine within the CC system was related to HS5 secretion.

A hierarchical clustering analysis based on cytokine concentration was performed for the three cell lines (

Figure 3-10).

With the Kasumi-1 cell line, GM-CSF, IL-1β, IL-4, and IL-18 showed the same trend of difference among culturing conditions as was noted in the previous experiment (Figure 3-7). However, in this experiment, the trend of difference between conditions changed as HS5 showed a trend to decrease in the concentration of TNF-α compared to the CC system. On the other hand, HS5 showed a trend of an increase in IL-2 concentration compared to other conditions.

In the current experiment, in the Kasumi-1 cell line, although CC (TW) didn't show the same trend of IL-6 increase compared to CC (C) as was noted in the previous experiment, IL-6 concentration showed a significant difference in CC (C) and CC (TW) compared to LC confirming the result seen before. However, both conditions of the CC system didn't show significant differences compared to HS5, suggesting that most of the IL-6 present in the CC system is secreted from HS5 (Figure 3-11; Figure 3-7).

In the ME-1 cell line, unexpectedly, the current experiment didn't confirm the result of the previous one. Moreover, the significant difference found in the first experiment between LC and CC regarding the following cytokines, GM-CSF, TNF-α, IL-2, IL-4, and IL-18, was turned into nonsignificant in the second one.

In the current experiment with the THP-1 cell line, it was noticed that most cytokines showed the same trend of difference among different culturing conditions compared to the previous experiment. However, there was a trend to decrease in IL-2 and IL-6 expression in CC (TW) compared to CC (C) and HS5 compared to the previous experiment.

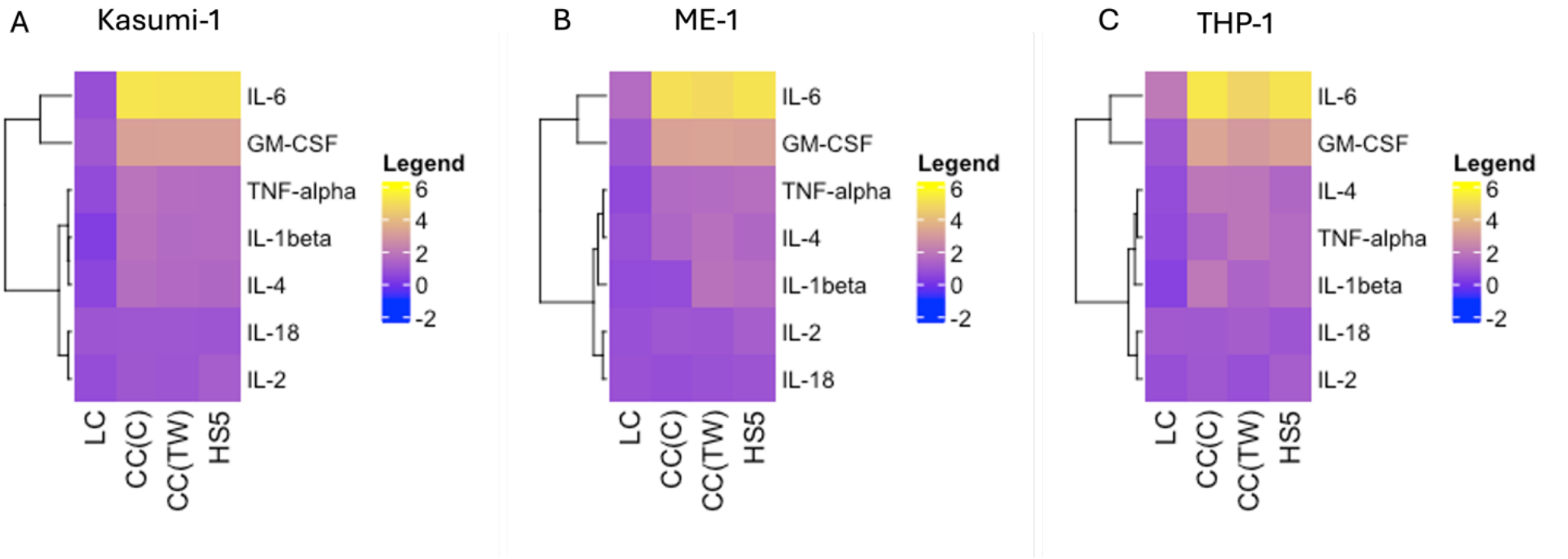

Figure 3-10 Hierarchical clustering analysis of different cytokine expression among AML cell lines.
Hierarchical clustering analysis heat map showing log10-transformed concentrations for seven cytokines (rows) for each culture condition (columns): liquid culture (LC), coculture with direct contact (CC (C)), coculture with indirect contact (CC (TW)), and HS5 alone. (A) Kasumi-1 (B) ME-1 (C) THP-1. Values are plotted as the mean of three independent experiments n=3. Log10 was used in the heat map to represent cytokine concentrations as different cytokines have variable levels between cell lines, with HS5 serving as a common reference for comparison across experiments.

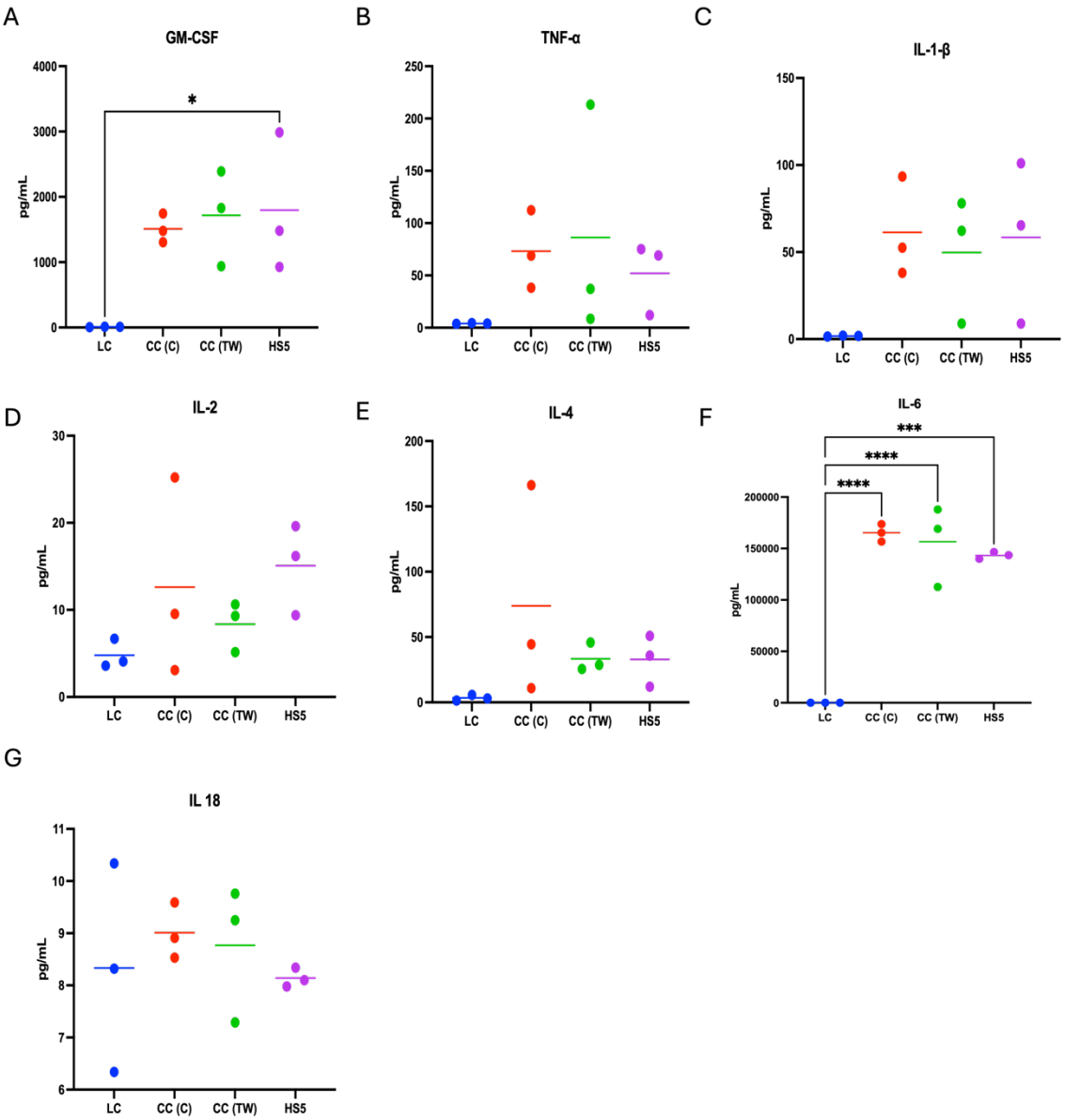

Figure 3-11 Secretome of Kasumi-1 cell line after 24 hours culture in experimental conditions. Various cytokine concentrations (picograms/mL, pg/mL) in the Kasumi-1 cell line in its different culturing conditions LC, CC (C), CC (TW) and HS5 cultured alone using multiplex immunoassay. HS5 is serving as a common reference for comparison across different cell lines. (A) GM-CSF, (B) TNF-α, (C) IL-1-β, (D) IL-2, (E) IL-4, (F) IL-6, (G) IL-18. Values are plotted as the mean of three independent experiments n=3. *P < 0.05, ***P < 0.001 ****P < 0.0001 are considered statistical significance using one-way ANOVA with Tukey's multiple comparisons test.

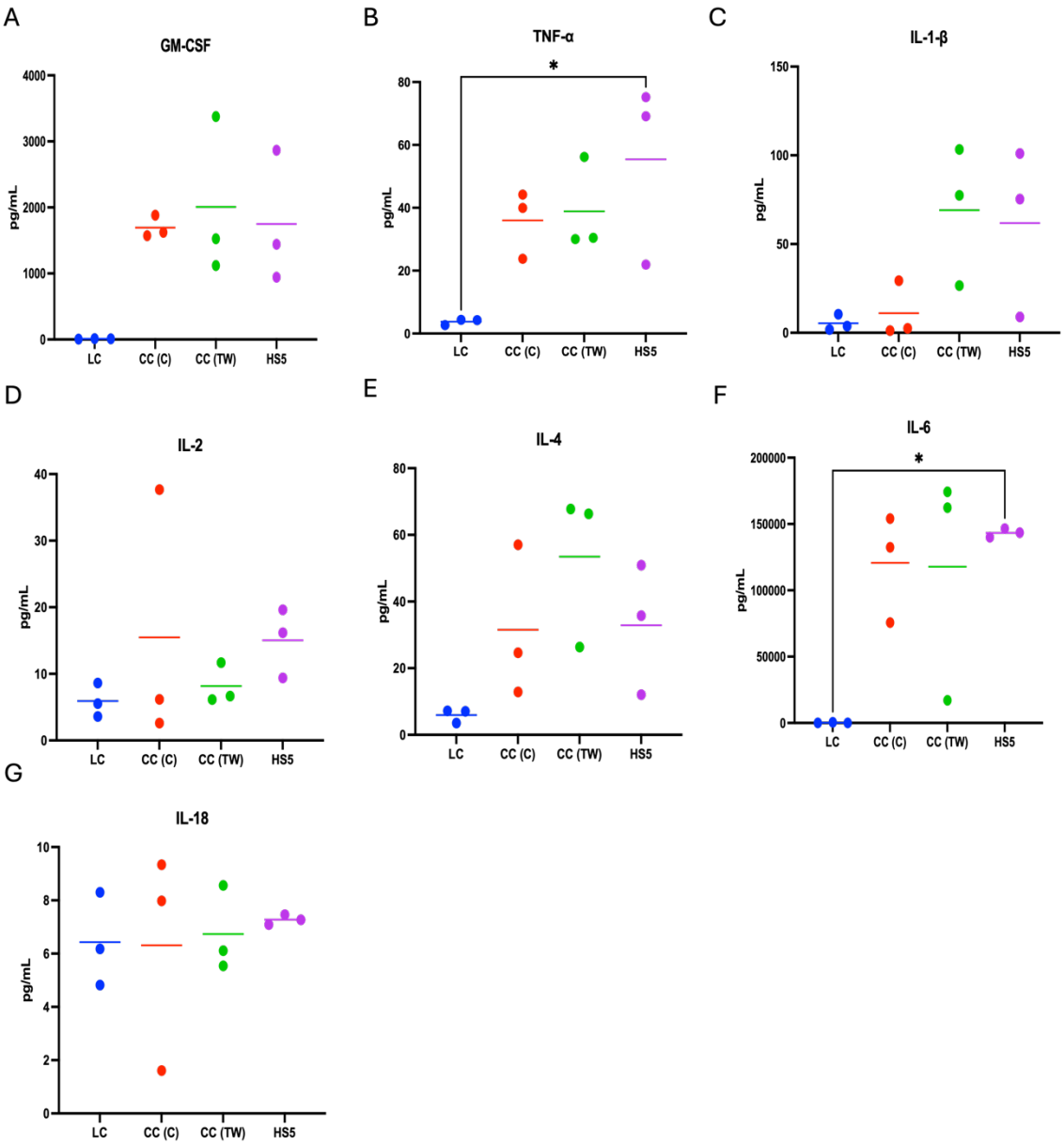

Figure 3-12 Secretome of ME-1 cell line after 24 hours culture in experimental conditions. Various cytokines concentrations (picograms/mL, pg/mL) in the ME-1 cell line in its different culturing conditions LC, CC (C), CC (TW) and HS5 cultured alone using multiplex immunoassay. HS5 is serving as a common reference for comparison across different cell lines. (A) GM-CSF, (B) TNF-α, (C) IL-1-β, (D) IL-2, (E) IL-4, (F) L-6, (G) IL-18. Values are plotted as the mean of three independent experiments n=3. *$P < 0.05$ is considered statistical significance using one-way ANOVA with Tukey's multiple comparisons test.

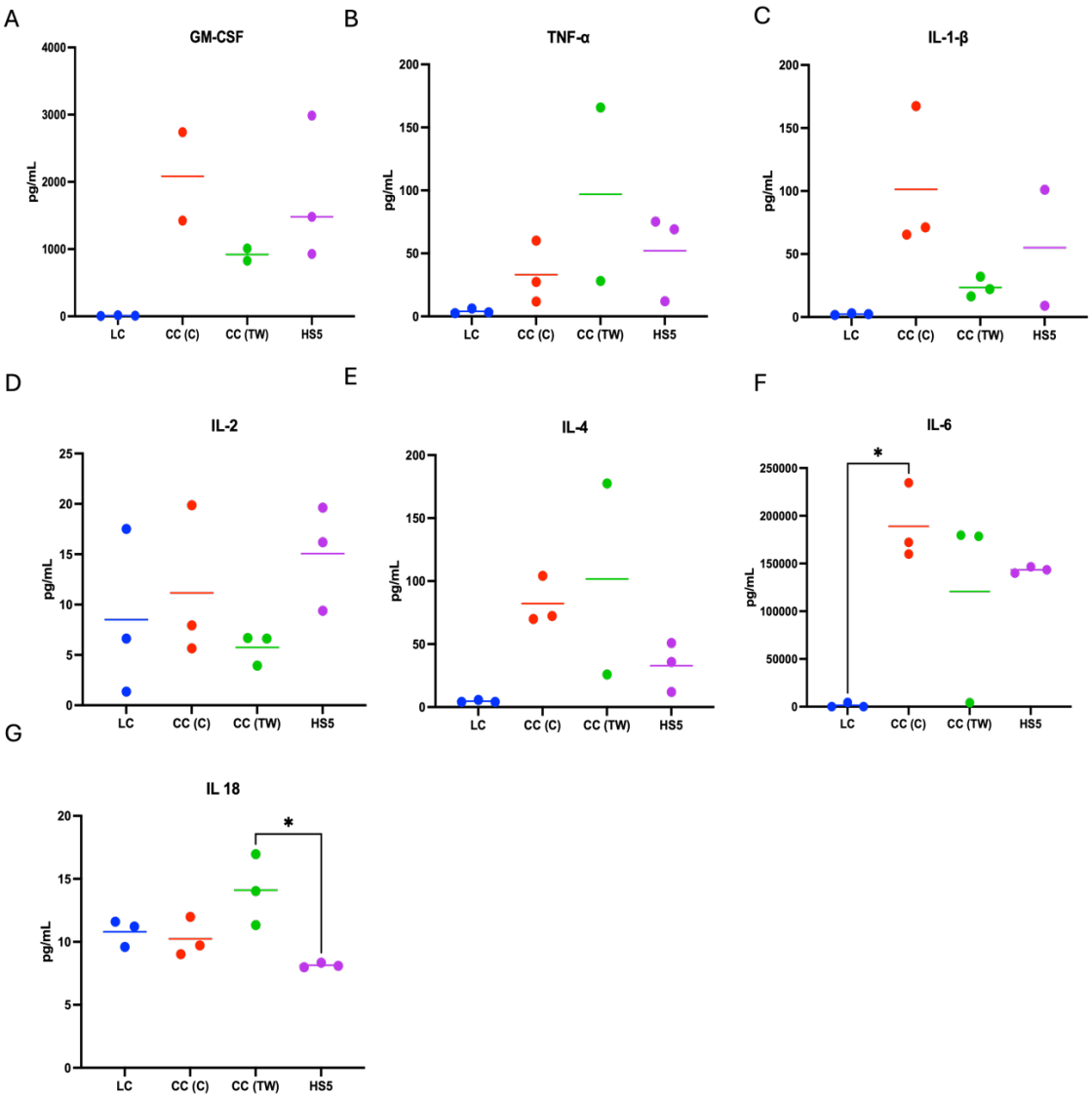

Figure 3-13 Secretome of THP-1 cell line after 24 hours culture in experimental conditions. Various cytokines concentrations (picograms/mL, pg/mL) in the THP-1 cell line in its different culturing conditions LC, CC (C), CC (TW) and HS5 cultured alone using multiplex immunoassay. HS5 is serving as a common reference for comparison across different cell lines. (A) GM-CSF, (B) TNF-α, (C) IL-1-β, (D) IL-2, (E) IL-4, (F) IL-6, (G) IL-18. Values are plotted as the mean of three independent experiments n=3, although in some conditions, only two independent replicates were available because the technical failure of cytokine detection resulted in missing some values. *P < 0.05 is considered statistical significance using one-way ANOVA with Tukey's multiple comparisons test.

3.4 Discussion

In this chapter we aimed to identify the cytokine secretome among different AML cell lines and to study its role in providing chemoresistance against standard chemotherapy. Based on preliminary results from a former PhD student in our lab, it was found that there were four specific cytokines present in a higher concentration within the CC system compared to the LC system with primary paediatric AML samples (Laing et al., 2025). The role of these four cytokines, namely IL-6, VEGF-A, SDF-1α, and HGF, were investigated for provision of AML chemoresistance.

As the previous results were done on primary paediatric samples, the Kasumi-1 cell line, which represents a paediatric core-binding factor AML with t(8;21) was used (Asou et al., 1991). Moreover, Luminex® immunoassay was done on Kasumi-1 cell line supernatants and from two other AML cell lines; ME-1 cell line, an adult core binding factor with inv(16) (p13q22) (Yanagisawa et al., 1991) and THP-1, a paediatric non-core binding factor AML with t(9;11) (Odero et al., 2000; Tsuchiya et al., 1980) to make a comparison of cytokine secretome between adult and paediatric AML cell lines and between AML cell lines with different cytogenetic abnormalities for future research projects.

VEGF-A binds and activates VEGFR-1 and VEGFR-2 to stimulate vascular permeability, angiogenesis, cell migration, and gene expression (Shibuya & Claesson-Welsh, 2006). VEGF and VEGFR have a role in angiogenesis through angiogenic signalling pathways. Researchers found that acute leukaemia cells use these pathways in both autocrine and paracrine modes to support AML cell viability, proliferation and migration (Fragoso et al., 2007). It was noticed that VEGF-A level in the plasma from AML patients was increased compared to normal individuals, who were considered the control group, referring to a prognostic implication for VEGF-A in AML (Aguayo et al., 2002). Adding VEGF-A to the Kasumi-1 cell line culture showed no difference in cell viability using apoptosis assay (Annexin-V / DAPI). However, it minimally supported Kasumi-1 chemoresistance to Ara-C but without statistical significant data, as the experiment was only duplicated (Figure 3-3).

IL-6 is one of a group of cytokines that stimulates the JAK-STAT pathway; it activates STAT3. IL-6 binds to a four-subunit complex, consisting of two gp130 subunits and two receptors (IL-6Rα); these receptors are responsible for JAK2 activation. Activated JAK2 phosphorylates STAT3 at tyrosine 705 (pY-STAT3). After dimerisation of phosphorylated STAT3 proteins, they are translocated to the nucleus to act as a transcription factor, causing regulation of prosurvival gene expression (Calò et al., 2003). STAT3 activation increases cell survival in the presence of cytotoxic chemotherapy at a clinical level (Hayakawa et al., 2013). Increased STAT3 activity has been associated with a low survival rate in many malignancies (Benekli et al., 2002).

Although studies had shown that IL-6 level and IL-6 gene expression were found to be increased in AML patients (Saadi et al., 2021) and had a role in determining the prognosis (Sanchez-Correa et al., 2013; Stevens et al., 2017), adding IL-6 to the Kasumi-1 cell line culture didn't show any difference in increasing cell viability using apoptosis assay (Annexin-V /DAPI). However, adding IL-6 to Kasumi-1 cells in combination with Ara-C minimally increased the percentage of cell survival. Moreover, it significantly decreased late apoptosis (Annexin-V + / DAPI +) compared to adding Ara-C alone without IL-6 (Figure 3-3, Figure 3-4).

Based on these experiments, it was found that IL-6 and VEGF-A did not affect cell viability and had little chemoresistant effect when combined with Ara-C. However, adding HGF and SDF-1α had neither survival nor chemoresistant action on the Kasumi-1 cell line.

One study has previously shown that the human HS5 BM immortalised stromal cell line protected AML cells against self and drug-induced apoptosis (Garrido et al., 2001).

In our lab experiment, the AML cell lines Kasumi-1, ME-1, SKNO-1, and THP-1 all show a degree of HS5-mediated chemoprotection. The way I used to show the chemoprotection is the difference between the LC and CC systems when adding the same Ara-C concentration to both. The other method is to see the effect of adding EC50 Ara-C within the CC system to show that adding EC50 Ara-C, calculated on LC, can't kill 50% of cells in CC. The ME-1 cell line shows the highest degree of HS5-mediated protection. This was manifested as a high level of

significance between LC and LC plus Ara-C (p=0.0002), which reverted to a level of no significance between CC and CC plus Ara-C (p=0.0645). Moreover, there is a statistically significant difference between LC plus Ara-C and CC plus Ara-C (p=0.0063). On the other hand, SKNO-1 showed the lowest chemoprotection, as there was no significant difference between LC and CC when adding Ara-C (p=0.2222) (Figure 3-5).

Applying ProcartaPlex™ immunoassay to the three cell line culture supernatants showed some degree of significance; Kasumi-1, ME-1, and THP-1 cell lines showed different cytokine expression, which may be important to elucidate the role of cytokines in providing AML survival. Our previous work showed only four cytokines present at a high concentration in CC compared to LC, (Laing et al., 2025) and by studying those cytokines, it was found that only IL-6 is the promising cytokine to work on. As a result of our previous work, another group of cytokines was chosen for the ProcartaPlex™ immunoassay to widen our scope of cytokines investigation and try to find other cytokines that might have a role in AML survival. Moreover, our last work on cytokines didn't show the role of cytokines alone, as there was no method of separation between AML cells and BMSC used, So different cultures were explored: AML cells cultured alone in liquid suspension culture (LC), AML cells cultured with stromal cells for 24 hours in direct contact (CC (C)), or AML cells cultured with stromal cells without direct contact through using transwell (CC (TW)), and immortalised stromal cells cultured alone (HS5).

From the heat map, it was found that nine cytokines were detected by multiplex immunoassay across the three AML cell lines. Kasumi-1, ME-1, and THP-1 and across different culturing conditions, LC, LC (C), LC (TW), and HS5. It was shown that IL-6 and GM-CSF were among the cytokines that are highly expressed in all cell lines and across different culturing conditions. IL-6 showed an increase in CC (TW) compared to HS5 and LC in Kasumi-1 and THP-1 cell lines, suggesting the effect of culturing AML cells with BMSC without direct contact on cytokines secretion and whether this would have a role on AML survival. Also, GM-CSF showed an increase in CC conditions compared to LC and HS5 in ME-1 cell line, suggesting the interplay role between AML cells and BMSC. Other cytokines are moderately expressed in all cell lines and across all conditions, with some variation between different culturing conditions.

ProcartaPlex™ immunoassay was done twice on the same cell lines. Between the experiments, unexpectedly, there were some differences in cytokine expression within the cell line itself, referring to the heterogeneity within the cell line among their replicates. Many cell lines were established based on their surface markers and genetic abnormalities. However, with every passage of cells within the cell line, various genetic alterations could accumulate. Although all the cell lines were authenticated before initiating experiments, genomic instability may lead to changes in the activity of the signalling pathway and cytokines working on it (Skopek et al., 2023).

In addition to AML heterogeneity, culturing conditions and technical variability should be taken into consideration, as any small changes in cell density between experiments result in a change in cytokines production (Godoy-Ramirez et al., 2004). Moreover, although the Luminex® immunoassay has the advantages of high sensitivity and multiplexing, technical variability might influence the production of cytokines leading to different changes among different experiments (Rountree et al., 2024).

On the other hand, although cell lines were used instead of primary samples for biological experiments for many reasons, cell lines are still different from the primary samples, which leads to different behaviour resulting in a dramatic change in cytokines secretome (Kaur & Dufour, 2012).

In the Kasumi-1 cell line, IL-1β, IL-6 and IL-18 were the only cytokines that preserved the same expression in both experiments. Of them, IL-6 and IL-18 were found to be present in a higher concentration in the CC system (C and TW) compared to LC and HS5 alone. Moreover, it was noticed that there were some cytokines, IL-1β, IL-2, and IL-4 present at a higher concentration in CC (C) compared to CC (TW) suggesting that there may be a role of direct contact between AML cells and stromal cells in producing these cytokines which might be responsible for stromal-mediated chemoprotection.

In the ME-1 cell line, GM-CSF, IL-1β, and IL-4 preserved the same trend toward an increase in CC (TW) compared to LC and HS5 in both experiments. The level of significance between CC (TW) and LC was lost in the second experiment in these cytokines, as the CC (C) cytokine expression differed between both experiments.

In the THP-1 cell line, there were a lot of missing values due to technical failure in detecting the fluorescence coming from the magnetic beads in the ProcartaPlex™ immunoassay; this technical failure couldn't be explained, but noticed more in the THP-1 cell line resulting in some conditions were represented by only two replicates or even one replicate, leading to no statistical analysis. However, GM-CSF, IL-1β, and IL-6 had consistent expression in both experiments in CC (C). These cytokines were present at a high concentration in CC (C) compared to LC and HS5, suggesting that direct contact with stromal cells might have a role in increasing the production of cytokines.

In conclusion, our results demonstrated that in the Kasumi-1 cell line, IL-6 concentration was increased within the CC system compared to LC and HS5 cultured alone. This result was consistent in all experiments done. Moreover, IL-6 increased late apoptosis when combined with Ara-C referring to its potential role in providing chemoresistance. In the next two chapters, IL-6 will be studied in detail regarding the signalling pathways that IL-6 works through and how could inhibiting the activation of these pathways lead to abolishing chemoresistance.

4 Result 2: Dasatinib minimally abrogates HS5-mediated protection in ME-1 cell line

4.1 Introduction

4.1.1 Heterogeneous response to HS5 mediated chemoresistance in AML cell lines.

It was shown in the previous chapter that HS5 can protect core binding factor paediatric cell line, Kasumi-1 with t(8;21), an adult cell line with inv(16), ME-1, and a non-core binding factor paediatric cell line, THP-1, from the effects of Ara-C. However, HS5 can't protect adolescent core binding factor cell line with t(8;21), SKNO-1 against standard chemotherapy (Table 4-1).

Table 4-1 Impact of HS5 on Ara-C chemosensitivity across AML subtypes

	Kasumi-1	ME-1	SKNO-1	THP-1
Core binding factor	✓	✓	✓	x
Age group	Paediatric	Adult	Adolescent	Paediatric
HS5 protection against Ara-C	✓	✓	X	✓

4.1.2 HS5 secretome is thought to have a role in chemoprotection.

Studies have shown that BM MSC is vital in leukaemogenesis (Blau et al., 2011) and takes part in chemoresistance through the secretion of specific soluble mediators (Kojima et al., 2011).

Using Luminex® technology, the ProcartaPlex™ immunoassay was used to determine the concentration of different cytokines secreted by HS5 and AML cell lines cultured alone (LC) and compared to the CC condition of AML cell line / HS5 together. From 11 cytokines analysed, there were five cytokines (GM-CSF, TNF-α IL-2, IL-6, IL-18) present at a higher level in CC (Direct and transwell) compared to AML LC or HS5 cultured alone in all studied cell lines. There was a statistically significant increase in IL-2 ($p=0.0006$, $n=3$) and IL-6 ($p=0.0277$, $n=3$) from Kasumi-

1 in CC compared to LC. The three other cytokines (GM-CSF, TNF-α IL-18) showed a significant increased level in the CC (C) compared to ME-1 LC and HS5 alone. These results lead us to think about the role of IL-6 in providing chemoresistance in paediatric AML and the chance of targeting either the cytokine or it's signalling pathway.

4.1.3 Non-canonical signalling Pathway of IL-6

Dr Laing (a former PhD student in our Lab) performed RNA sequencing (not published yet) on six samples from paediatric AML patients with different cytogenetic and molecular mutations to show global transcriptome analysis of AML blasts in CC compared to LC.

Regarding IL-6 pathways, GSEA was performed with five gene sets. IL-6-related pathways were found to be significantly enriched in the AML cells from CC compared to LC in four out of the five gene sets, specifically:

1) Reactome IL-6 family signalling
2) Gene Ontology (GO) IL-6-mediated signalling pathway
3) Biocarta IL-6 pathway
4) Brocke apoptosis reversed by IL-6

From the heat map (Figure 4-1) which shows highly enriched genes in the leading-edge subsets in the previous four IL-6-related pathways, it was noticed that Yes-associated protein (YAP) was a significantly upregulated gene in AML blasts from CC compared to LC in GO IL-6-mediated signalling pathway (Laing, 2021). Studying GO IL-6-mediated signalling pathway, it was found that SRC is one of the molecules forming this pathway.

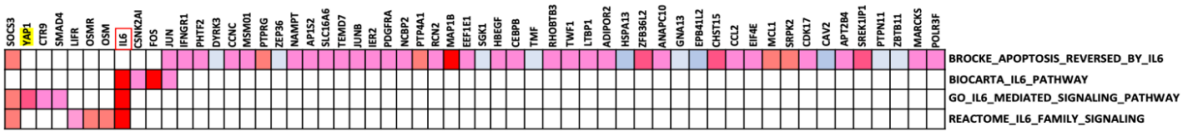

Figure 4-1 Heat map shows highly enriched genes in the leading-edge subsets in the four IL-6-mediated pathways.
(Laing, 2021)

Studies have found that there is another STAT-independent pathway that IL-6 is involved in. Upon binding of IL-6 to its receptor and gp130, a co-receptor for IL-

6, this binding complex, in addition to stimulating JAK-STAT, stimulates SFK which include nine members of non-receptor tyrosine kinases, SRC, FYN, YES, LCK, HCK, BLK, FGR, LYN, and YRK. SRC and YES activate YAP and the transcriptional coactivator with PDZ-binding motif (TAZ). YAP and TAZ are hippo signalling pathway members and transcription co-activators, kept inactive in the cytoplasm until activation. This activation would be through direct phosphorylation of YAP tyrosine residue (Y357) or Hippo signalling inhibition through YAP Serine phosphorylation (S127). Once activated, YAP will enter the nucleus and bind to transcription factors as Transcriptional Enhanced Associate Domain (TEAD) to control downstream target genes like Connective Tissue Growth Factor (*CTGF*), cysteine-rich angiogenic inducer 61(*CYR61*), and Cellular Communication Network Factor 1 (*CCN1*) which are responsible for tissue growth, proliferation, migration, invasion, and cell survival (Figure 4-2) (Azar et al., 2020).

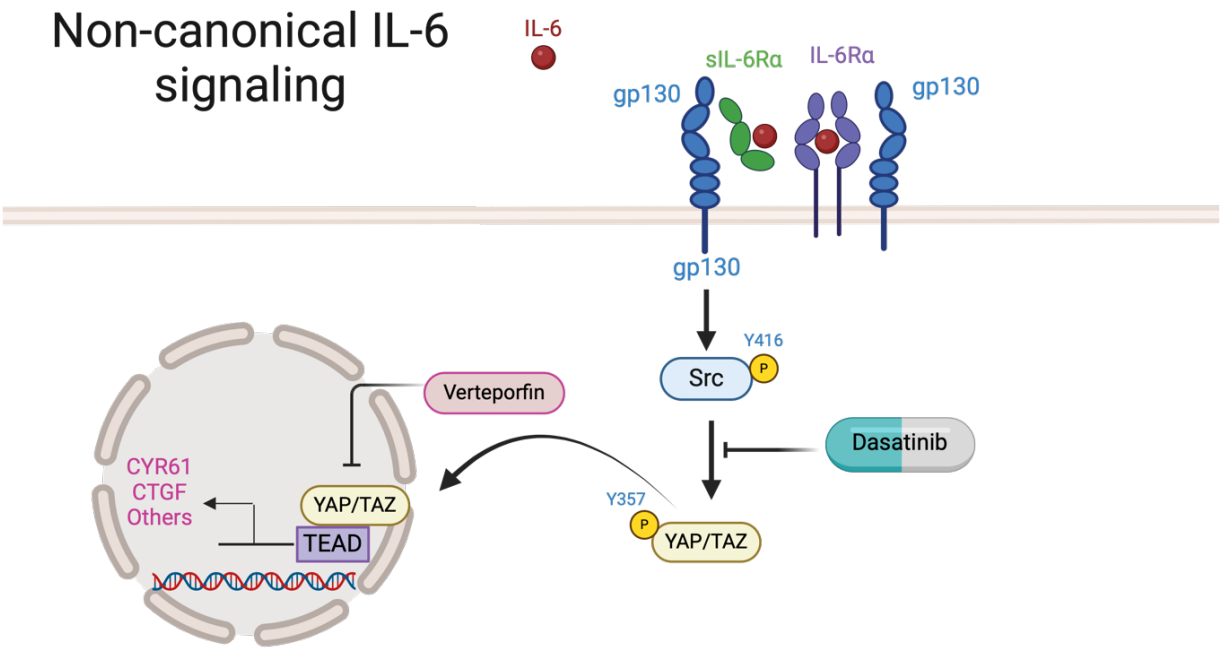

Figure 4-2 Schematic figure showing the noncanonical IL-6 signalling pathway.
IL-6/IL-6R/gp130 complex stimulates the SRC/YAP/CYR61 signalling pathway. Dasatinib (BMS-354825) is an SRC/ABL tyrosine kinase inhibitor, that inhibits YES (SRC member) from activating YAP. Verteporfin, a photosensitizer, is used as an inhibitor of the interaction of YAP with TEAD, which, in turn, blocks transcriptional activation of targets downstream of YAP as *CYR61* and *CTGF.*

4.2 Aims and Objectives

We have shown in our previous result chapter, that IL-6 as well as CC with HS5 provide chemoprotection against standard chemotherapy. Moreover, the ProcartaPlex™ immunoassay showed an increased IL-6 concentration in CC supernatant compared to LC. Depending on the IL-6 mediated pathway, that was shown to be enriched in AML blast CC compared to LC, and the fact that IL-6 has a non-canonical pathway stimulating the SRC/YAP signalling pathway, inhibiting this pathway may additively affect the abolition of chemoprotection-induced CC. Therefore, the following aims were developed to investigate the SRC/YAP signalling pathway:

1) Investigate SRC signalling gene expression in LC and CC to see if CC has a role in gene expression changes;

2) Investigate protein expression of different genes involved in the SRC signalling pathway and see if it differs between LC and CC;

3) Determine the dasatinib concentration that can be used for SRC inhibition in further experiments;

4) Investigate the effect of dasatinib on the inhibition of SRC phosphorylation and whether this inhibition affects cell viability, cell proliferation, cell cycle, and apoptosis in AML cell line.

4.3 Results

4.3.1 Investigation of SRC/YAP signalling in CC compared to LC in different AML cell lines

4.3.1.1 CC changes gene expression in the SRC signalling pathway.

From the results of the investigation as to which cell lines are protected against Ara-C when cocultured with HS5, two cell lines that HS5 could protect against chemotherapy were chosen; one represents paediatric, (Kasumi-1 cell line) and one represents adult AML (ME-1 cell line). Also, another protected cell line (THP-1 cell line) to represent a paediatric non-core binding factor was used for comparison.

From the SRC signalling pathway that IL-6 is activating, three different genes were chosen to study; *SRC* as this is an upstream kinase that should be stimulated by IL-6/gp130 complex, *YAP* as 'midstream' pathway that is activated because of SRC activation, and *CYR61*, a downstream pathway and one of the final target genes that affect cell survival and proliferation.

The RT-qPCR (Figure 4-3) analysis was performed on the three genes selected and on the three different cell lines in LC and CC to see if CC affected gene expression. The results showed that CC was able to upregulate the *SRC* gene in all cell lines examined with a significant increase in CC on the ME-1 cell line ($p=0.0082$, $n=5$) (Figure 4-3, B and D). Regarding the midstream pathway gene (*YAP*), Kasumi-1 didn't show any expression either in LC or CC (Figure 4-3, A and E) and only very low expression in ME-1 was observed (Figure 4-3 B and E), however, it is overexpressed in CC in THP-1 but with no significant difference between LC and CC (Figure 4-3 C and E). Moreover, *CYR61* (the target gene and one of the downstream genes in the pathway) showed over-expression in the core binding factor cell lines (Kasumi-1 and ME-1 without showing a significant difference between LC and CC Figure 4-3, A, B and F). However, *CYR61* didn't show expression difference between LC and CC in THP-1 cell line. Figure 4-3 C and F).

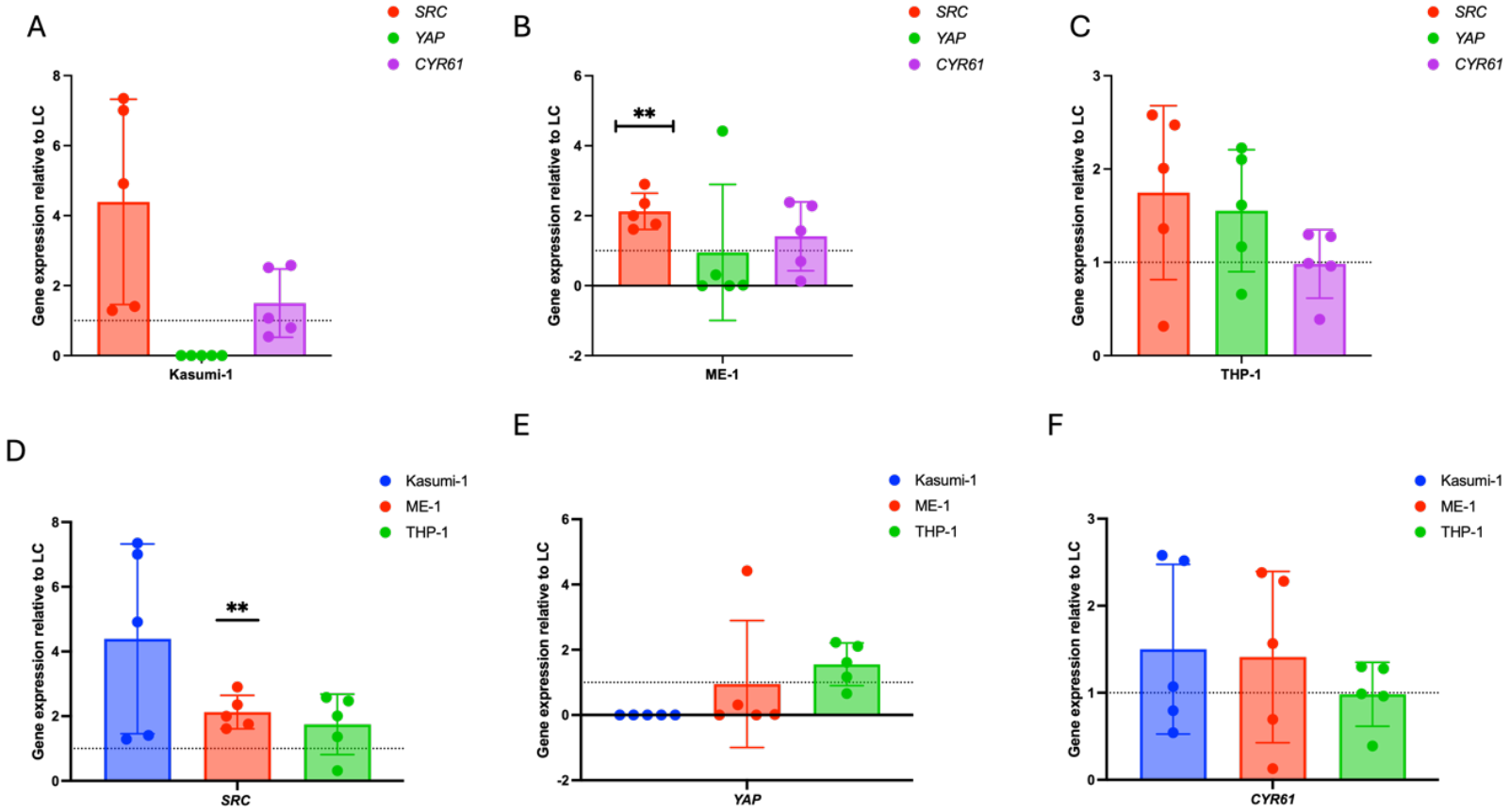

Figure 4-3 SRC signalling pathway genes expression in CC (Using Transwell) normalised to LC in different AML cell lines.
(A) Relative mRNA expression of *SRC*, *YAP*, and *CYR61* in Kasumi-1 cell line detected by RT-qPCR after 24 hours of culture. (B) ME-1 cell line (C) THP-1 cell line. (D) Relative mRNA expression of the *SRC* gene in Kasumi-1, ME-1 and THP-1. (E) *YAP*. (F) *CYR61*. * (A, B, C) are the same data as (D, E, F). All data are for CC normalised to LC, which is scaled to 1 for each gene. Graphs are shown as the mean ± S.D. of five independent experiments, n=5. Statistically significant differences were determined by a paired t-test. ** $p<0.01$.

4.3.1.2 Protein expression differs between LC and CC amongst AML cell lines.

Western blot analysis was performed on the same cell lines and culture conditions assessed for gene expression to show whether the difference in gene expression would be translated and manifested at a protein level. Phospho-SRC (Y416), total SRC, YAP and CYR61 were evaluated on LC and CC (using transwell insert) after 24-hours incubation. Three different cell lines (Kasumi-1, ME-1 and THP-1) were examined. Autophosphorylation of SRC protein showed lower expression in CC compared to LC in all cell lines examined without significant differences between the cell lines. However, total SRC showed significantly higher expression in CC for ME-1($p=0.0001$, $n=3$) (Figure 4-4 B, E) and THP-1 ($p=0.0013$, $n=3$) (Figure 4-4 C, F) cell lines, it demonstrated a non-significant trend to lower expression in Kasumi-1 in CC (Figure 4-4 A, D).

Regarding YAP, a midstream protein in the SRC signalling pathway, it was not expressed in either Kasumi-1 or ME-1 cell lines (Figure 4-4 A, B, D, F) but showed minimal expression in THP-1(Figure 4-4 C, F) with a significantly higher expression in CC than LC ($p=0.0069$, $n=3$). CYR61 protein didn't show expression in Kasumi-1(Figure 4-4 A, D) but did show higher expression in ME-1 CC compared to LC (Figure 4-4 B, E) and lower expression in THP-1 CC compared to LC without any significant difference between the two conditions (Figure 4-4 C, F).

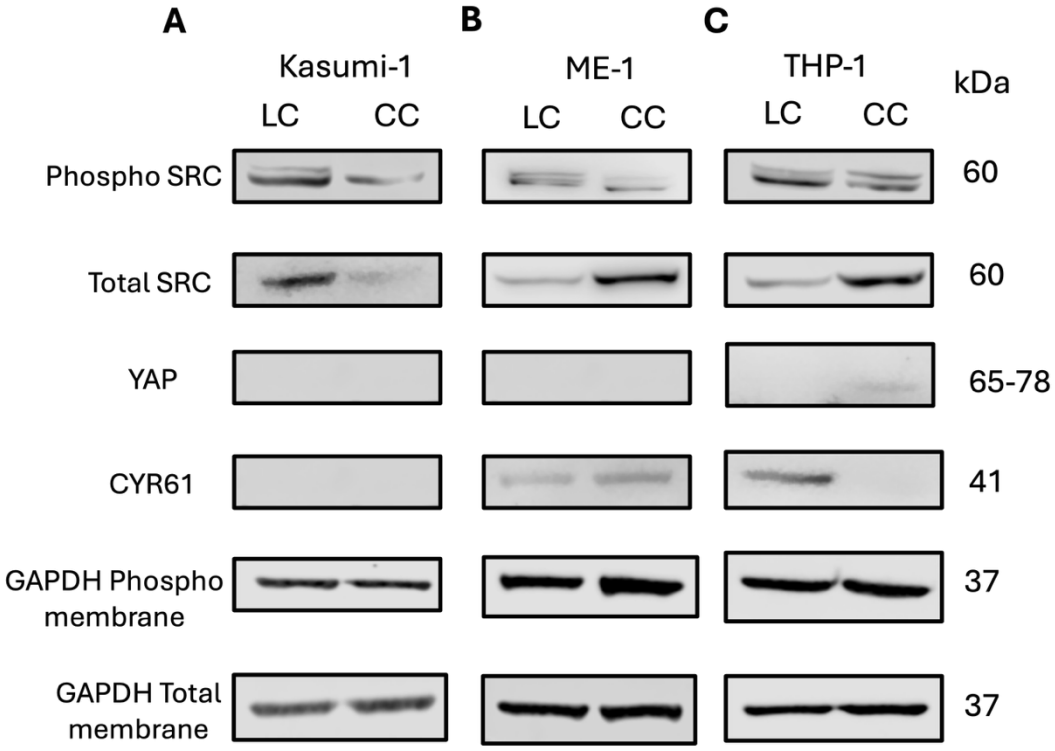
A
B
C
Kasumi-1
ME-1
THP-1
LC
CC
LC
CC
LC
CC
kDa
Phospho SRC
Total SRC
YAP
CYR61
GAPDH Phospho membrane
GAPDH Total membrane
60
60
65-78
41
37
37

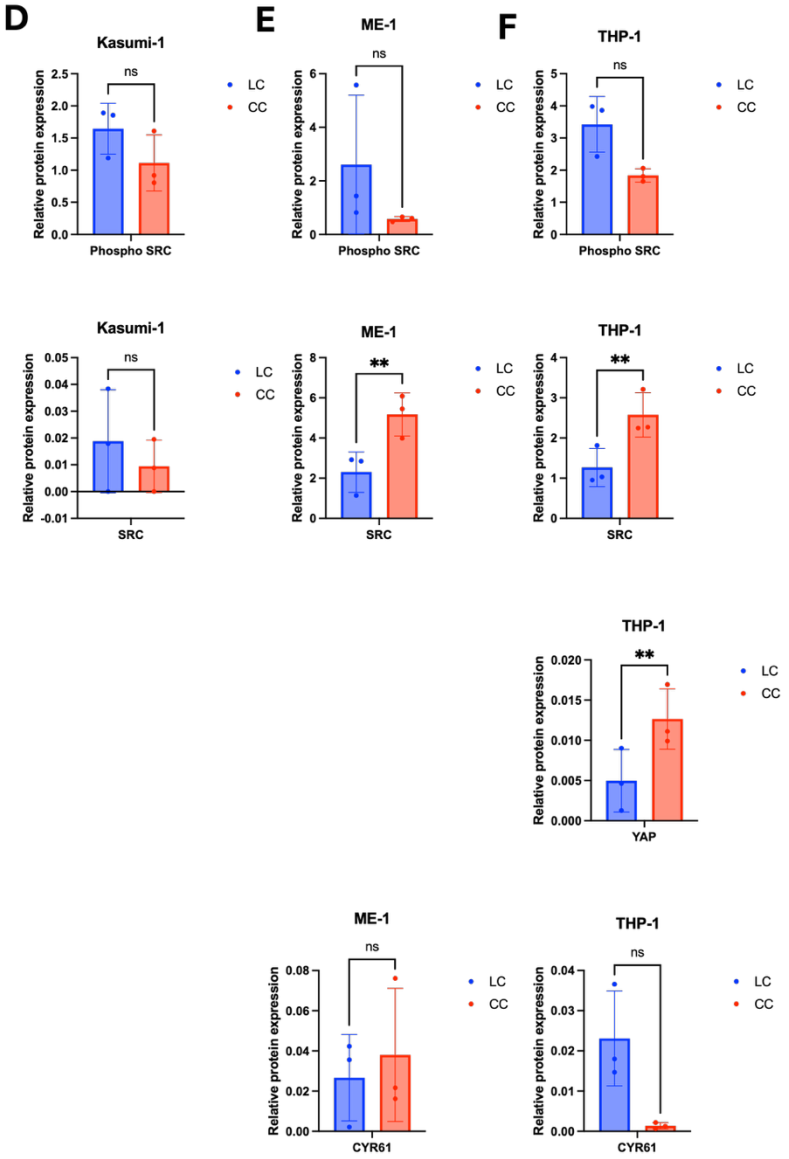
D
E
F
Kasumi-1
ME-1
THP-1
ns
**
Relative protein expression
Phospho SRC
SRC
YAP
CYR61
LC
CC

Figure 4-4 SRC signalling pathway protein expression in LC and CC (Using Transwell) in different AML cell lines.
(A, D) Western blotting analysis of relative protein expression of SRC (Phospho SRC Y416 and total SRC), YAP, and CYR61 in Kasumi-1. (B, E) ME-1. (C, F) THP-1. Densitometry was calculated relative to the corresponding GAPDH. Each bar represents the mean ± SD of three independent experiments n=3, and statistically significant differences were determined by paired t-test. ** $p<0.01$. All antibodies, Phospho-SRC, YAP, CYR61 are blotted on one membrane, and total SRC was blotted on another membrane. Representatives immunoblot images are shown. For Kasumi-1, phospho-SRC and its corresponding GAPDH were taken from replicate 1, while total SRC and its GAPDH were taken from replicate 2. For ME-1, phospho-SRC, CYR61, and their GAPDH were taken from replicate 3, while total SRC and its GAPDH were taken from replicate 1. For THP-1, all panels were taken from replicate 2. Full blots from three independent biological replicates are provided in the Appendix (Figure 6-1- Figure 6-5).

4.3.2 Dasatinib inhibits autophosphorylation of SRC in ME-1 cell line

Based on the result of *SRC* gene expression and total SRC protein expression in the ME-1 cell line which shows a significant increase in CC compared to LC, the ME-1 cell line was chosen for further experiments. The concentration-response relationship of dasatinib is critical for determining its optimal therapeutic window, balancing efficacy with potential toxicity. Based on previous studies, different dasatinib concentrations were chosen to be examined for autophosphorylation inhibition of SRC tyrosine kinase. Cells were treated for 30 mins with dasatinib in the following concentrations (1,5,10,50,100,500nM) and phospho SRC was analysed. It was shown that all concentrations were able to inhibit the autophosphorylation of SRC and 1nM could be used for further experiments as SRC inhibitor (Figure 4-5).

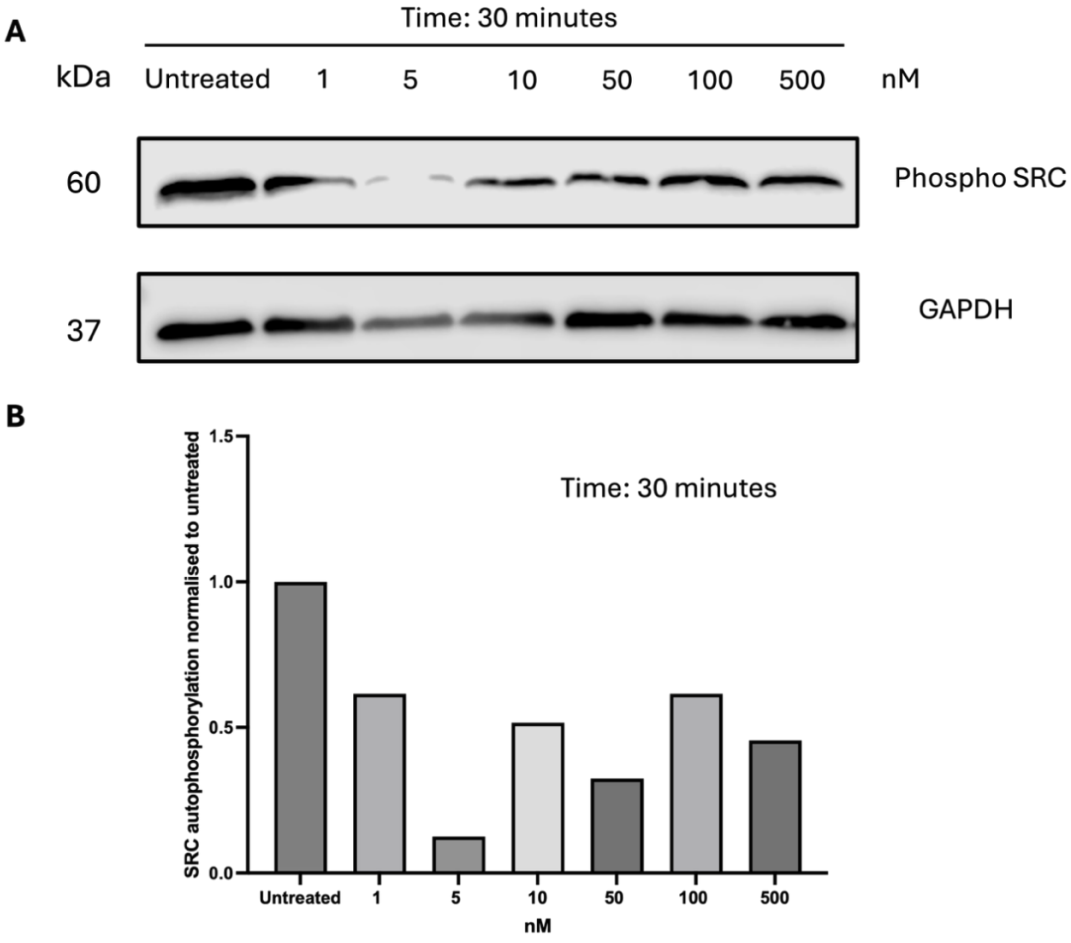

Figure 4-5 Dasatinib inhibits SRC autophosphorylation in the ME-1 cell line.
ME-1 cell line was treated with different concentrations of dasatinib (1,5,10,50,100,500nM) for 30 mins, (A) Western blot bands of phospho SRC (Y416), all data were normalised to GAPDH. (B) The graph shows autophosphorylation of SRC normalised to the untreated sample. n=1. Full membrane is shown in the Appendix Figure 6-9

A time course experiment was done to find the optimum time for dasatinib to work using the previously determined concentration (1nM), a range of short-term time points was examined (5,10,15,30 mins). SRC autophosphorylation was determined using western blot analysis. It was shown that dasatinib can inhibit SRC autophosphorylation at an earlier time (5 mins) and reach its maximum inhibitory effect at 30 mins (Figure 4-6). Other time points, up to 24 hours, were examined to determine how long this inhibitory effect lasts.

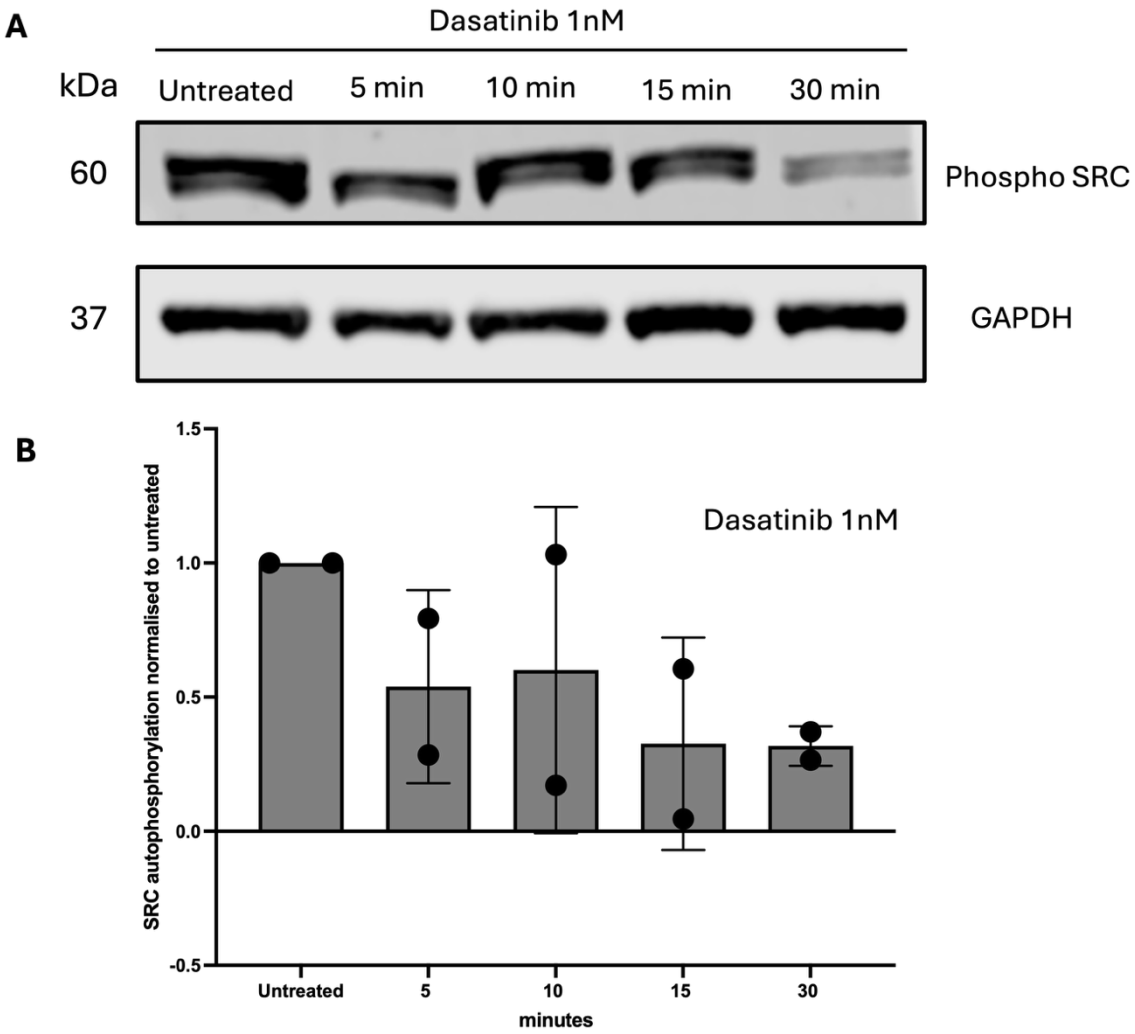

Figure 4-6 Dasatinib inhibits SRC autophosphorylation in ME-1 cell line across different time points.
ME-1 cell line was treated with 1nM of dasatinib for different time points (5, 10, 15, and 30 mins) (A) Western blot bands of phospho SRC (Y416), all data were normalised to GAPDH then to untreated. (B) graph shows autophosphorylation of SRC normalised to untreated sample. n=2. Full membrane is shown in the Appendix (**Figure 6-6**).

Timepoint analysis reveals that dasatinib inhibitory effects on SRC phosphorylation and downstream signalling pathways occur rapidly, starting at 5 mins and sustained for one hour after applying the drug. This inhibitory effect disappears after one hour of drug administration (Figure 4-7). It was noticed that the

housekeeping protein used in this experiment (GAPDH) was decreasing over time, this might be related to the biological effect of dasatinib or technical error caused by loading inconsistencies. Dasatinib is a tyrosine kinase inhibitor and can influence various cellular processes including metabolism, GAPDH is a key enzyme of glycolysis and its expression can be influenced by changes in metabolic states. So, dasatinib may be affecting the metabolic state of the cells, leading to a reduction in GAPDH levels over time. To confirm this explanation, other housekeeping proteins could be used like β-actin or tubulin.

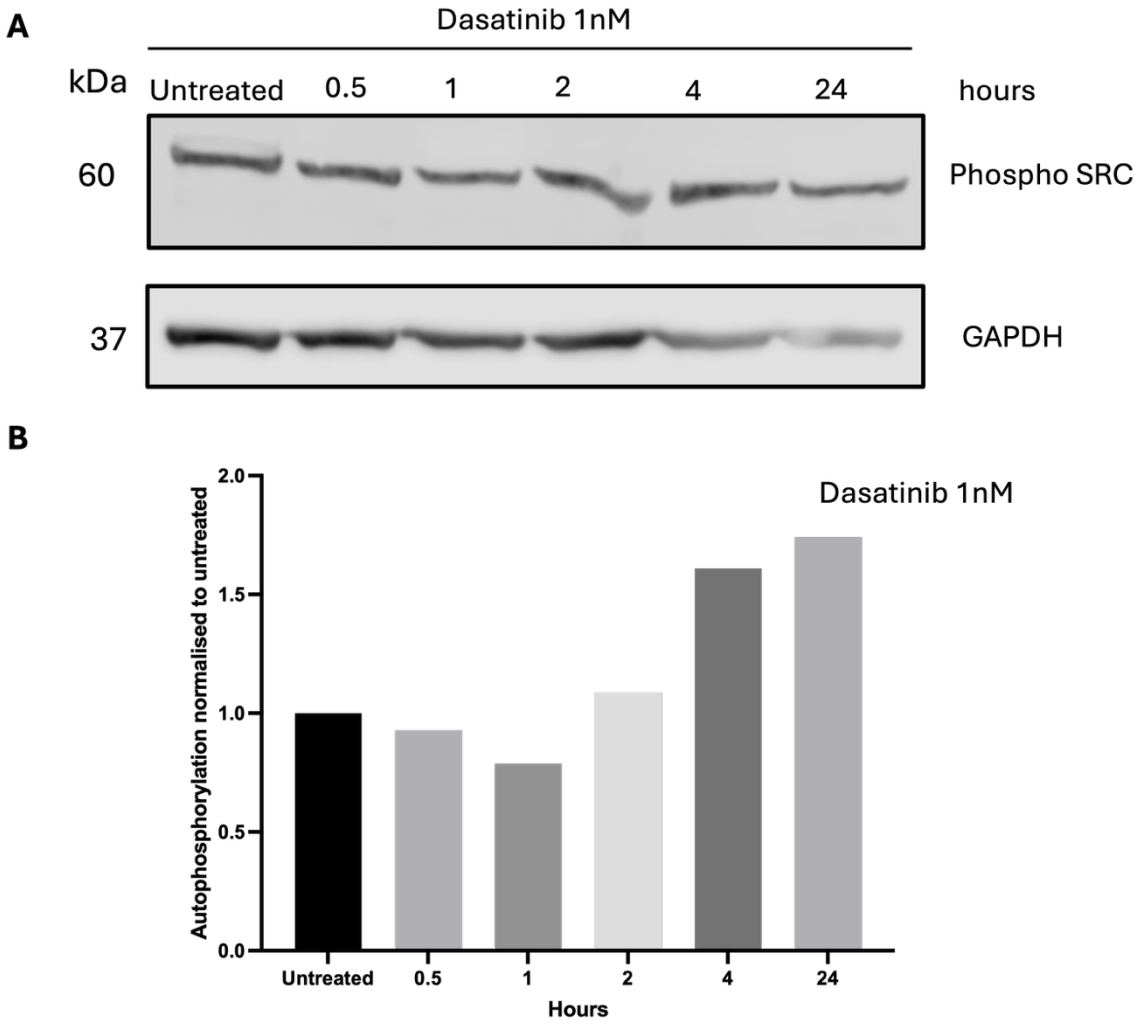

Figure 4-7 Dasatinib inhibitory effect on SRC autophosphorylation in ME-1 cell line was abolished after one hour of administration.
ME-1 cell line was treated with 1nM of dasatinib for different time points (0.5, 1, 2, and 4 hours) (A) Western blot bands of phospho SRC (Y416), all data were normalised to GAPDH then to untreated. (B) graph shows autophosphorylation of SRC normalised to untreated sample. n=1. Full membrane is shown in the Appendix (**Figure 6-7**).

4.3.3 Effect of dasatinib on ME-1 cell viability, cell proliferation and cell cycle analysis.

4.3.3.1 Dasatinib does not affect AML cell survival and cell proliferation but affects the cell cycle at a 48-hours.

To see the effect of dasatinib on ME-1 cell viability, a 48-hours time point was chosen as ME-1 cells double in number every 48 hours. HS5 stromal cells were seeded 24 hours in advance, with ME-1 split at the same time to avoid lag in growth phase effect, then ME-1 cells (including cells stained with CTV for cell proliferation experiment) were added to HS5. Ara-C at EC_{50} and dasatinib in its defined concentration were added and cells were cultured for 48 hours in the incubator at 37°C, 5% CO_2. After that, cells were collected for apoptosis, cell cycle and proliferation (CTV) assays.

In the apoptosis assay, in LC, Ara-C killed from 25 to 30% of ME-1 cells showing a significant difference in cell viability between LC and LC with Ara-C, However, in CC, Ara-C couldn't kill the same percentage of cells killed in LC although using the same concentration of Ara-C, it only killed from 10 to 15% of cells, owing to HS5's protective effect against Ara-C. Adding dasatinib in its defined dose in LC didn't show any difference to LC without any drugs suggesting that dasatinib has no cytotoxic action on its own, testing dasatinib as an adjuvant to Ara-C by adding it to Ara-C in CC condition showed no added action on cell viability and no statistically difference to the CC without Ara-C (Figure 4-8) n=4.

Regarding cell proliferation analysis, it was noticed that CC either alone or treated with dasatinib showed more proliferation status than LC. Adding Ara-C in CC showed no increase in proliferation than in LC + Ara-C suggesting that HS5 mediated protection doesn't include an increase in cell proliferation. Adding dasatinib to LC didn't affect cell proliferation status compared to LC without adding any drugs. Moreover, adding dasatinib with Ara-C didn't affect cell proliferation. (n=3, Figure 4-9, A and B).

Cell cycle analysis confirms apoptosis and cell proliferation results, as subG1 which represents the apoptotic cells didn't differ between CC with Ara-C only and CC with dasatinib and Ara-C (Figure 4-10). Also, there is no significant difference in cell cycle phases between adding dasatinib to Ara-C and using Ara-C alone.

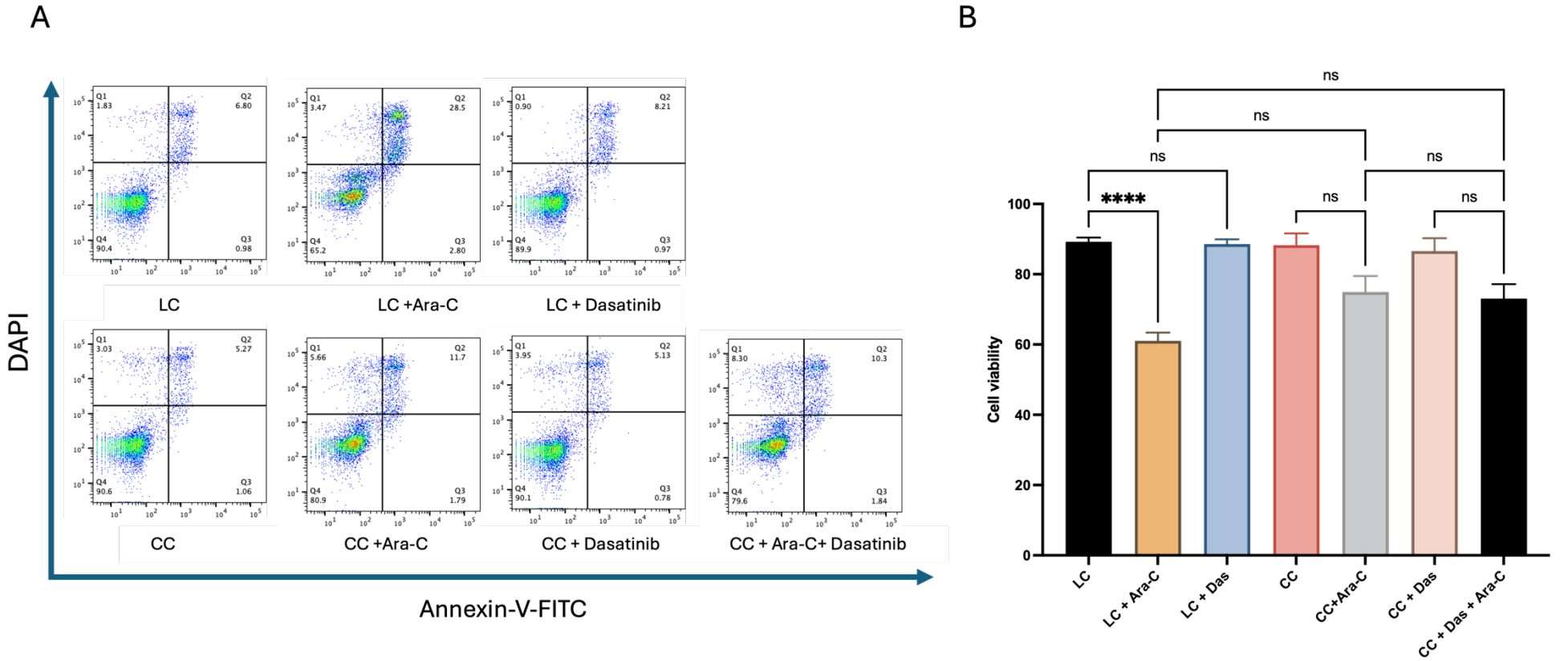

Figure 4-8 Apoptosis assay in ME-1 cell line with EC50 Ara-C and 1nM dasatinib after 48-hours culture.
(A) Representative flow cytometry showing apoptosis with Annexin-V/DAPI in LC and CC (Direct contact) with and without Ara-C and dasatinib, LC + dasatinib +Ara-C is missed. (B) graph showing the percentage of Annexin-V (-) and DAPI (-) in different conditions. Each bar represents the mean ± SD of four independent experiments n=4, and ****$P < 0.0001$ is considered statistical significance using one-way ANOVA with Tukey's multiple comparisons test.

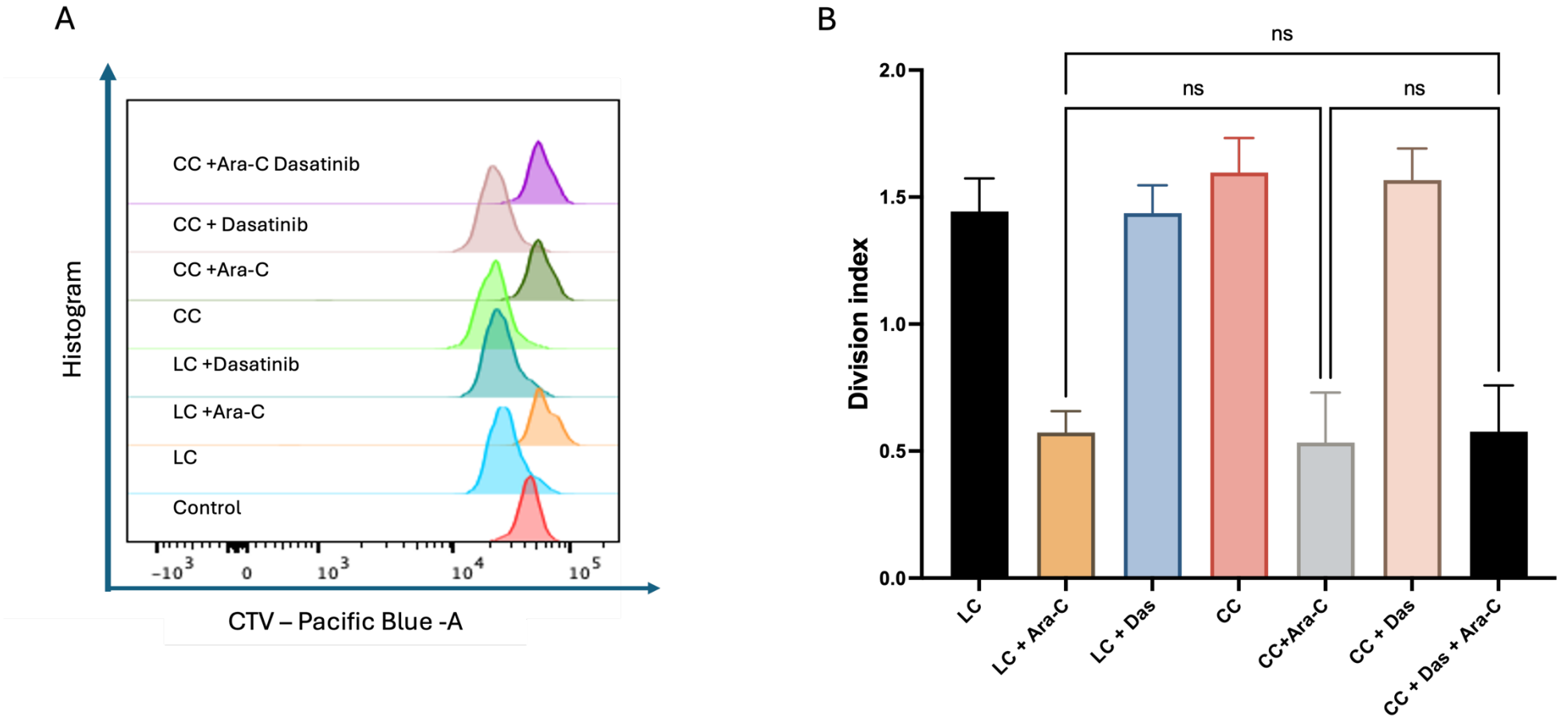

Figure 4-9 Cell proliferation assay in ME-1 cell line with EC50 Ara-C and 1nM dasatinib after 48-hours culture.
(A) CTV histogram showing the geometric mean of CTV stain in LC and CC (Direct contact) with and without Ara-C and dasatinib in comparison to control. (B) graph showing the division index in LC and CC with and without drugs. Each bar represents the mean ± SD of three independent experiments n=3.

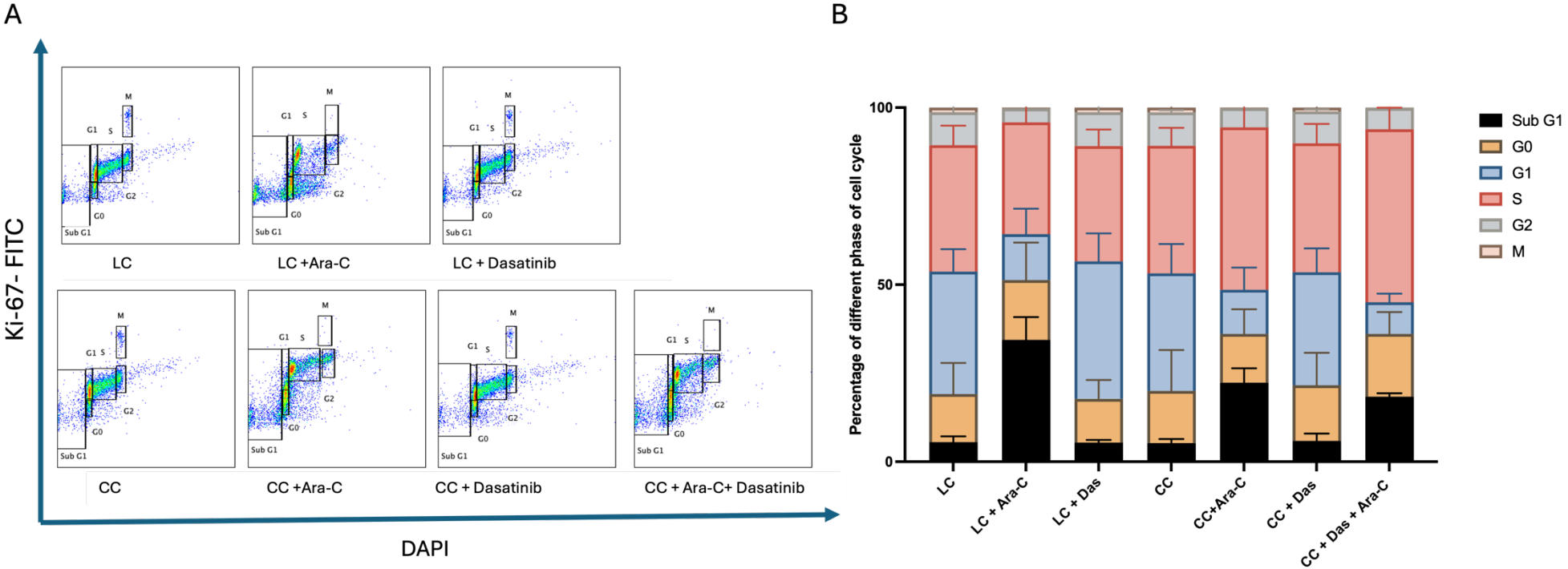

Figure 4-10 Cell cycle analysis of ME-1 cells in LC and CC (Direct contact) in the presence of Ara-C and dasatinib cultured for 48 hours.
(A) Representative flow cytometry of cell cycle assay showing different phases of the cell cycle in different conditions. (B) graph showing the percentage of cells in different phases of the cell cycle among different conditions. Each bar represents the mean of three independent experiments n=3, and $*P < 0.05$, $**P < 0.01$, $***P < 0.001$ are considered as statistical significance using one-way ANOVA with Tukey's multiple comparisons test.

4.3.3.2 Dasatinib had minimal effect on cell count, apoptosis, and cell cycle at a 72-hours.

The previous result shows that there is no difference between adding dasatinib to Ara-C or using Ara-C alone at a 48-hours time point regarding the Annexin/DAPI method, so a longer time point (72 hours) was used with adding dasatinib every 24 hours after culturing. Other apoptosis methods were used, so the apoptosis process could be measured at the level of the nucleus using cleaved PARP and cleaved caspase. Moreover, cell counts were performed to determine the absolute count at the end of the experiment in the different conditions.

Absolute cell count using TB exclusion was done on the ME-1 cell line to compare CC with or without EC_{50} Ara-C and dasatinib added either once at the start of culture or every 24 hours using the previously determined concentration (1nM) (Figure 4-11).

Apoptosis assay using Annexin-V and DAPI after culturing the ME-1 cell line for 72 hours shows similar results as at 48 hours. There was no significant difference between CC with Ara-C alone compared to CC with Ara-C and dasatinib, However, when the cells were treated with dasatinib every 24 hours, it showed a very minimal decrease in survival compared to CC with dasatinib added once at the start of culture. There was no statistically significant difference between the two conditions (Figure 4-12).

Cell cycle analysis at 72 hours showed the same result as at 48 hours as there was no significant difference between CC with Ara-C alone and CC with Ara-C and dasatinib (Figure 4-13). Moreover, adding dasatinib every 24 hours didn't show a difference in subG1 compared to when dasatinib was added once at the start of culture. Also, the G0 percentage didn't show a difference when dasatinib was added every 24 hours compared to adding it at the start of culture only.

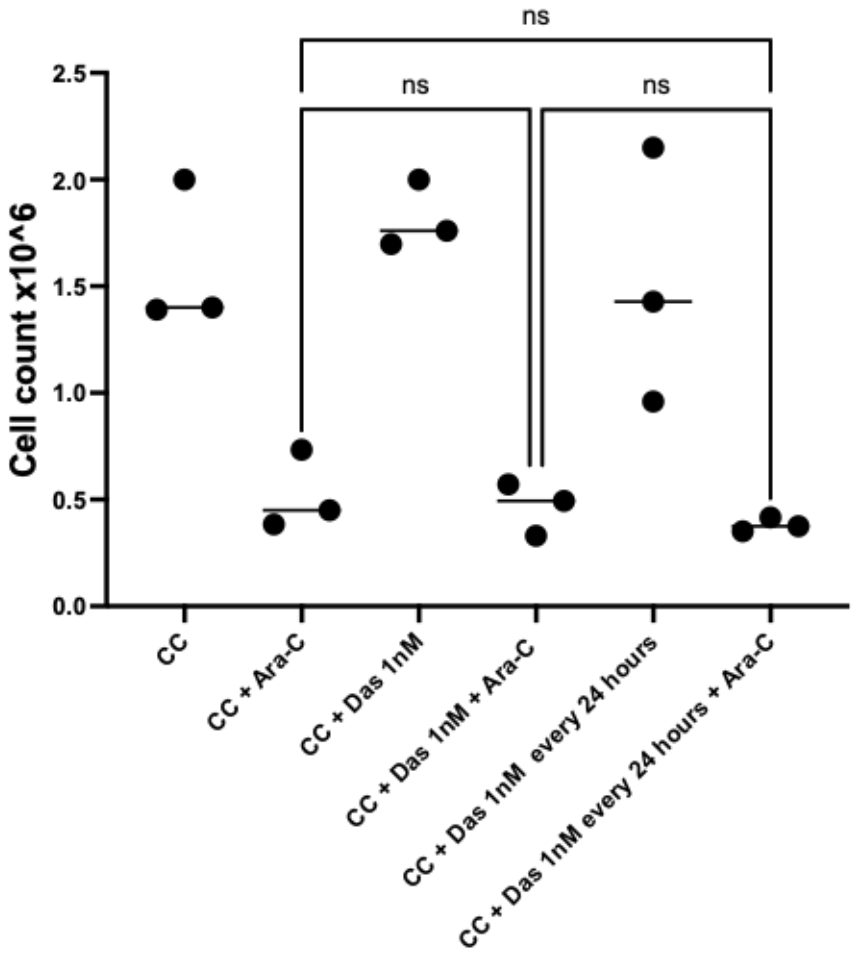

Figure 4-11 Absolute cell count using TB on ME-1 cell line after 72 hours of culturing in direct contact with HS5.
Each dot represents one independent replicate n=1, the line represents the median of three independent experiments, and *P < 0.05 is considered as statistical significance using one-way ANOVA with Tukey's multiple comparisons test.

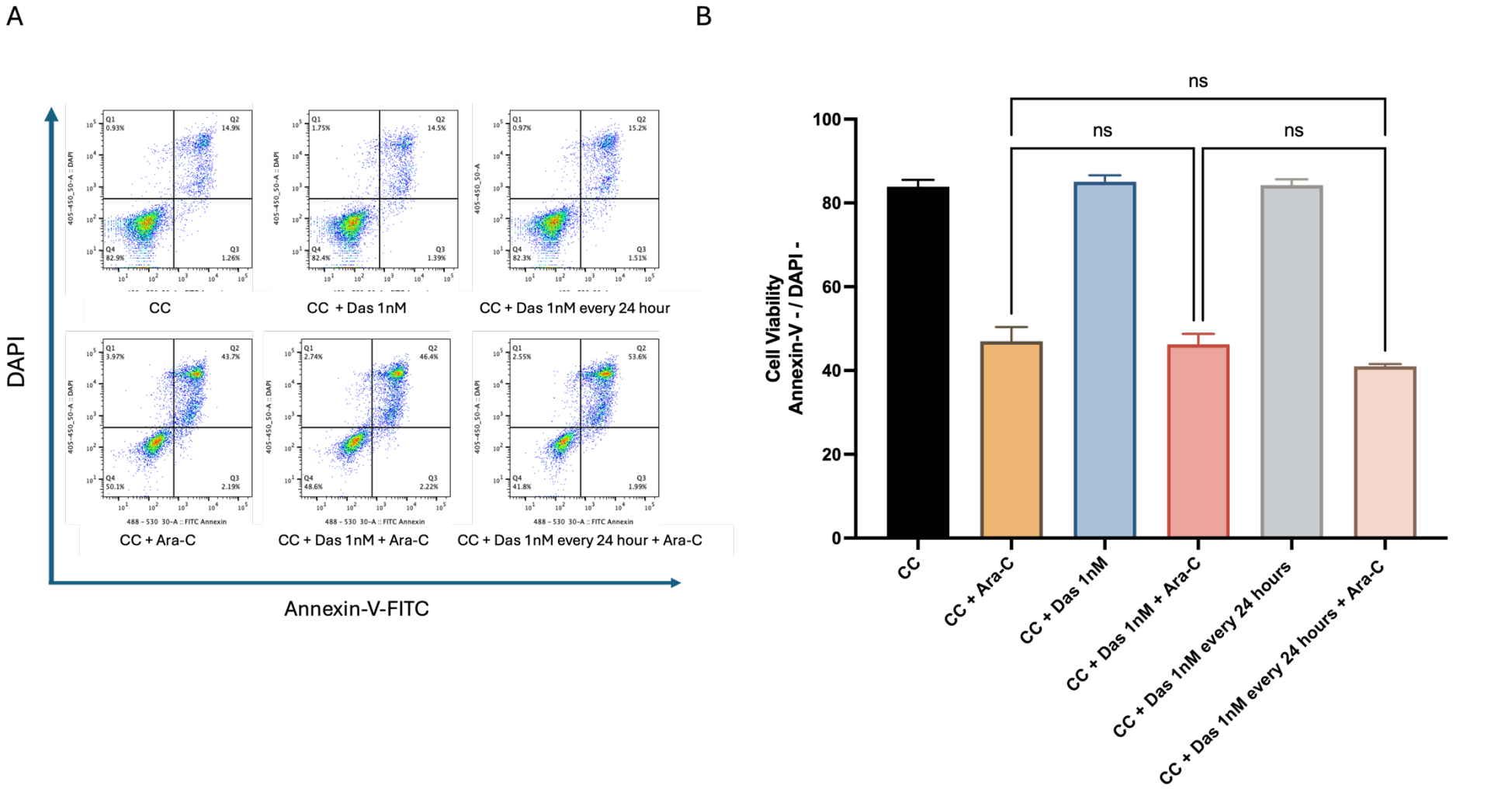

Figure 4-12 Apoptosis assay in ME-1 cell line with EC50 Ara-C and 1nM dasatinib after 72 hours culture.
(A) representative flow cytometry showing apoptosis with Annexin-V/DAPI in CC (Direct contact) with and without Ara-C and dasatinib applied once at the start of culture or every 24 hours. (B) graph showing the percentage of Annexin-V (-) and DAPI (-) in different conditions. Each bar represents the mean ± SD of four independent experiments n=4, and *$P < 0.05$ is considered as statistical significance using one-way ANOVA with Tukey's multiple comparisons test.

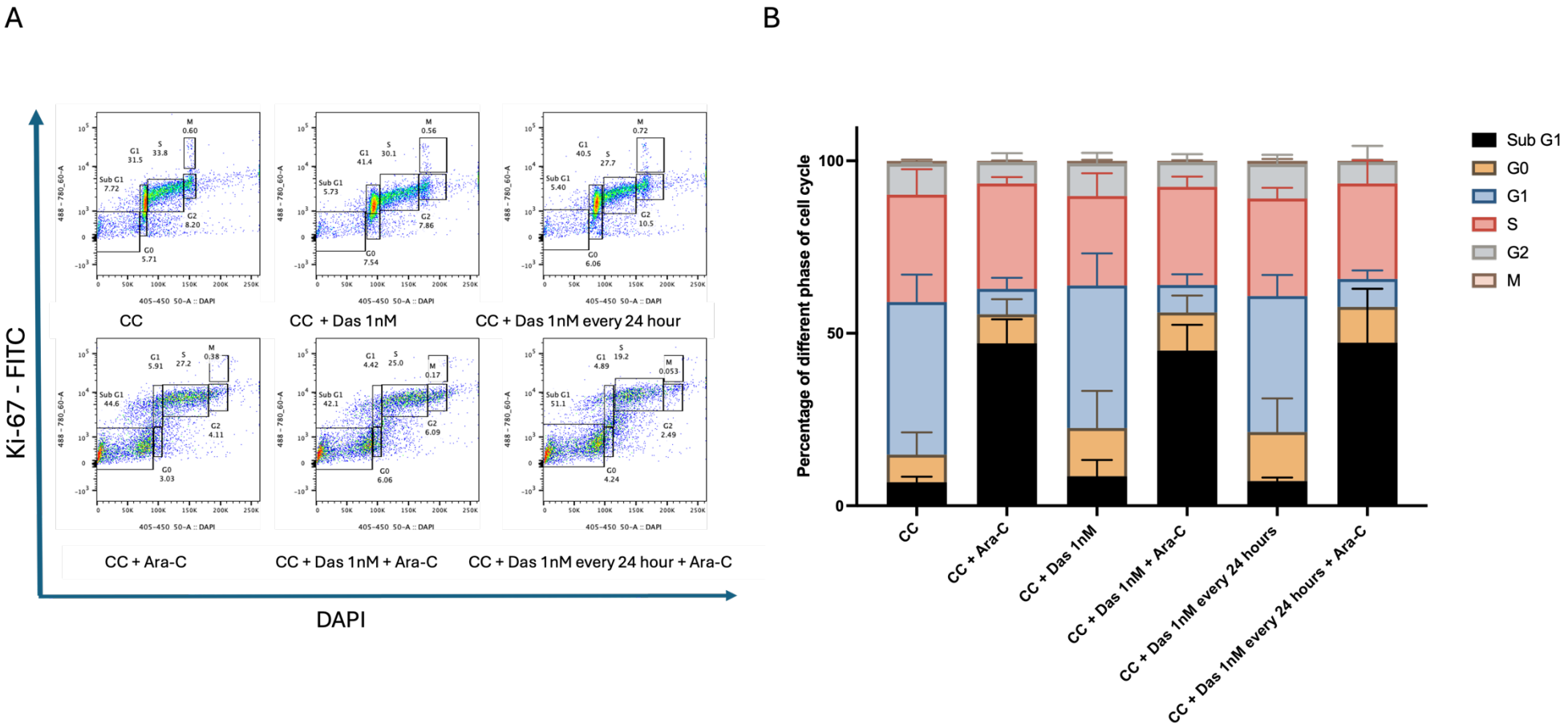

Figure 4-13 Cell cycle analysis of ME-1 cells in CC (Direct contact) in the presence of Ara-C and dasatinib at 72 hours with dasatinib added once at the start of culture or every 24 hours.

(A) representative flow cytometry of cell cycle assay showing different phases of the cell cycle in different conditions. (B) graph showing the percentage of cells in different phases of the cell cycle among various conditions. Each bar represents the mean of three independent experiments n=3, and $*P < 0.05$ is considered as statistical significance using one-way ANOVA with Tukey's multiple comparisons test.

4.3.3.3 C-PARP and c-Caspase as apoptotic markers to examine the dasatinib role in AML cell viability

Cleaved Poly ADP-ribose polymerase (c-PARP) is a protein involved in DNA repair. During apoptosis, caspases cleave PARP, forming a cleaved PARP fragment (c-PARP) (Herceg & Wang, 2001). C-PARP protein detection by western blot was done at 72 hours on CC with Ara-C and dasatinib added once at the start of culture, or repeatedly every 24 hours (Figure 4-14). Western blot bands showed that Ara-C increased c-PARP protein as a result of the apoptosis process. Moreover, adding dasatinib either once at the start, or every 24 hours during culture enhances the apoptosis process by increasing c-PARP protein. It was noticed that adding dasatinib every 24 hours boosted the apoptosis effect of Ara-C.

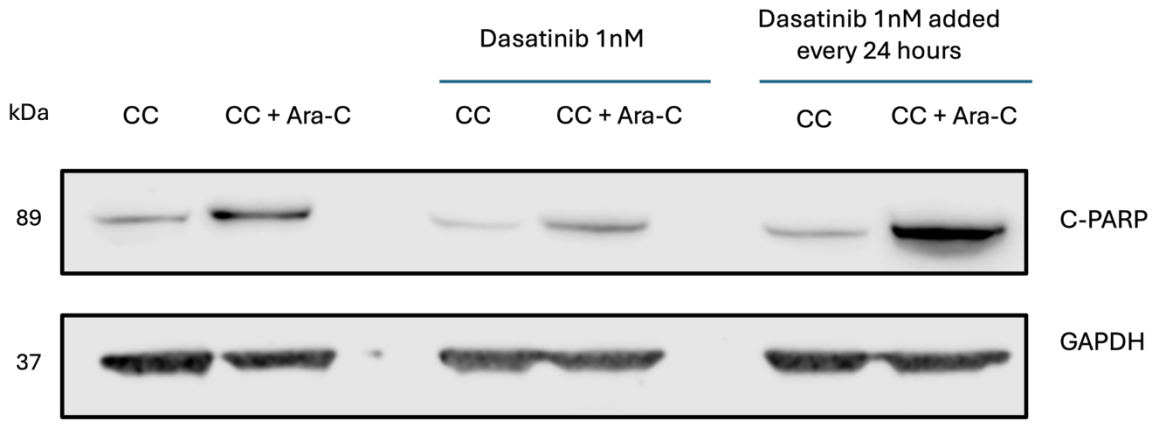

Figure 4-14 western blot bands for c-PARP in CC (Using Transwell) with EC50 Ara-C and 1nM dasatinib after 72 hours of culture.
ME-1 cell line was cultured with HS5 with and without Ara-C, and dasatinib was added either once at the start of culture or every 24 hours. n=1. Full membrane is shown in the Appendix (**Figure 6-8**).

To confirm the results of Annexin-V/DAPI and c-PARP, cleaved caspase-3 (c-Caspase) was done by flow cytometry, and the result showed that adding dasatinib once at the start of culture improved the apoptotic effect of Ara-C compared to adding it every 24 hours or not adding it at all. However, there is no statistically significant difference between adding it or not (Figure 4-15).

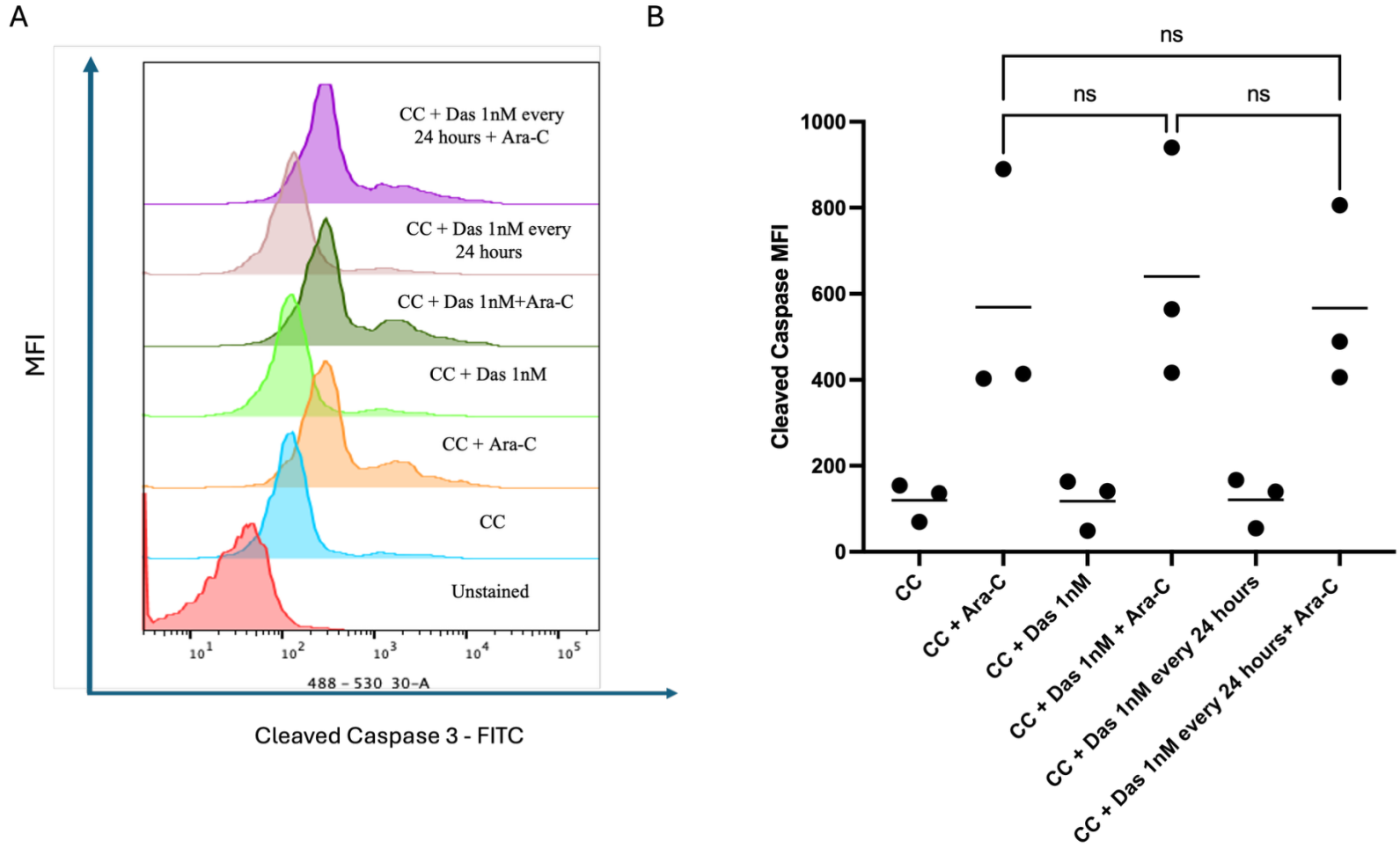

Figure 4-15 C-Caspase-3 in ME-1 CC (Direct contact) with EC50 Ara-C and 1nM dasatinib after 72 hours of culture.
(A) C-Caspase histogram showing the mean fluorescence intensity (MFI) of c-Caspase stain in CC with and without Ara-C and dasatinib added once or every 24 hours compared to control. (B) graph showing c-Caspase MFI in CC with and without drugs. (n=3) P values were determined using one-way ANOVA with Tukey's multiple comparisons test, ns=non-significant.

4.4 Discussion:

IL-6 is a pro-inflammatory marker secreted from AML cells during infiltration of BMME due to AML cell interaction and has a vital role in chemoresistance in malignancy. The underlying mechanisms of this chemoresistance are not yet clear. One of the potential mechanisms is the role of IL-6 in lipid metabolism and CD36-mediated fatty acid uptake (Y. Zhang et al., 2022). Another possible mechanism is activating the JAK-STAT signalling pathway that regulates prosurvival gene expression inside the nucleus (Benekli et al., 2002).

Studies found that there is another STAT-independent pathway that IL-6 works on. Upon binding of IL-6 to the IL-6 receptor and gp130, a co-receptor for IL-6, this binding complex, in addition to stimulating JAK-STAT, stimulates SFK (Azar et al., 2020). Based on the previous chapter result of ProcartaPlex™ immunoassay showing that IL-6 is highly secreted within CC compared to LC and HS5 alone, and on Dr Laing's data showing that four out of five of IL-6 mediated signalling pathways are significantly enriched in CC compared to LC in six paediatric AML samples (showed in Figure 4-1), it was hypothesised that SRC signalling activation may have a role in BMME-mediated chemoresistance.

Based on this hypothesis, SRC signalling pathway gene and protein expression were investigated. From the SRC signalling pathway that IL-6 is working on, three different genes were chosen for study; *SRC* as this is an upstream kinase that should be stimulated by IL-6/gp130 complex, SRC is one of the SFK, contains eight members, one of them is YES, YES activates Yes-associated protein (YAP) by direct phosphorylation leading to nuclear translocation to activate target gene transcription (Taniguchi et al., 2015). *YAP* is a midstream pathway molecule that is activated because of SRC activation, YAP is a transcription co-activator and a key member in hippo signalling pathway, YAP is responsible for cell proliferation, once cells proliferate to a high density, hippo pathway is activated leading to YAP phosphorylation (S127) and retention in the cytoplasm to be degraded by ubiquitination. Direct phosphorylation of YAP (Y357) or unphosphorylated YAP enter the nucleus activating the transcription factors for genes involved in cell proliferation and apoptosis (Hsu et al., 2020). *CYR61* is a downstream molecule and one of the final target genes that affects cell survival and proliferation.it is

one of the target genes for YAP (Y. Wang et al., 2022) and contributes to mitoxantrone resistance in AML (Long et al., 2015).

It was found that only the *SRC* gene was overexpressed in CC in comparison to LC in the adult core binding factor AML cell line (ME-1), However, *YAP* and *CYR61* didn't show a statistically significant difference in Kasumi-1, ME-1 and THP-1 in both LC and CC. This could be explained by either the SRC signalling pathway working through other genes that need to be studied or IL-6 having no major effect through this non-canonical signalling pathway.

Although *SRC* was overexpressed in CC compared to LC which might mean an increase in protein function, SRC autophosphorylation was found to be less expressed in CC. This suggests that there is no strong relation between gene expression and its function through phosphorylation. So, the gene product might work more through other post-translational modifications rather than phosphorylation, as the total SRC protein is higher in CC compared to LC.

The hypothesis depended on IL-6 acting through non-canonical signalling which has YAP and CYR61 in the pathway. It was found that YAP and CYR61 were not much expressed in our studied cell lines, although there are published studies on these genes in AML (Chen et al., 2017; Feng et al., 2022; Song et al., 2023).

Although midstream (*YAP*) and downstream genes (*CYR61*) are not much expressed in our studied cell lines, experiments were performed as the upstream gene and protein (SRC) were overexpressed in CC compared to LC and so the drug selected to be tested was dasatinib which acts as SRC tyrosine kinase inhibitor.

Based on previous studies working on dasatinib, different concentrations were used to determine the lowest concentration that inhibits signalling with the least cytotoxic effect. One nanomolar was found to inhibit SRC autophosphorylation to 50% compared to the untreated sample which was found to be the lowest dose that has no cytotoxicity on our studied cell line and could provide its inhibitory effect.

Regarding the timepoint at which dasatinib has its action, shorter timepoints were examined, depending on our previous knowledge that phosphorylation happens

within seconds (Blazek et al., 2015), and it was found that inhibition of phosphorylation starts at 5 mins but reaches its maximum inhibition at 30 mins. However, it is important to know for how long this inhibition lasted and how often the drug would be effective on repeated dosing, so, a further experiment was done with a longer timepoint starting from 30 mins, the zenith of maximum inhibition, until 24 hours and it was found that the inhibition last for only one hour and the inhibitory effect started to be abolished from 2-hours timepoint until 24 hours. It was also noticed that the autophosphorylation gained after inhibition with dasatinib was much higher than the autophosphorylation without adding the drug.

Regarding cell cycle analysis, data showed that dasatinib increased the percentage of cells entering G0, either alone or in combination with Ara-C, when cells were treated for 48 hours. G0 is the resting phase of the cell cycle; cells in this phase are neither dividing nor preparing for division. These cells are mainly categorised into three groups: senescent, quiescent, and differentiated (Patt & Quastler, 1963). Senescence is an irreversible state resulting from DNA damage, meaning the cells are still viable and perform normal cellular processes, but can't proliferate. Quiescence means that the cells aren't proliferating, but this condition is reversible whenever growth factors are available. In a differentiated state, cells will never proliferate as they have reached their end stage of maturation.

Because dasatinib caused G0 to increase when added to Ara-C in CC compared to CC with Ara-C alone, investigation of the drug at a later timepoint (72 hours) was applied to see the effect of the drug and the fates of cells that were in G0 as the drug might need more time to affect the cell viability. Also, investigating cell viability using absolute cell count and apoptosis assays using methods that can measure earlier stages, e.g. measuring c-PARP and c-Caspase confirmed the previous results of minimal effect of dasatinib when Annexin /DAPI stain was applied as the Annexin-V/DAPI technique represents the morphological and late aspect of apoptosis.

Moreover, dasatinib was added more frequently (every 24 hours), based on the working hypothesis that dasatinib, which works through the inhibition of SRC phosphorylation, might regain its phosphorylation after one hour of applying the

drugs. One study has shown that SRC phosphorylation returns rapidly after inhibition using SRC inhibitors such as dasatinib (Luo et al., 2008)). Luo et al. showed that after treating PC-3 cells (human prostate tumour cells) with dasatinib, p-SRC was completely inhibited at 3 hours. However, this phosphorylation maximally recovered between 7 and 17 hours and came back completely at 24 hours. It was found that some factors within the pathway could stop the drug from having its targeted effect (Konig et al., 2008). Although dasatinib can inhibit SRC phosphorylation, which should affect cell viability and cell proliferation, some growth factor receptors being continuously stimulated prevent alteration in the apoptotic regulatory mechanisms after dasatinib treatment (Konig et al., 2008).

Results of apoptosis using c-PARP have shown that adding dasatinib augmented the apoptotic effect of Ara-C in the CC condition. However, this result was not correlated with Annexin-V/DAPI assay or cleaved caspase-3 assay, the idea of apoptosis timing could explain this. Annexin-V is a molecule that binds PS, a phospholipid normally located on the inner surface of the plasma membrane. During apoptosis, PS is translocated from the inner to the outer surface of the plasma membrane. Annexin V can bind to PS exposed on the outer surface of apoptotic cells, making it a marker for early-stage apoptosis.
On the other hand, PARP is a protein responsible for DNA repair. During apoptosis, caspases cleave PARP, forming a cleaved PARP fragment (c-PARP). Detection of c-PARP indicates the activation of caspases, which are key components of the apoptosis pathway. Therefore, c-PARP serves as a marker for late-stage apoptosis (Figure 4-16). So, in some cases, specific apoptotic stimuli such as oxidative stress and targeted molecular therapies might cause DNA damage resulting from caspase activation and PARP cleavage without significant changes in membrane permeability which results in increased c-PARP without change Annexin-V (Elmore, 2007).

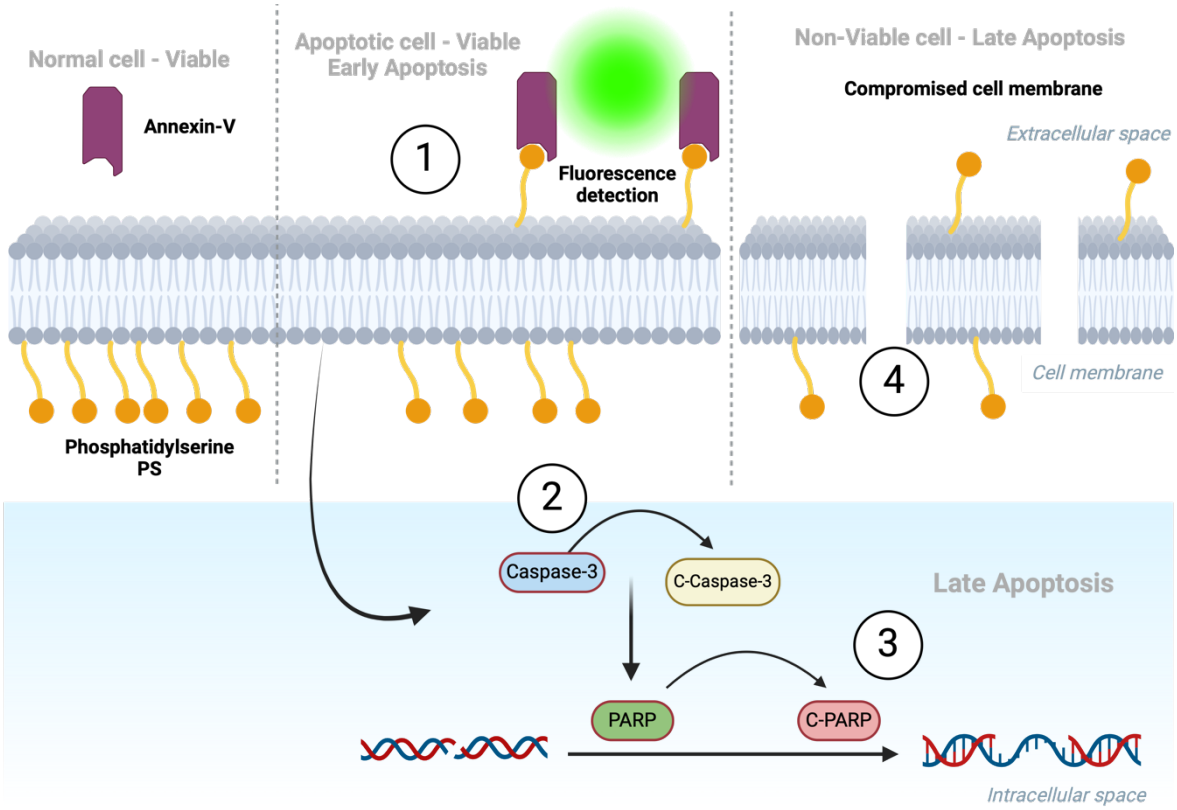

Figure 4-16 Schematic illustration showing the sequence of apoptosis progression.
The sequence of apoptosis events emphasises the critical molecular changes that occur during apoptosis, from the early activation of apoptotic markers and caspases to the eventual breakdown of cellular structures and DNA fragmentation.

Moreover, c-PARP can be increased while caspase-3 is not changed, this could be owing to the cleavage of PARP related to alternative caspase activation such as caspase-7 and caspase-6 (Fuentes-Prior & Salvesen, 2004). Also, PARP-1 can be cleaved by proteases other than caspases. Specifically, of note, PARP-1 is a substrate for several proteases including calpains, cathepsins, granzymes, and MMPs, which can cleave PARP-1 into various fragments resulting in increased c-PARP without caspase-3 changes (Chaitanya et al., 2010).

In conclusion, the findings of this chapter highlight the role of SRC signalling in AML chemoresistance, as it is expressed in the CC condition. Inhibiting the pathway using dasatinib didn't significantly abrogate HS5-mediated chemoprotection. We thought that the chemoprotection related to cytokines secreted by the CC condition, including IL-6 and the SRC signalling pathway, is considered a non-canonical pathway for IL-6, so the next chapter will discuss the role of JAK-STAT signalling pathway in providing chemoresistance and how inhibiting it using ruxolitinib could be effective.

5 Result 3: Ruxolitinib abrogates stromal cell-mediated chemoresistance by JAK-STAT pathway inhibition

5.1 Introduction

Studies showed that the molecular mechanism of BMSC-mediated chemoresistance is partly related to cytokines secretion; IL-6 is considered one of the main cytokines secreted by BMSC (Kyurkchiev, 2014). Many studies are exploring how IL-6 can increase AML cell viability (Hou et al., 2020, 2023; Li et al., 2024; Lu et al., 2023; Mei et al., 2022; Stevens et al., 2017; Y. Zhang et al., 2022).

As discussed in the previous chapter, IL-6 can work through a non-canonical signalling pathway by stimulating SRC/YAP signalling resulting in the transcription of survival and proliferation genes as *CYR61* inside the nucleus, providing AML cells with increased viability and proliferation. Our investigation into this pathway was prompted by the observation that CC enhances SRC expression in the ME-1 cell line at both the gene and protein levels. Additionally, RNA sequencing data from CC of six paediatric AML samples revealed an enrichment of the *YAP* gene in one of the five gene sets of IL-6 pathways performed by GSEA, this pathway is the GO IL-6-mediated signalling pathway (Laing, 2021).

Based on these findings, we attempted to use dasatinib, a licensed SRC/ABL inhibitor (Blake et al., 2008), as an adjuvant to the standard chemotherapy agent, Ara-C. However, dasatinib did not significantly affect AML cell line cell proliferation, viability, or cell cycle. Several factors may account for this lack of efficacy. Firstly, the pathway we studied is not the primary pathway through which IL-6 exerts its effects, as IL-6 predominantly signals via the JAK-STAT pathway. secondly, the *YAP* gene wasn't found to be expressed in our investigated cell lines, Kasumi-1, or showed lower expression in ME-1 and THP-1. However, it was decided to start this investigation with the non-canonical signalling pathway, as we had shown that the CC system significantly upregulated *SRC* gene and protein expression in ME-1 cell line.

Experiments were refocussed to work on the main signalling pathway, i.e., JAK-STAT pathway. Additionally, HS5 cells may secrete other cytokines that protect

AML cells against Ara-C, these cytokines may not work on the SRC/YAP signalling pathway but work through the JAK-STAT signalling pathway.

IL-6 activates the JAK-STAT signalling pathway which phosphorylates STAT3, a transcription factor responsible for the regulation of many proliferative and survival genes (Sansone & Bromberg, 2012). Serine phosphorylated STAT3 (pS-STAT3) was shown to alter mitochondrial OXPHOS, resulting in AML chemoresistance (Hou et al., 2020). Small, intracellular, calcium-sensing molecules, S100A8 and S100A9 which can modulate some cellular processes such as cell proliferation and differentiation were found to be upregulated in AML cells cocultured with BMSC through IL-6/JAK-STAT signalling activation (Böttcher et al., 2022).

Ruxolitinib (previously known as INCB018424) belongs JAK inhibitor group. Nowadays, it is used clinically in the treatment of JAK2 *V617F*-positive myeloproliferative neoplasms, including intermediate or high-risk myelofibrosis and polycythaemia vera (Bose & Verstovsek, 2017). As a JAK inhibitor drug, together with the fact that IL-6 works through JAK-STAT signalling, it was hypothesised that ruxolitinib may act as targeted therapy for BMSC-mediated chemoresistance aiming to overcome AML chemoresistance leading to relapse.

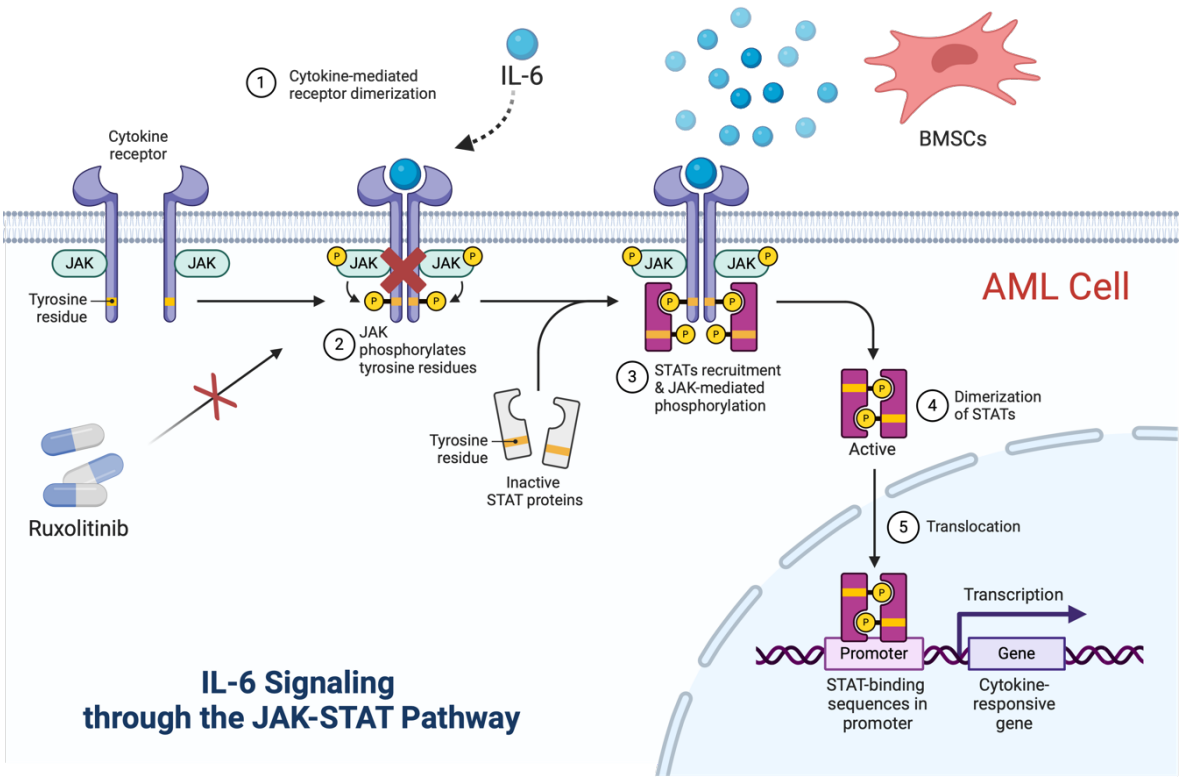

Figure 5-1 JAK-STAT signalling pathway activation through IL-6 secreted from BMSC and the effect of ruxolitinib inhibition on this pathway.
The figure shows an example of stimulation of the JAK-STAT pathway by binding IL-6 to its receptor, causing receptor conformational changes and autophosphorylation of JAK2, leading to STAT3 recruitment, phosphorylation and dimerisation, then entering the nucleus for survival gene transcription. Ruxolitinib, a JAK inhibitor, competitively inhibits ATP-binding catalytic sites on JAK1 and JAK2.

5.2 Aims and objectives

Based on the previous results showing that SRC/YAP signalling is not significantly effective in mediating cellular chemoresistance, it is hypothesised that IL-6, secreted by the HS5 cell line, exerts its chemoresistant effect through activation of the JAK-STAT signalling pathway, which, if inhibited, could eliminate the HS5-mediated chemoprotection, thereby increasing the sensitivity of the AML cell line to Ara-C. The following research aims were developed:

1) Confirm stimulation of JAK-STAT signalling pathway in Kasumi-1 cell line by exogenous IL-6 and CC system;

2) Find the lowest ruxolitinib concentration that totally inhibits JAK-STAT signalling in the Kasumi-1 cell line;

3) Investigate the effect of ruxolitinib on Kasumi-1 cell viability and proliferation within CC;

4) Confirm the role of cytokines secreted by excluding direct contact role using transwell;

5) Compare the chemoprotective effect of primary paediatric AML stromal cells and the HS5 cell line on the Kasumi-1 cell line.

5.3 Results

5.3.1 IL-6 and CC stimulate JAK-STAT signalling pathway

In our previous work, the concentration of IL-6 was noticed to be increased in CC compared to LC using Luminex® assay in primary paediatric AML samples; IL-6 was detected as low as 5ng/mL (Laing et al., 2025). JAK-STAT signalling was tested for its stimulation either by adding IL-6 to the Kasumi-1 cell line or the CC system.

pS-STAT3 (Y705) was measured by flow cytometry to show the effect of adding IL-6 and CC (Kasumi-1 / HS5) on STAT3 phosphorylation. Phosphorylation of STAT3 was evident in both situations; LC after adding IL-6 for 30 mins and the CC system (Figure 5-2).

The result showed that CC and exogenous IL-6 at a concentration of 10ng/mL in LC can stimulate JAK-STAT signalling and phosphorylate STAT3 at tyrosine residue 705 (Y705). CC significantly phosphorylates STAT3 compared to autophosphorylation of LC (p=0.0138, n=5). However, adding IL-6 10ng/mL phosphorylates STAT3 but without a significant difference to LC autophosphorylation.

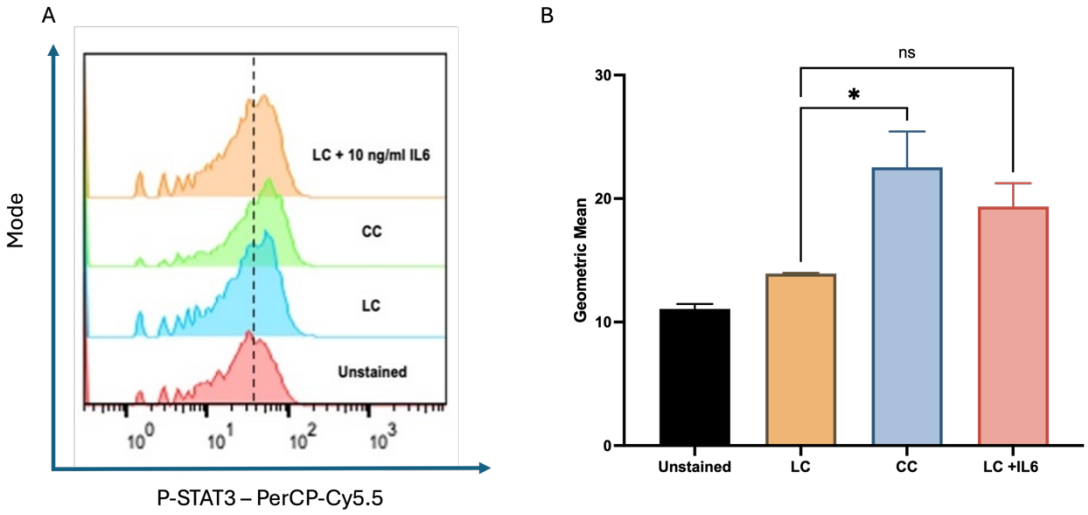

Figure 5-2 CC and exogenous IL-6 phosphorylate STAT3 via stimulation of JAK-STAT signalling pathway.
(A) Mode, represented by the peak of the curve, of pSTAT3 (Y705) in Kasumi-1 cell line in liquid culture (LC), LC + IL-6 (10ng/mL), and coculture (CC). (B) Geometric mean (GM) of pSTAT3 (Y705) in LC, LC + IL-6 and CC compared to the LC autophosphorylation (unstained control). Each bar represents the mean ± S.D of five independent experiments n=5, and *P < 0.05 is considered statistical significance using one-way ANOVA with Tukey's multiple comparisons test, ns=non-significant.

5.3.2 Ruxolitinib effectively inhibits JAK/STAT signalling in LC + IL-6 and CC.

We tested a range of ruxolitinib concentrations, the objective was to select the lowest concentration capable of completely inhibiting pSTAT3 for further experiments.

The result showed that all ruxolitinib concentrations used in this experiment significantly inhibited JAK-STAT signalling pathway. The lowest (0.5μM) concentration of ruxolitinib inhibited pSTAT3 with a statistically significant difference compared to no drug control (p=0.0088, n=5). and was selected for use in further experiments (Figure 5-3).

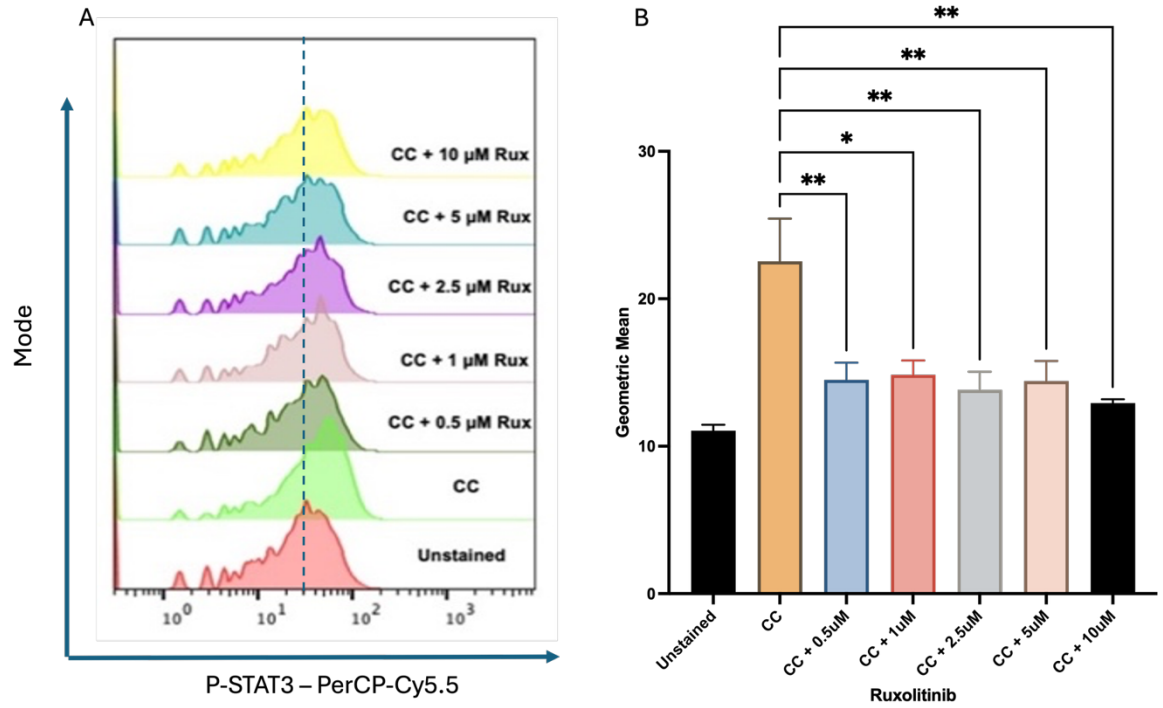

Figure 5-3 Different doses of ruxolitinib inhibit JAK2 resulting in decreasing STAT3 phosphorylation (Y705) induced by HS5 in Kasumi-1 CC.
(A) Mode, representing the most frequent intensity value, of pSTAT3 (pY705) in Kasumi-1 cell line in CC and with different ruxolitinib concentrations. (B) The graph shows the GM of pSTAT3 (Y705) in CC with ruxolitinib compared to the no-drug control. Each bar represents the mean ± S.D of five independent experiments n=5, and *P < 0.05, **P < 0.01, ***P < 0.001 are considered statistical significance using one-way ANOVA with Tukey's multiple comparisons test.

5.3.3 Ruxolitinib has no cytotoxic effect amongst AML cell lines

To investigate any synergy effect between ruxolitinib, as JAK-STAT inhibitor, and Ara-C, as standard chemotherapeutic drug used mainly in the induction phase for AML treatment, it was important first to make sure that ruxolitinib had no non-specific cytotoxic effect on AML cells. In further experiments, if ruxolitinib led to a decrease in AML cell viability, this effect could be inferred as a result of JAK-STAT inhibition, not to any non-specific toxicity effect.

In the next experiment, different ruxolitinib concentrations were used to examine its cytotoxic effect on different AML cell lines. Also, different time points were used to make sure that the drug had no temporal toxic effect when cells were incubated with the drug for a longer time.

Using apoptosis assay (Annexin-V and DAPI), three AML cell lines, Kasumi-1, SKNO-1 as a paediatric and ME-1 as an adult, were selected as they are core binding factors. They were tested for cell viability after adding different doses of ruxolitinib, 0.5,2.5,5,10μM, and incubated for 24, 48 and 72 hours.

Regarding the Kasumi-1 cell line, it was noticed that there was a trend towards a decrease in cell survival when using ruxolitinib (0.5μM) at a 24-hours time point. However, there was no statistically significant difference between using the drug and no drug control (Figure 5-4).

On the other hand, the ME-1 cell line didn't show any alteration in cell survival after adding all defined doses of ruxolotinib and at all time points investigated (Figure 5-4).

In SKNO-1 cell line, there is a trend to decrease in cell viability while increasing the dose of ruxolitinib at 48- and 72-hours time points with no obvious changes at a 24-hours time point. There is no significant difference in cell survival between 0.5μM and VC at the three defined time points (Figure 5-4).

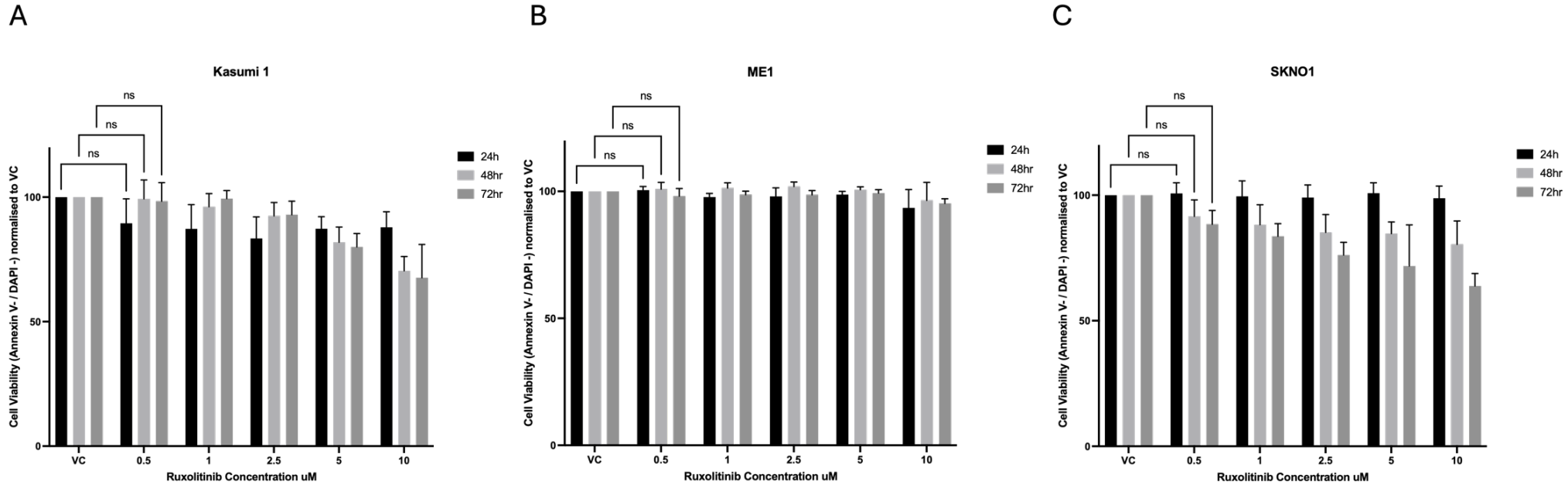

Figure 5-4 Cytotoxic effect of ruxolitinib on Kasumi-1, ME-1, SKNO-1 cell viability at 24, 48, and 72 hours time points.
Apoptosis assay (Annexin-V/DAPI) showed the cytotoxic effect of different doses of ruxolitinib on (A) Kasumi-1 cell line, (B) ME-1 cell line, (C) SKNO-1 at 24, 48 and 72 hours. Each bar represents the mean ± S.D of three independent experiments n=3. There was no statistical significance using one-way ANOVA with Tukey's multiple comparisons test. VC; vehicle control.

5.3.4 Ruxolitinib and Ara-C have no cytotoxic synergistic effect in LC on AML cell viability

From the previous experiments, it was shown that ruxolitinib could inhibit JAK-STAT signalling (pS-STAT3) stimulated either by exogenous IL-6 or CC and has no cytotoxic effect on AML cell viability. However, to investigate whether inhibition of JAK-STAT signalling within CC affected cell viability, we first examined any co-operative effect in LC to see if ruxolitinib has a role in decreasing AML cell viability in absence of JAK-STAT stimulation by CC.

Using the Kasumi-1 cell line, apoptosis assay (Annexin-V/DAPI) showed that there were no significant changes when adding ruxolitinib (0.5μM) to EC_{50} Ara-C (150nM) in LC; 50 per cent of Kasumi-1 cells were lost. Hence, when ruxolitinib was added to EC_{50} Ara-C, and cell viability didn't change, this inferred that the killing effect was only because of Ara-C (Figure 5-5).

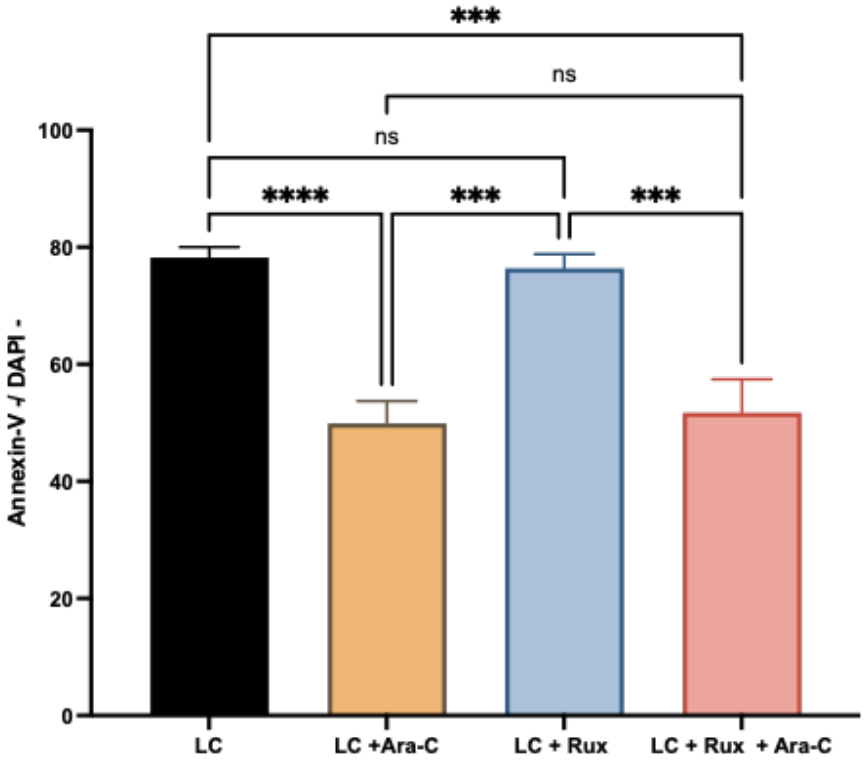

Figure 5-5 Ruxolitinib doesn't decrease Kasumi-1 cell viability when added to LC with EC_{50} Ara-C at a 48-hours time point.
Apoptosis assay (Annexin-V/DAPI) didn't show a decrease in cell survival after adding ruxolitinib (0.5μM) to Ara-C (150nM) in LC for 48 hours. Each bar represents the mean ± S.D of three independent experiments n=3, and ***P < 0.001, ****P < 0.0001 are considered statistically significant using one-way ANOVA with Tukey's multiple comparisons test.

5.3.5 HS5 cells are unaffected by ruxolitinib and Ara-C

After proving that ruxolitinib did not augment the killing effect of Ara-C, we needed to make sure that ruxolitinib did not affect HS5 cell viability. This was to confirm that any decrease of cell viability in CC is related to JAK-STAT signalling inhibition and not to a decrease in HS5-mediated protection through the killing of the stromal cells by ruxolitinib or Ara-C.

In this experiment, Kasumi-1 and HS5 cells were cocultured, HS5 were trypsinized and collected after 48 hours of culture; HS5 cells were separated from Kasumi-1 cells using their CD73 expression. CD73-positive cells were then investigated using apoptosis assay (Annexin-V/DAPI).

The result showed that Ara-C (150nM; EC_{50} in Kasumi-1) had no killing effect on HS5 cells. However, ruxolitinib (0.5μM) had a minimal killing effect on HS5, but without reaching a statistical significance compared to absence of ruxolitinib (Figure 5-6).

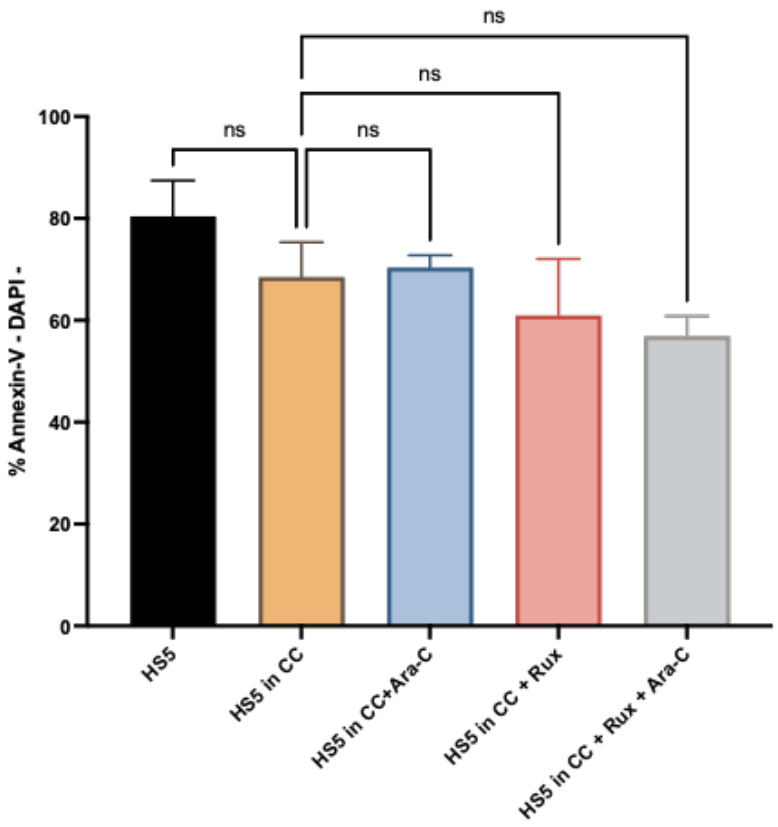

Figure 5-6 Ara-C and ruxolitinib do not kill HS5 cells after coculturing with Kasumi-1 cell line for 48 hours.
Apoptosis assay shows HS5 cells within the CC system aren't affected by Ara-C (150nM) or ruxolitinib (0.5μM). Each bar represents the mean ± S.D of three independent experiments n=3. There was no statistical significance using one-way ANOVA with Tukey's multiple comparisons test.

5.3.6 The JAK1/2 inhibitor ruxolitinib abrogates HS5-mediated chemoprotection in Kasumi-1 cell line

From previous experimentation, the lowest concentration that could inhibit the JAK-STAT pathway was found to be 0.5μM of ruxolitinib. This specific concentration was proven to have no cytotoxic action against AML cells in LC or stromal cells cultured alone. Hence, there was confidence that any biological activity noticed in subsequent experiments within the CC system would be owing to the inhibition of the JAK-STAT signalling pathway.

Next, inhibiting JAK-STAT signalling using ruxolitinib would be investigated on Kasumi-1 survival and whether using it would increase sensitivity to the standard chemotherapeutic drug, Ara-C.

It was noticed that in the Kasumi-1 cell line, there was a significant difference in cell viability using apoptosis assay (Annexin-V / DAPI) between LC with and without Ara-C ($p=0.0099$, $n=3$) when EC_{50} of the drug was used, which will be used as control for the CC system. No significant difference between CC with and without Ara-C was identified, suggesting the CC system provides chemoprotection against Ara-C. After adding ruxolitinib to Ara-C, there was a significant difference in Kasumi-1 survival in CC compared to ruxolitinib alone ($p=0.0026$, $n=3$). Moreover, there was a significant difference regarding Kasumi-1 cell viability between CC with Ara-C alone and CC with ruxolitinib and Ara-C ($p=0.021$, $n=3$). (Figure 5-7). Conditions of LC with ruxolitinib and with both ruxolitinib and Ara-C weren't included in this experiment as they were studied before (Figure 5-4, Figure 5-5).

Cell cycle analysis confirmed the results of the apoptosis assay; it was noticed that there is a significant increase in subG1 in all conditions with Ara-C compared to conditions without Ara-C. However, the degree of significance varied among them. Adding Ara-C to LC showed a highly significant difference compared to LC without Ara-C ($p= < 0.0001$, $n=3$). In CC the significance between Ara-C and no-Ara-C condition was less profound than that found in LC ($p=0.0241$, $n=3$). However, adding both ruxolitinib and Ara-C to CC resulted in highly significant apoptosis as compared to CC with ruxolitinib alone with a marked increase in the subG1 fraction ($p= < 0.0001$, $n=3$) (Figure 5-8).

Proliferation (CTV) assay was performed on the same conditions to determine how cells responded to adding the drug. It was noticed that Ara-C and ruxolitinib within the LC system inhibited cell proliferation but without significant difference compared to LC without drugs. In the CC system, Ara-C and ruxolitinib inhibit cell proliferation when applied on their own. However, adding ruxolitinib with Ara-C magnified the inhibition effect resulting in a highly significant difference compared to CC without drugs ($p=0.008$, $n=3$) (Figure 5-9).

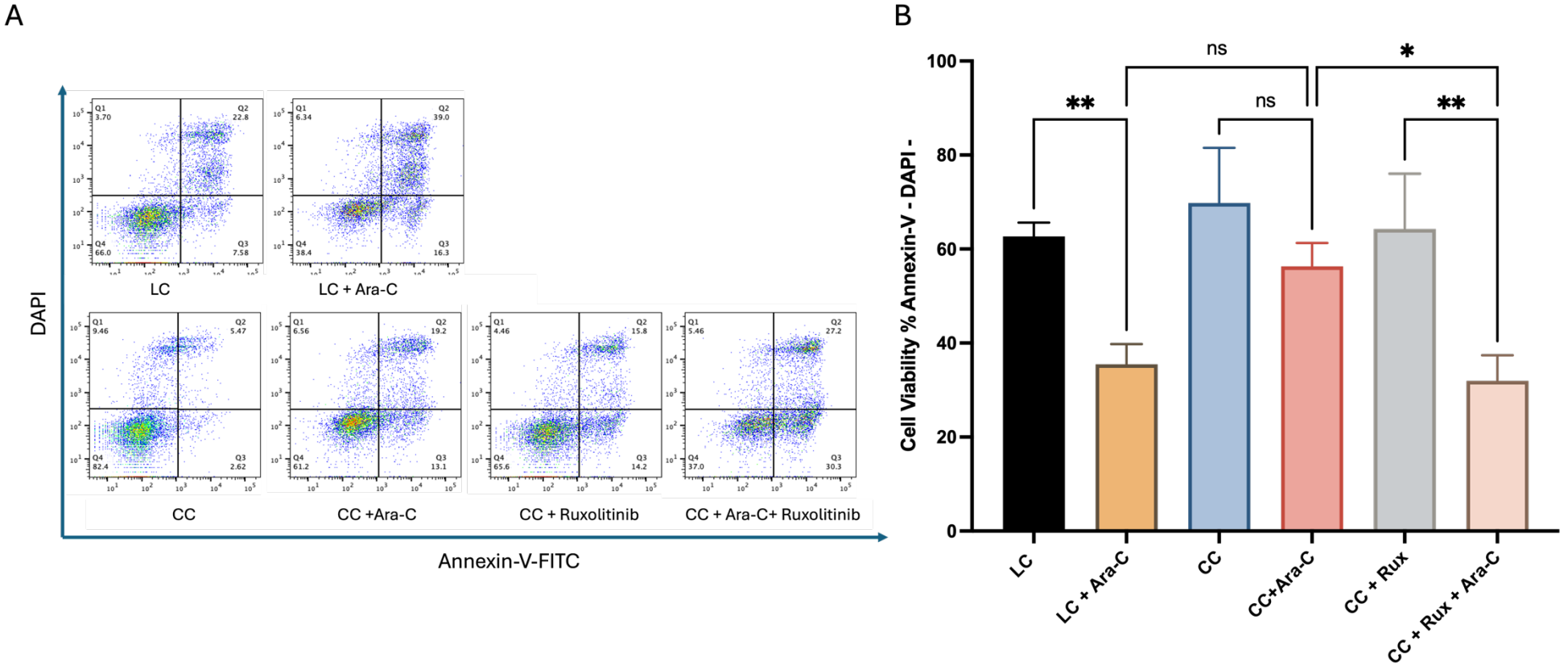

Figure 5-7 Ruxolitinib can abolish HS5-mediated chemoprotection.
(A) Representative flow cytometry dot plots showing apoptosis with Annexin-V/DAPI in liquid culture (LC) and coculture (CC) with and without Ara-C (150nM) and ruxolitinib (0.5μM). (B) Percentage of viable cells (Annexin-V - / DAPI -) in LC versus CC with and without Ara-C and ruxolitinib, n=3. *$P < 0.05$, **$P < 0.01$ are considered statistically significant using one-way ANOVA with Tukey's multiple comparisons test. Error bars indicate the standard error for 3 biological replicates of each sample n=3, mean ± SD.

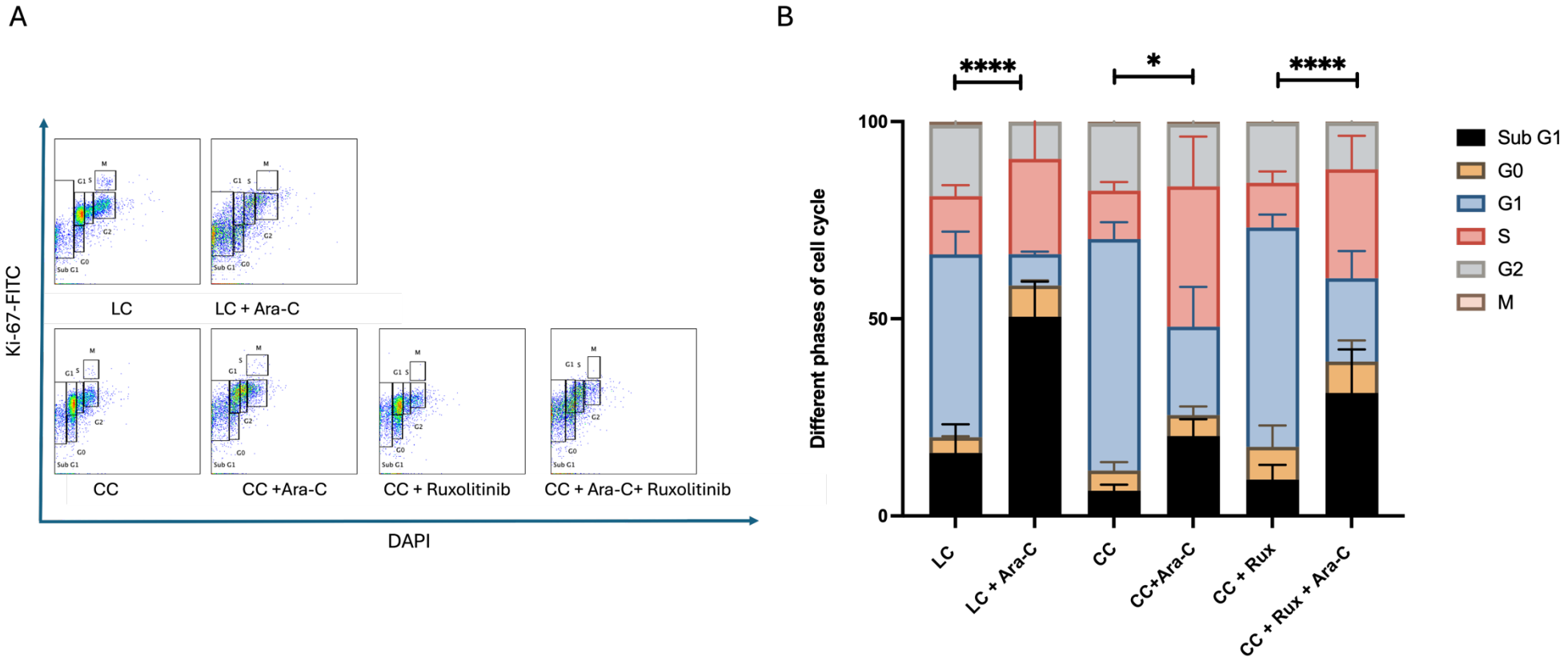

Figure 5-8 Cell cycle analysis shows that ruxolitinib abrogates HS5-mediated chemoprotection.
(A) Representative flow cytometry dot plots showing cell cycle with Ki-67/DAPI in liquid culture (LC) and coculture (CC) with and without Ara-C (150nM) and ruxolitinib (0.5μM). (B) Percentage of different phases of the cell cycle in LC versus CC with and without Ara-C and ruxolitinib, (significance over the graph related to subG1 only; n=3). *P < 0.05, ****P < 0.0001 are considered statistically significant using two-way ANOVA with Tukey's multiple comparisons test. Error bars indicate the standard error for three biological replicates of each sample, n=3, mean ± SD.

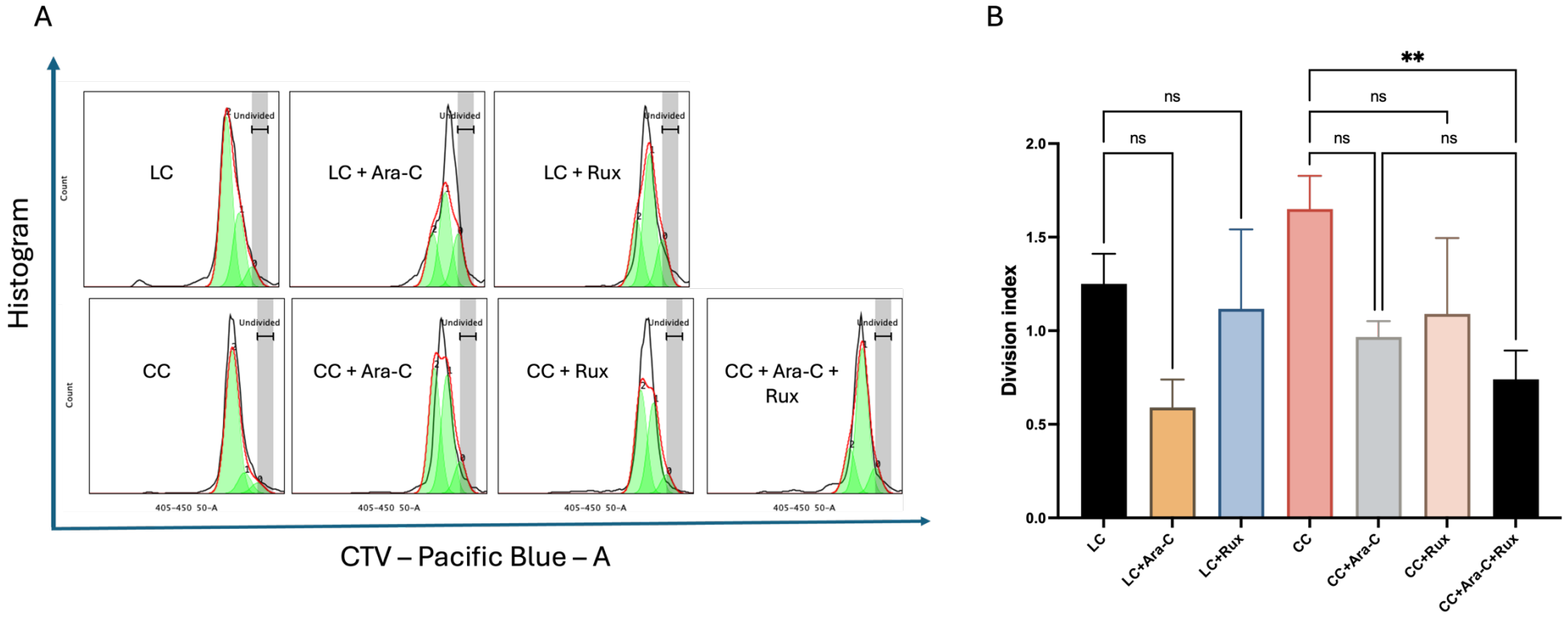

Figure 5-9 Ruxolitinib has a co-operative effect on cell proliferation inhibition by Ara-C within the CC system.
(A) CTV assay showed a histogram of cell proliferation in LC and CC with and without drugs. (B) The graph shows the division index of the Kasumi-1 cell line in LC and CC with and without (150nM) Ara-C and (0.5μM) ruxolitinib, n=3. $^{**}P < 0.01$ is considered statistically significant using one-way ANOVA with Tukey's multiple comparisons test, ns=non-significant. Error bars indicate the standard error for 3 biological replicates of each sample n=3, mean ± SD.

5.3.7 AML cell interaction with BMSC has a role in stimulating JAK-STAT signalling that may be inhibited by ruxolitinib

From a previous experiment, it was found that ruxolitinib could overcome stroma-induced apoptosis inhibition. It was inferred that the apoptosis inhibition was related to JAK-STAT signalling pathway activation within the CC system. However, we needed to know whether the stimulation of the pathway was owing to cytokines and chemokines in HS5 supernatant, or the cell interaction between AML and stromal cells.

A transwell (TW) assay was introduced in the next experiment using a permeable membrane that allows cytokines and chemokines to pass freely between AML and stromal cells without direct cell contact.

Apoptosis and cell cycle analyses were done on LC, as control, and CC using TW; Ara-C and ruxolitinib were applied to see their effect on apoptosis and cell cycle.

It was noticed that there was a statistically significant difference between CC with Ara-C and ruxolitinib compared to CC with ruxolitinib alone ($p=0.0489$, $n=3$).This degree of significance was lower than the degree of significance in the experiment without TW assay ($p=0.0241$) in Figure 5-7. Ruxolitinib may work better when cells interact, indicating that cell-to-cell contact has a vital role in stimulating the JAK-STAT signalling pathway, and ruxolitinib could overcome apoptosis inhibition caused by JAK stimulation (Figure 5-10).

In cell cycle analysis, all subG1 phases in conditions with Ara-C were compared, and it was noticed that CC with Ara-C showed a significant decrease in subG1 compared to LC with Ara-C ($p=0.01$, $n=3$). However, no significant difference was noticed after adding ruxolitinib to the Ara-C within the CC system (Figure 5-11).

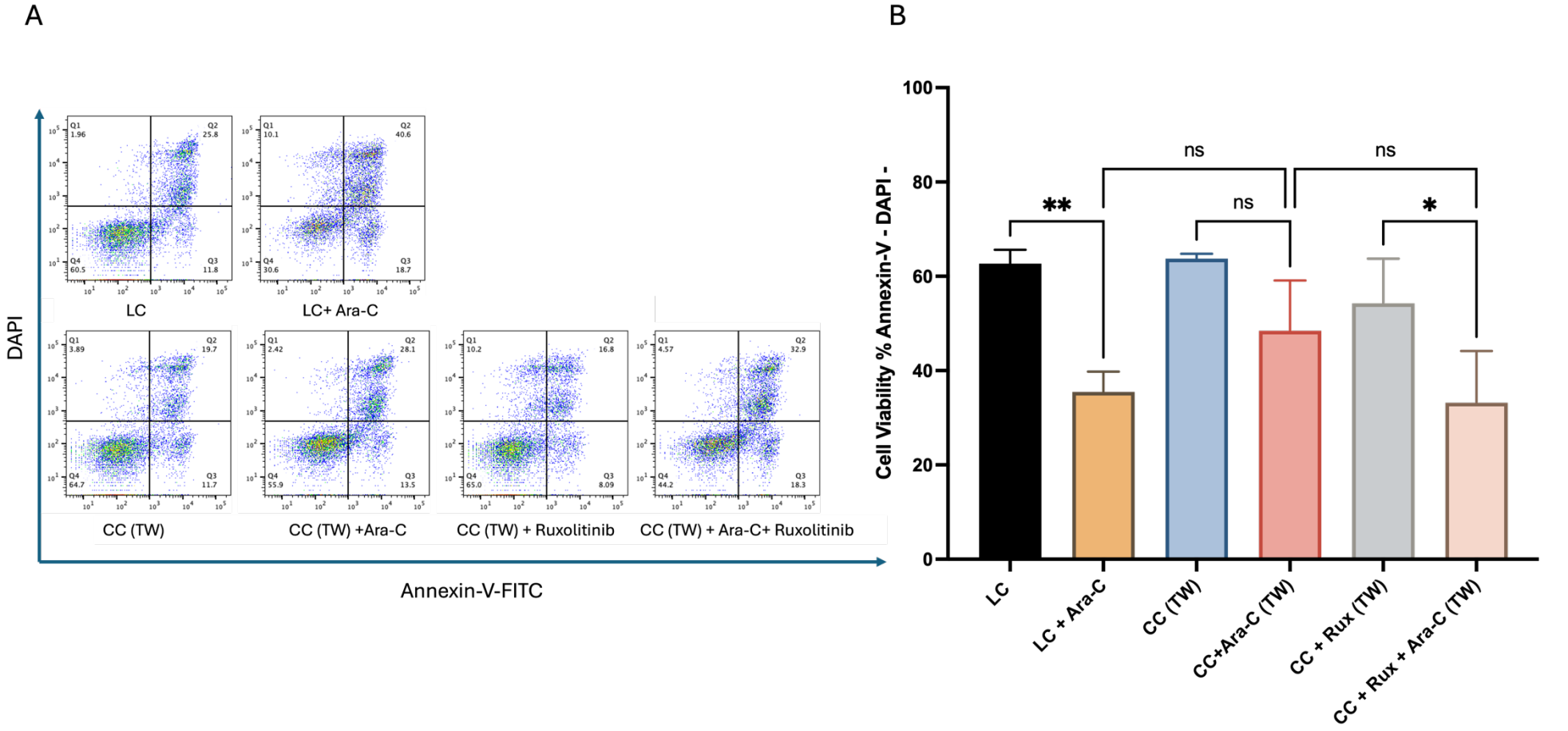

Figure 5-10 Ruxolitinib abolished HS5 supernatant-mediated chemoprotection.
(A) Representative flow cytometry showing apoptosis with Annexin-V/DAPI in LC and CC supernatant using transwell assay (TW) with and without Ara-C and ruxolitinib. (B) Percentage of viable cells (Annexin-V - / DAPI -) in LC Vs CC supernatant using TW with and without Ara-C and ruxolitinib n=3. *$P < 0.05$, **$P < 0.01$ are considered statistically significant using one-way ANOVA with Tukey's multiple comparisons test. ns=non-significant. Error bars indicate the standard error for 3 biological replicates of each sample n=3, mean ± SD.

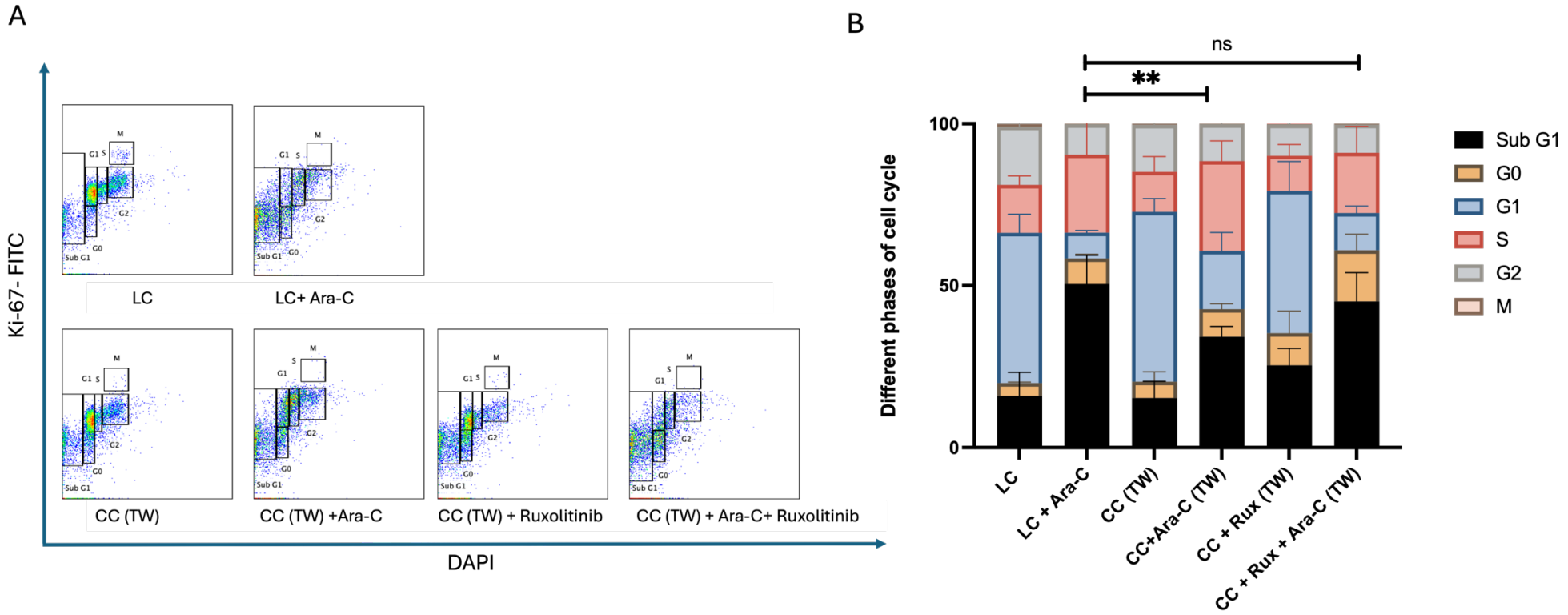

Figure 5-11 Cell cycle analysis shows that ruxolitinib abrogated HS5 supernatant-mediated chemoprotection.
(A) Representative flow cytometry dot plot showing cell cycle with Ki-67/DAPI in LC and CC using transwell with and without Ara-C and ruxolitinib. (B) Percentage of different phases of the cell cycle in LC Vs CC without cell contact with and without Ara-C and ruxolitinib, (significance star over the graph related to subG1 only) n=3. $^{**}P < 0.01$ is considered statistically significant using two-way ANOVA with Tukey's multiple comparisons test. Ns=non-significant. Error bars indicate the standard error for 3 biological replicates of each sample n=3, mean ± SD.

5.3.8 Ruxolitinib can abolish primary paediatric stromal-mediated protective effect

The next step in the investigation was to compare AML paediatric stromal cells to HS5 (adult) cell line to see if the same protective effect was present and whether ruxolitinib was able to abolish primary BMSC-mediated protection. The Kasumi-1 cell line was cocultured with two different paediatric (P-) AML BMSC samples, isolated from two AML paediatric patients (pAML022 and pAML026)

Using Annexin-V / DAPI apoptosis assay, it was noticed that CC of Kasumi-1 with paediatric AML (pAML) stromal cells had minimal protection against Ara-C in direct contact showing a significant difference between LC + Ara-C and CC + Ara-C. However, this protection wasn't present when using TW assay. In direct contact, ruxolitinib minimally inhibited stromal cell-mediated protection that didn't reach a level of significance between CC + Ara-C or CC + Rux + Ara-C. However, in TW assay, where there is no direct contact between AML cells and stromal cells, there was no AML stromal cell-mediated protection against Ara-C, with no added effect of ruxolitinib (

Figure 5-12).

Cell cycle analysis confirmed the results of the apoptosis assay. In direct contact conditions there was a decrease in subG1 (representing the apoptotic phase), in CC + Ara-C compared to LC + Ara-C but without significant difference between the two conditions. There was a trend toward increased subG1 fraction when adding ruxolitinib to Ara-C in the CC condition. Other than subG1, there was no noticeable difference among all conditions regarding cell cycle phases (Figure 5-13 A).

In the TW assay, there is no significant difference in cell cycle phases among all culture conditions explored (Figure 5-13 B).

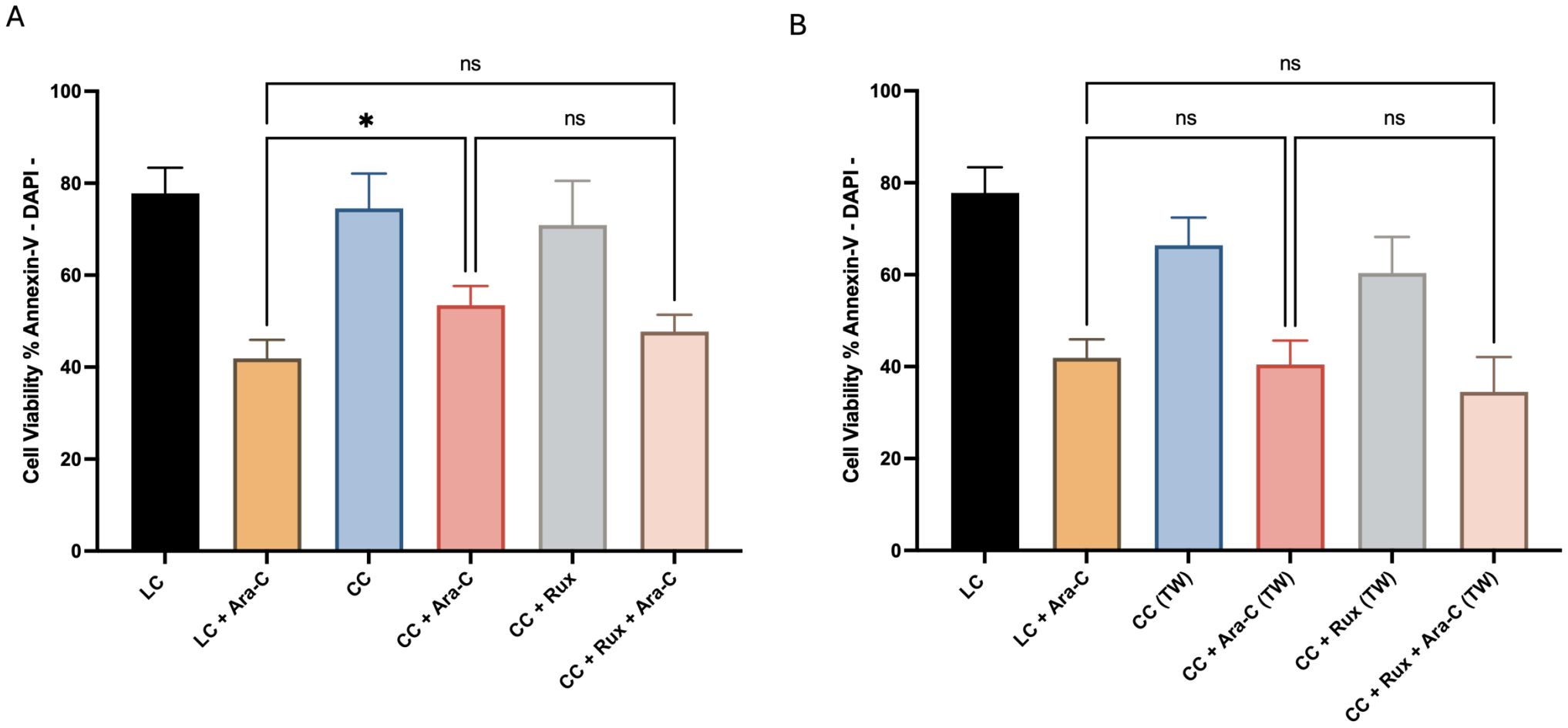

Figure 5-12 Ruxolitinib cannot eliminate paediatric bone marrow stromal cell-mediated chemoprotection when in direct contact with Kasumi-1 cell line.
(A) Apoptosis assay (Annexin-V / DAPI) shows cell viability percentage in LC and CC with and without Ara-C and ruxolitinib in direct contact. (B) Transwell assay. n=6. *$P < 0.05$, is considered statistically significant using one-way ANOVA with Tukey's multiple comparisons test. Error bars indicate the standard error for three biological replicates of each sample over 2 pAML stromal cell lines n=3, mean ± SD.

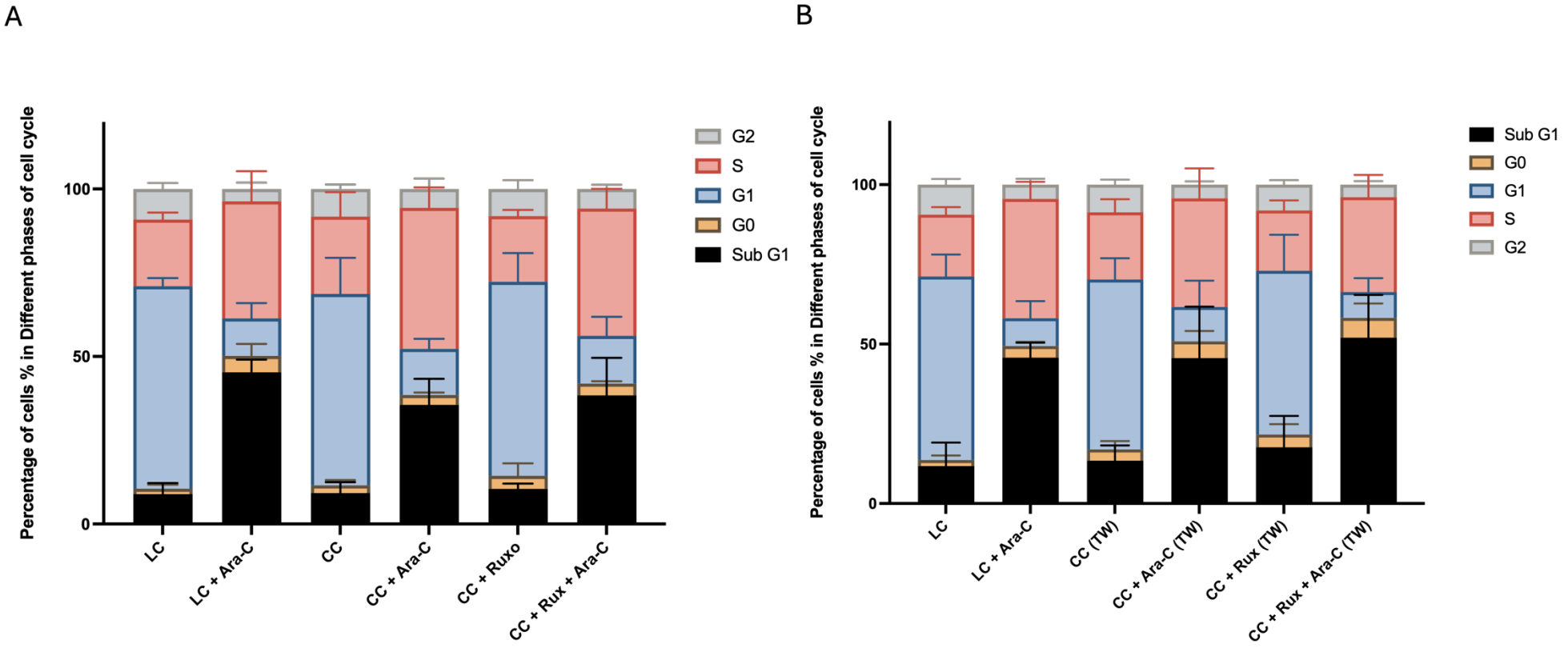

Figure 5-13 Paediatric AML bone marrow stromal cells have a very minimal protection effect on Kasumi-1 cell line against Ara-C when in direct contact condition.

(A) Cell cycle assay shows percentage of different phases of cell cycle in LC and CC with and without Ara-C and ruxolitinib in direct contact. (B) Transwell assay (TW); n=4. There was no statistical significance using two-way ANOVA with Tukey's multiple comparisons test. Error bars indicate the standard error for 2 biological replicates of each sample over 2 pAML stromal cells n=3, mean ± SD.

5.4 Discussion

Within this chapter, we concentrate on studying the interplay between JAK-STAT signalling activation and chemoresistance provided by stromal cells. As shown in the last chapter, dasatinib, an SRC/ABL inhibitor, could abolish the chemoprotective effect of stromal cells on the adult AML cell line ME-1 without showing a significant difference in ME-1 cell viability using apoptosis assay (Annexin-V/DAPI) between adding dasatinib to Ara-C and adding Ara-C alone. It was necessary to investigate the main signalling pathway which IL-6 activates and examine how effective inhibition of this signalling was in abrogating the chemoprotective effect of BMSC.

In the last chapter, we chose ME-1 cell line to examine as this was the only cell line that showed a statistical difference between LC and CC regarding *SRC* gene and protein expression. However, in this chapter, we used the Kasumi-1 cell line to represent paediatric AML as the ProcartaPlex™ findings with this cell line showed that IL-6 was present in CC in a high concentration compared to LC (p=0.0277, n=3) and HS5 cultured alone. Moreover, previous data showed an increased concentration of IL-6 in CC compared to LC in the primary paediatric AML samples (Laing et al., 2025).

Before testing any drug and its role in overcoming resistance to apoptosis in the Kasumi-1 cell line, we needed first to confirm that either adding exogenous IL-6 to LC or the CC system was able to stimulate JAK-STAT signalling and phosphorylate STAT3 that will then act as a transcription factor inside the nucleus, driving proliferative and survival gene expression.

The results showed that the CC system phosphorylated STAT3 (Y705) with a statistically significant difference compared to autophosphorylation in LC. However, adding exogenous IL-6 didn't reach the same level of phosphorylation. This could be explained by the co-operation of multiple cytokines and chemokines secreted by HS5 that can stimulate JAK-STAT signalling and phosphorylate STAT3.

Our results were found to be in agreement with a study tested the effect of HS5 conditioned medium (CM) and exogenous cytokines secreted by HS5, such as G-CSF, GM-CSF, IL-6, and IL-8, on the phosphorylation of different signalling

pathways in primary AML patient samples (pERK, pAkt, p-STAT3, and p-STAT5). They found that HS5 CM, as well as G-CSF and GM-CSF, have the potential to induce STAT-5 phosphorylation in three patient samples. However, in our study, STAT-3 was chosen as it is the main downstream signalling molecule stimulated by Jak1/2 and inhibited by ruxolitinib, which is the core drug of our study. Taken together, it was found that IL-6, although it phosphorylates STAT-3, is not the primary cytokine present in HS5 compared to other cytokines or the HS5 CM (Karjalainen et al., 2017).

The next step was to determine the ideal ruxolitinib concentration for use in further experiments. Two ways to detect the optimum usable concentration of the drug: the $IC_{50,}$ which inhibits 50% phosphorylation, and the second way to determine the minimum concentration that could be used to fully inhibit the phosphorylation. Normally, IC_{50} should be used when comparing the potency of inhibitors, however, here, it was necessary to completely inhibit phosphorylation of STAT3 to accurately know how the stimulation of JAK-STAT signalling plays a role in providing chemoresistance.

Based on a study (Habbel et al., 2020) that used ruxolitinib in *ex-vivo* experiments, different concentrations were chosen across a range, and it was found that 0.5μM was the minimum concentration tested that was able to fully inhibit STAT3 phosphorylation.

To investigate the effect of ruxolitinib on AML cell line survival and whether adding this drug to standard chemotherapy would potentiate its action, many factors needed to excluded. Firstly, ruxolitinib shouldn't kill AML cells on its own to make sure that the adjuvant effect was related to JAK-STAT inhibition rather than broad cytotoxic properties of the drug. Secondly, ruxolitinib shouldn't have any synergistic effect to standard chemotherapy in LC, as our study concentrates on abolishing the CC chemoprotective effect. Thirdly, ruxolitinib shouldn't have any cytotoxic action on HS5 cells as well as Ara-C, because killing stromal cells means that the drug works through its cytotoxic properties, not through JAK-STAT signalling inhibition.

In the previous result section, all three factors, cytotoxic effect on AML cells in LC, cytotoxic action on HS5, and synergistic action with Ara-C on AML cells, were

assayed using apoptosis assay (Annexin-V / DAPI stain) which showed that ruxolitinib had no cytotoxic action on Kasumi-1 cell line in LC condition (Figure 5-4), had no synergistic effect when added to Ara-C (at its EC_{50}) in LC (Figure 5-5), and had no cytotoxic activity on HS5 (Figure 5-6). Similar results were seen for Ara-C (Figure 5-6). From all previous results, any elimination of chemoprotective action provided by stromal cells within the CC system would be solely inferred to be through inhibition of JAK-STAT pathway signalling activation.

To investigate the role of ruxolitinib on Kasumi-1 cell survival, apoptosis assay (Annexin-V/DAPI) was performed and showed that while Ara-C killed 50% of cells within LC as predicted at its EC_{50}, the concentration couldn't kill the same percentage within the CC system, supporting the findings from the first results chapter that HS5 provide some chemoprotection to Kasumi-1 cells (Figure 3-3,Figure 3-4). Adding ruxolitinib to Ara-C in CC decreased AML cell viability by nearly 50%, indicating that ruxolitinib could abrogate the HS5-mediated chemoprotection. Adding ruxolitinib in combination with Ara-C in CC killed nearly the same percentage of cells as Ara-C alone in LC, indicating that ruxolitinib, as a JAK inhibitor, could be used with standard chemotherapy to eliminate BMSC-mediated microenvironment protection.

To confirm the apoptosis result and know more about the behaviour of the cells, cell cycle analysis was done. SubG1 cells, representing the apoptotic cells, confirmed what the apoptosis assay demonstrated regarding ruxolitinib ability to eliminate CC-mediated chemoresistance.

On the other hand, it was noticed that the G2 phase within the CC condition with Ara-C didn't change compared to without Ara-C, although Ara-C likely stopped DNA replication during the S phase of the cell cycle, leading to an increase in the percentage of S phase at the expense of G2 phase. With no change in G2 within CC with Ara-C compared to CC alone, cells preserve the ability to proliferate in the presence of Ara-C. Adding ruxolitinib to Ara-C (minimally) decreased the percentage of G2, suggesting that ruxolitinib may have a role in decreasing cell proliferation.

CTV cell proliferation tracking assay was done to assess the proliferation status within the CC system and to compare it to the LC condition. The result showed

that although Ara-C and ruxolitinib were able to decrease cell proliferation in both LC and CC, both drugs' activity didn't reach statistical significance compared to the no drug control. However, adding ruxolitinib to Ara-C within the CC system significantly decreased cell proliferation. Unfortunately, we can't relate the effect of ruxolitinib to overcoming HS5-mediated chemoresistance as the experiment missed the condition of adding ruxolitinib to Ara-C within the LC system, which might show a significant decrease of cell proliferation implying no role in abolishing the chemoprotective action of the CC.

Transwell assay was applied to investigate the role of direct cell-to-cell contact versus role of secreted cytokines between Kasumi-1 and HS5 cells in stimulating the JAK-STAT signalling pathway and its effect on cell survival. It was found that ruxolitinib has a profound killing effect when applied to Kasumi-1 cells in direct contact with HS5 compared to no cell-to-cell contact (transwell). This suggests that direct contact between the cells has a role in stimulating JAK-STAT signalling as well as cytokines and chemokines, including IL-6, secreted by HS5. Moreover, it was noticed that cell viability during direct contact was better than their corresponding conditions after using transwell assay, indicating that direct cell-to-cell contact between cells plays a vital role in increasing AML cell viability. However, adding ruxolitinib to Ara-C resulted in a profound decrease in cell viability within the direct contact condition compared to the non-contact transwell experiment, suggesting that ruxolitinib was able to completely inhibit JAK-STAT signalling stimulation through inhibition of STAT3 Y705 phosphorylation by flow cytometry showed in (Figure 5-3) which has an important role in maintaining cell viability within CC with direct contact.

All the previous experiments used the HS5 cell line representing normal bone marrow stromal cells. Some studies showed that AML infiltration changes the bone marrow microenvironment, including stromal cells to act as a refuge for AML cells from chemotherapy, and in vitro 3D culturing of AML cells with AML BMME showed more resistance to chemotherapy than AML cells cultured with healthy BMME (Cheung et al., 2025; Civini et al., 2013). Stromal cells from an infiltrated leukaemia bone marrow niche needed to be examined for their protective role against AML standard chemotherapy. Two BMSC samples isolated from two different pAML patients were used in CC with Kasumi-1 cell line to compare the

protective action of both samples to the HS5 cell line, and to see whether ruxolitinib exerted the same effect on them as on HS5.

It was noticed that the CC system using pAML samples didn't provide the same level of protection as HS5 in the direct contact assay and the CC system didn't protect Kasumi-1 cell line when cocultured using transwell assay. There may be questions around testing an immortal cell line with primary patient stromal cells, or discrepancy may be owing to the ratio between stromal cells and Kasumi-1 cell line that could be increased from 1:2 to 1:1 when primary bone marrow support material is used. One study showed how increasing the ratio of HS5 to Kasumi-1 cells resulted in decreasing early apoptosis, suggesting that the ratio between AML cells and stromal cells has a vital role in providing chemoresistance (Yu et al., 2023). Further experiments should be done to investigate why the HS5 cell line could provide chemoprotection against the AML cell line, although patient stromal cells isolated from AML patient samples couldn't provide the same level of protection.

Based on the difference between immortalised cells like HS5 and primary stromal cells, we can hypothesise why HS5 could provide more protection to AML than primary AML stromal cells. In vitro uses of primary cells will lead to continuous loss of proliferation and premature senescence despite preserving its viability and metabolism, on the other hand, immortalised cells kept proliferating, leading to reduced senescent status, which is suggested to be favourable regarding AML survival (Y. Wang et al., 2019).

Immortalised HS5 is thought to secrete more cytokines than primary cells; this may be referred to as genetic engineering of the cell line that exhibits a higher synthetic and metabolic activity with a consistent ability to proliferate. Due to active growth and proliferation of the cell line, some cytokines related to growth and proliferation might be secreted in a higher concentration compared to primary AML cells as IL-6 and GM-CSF, which were found to be highly secreted in HS5 in our ProcartaPlex™ results (Figure 3-6) (

Figure 3-10). As we try to elucidate the role of those cytokines in providing AML cell viability, HS5-mediated protection, which is higher than primary AML stromal cells, could be explained. So, primary stromal cells, either from healthy donors or

from AML patients, need to be compared with the HS5 cell line regarding cytokine secretion.

Another hypothesis that might be related to why primary AML stromal cells didn't provide full chemoprotection as HS5 did is that the culture was between AML cell lines with primary AML stromal cells, not primary AML cells. This means, as we discussed before, that AML cell lines could be more proliferative and resistant to chemotherapy than primary AML cells, and this results in primary AML stromal cells not conferring the same level of protection as HS5. So, it is important that primary AML cells should be cultured with primary AML stromal cells, and all results should be compared with the AML cell line cultured with the HS5 cell line.

As the level of protection provided by patients' stromal cells was not significant, especially within the transwell assay, investigating the role of ruxolitinib in providing chemosensitivity and increasing survival was difficult. Ruxolitinib showed a trend toward decreased leukaemia cell viability within direct cell-to-cell contact (to primary paediatric AML stromal cells) assay. However, the result was not as significant as using HS5.

In summary, ruxolitinib eliminated the chemoprotective effect mediated by human immortalised HS5 stromal cell line; this effect needed more investigation with patient stromal cells. Patient BMSC samples were investigated in comparison to HS5 to see whether the addition of ruxolitinib could restore Kasumi-1 chemosensitivity. Direct contact between AML cells and stromal cells within BMME has a vital role in providing chemoprotection against standard chemotherapy, and ruxolitinib works better to reverse this within a cell-to-cell contact environment in our *in vitro* modelling.

6 General Discussion and Future Work

AML is a heterogeneous leukaemia, predominantly a disease of the elderly, but affecting both adults and children. It is characterised by various cytogenetic abnormalities and mutations (Snaith et al., 2024). Furthermore, the patient's responses to standard chemotherapy, their underlying co-morbidities and the prognosis of different AML sub-types add to this heterogeneity. Conversely, chemoresistance and relapse occur in a high percentage of patients, is a critical area of unmet clinical need and requires further study urgently. Consequently, a deeper understanding of the disease's pathogenesis is essential, and personalised medicine will be necessary to treat those patients (Neoplasia, 2015). Another approach to combating the disease is to target any support mechanisms of leukaemia, e.g. the leukaemic niche, that aid in the growth, proliferation, and survival of leukaemia cells (Mukherjee & Sekeres, 2019).

The core of this thesis is trying to understand and delineate the role of the BMME in providing AML chemoresistance and relapse. As discussed in the main introduction, the bone marrow niches, endosteal and vascular, confer chemoresistance to AML LSC through a series of modulations in stromal cells and in other BMME cells to help LSC escape all types of attack, such as chemotherapy and the immune system (Boutin et al., 2020; Hou et al., 2020; Konopleva et al., 2002; Long et al., 2015; Miari & Williams, 2024).

This chemoresistance manifested through the interplay between leukaemia and the BMME, cytokines and chemokines play a significant role in stimulating the signalling pathways that lead to survival and proliferation. Proliferative gene transcription and translation ultimately contribute to the growth of the LSC (Yao et al., 2021).

We found that stromal cells secrete a group of cytokines and chemokines that have a role in AML chemoresistance through various pathway stimulation. By targeting those pathways, we noticed that we could increase AML chemosensitivity to standard chemotherapy. This finding will lead to further study of the stromal cell secretome and its involved signalling pathways aiming to target them with adjuvant drugs which will be more effective and less cytotoxic.

This work fills the gap left by a former PhD student in our lab who found that culturing AML cells with stromal cells confers chemoresistance to standard chemotherapy (Laing, 2021). Using a ProcartaPlex™ immunoassay for supernatants and RNA sequencing for cells after culturing, multiple cytokines and chemokines, IL-6, VEGF-A, HGF, and SDF-1α, were present in higher concentrations during culturing cells with MSCs compared to the AML cells cultured alone (Laing et al., 2025). This raised questions regarding those specific cytokines and their role in providing chemoresistance and relapse.

All experiments described in this thesis were performed on cell lines with well described cytogenetic profiles to understand how different subtypes of AML are affected by manipulation of cytokines in the BMME. This was a critical step before undertaking further experiments on primary AML samples with a wide variety of AML cytogenetic abnormalities. By applying those cytokines (IL-6, VEGF-A, HGF, and SDF-1α) to the Kasumi-1 cell line, it was noticed that only IL-6 and, to a lesser extent, VEGF-A increased cell viability and decreased apoptosis. This led us to undertake further experiments to study more cytokines, and also confirm the results observed with IL-6 in the experiments described. Before using the Luminex® technique on different AML cell lines, it is essential to determine whether AML cell lines receive a protective effect from the stromal cell line HS5 or if they do not respond to its chemoprotective influence as the Luminex® technique will be used to screen cytokines produced by AML cell lines when cultured alone, in contact with HS5, or by HS5 alone. The goal is to correlate differences in cytokine levels across these conditions with the responsiveness of AML cells to HS5's protective effects.

A group of cell lines were chosen depending on the age of the patients to include both adults, the ME-1 cell line, paediatric, Kasumi-1 and THP-1, and adolescents, SKNO-1. Also, these cell lines were chosen to be classified into core binding factor leukaemia cell lines, Kasumi-1, ME-1, and SKNO-1 and non-core binding factor cell line, THP-1. All the chosen cell lines were tested for their response to the standard chemotherapy agent Ara-C after culturing them with HS5 cells, a healthy stromal cell line, to get more knowledge regarding which AML cell lines receive protection from HS5.

As we discussed in the first result chapter and based on the heterogeneity of AML, it was found that HS5 could confer chemoresistance and provide cell protection to Kasumi-1, ME-1, and THP-1, but no protection was provided to SKNO-1.

One core factor of AML heterogeneity is the protective effect received by the BMME. As we highlighted in the main introduction chapter, the BMME has a pivotal role in providing chemoresistance to AML. However, our experiments demonstrated that one cell line of AML, SKNO-1, didn't receive protection from the stromal cell line, HS5. Although SKNO-1, Kasumi-1, and ME-1 are core binding factor AML cell lines, and SKNO-1 and Kasumi-1 share the same cytogenetic abnormality, t(8;21), they didn't show the same response to HS5 mediated protection. This could suggest that there are different mechanisms of HS5-mediated protection unrelated to cytogenetic abnormalities. Hence, the study of the BMME secretome was identified as an important area for further study for elucidating chemoprotective mechanism.

The AML cell lines which showed to be chemoprotective, Kasumi-1, ME-1, THP-1, were used for cytokines screening by ProcartaPlex™ immune assay. The results of this ProcartaPlex™ assay will be used in future experiments to further investigate the prosurvival role of those cytokines found to be present in a higher concentration in coculture compared to LC or HS5 alone, such as GM-CSF and IL-2. These experiments will be performed on primary AML samples, aiming to block these cytokines using available drugs to validate the role of these cytokines on AML survival, proliferation, growth, and chemoresistance.

IL-6 is one of the most pro-inflammatory cytokines found within AML and secreted by both AML cells and MSCs (Saadi et al., 2021; Sanchez-Correa et al., 2013). Based on the finding that IL-6 provides AML chemoresistance and decreases AML apoptosis, this thesis discussed the signalling pathway stimulated by IL-6; either the classical pathway through JAK-STAT signalling or the non-canonical pathway through the SRC-YAP-CYR61 signalling axis.

Because IL-6 acts through classical and non-canonical pathways, both types of signalling pathways were under consideration for further investigation after confirming that the genes and proteins of these signalling pathways were

upregulated and overexpressed in the CC conditions compared to LC. This confirmed their role in providing chemoresistance to AML cell lines.

Two different FDA-approved drugs were chosen to be tested to understand their effect on AML: dasatinib, approved for CML, and ruxolitinib, approved for myelofibrosis (J. Mascarenhas & Hoffman, 2012). Ruxolitinib was chosen as a JAK inhibitor because it will stop JAK-STAT signalling stimulation produced by IL-6, while dasatinib was chosen because it is an SRC inhibitor for stopping SRC-YAP stimulation (Blake et al., 2008). Although the synergistic drug effect wasn't investigated, adding ruxolitinib to standard chemotherapy resulted in an increase in AML sensitivity to Ara-C and a statistical difference regarding cell viability between cells treated with Ara-C and ruxolitinib in combination compared to cells treated with Ara-C alone. However, adding dasatinib to the same culture conditions didn't show the same inhibitory effect as ruxolitinib.

It should be noted that the ruxolitinib was tested on the Kasumi-1 cell line only, a paediatric core-binding factor cell line as Kasumi-1 was the only cell line that showed response to IL-6 by decreasing the percentage of cells in late apoptosis by Annexin/ DAPI; this was considered a surrogate for improved cell survival. However, dasatinib was tested on the ME-1 cell line, an adult core binding factor cell line as ME-1 is the only cell line that showed SRC upregulation in CC compared to LC. Variation in results between ruxolitinib and dasatinib might be due to the different cell lines used or to the effects of the signalling pathway being studied, as JAK-STAT signalling is the main pathway stimulated by IL-6 and as IL-6 was found to affect AML cell apoptosis in the Kasumi-1 cell line, so ruxolitinib showed better result than dasatinib.

Unfortunately, IL-6 prosurvival role wasn't tested on the ME-1 cell line. Instead, SRC gene expression was tested and was found to be upregulated in CC in the ME-1 cell line, so dasatinib was used to further investigate the SRC-YAP-CYR61 in the ME-1 cell line. Although dasatinib didn't show the effective action that was hypothesised regarding abolishing chemoprotection provided by stromal cells, the drug should be the subject of further study in AML as it shows a decrease in growth in the SKNO-1 cell line bearing the c-KIT mutation (Heo et al., 2017). Investigating the effect of dasatinib on more AML cell lines to further elucidate its mechanism of action to treat AML is required, especially with recent publication showing the

promising therapeutic approach in treating core binding factor AML (Srinivasan, 2024).

Moreover, heterogeneity between AML subtypes and between different age groups should be counted toward different cell behaviours to different drugs. Indeed, precision medicine should be a key aim nowadays because of the complex heterogeneity among AML cases.

For an understanding of the mechanisms through which the BMME confers chemoresistance, experiments were done to elucidate the role of cell-to-cell contact and whether this chemoprotection is related solely to cytokine and chemokine secretion or whether the contact between cells plays a role.

Experiments were based mainly on comparing LC and CC to investigate the role of BMME cells and their secretome. Another technique which we could have considered is to use the conditioned medium produced from culturing stromal cells alone. This method was used in a study, demonstrated that stromal cells promote the expression of S100A8/A9 through both cell-to-cell contact-dependent and contact-independent mechanisms (Böttcher et al., 2022). However, using a semipermeable membrane (transwell assay) and direct cell-to-cell contact were enough to prove the role of cell-to-cell contact and validate the effect of cytokines and chemokines presented in the media surrounding the cells. It was noticed that the chemoprotection provided through cell-to-cell contact is better than through non-contact-dependent mechanisms. However, there was a protection effect in both conditions, suggesting that secretome and direct contact have a role in providing chemoresistance.

One study noticed that stromal cells could confer chemoresistance, this chemoresistance was referred to stroma-dependent ABC transporter activation after direct contact between leukaemia blast cells and stromal cells isolated either from a healthy donor or leukaemia patients (Boutin et al., 2020). This highlights another research gap, which needs to be filled regarding what is the main mechanism responsible for providing chemoresistance and driving or contributing to relapse of AML.

Future work will be based on exploring the heterogeneity of AML, focusing on the mechanism of BMME-dependent chemoresistance and trying to identify further FDA-approved drugs with fewer side effects, which alter the BMME in AML, and could be used for future clinical trials to improve the treatment and outcomes of AML. Based on the results of the ProcartaPlex™ showing that GM-CSF and IL-2 were present in a higher concentration in CC compared to LC, a proposal of research was developed to investigate the role of GM-CSF as a cytokine which contributes to chemoresistance, and whether blocking its action using a targeted drug, such as mavrilimumab, could abolish stromal cell-dependent chemoresistance. GM-CSF works through three different signalling pathways, PI3K-AKT, JAK-STAT5, and RAS-MAPK-ERK and is thought to have a dual effect regarding its role in AML survival and proliferation which need to be further elucidated (Faderl et al., 2003; A. Kumar et al., 2022).

Moreover, a massive effort should be put towards precision/personalised medicine to select the most effective drug suitable for each patient. The new era of personalised medicine is targeting the patient genome, not the leukaemia itself, so BMME could be targeted to prevent its transformation into a leukaemia-permissive microenvironment, helping leukaemia cells to survive and grow.

Future work should incorporate advanced 3D *in vitro* culture systems to better replicate the dynamic and heterogeneous BMME and its role in AML chemoresistance. 3D modelling is considered the next graduated step after doing experiments in 2D and before trying the murine model. Unlike traditional 2D cultures, 3D models can integrate key microenvironmental components as cells, extracellular matrix, and soluble factors, allowing more physiologically relevant interactions between LSCs and their niche. Scaffold-based and dynamic bioreactor systems have demonstrated superior capacity to preserve LSC quiescence, enhance adhesion-mediated resistance, and model metabolic adaptations under stress, thus providing a more accurate platform for testing novel therapeutic strategies(Al-Kaabneh et al., 2022). Personalised approaches, using patient-derived cells cultured in tailored 3D BM-mimetic systems, could enable the identification of patient-specific signalling pathways and drug sensitivities, ultimately guiding more effective, targeted treatment regimens aimed at eradicating both bulk leukaemic cells and LSCs.

After getting confidence in the results, either using a 2D or 3D model, future research should employ advanced murine models that closely reproduce the genetic, phenotypic, and microenvironmental features of human AML. Progress in genetically engineered strains and patient-derived xenograft (PDX) systems now allows the investigation of leukaemic stem cell dynamics, clonal evolution, and therapy-driven selection within an intact immune and stromal framework. Incorporating models with humanised bone marrow niches or immune components can further enhance translational relevance by preserving key interactions between AML cells, their microenvironment, and immune surveillance (Kurtz et al., 2022). Such models represent a critical step between *in vitro* experiments and clinical application, providing a robust platform for evaluating novel targeted agents, combination strategies, and resistance mechanisms, ultimately paving the way for more effective and individualised therapeutic approaches in AML.

Our further plan is to apply all these findings to primary AML samples of different AML cytogenetics to explore more about the heterogeneity and whether these cytokine inhibitors are effective in treating AML.

Overall, this thesis has expanded our knowledge of the BMME secretome. We have presented data outlining how the secretome differs among culture conditions, either LC or CC with and without direct stromal contact, proving the interplay between AML cells and stromal cells. We have highlighted the role of cytokines present in a higher concentration in CC compared to LC in providing growth, survival, proliferation advantage and contributing to chemoresistance. We have identified potential therapeutic targets for AML treatment using FDA-approved drugs, ruxolitinib and dasatinib, currently approved for non-AML conditions. These drugs may be investigated in upcoming clinical trials to overcome BMME-mediated chemoresistance and enhance AML treatment efficacy.

Appendix

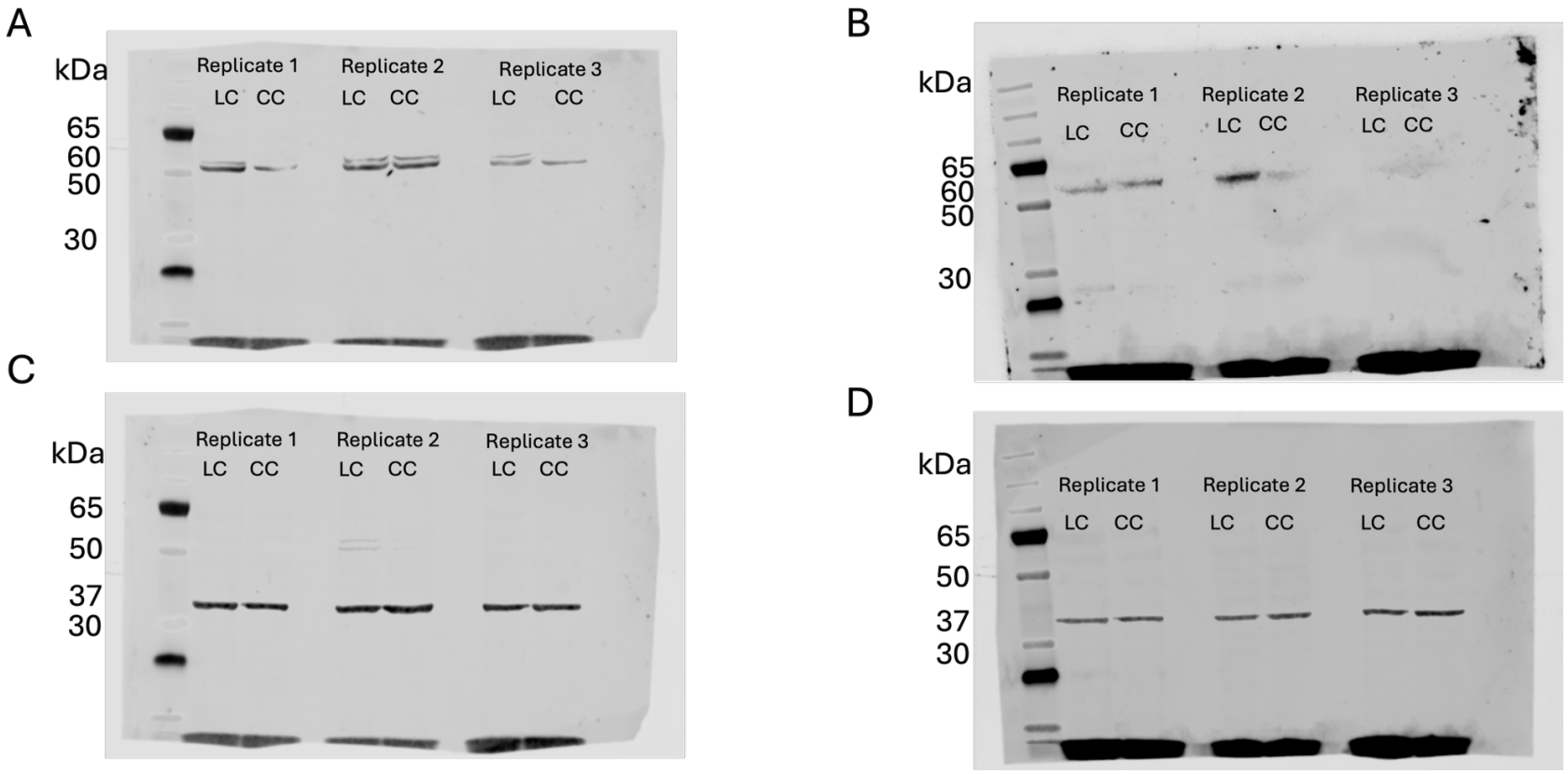

Figure 6-1 Immunoblot analysis of phospho- and total SRC expression in Kasumi-1 cells cultured under LC and CC conditions using a transwell system. (A) Phospho-SRC (60 kDa) expression across three biological replicates. (B) Total SRC expression (60 kDa) was detected on a separate membrane. (C) GAPDH (37 kDa) loading control corresponding to the phospho-SRC blot in (A). (D) GAPDH (37 kDa) loading control corresponding to the total SRC blot in (B). Phospho- and total SRC signals were normalised to their respective GAPDH signals on the same membranes. (Figure 4-4A in the main text)

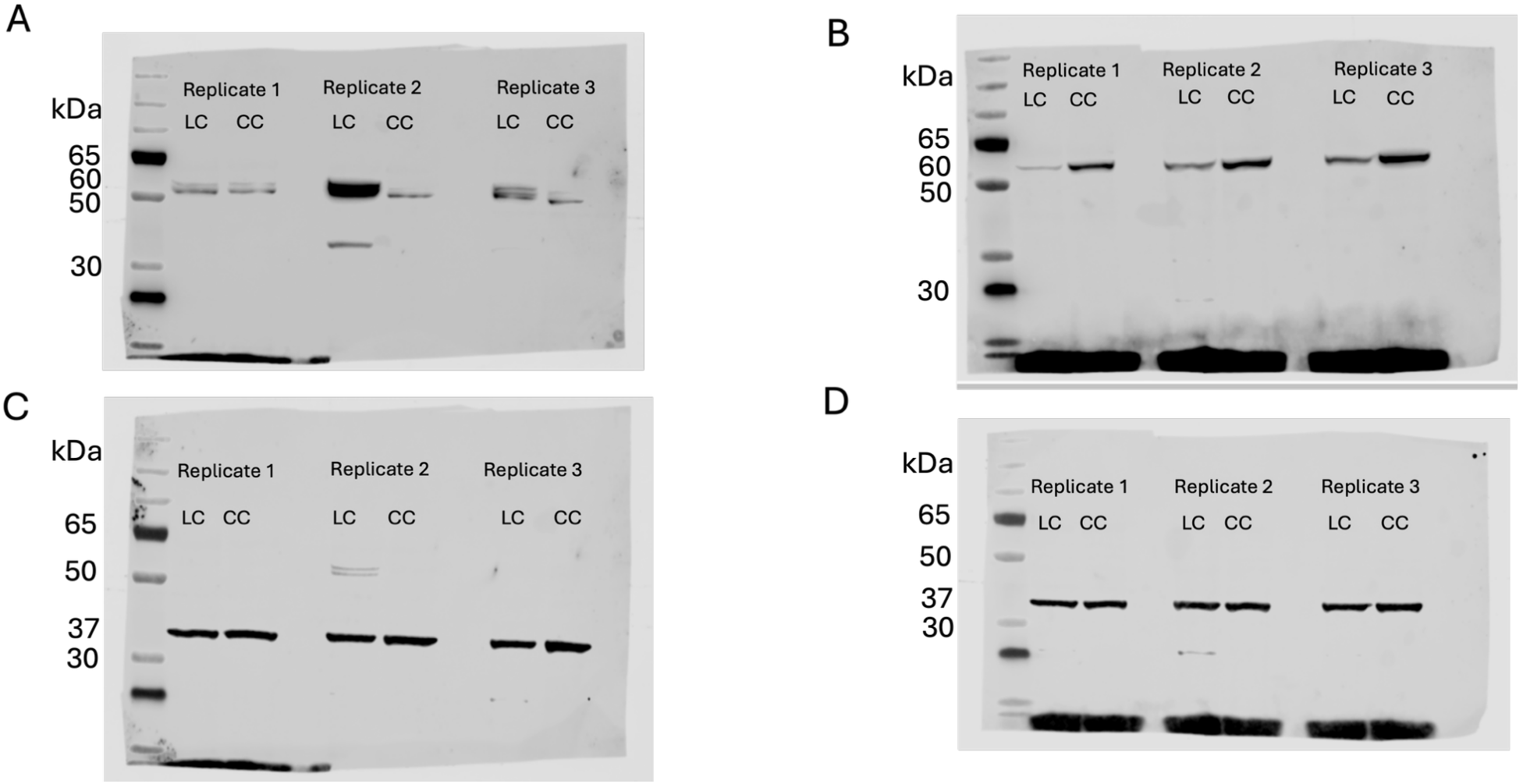

Figure 6-2 Immunoblot analysis of phospho- and total SRC expression in ME-1 cells cultured under LC and CC conditions using a transwell system.
(A) Phospho-SRC (60 kDa) expression across three biological replicates. (B) Total SRC expression (60 kDa) was detected on a separate membrane. (C) GAPDH (37 kDa) loading control corresponding to the phospho-SRC blot in (A). (D) GAPDH (37 kDa) loading control corresponding to the total SRC blot in (B). Phospho- and total SRC signals were normalised to their respective GAPDH signals on the same membranes. (Figure 4-4B in the main text)

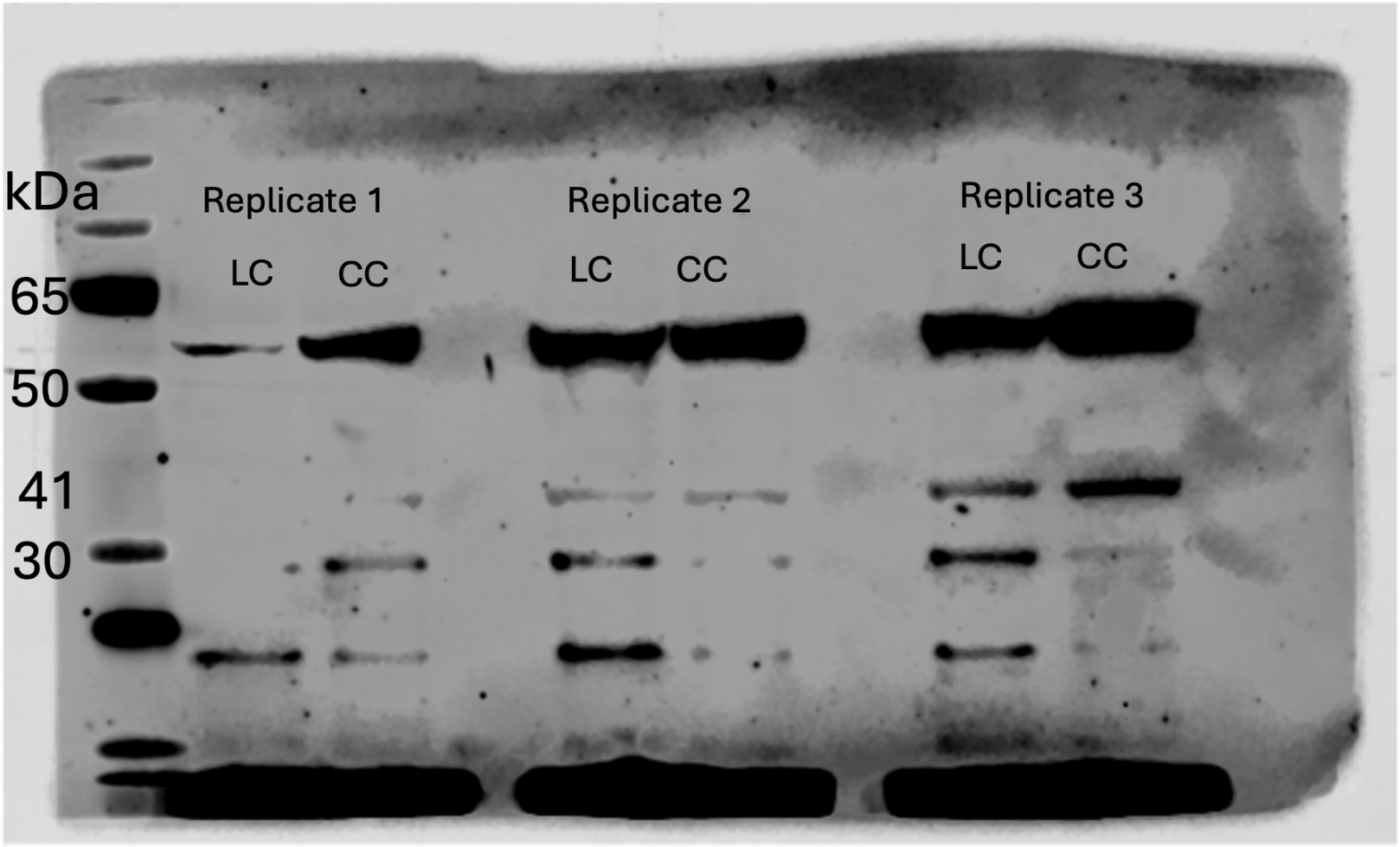

Figure 6-3 Immunoblot analysis of YAP and CYR61 expression in ME-1 cells cultured under LC and CC conditions using a transwell system.
CYR61 (41 kDa) expression across three biological replicates. Signals were normalised to their respective GAPDH signals on the same membranes (Figure 6-2 C). (Figure 4-4B in the main text)

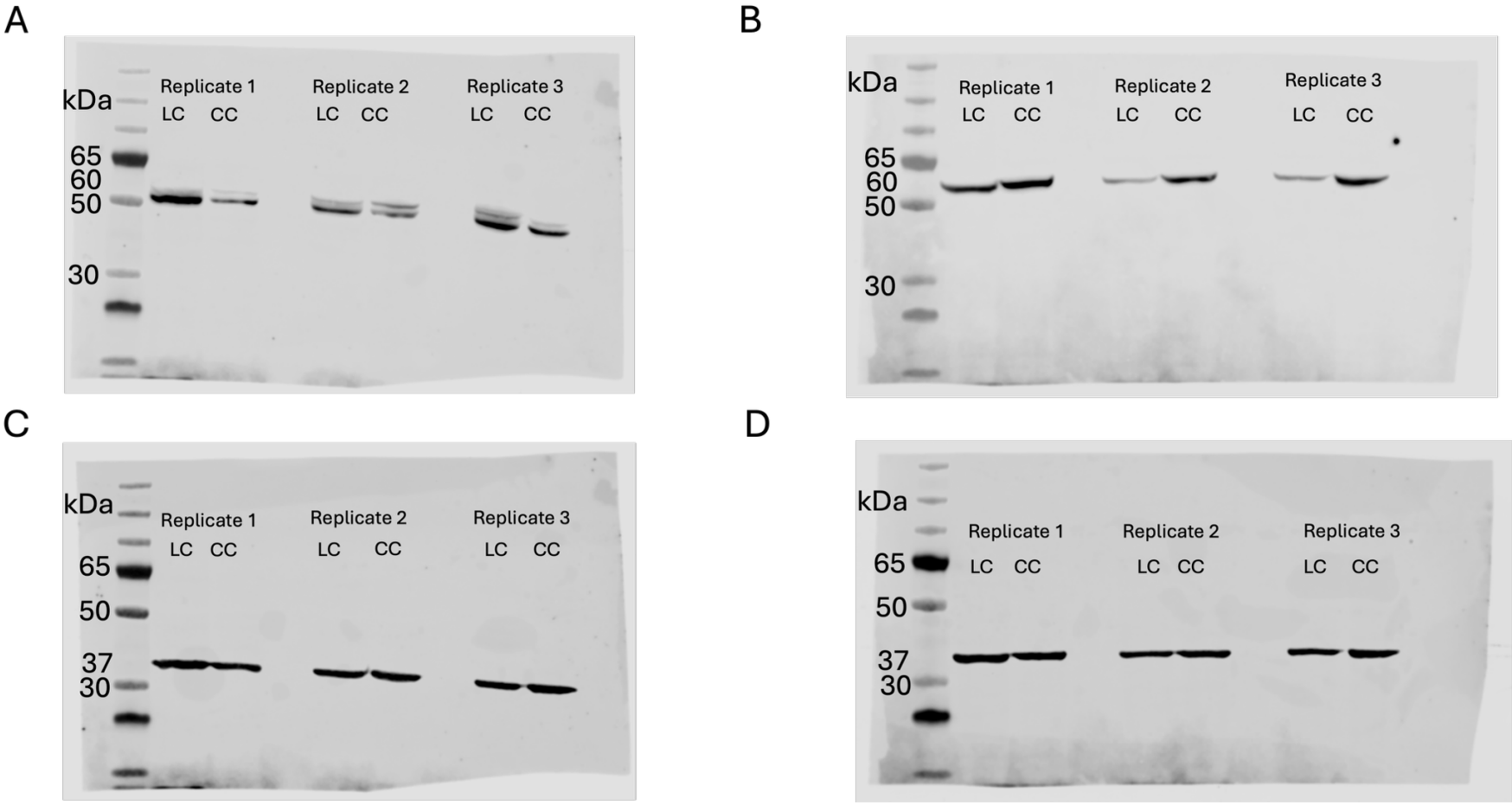

Figure 6-4 Immunoblot analysis of phospho- and total SRC expression in THP-1 cells cultured under LC and CC conditions using a transwell system.
(A) Phospho-SRC (60 kDa) expression across three biological replicates. (B) Total SRC expression (60 kDa) was detected on a separate membrane. (C) GAPDH (37 kDa) loading control corresponding to the phospho-SRC blot in (A). (D) GAPDH (37 kDa) loading control corresponding to the total SRC blot in (B). Phospho- and total SRC signals were normalised to their respective GAPDH signals on the same membranes. (Figure 4-4C in the main text)

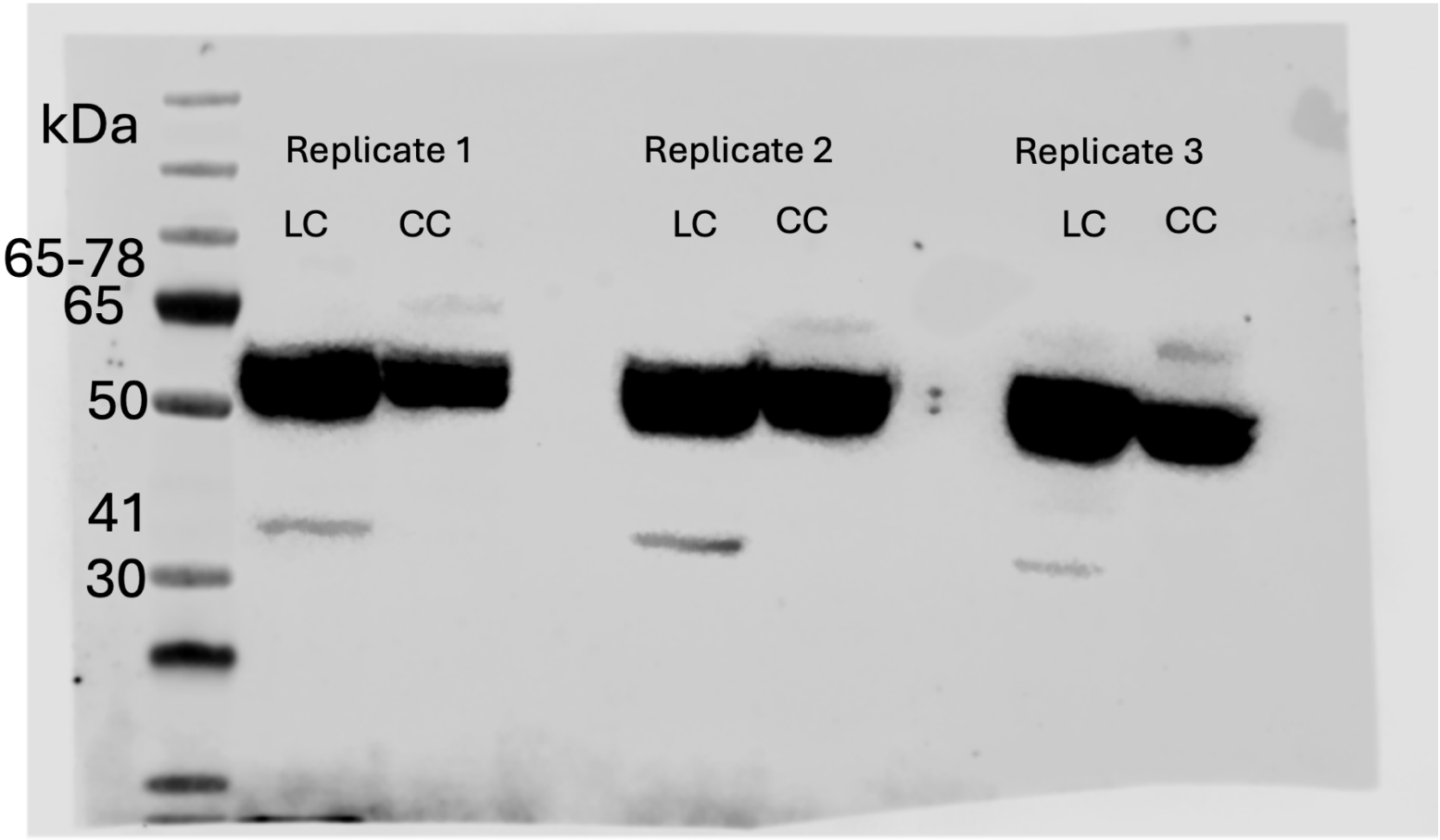

Figure 6-5 Immunoblot analysis of YAP and CYR61 expression in THP-1 cells cultured under LC and CC conditions using a transwell system.
YAP (65-78 kDa) and CYR61 (41 kDa) expression across three biological replicates. Signals were normalised to their respective GAPDH signals on the same membranes (Figure 6-4C). (Figure 4-4C in the main text)

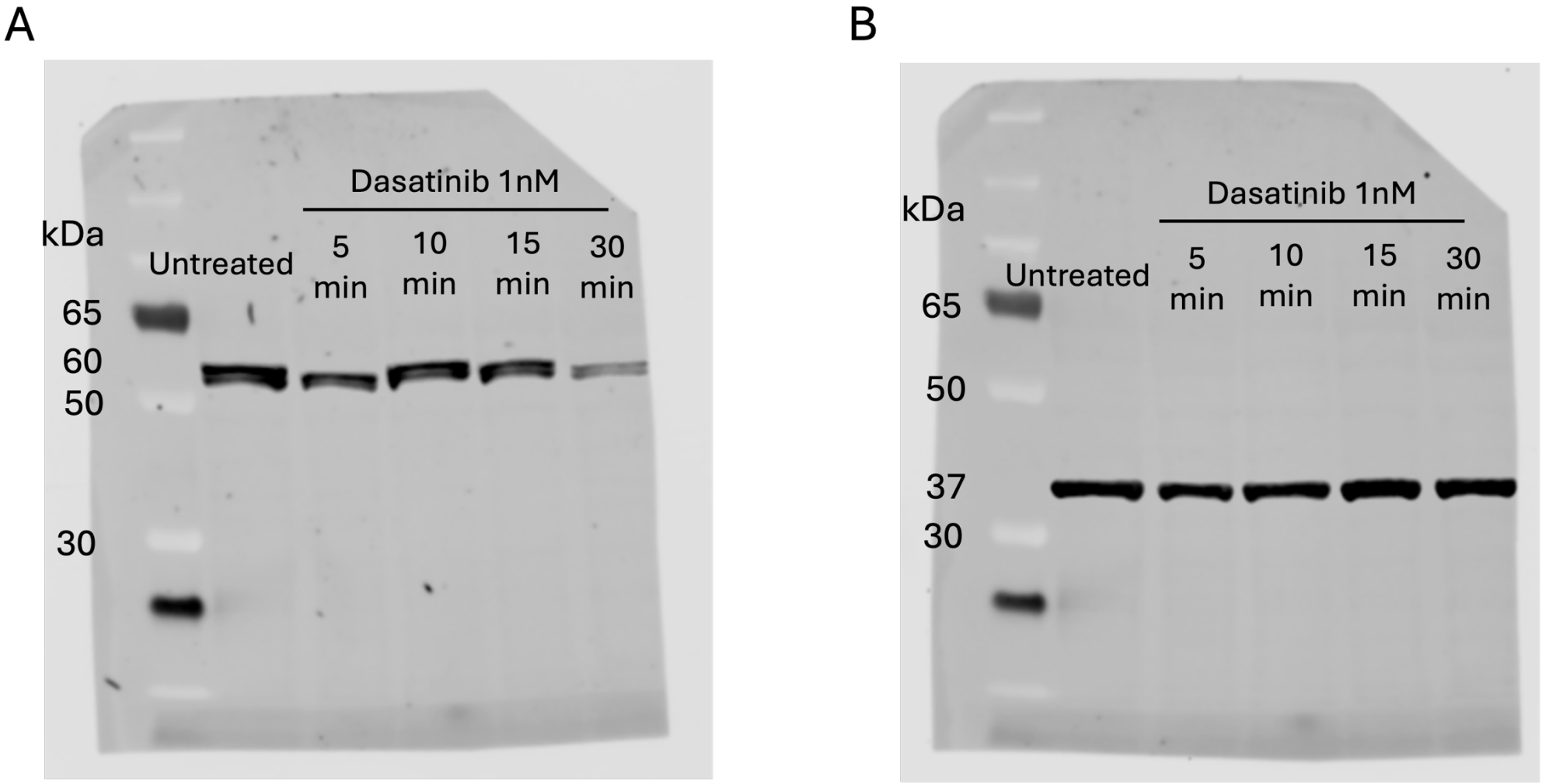

Figure 6-6 Full blotting membrane showing inhibition of SRC autophosphorylation in the ME-1 cell line by Dasatinib across different time points.
(A) phospho-SRC (60kDa), (B) GAPDH (37kDa). Signals were normalised to GAPDH. (Figure 4-6 in the main text)

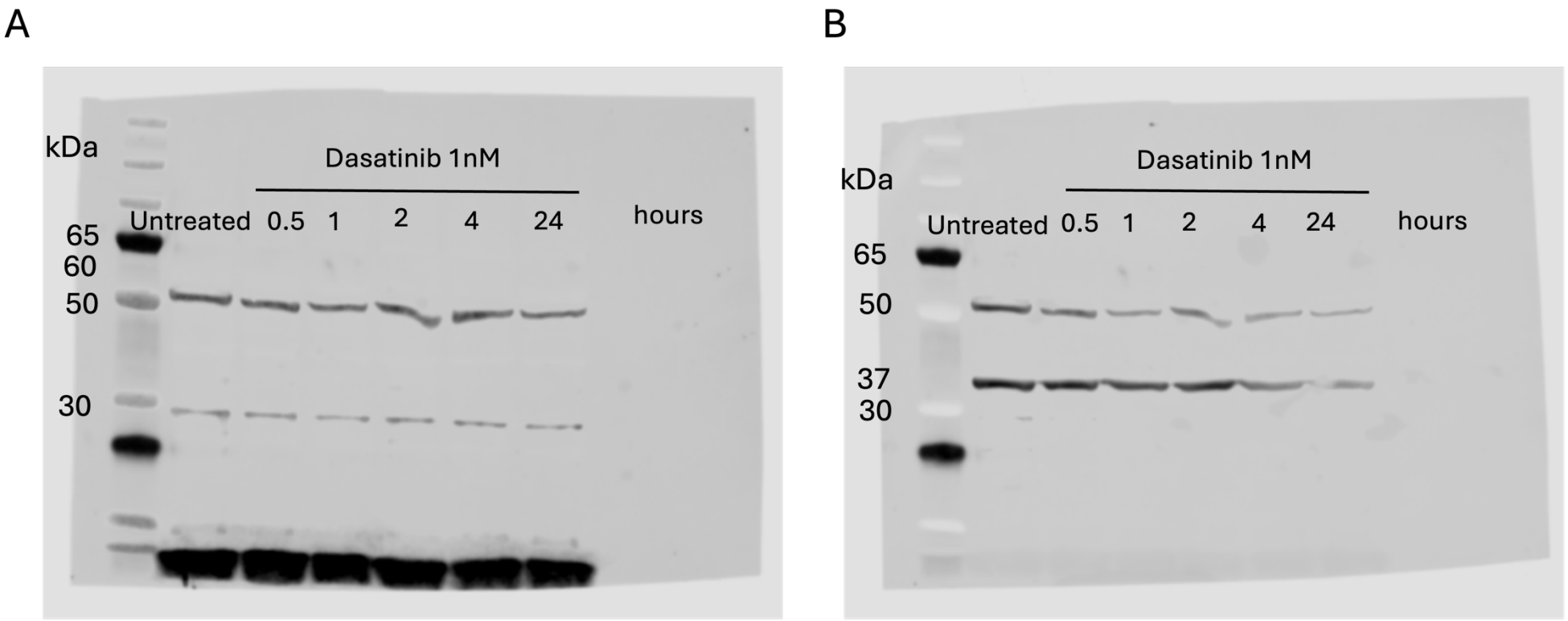

Figure 6-7 Full blotting membrane showing restoration of SRC autophosphorylation in the ME-1 cell line after 24hours of treatment by dasatinib.
(A) phospho-SRC (60kDa), (B) GAPDH (37kDa). Signals were normalised to GAPDH. (Figure 4-7 in the main text)

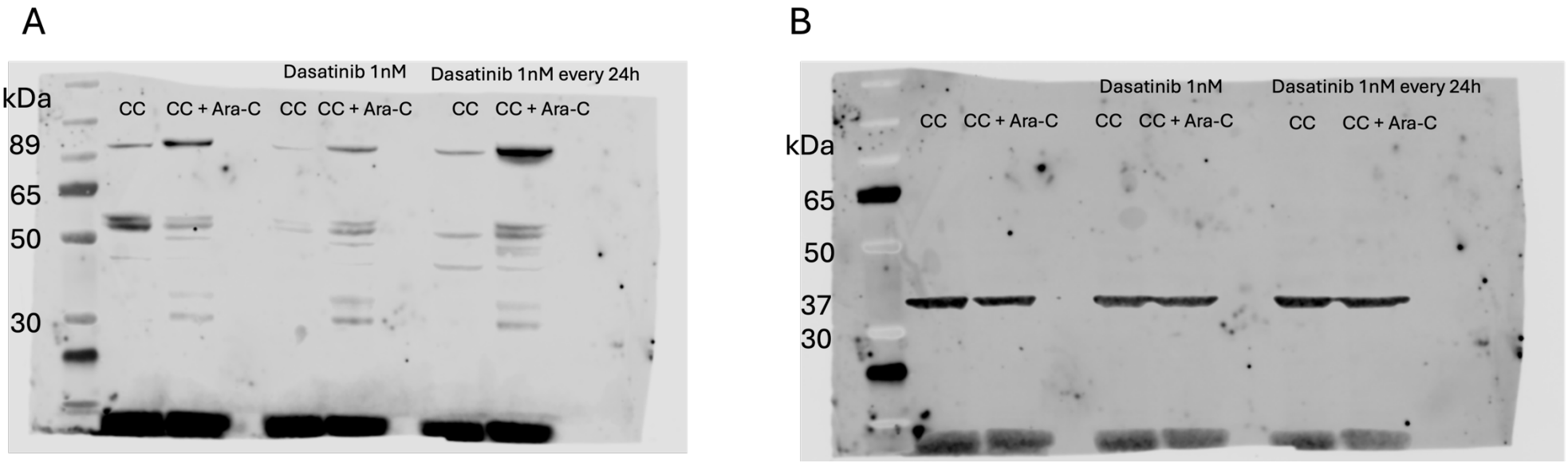

Figure 6-8 Full membrane blot showing apoptosis after culturing the ME-1 cell line with Dasatinib once and every 24 hours for 48 hours.
(A) C-PARP (89kDa), (B) GAPDH (37kDa). Signals were normalised to GAPDH. (Figure 4-14 in the main text)

A

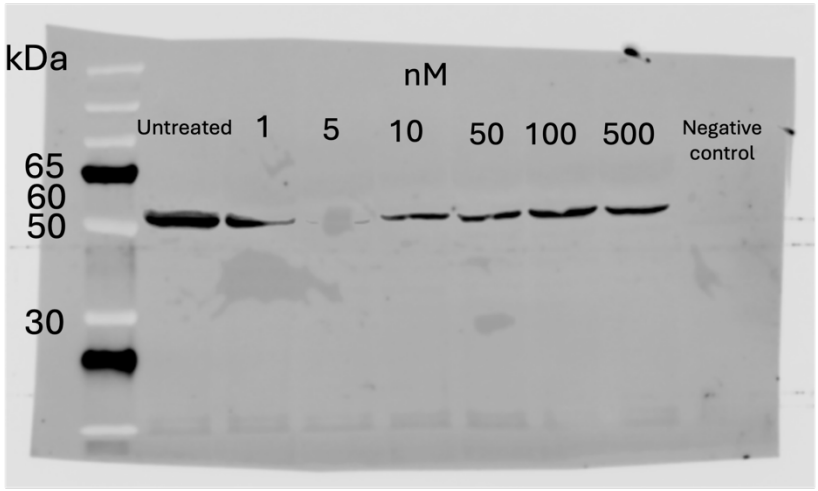

B

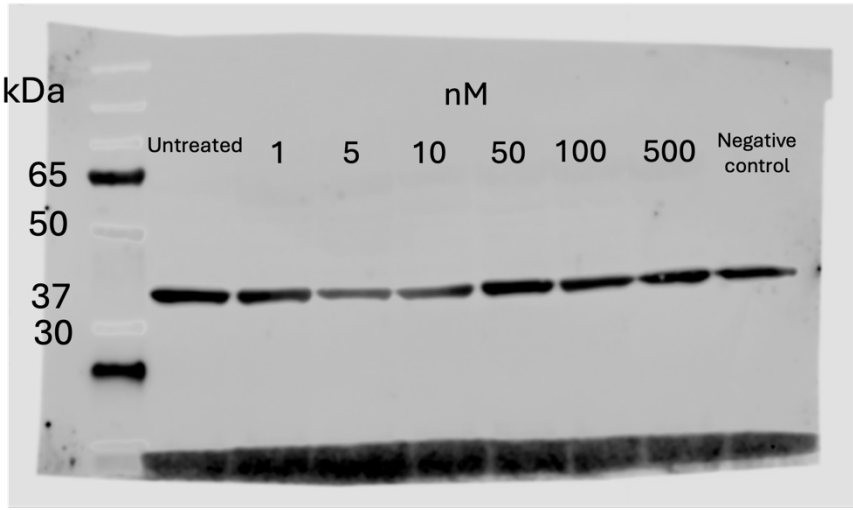

Figure 6-9 Full blotting membrane showing inhibition of SRC autophosphorylation in the ME-1 cell line by Dasatinib at 30 min time point using different concentrations.
(A) phospho-SRC (60kDa), (B) GAPDH (37kDa). Signals were normalised to GAPDH. (Figure 4-5 in the main text)

7 List of References

Abaza, Y., & Zeidan, A. M. (2022). Immune Checkpoint Inhibition in Acute Myeloid Leukemia and Myelodysplastic Syndromes. *Cells*, *11*(14), 2249. https://doi.org/10.3390/cells11142249

Abdel-Wahab, O., Manshouri, T., Patel, J., Harris, K., Yao, J., Hedvat, C., Heguy, A., Bueso-Ramos, C., Kantarjian, H., Levine, R. L., & Verstovsek, S. (2010). Genetic Analysis of Transforming Events That Convert Chronic Myeloproliferative Neoplasms to Leukemias. *Cancer Research*, *70*(2), 447–452. https://doi.org/10.1158/0008-5472.CAN-09-3783

Aguayo, A., Kantarjian, H. M., Estey, E. H., Giles, F. J., Verstovsek, S., Manshouri, T., Gidel, C., O'Brien, S., Keating, M. J., & Albitar, M. (2002). Plasma vascular endothelial growth factor levels have prognostic significance in patients with acute myeloid leukemia but not in patients with myelodysplastic syndromes. *Cancer*, *95*(9), 1923–1930. https://doi.org/10.1002/cncr.10900

Ahmed, H. M. M. A., Al-Matary, Y. S., Nimmagadda, S. C., Fiori, M., Patnana, P. K., Frank, D., Wei, L., Schütte, J., May, T., Goethert, J. R., Schroeder, T., Buttkereit, U., Recher, C., Rodríguez-Paredes, M., Koenig, T., Hartmann, W., Tuckermann, J., Opalka, B., Lenz, G., & Khandanpour, C. (2020). AML Associated Mesenchymal Stroma Cells Support Growth of AML Cells As a Result of Activated Notch Signaling and This Can be Targeted By Dexamethasone. *Blood*, *136*(Supplement 1), 1–1. https://doi.org/10.1182/blood-2020-134177

Al-Kaabneh, B., Frisch, B., & Aljitawi, O. S. (2022). The Potential Role of 3D In Vitro Acute Myeloid Leukemia Culture Models in Understanding Drug Resistance in Leukemia Stem Cells. In *Cancers* (Vol. 14, Issue 21). MDPI. https://doi.org/10.3390/cancers14215252

Anguille, S., Van de Velde, A. L., Smits, E. L., Van Tendeloo, V. F., Juliusson, G., Cools, N., Nijs, G., Stein, B., Lion, E., Van Driessche, A., Vandenbosch, I., Verlinden, A., Gadisseur, A. P., Schroyens, W. A., Muylle, L., Vermeulen, K., Maes, M.-B., Deiteren, K., Malfait, R., … Berneman, Z. N. (2017). Dendritic cell vaccination as postremission treatment to prevent or delay relapse in acute myeloid leukemia. *Blood*, *130*(15), 1713–1721. https://doi.org/10.1182/blood-2017-04-780155

Appeldoorn, T. Y. J., Munnink, T. H. O., Morsink, L. M., Hooge, M. N. L., & Touw, D. J. (2023). Pharmacokinetics and Pharmacodynamics of Ruxolitinib: A Review. *Clinical Pharmacokinetics*, *62*(4), 559–571. https://doi.org/10.1007/s40262-023-01225-7

Arranz, L., Sánchez-Aguilera, A., Martín-Pérez, D., Isern, J., Langa, X., Tzankov, A., Lundberg, P., Muntión, S., Tzeng, Y.-S., Lai, D.-M., Schwaller, J., Skoda, R. C., & Méndez-Ferrer, S. (2014). Neuropathy of haematopoietic stem cell niche is essential for myeloproliferative neoplasms. *Nature*, *512*(7512), 78–81. https://doi.org/10.1038/nature13383

Asou, H., Tashiro, S., Hamamoto, K., Otsuji, A., Kita, K., & Kamada, N. (1991). Establishment of a human acute myeloid leukemia cell line (Kasumi-1) with 8;21 chromosome translocation. *Blood*, *77*(9), 2031–2036.

Azar, W. J., Christie, E. L., Mitchell, C., Liu, D. S., Au-Yeung, G., & Bowtell, D. D. L. (2020). Noncanonical IL6 Signaling-Mediated Activation of YAP Regulates Cell Migration and Invasion in Ovarian Clear Cell Cancer. *Cancer*

Research, *80*(22), 4960–4971. https://doi.org/10.1158/0008-5472.CAN-19-3044

Barbullushi, K., Rampi, N., Serpenti, F., Sciumè, M., Fabris, S., De Roberto, P., & Fracchiolla, N. S. (2022). Vaccination Therapy for Acute Myeloid Leukemia: Where Do We Stand? *Cancers*, *14*(12), 2994. https://doi.org/10.3390/cancers14122994

Barnhouse, V., Petrikas, N., Crosby, C., Zoldan, J., & Harley, B. (2021). Perivascular Secretome Influences Hematopoietic Stem Cell Maintenance in a Gelatin Hydrogel. *Annals of Biomedical Engineering*, *49*(2), 780–792. https://doi.org/10.1007/s10439-020-02602-0

Bazinet, A., & Assouline, S. (2021). A review of FDA-approved acute myeloid leukemia therapies beyond '7 + 3.' In *Expert Review of Hematology* (Vol. 14, Issue 2, pp. 185–197). Taylor and Francis Ltd. https://doi.org/10.1080/17474086.2021.1875814

Behrmann, L., Wellbrock, J., & Fiedler, W. (2018). Acute Myeloid Leukemia and the Bone Marrow Niche—Take a Closer Look. *Frontiers in Oncology*, *8*. https://doi.org/10.3389/fonc.2018.00444

Benekli, M., Xia, Z., Donohue, K. A., Ford, L. A., Pixley, L. A., Baer, M. R., Baumann, H., & Wetzler, M. (2002). Constitutive activity of signal transducer and activator of transcription 3 protein in acute myeloid leukemia blasts is associated with short disease-free survival. *Blood*, *99*(1), 252–257. https://doi.org/10.1182/blood.V99.1.252

Bennett, J. M., Catovsky, D., Daniel, M., Flandrin, G., Galton, D. A. G., Gralnick, H. R., & Sultan, C. (1976). Proposals for the Classification of the Acute Leukaemias FRENCH-AMERICAN-BRITISH(FAB) CO-OPERATIVE GROUP. *British Journal of Haematology*, *33*(4), 451–458. https://doi.org/10.1111/j.1365-2141.1976.tb03563.x

Blake, S., Hughes, T. P., Mayrhofer, G., & Lyons, A. B. (2008). The Src/ABL kinase inhibitor dasatinib (BMS-354825) inhibits function of normal human T-lymphocytes in vitro. *Clinical Immunology*, *127*(3), 330–339. https://doi.org/10.1016/j.clim.2008.02.006

Blau, O., Baldus, C. D., Hofmann, W.-K., Thiel, G., Nolte, F., Burmeister, T., Türkmen, S., Benlasfer, O., Schümann, E., Sindram, A., Molkentin, M., Mundlos, S., Keilholz, U., Thiel, E., & Blau, I. W. (2011). Mesenchymal stromal cells of myelodysplastic syndrome and acute myeloid leukemia patients have distinct genetic abnormalities compared with leukemic blasts. *Blood*, *118*(20), 5583–5592. https://doi.org/10.1182/blood-2011-03-343467

Blau, O., Hofmann, W.-K., Baldus, C. D., Thiel, G., Serbent, V., Schümann, E., Thiel, E., & Blau, I. W. (2007). Chromosomal aberrations in bone marrow mesenchymal stroma cells from patients with myelodysplastic syndrome and acute myeloblastic leukemia. *Experimental Hematology*, *35*(2), 221–229. https://doi.org/10.1016/j.exphem.2006.10.012

Blazek, M., Santisteban, T. S., Zengerle, R., & Meier, M. (2015). Analysis of fast protein phosphorylation kinetics in single cells on a microfluidic chip. *Lab on a Chip*, *15*(3), 726–734. https://doi.org/10.1039/c4lc00797b

Bose, P., & Verstovsek, S. (2017). JAK2 inhibitors for myeloproliferative neoplasms: What is next? *Blood*, *130*(2), 115–125. https://doi.org/10.1182/blood-2017-04-742288

Böttcher, M., Panagiotidis, K., Bruns, H., Stumpf, M., Völkl, S., Geyh, S., Dietel, B., Schroeder, T., Mackensen, A., & Mougiakakos, D. (2022). Bone marrow stroma cells promote induction of a chemoresistant and prognostic unfavorable S100A8/A9high AML cell subset. *Blood Advances*, *6*(21), 5685–5697. https://doi.org/10.1182/bloodadvances.2021005938

Boutin, L., Arnautou, P., Trignol, A., Ségot, A., Farge, T., Desterke, C., Soave, S., Clay, D., Raffoux, E., Sarry, J. E., Malfuson, J. V., Lataillade, J. J., Le Bousse-Kerdilès, M. C., & Anginot, A. (2020). Mesenchymal stromal cells confer chemoresistance to myeloid leukemia blasts through Side Population functionality and ABC transporter activation. *Haematologica*, *105*(4), 987–998. https://doi.org/10.3324/haematol.2018.214379

Brenner, A. K., Nepstad, I., & Bruserud, Ø. (2017). Mesenchymal stem cells support survival and proliferation of primary human acute myeloid leukemia cells through heterogeneous molecular mechanisms. *Frontiers in Immunology*, *8*(FEB). https://doi.org/10.3389/fimmu.2017.00106

Bresnick, A. R., Weber, D. J., & Zimmer, D. B. (2015). S100 proteins in cancer. *Nature Reviews Cancer*, *15*(2), 96–109. https://doi.org/10.1038/nrc3893

Brune, M. (2006). Improved leukemia-free survival after postconsolidation immunotherapy with histamine dihydrochloride and interleukin-2 in acute myeloid leukemia: results of a randomized phase 3 trial. *Blood*, *108*(1), 88–96. https://doi.org/10.1182/blood-2005-10-4073

Brunner, A. M., Esteve, J., Porkka, K., Knapper, S., Traer, E., Scholl, S., Garcia-Manero, G., Vey, N., Wermke, M., Janssen, J., Narayan, R., Loo, S., Kontro, M., Ottmann, O., Naidu, P., Pelletier, M., Han, M., Lewandowski, A., Zhang, N., … Tovar, N. (2021). Efficacy and Safety of Sabatolimab (MBG453) in Combination with Hypomethylating Agents (HMAs) in Patients (Pts) with Very High/High-Risk Myelodysplastic Syndrome (vHR/HR-MDS) and Acute Myeloid Leukemia (AML): Final Analysis from a Phase Ib Study. *Blood*, *138*(Supplement 1), 244–244. https://doi.org/10.1182/blood-2021-146039

Bryan, J. C., & Verstovsek, S. (2016). Overcoming treatment challenges in myelofibrosis and polycythemia vera: the role of ruxolitinib. *Cancer Chemotherapy and Pharmacology*, *77*(6), 1125–1142. https://doi.org/10.1007/s00280-016-3012-z

Burt, R., Dey, A., Aref, S., Aguiar, M., Akarca, A., Bailey, K., Day, W., Hooper, S., Kirkwood, A., Kirschner, K., Lee, S.-W., Celso, C. Lo, Manji, J., Mansour, M. R., Marafioti, T., Mitchell, R. J., Muirhead, R. C., Cheuk, K., Ng, Y., … Fielding, A. K. (2019). *Activated stromal cells transfer mitochondria to rescue acute lymphoblastic leukemia cells from oxidative stress*. http://ashpublications.org/blood/article-pdf/134/17/1415/1502485/bloodbld2019001398.pdf

Calò, V., Migliavacca, M., Bazan, V., Macaluso, M., Buscemi, M., Gebbia, N., & Russo, A. (2003). STAT Proteins: From Normal Control of Cellular Events to Tumorigenesis. *Journal of Cellular Physiology*, *197*(2), 157–168. https://doi.org/10.1002/jcp.10364

CALVI, L. M. (2006). Osteoblastic Activation in the Hematopoietic Stem Cell Niche. *Annals of the New York Academy of Sciences*, *1068*(1), 477–488. https://doi.org/10.1196/annals.1346.021

Calvi, L. M., Adams, G. B., Weibrecht, K. W., Weber, J. M., Olson, D. P., Knight, M. C., Martin, R. P., Schipani, E., Divieti, P., Bringhurst, F. R., Milner, L. A., Kronenberg, H. M., & Scadden, D. T. (2003). Osteoblastic cells regulate the haematopoietic stem cell niche. *Nature*, *425*(6960), 841–846. https://doi.org/10.1038/nature02040

Cao, Y., Wei, J., Zou, L., Jiang, T., Wang, G., Chen, L., Huang, L., Meng, F., Huang, L., Wang, N., Zhou, X., Luo, H., Mao, Z., Chen, X., Xie, J., Liu, J., Cheng, H., Zhao, J., Huang, G., … Zhou, J. (2020). Ruxolitinib in treatment of severe coronavirus disease 2019 (COVID-19): A multicenter, single-blind, randomized controlled trial. *Journal of Allergy and Clinical Immunology*, *146*(1), 137-146.e3. https://doi.org/10.1016/j.jaci.2020.05.019

Chaitanya, G. V., Alexander, J. S., & Babu, P. P. (2010). PARP-1 cleavage fragments: Signatures of cell-death proteases in neurodegeneration. In *Cell Communication and Signaling* (Vol. 8). https://doi.org/10.1186/1478-811X-8-31

Chen, M., Wang, J., Yao, S. F., Zhao, Y., Liu, L., Li, L. W., Xu, T., Gan, L. G., Xiao, C. L., Shan, Z. L., Zhong, L., & Liu, B. Z. (2017). Effect of YAP inhibition on human leukemia HL-60 cells. *International Journal of Medical Sciences*, *14*(9), 902–910. https://doi.org/10.7150/ijms.19965

Chen, P., Jin, Q., Fu, Q., You, P., Jiang, X., Yuan, Q., & Huang, H. (2016). Induction of multidrug resistance of acute myeloid leukemia cells by cocultured stromal cells via upregulation of the PI3K/Akt signaling pathway. *Oncology Research*, *24*(4), 215–223. https://doi.org/10.3727/096504016X14634208143021

Cheng, F., Xu, Q., Li, Q., Cui, Z., Li, W., & Zeng, F. (2023). Adverse reactions after treatment with dasatinib in chronic myeloid leukemia: Characteristics, potential mechanisms, and clinical management strategies. *Frontiers in Oncology*, *13*. https://doi.org/10.3389/fonc.2023.1113462

Cheng, J., Li, Y., Liu, S., Jiang, Y., Ma, J., Wan, L., Li, Q., & Pang, T. (2019). CXCL8 derived from mesenchymal stromal cells supports survival and proliferation of acute myeloid leukemia cells through the PI3K/AKT pathway. *The FASEB Journal*, *33*(4), 4755–4764. https://doi.org/10.1096/fj.201801931R

Cheung, H. L., Wong, Y. H., Li, Y. Y., Yang, X., Ko, L. H., Tan Kabigting, J. E., Chan, K. C., Leung, A. Y. H., & Chan, B. P. (2025). Microenvironment matters: In vitro 3D bone marrow niches differentially modulate survival, phenotype and drug responses of acute myeloid leukemia (AML) cells. *Biomaterials*, *312*. https://doi.org/10.1016/j.biomaterials.2024.122719

Chien, S., Haq, S. U., Pawlus, M., Moon, R. T., Estey, E. H., Appelbaum, F. R., Othus, M., Magnani, J. L., & Becker, P. S. (2013). Adhesion Of Acute Myeloid Leukemia Blasts To E-Selectin In The Vascular Niche Enhances Their Survival By Mechanisms Such As Wnt Activation. *Blood*, *122*(21), 61–61. https://doi.org/10.1182/blood.V122.21.61.61

Ciciarello, M., Corradi, G., Sangaletti, S., Bassani, B., Simonetti, G., Vadakekolathu, J., Marconi, G., Martinelli, G., Colombo, M. P., Rutella, S., Cavo, M., & Curti, A. (2019). Interferon-γ-Dependent Inflammatory Signature in Acute Myeloid Leukemia Cells Is Able to Shape Stromal and Immune Bone Marrow Microenvironment. *Blood*, *134*(Supplement_1), 1212–1212. https://doi.org/10.1182/blood-2019-126512

Civini, S., Jin, P., Ren, J., Sabatino, M., Castiello, L., Jin, J., Wang, H., Zhao, Y., Marincola, F., & Stroncek, D. (2013). Leukemia cells induce changes in human bone marrow stromal cells. *Journal of Translational Medicine*, *11*(1), 1–14. https://doi.org/10.1186/1479-5876-11-298

Corradi, G., Bassani, B., Simonetti, G., Sangaletti, S., Vadakekolathu, J., Fontana, M. C., Pazzaglia, M., Gulino, A., Tripodo, C., Cristiano, G., Bandini, L., Ottaviani, E., Ocadlikova, D., Piccioli, M., Martinelli, G., Colombo, M. P., Rutella, S., Cavo, M., Ciciarello, M., & Curti, A. (2022). Release of IFNγ by Acute Myeloid Leukemia Cells Remodels Bone Marrow Immune Microenvironment by Inducing Regulatory T Cells. *Clinical Cancer Research*, *28*(14), 3141–3155. https://doi.org/10.1158/1078-0432.CCR-21-3594

Corrado, C., Raimondo, S., Saieva, L., Flugy, A. M., De Leo, G., & Alessandro, R. (2014). Exosome-mediated crosstalk between chronic myelogenous leukemia cells and human bone marrow stromal cells triggers an Interleukin 8-

dependent survival of leukemia cells. *Cancer Letters*, *348*(1–2), 71–76. https://doi.org/10.1016/j.canlet.2014.03.009

Curti, A., Pandolfi, S., Valzasina, B., Aluigi, M., Isidori, A., Ferri, E., Salvestrini, V., Bonanno, G., Rutella, S., Durelli, I., Horenstein, A. L., Fiore, F., Massaia, M., Colombo, M. P., Baccarani, M., & Lemoli, R. M. (2007). Modulation of tryptophan catabolism by human leukemic cells results in the conversion of CD25− into CD25+ T regulatory cells. *Blood*, *109*(7), 2871–2877. https://doi.org/10.1182/blood-2006-07-036863

Daver, N., Alotaibi, A. S., Bücklein, V., & Subklewe, M. (2021). T-cell-based immunotherapy of acute myeloid leukemia: current concepts and future developments. *Leukemia*, *35*(7), 1843–1863. https://doi.org/10.1038/s41375-021-01253-x

de Freitas, F. A., Levy, D., Reichert, C. O., Sampaio-Silva, J., Giglio, P. N., de Pádua Covas Lage, L. A., Demange, M. K., Pereira, J., & Bydlowski, S. P. (2024). Influence of Human Bone Marrow Mesenchymal Stem Cells Secretome from Acute Myeloid Leukemia Patients on the Proliferation and Death of K562 and K562-Lucena Leukemia Cell Lineages. *International Journal of Molecular Sciences*, *25*(9). https://doi.org/10.3390/ijms25094748

Deininger, M. W. N., Tyner, J. W., & Solary, E. (2017). Turning the tide in myelodysplastic/myeloproliferative neoplasms. *Nature Reviews Cancer*, *17*(7), 425–440. https://doi.org/10.1038/nrc.2017.40

Dias, S., Shmelkov, S. V., Lam, G., & Rafii, S. (2002). VEGF165 promotes survival of leukemic cells by Hsp90-mediated induction of Bcl-2 expression and apoptosis inhibition. *Blood*, *99*(7), 2532–2540. https://doi.org/10.1182/blood.V99.7.2532

Ding, L., Ley, T. J., Larson, D. E., Miller, C. A., Koboldt, D. C., Welch, J. S., Ritchey, J. K., Young, M. A., Lamprecht, T., McLellan, M. D., McMichael, J. F., Wallis, J. W., Lu, C., Shen, D., Harris, C. C., Dooling, D. J., Fulton, R. S., Fulton, L. L., Chen, K., … DiPersio, J. F. (2012). Clonal evolution in relapsed acute myeloid leukaemia revealed by whole-genome sequencing. *Nature*, *481*(7382), 506–510. https://doi.org/10.1038/nature10738

Döhner, H., Wei, A. H., Appelbaum, F. R., Craddock, C., DiNardo, C. D., Dombret, H., Ebert, B. L., Fenaux, P., Godley, L. A., Hasserjian, R. P., Larson, R. A., Levine, R. L., Miyazaki, Y., Niederwieser, D., Ossenkoppele, G., Röllig, C., Sierra, J., Stein, E. M., Tallman, M. S., … Löwenberg, B. (2022). Diagnosis and management of AML in adults: 2022 recommendations from an international expert panel on behalf of the ELN. *Blood*, *140*(12), 1345–1377. https://doi.org/10.1182/blood.2022016867

Dong, L., Yu, W.-M., Zheng, H., Loh, M. L., Bunting, S. T., Pauly, M., Huang, G., Zhou, M., Broxmeyer, H. E., Scadden, D. T., & Qu, C.-K. (2016). Leukaemogenic effects of Ptpn11 activating mutations in the stem cell microenvironment. *Nature*, *539*(7628), 304–308. https://doi.org/10.1038/nature20131

Duarte, D., Hawkins, E. D., Akinduro, O., Ang, H., De Filippo, K., Kong, I. Y., Haltalli, M., Ruivo, N., Straszkowski, L., Vervoort, S. J., McLean, C., Weber, T. S., Khorshed, R., Pirillo, C., Wei, A., Ramasamy, S. K., Kusumbe, A. P., Duffy, K., Adams, R. H., … Lo Celso, C. (2018). Inhibition of Endosteal Vascular Niche Remodeling Rescues Hematopoietic Stem Cell Loss in AML. *Cell Stem Cell*, *22*(1), 64-77.e6. https://doi.org/10.1016/j.stem.2017.11.006

Eghtedar, A., Verstovsek, S., Estrov, Z., Burger, J., Cortes, J., Bivins, C., Faderl, S., Ferrajoli, A., Borthakur, G., George, S., Scherle, P. A., Newton, R. C., Kantarjian, H. M., & Ravandi, F. (2012). Phase 2 study of the JAK kinase

inhibitor ruxolitinib in patients with refractory leukemias, including postmyeloproliferative neoplasm acute myeloid leukemia. *Blood*, *119*(20), 4614–4618. https://doi.org/10.1182/blood-2011-12-400051

Eichenfield, L. F., Simpson, E. L., Papp, K., Szepietowski, J. C., Blauvelt, A., Kircik, L., Silverberg, J. I., Siegfried, E. C., Kuligowski, M. E., Venturanza, M. E., Kallender, H., Ren, H., & Paller, A. S. (2024). Efficacy, Safety, and Long-Term Disease Control of Ruxolitinib Cream Among Adolescents with Atopic Dermatitis: Pooled Results from Two Randomized Phase 3 Studies. *American Journal of Clinical Dermatology*, *25*(4), 669–683. https://doi.org/10.1007/s40257-024-00855-2

Elmore, S. (2007). Apoptosis: a review of programmed cell death. *Toxicologic Pathology*, *35*(4), 495–516. https://doi.org/10.1080/01926230701320337

Erba, H. P., Montesinos, P., Kim, H. J., Patkowska, E., Vrhovac, R., Žák, P., Wang, P. N., Mitov, T., Hanyok, J., Kamel, Y. M., Rohrbach, J. E. C., Liu, L., Benzohra, A., Lesegretain, A., Cortes, J., Perl, A. E., Sekeres, M. A., Dombret, H., Amadori, S., … Schlenk, R. F. (2023). Quizartinib plus chemotherapy in newly diagnosed patients with FLT3-internal-tandem-duplication-positive acute myeloid leukaemia (QuANTUM-First): a randomised, double-blind, placebo-controlled, phase 3 trial. *The Lancet*, *401*(10388), 1571–1583. https://doi.org/10.1016/S0140-6736(23)00464-6

Essers, M. A. G., & Trumpp, A. (2010). Targeting leukemic stem cells by breaking their dormancy. *Molecular Oncology*, *4*(5), 443–450. https://doi.org/10.1016/j.molonc.2010.06.001

Faderl, S., Harris, D., Van, Q., Kantarjian, H. M., Talpaz, M., & Estrov, Z. (2003). Granulocyte-macrophage colony-stimulating factor (GM-CSF) induces antiapoptotic and proapoptotic signals in acute myeloid leukemia. *Blood*, *102*(2), 630–637. https://doi.org/10.1182/blood-2002-06-1890

Feng, P., Zhang, J., Zhang, J., Liu, X., Pan, L., Chen, D., Ji, M., Lu, F., Li, P., Li, G., Sun, T., Li, J., Ye, J., & Ji, C. (2022). Deacetylation of YAP1 Promotes the Resistance to Chemo- and Targeted Therapy in FLT3-ITD+ AML Cells. *Frontiers in Cell and Developmental Biology*, *10*. https://doi.org/10.3389/fcell.2022.842214

Forte, D., García-Fernández, M., Sánchez-Aguilera, A., Stavropoulou, V., Fielding, C., Martín-Pérez, D., López, J. A., Costa, A. S. H., Tronci, L., Nikitopoulou, E., Barber, M., Gallipoli, P., Marando, L., Fernández de Castillejo, C. L., Tzankov, A., Dietmann, S., Cavo, M., Catani, L., Curti, A., … Méndez-Ferrer, S. (2020). Bone Marrow Mesenchymal Stem Cells Support Acute Myeloid Leukemia Bioenergetics and Enhance Antioxidant Defense and Escape from Chemotherapy. *Cell Metabolism*, *32*(5), 829-843.e9. https://doi.org/10.1016/j.cmet.2020.09.001

Fragoso, R., Elias, A. P., & Dias, S. (2007). Autocrine VEGF loops, signaling pathways, and acute leukemia regulation. *Leukemia & Lymphoma*, *48*(3), 481–488. https://doi.org/10.1080/10428190601064720

Fuentes-Prior, P., & Salvesen, G. S. (2004). The protein structures that shape caspase activity, specificity, activation and inhibition. *The Biochemical Journal*, *384*(Pt 2), 201–232. https://doi.org/10.1042/BJ20041142

Garrido, S. M., Appelbaum, F. R., Willman, C. L., & Banker, D. E. (2001). Acute myeloid leukemia cells are protected from spontaneous and drug-induced apoptosis by direct contact with a human bone marrow stromal cell line (HS-5). *Experimental Hematology*, *29*(4), 448–457. https://doi.org/10.1016/S0301-472X(01)00612-9

Giannopoulos, K. (2019). Targeting Immune Signaling Checkpoints in Acute Myeloid Leukemia. *Journal of Clinical Medicine*, *8*(2), 236. https://doi.org/10.3390/jcm8020236

Godoy-Ramirez, K., Franck, K., Mahdavifar, S., Andersson, L., & Gaines, H. (2004). Optimum culture conditions for specific and nonspecific activation of whole blood and PBMC for intracellular cytokine assessment by flow cytometry. *Journal of Immunological Methods*, *292*(1–2), 1–15. https://doi.org/10.1016/j.jim.2004.04.028

Goker Bagca, B., & Biray Avci, C. (2020). The potential of JAK/STAT pathway inhibition by ruxolitinib in the treatment of COVID-19. *Cytokine & Growth Factor Reviews*, *54*, 51–61. https://doi.org/10.1016/j.cytogfr.2020.06.013

Goulard, M., Dosquet, C., & Bonnet, D. (2018). Role of the microenvironment in myeloid malignancies. *Cellular and Molecular Life Sciences*, *75*(8), 1377–1391. https://doi.org/10.1007/s00018-017-2725-4

Greiner, J., Götz, M., & Wais, V. (2022). Increasing Role of Targeted Immunotherapies in the Treatment of AML. *International Journal of Molecular Sciences*, *23*(6), 3304. https://doi.org/10.3390/ijms23063304

Gurney, M., & O'Dwyer, M. (2021). Realizing Innate Potential: CAR-NK Cell Therapies for Acute Myeloid Leukemia. *Cancers*, *13*(7), 1568. https://doi.org/10.3390/cancers13071568

Habbel, J., Arnold, L., Chen, Y., Ollmann, M. M., Bruderek, K., Brandau, S., Uhrsen, U. D., & Hanoun, M. (2020). Inflammation-driven activation of JAK/STAT signaling reversibly accelerates acute myeloid leukemia in vitro. *Blood Advances*, *4*(13), 3000–3010. https://doi.org/10.1182/bloodadvances.2019001292

Han, L., Schuringa, J. J., Mulder, A., & Vellenga, E. (2010). Dasatinib impairs long-term expansion of leukemic progenitors in a subset of acute myeloid leukemia cases. *Annals of Hematology*, *89*(9), 861–871. https://doi.org/10.1007/s00277-010-0948-7

Hanoun, M., Zhang, D., Mizoguchi, T., Pinho, S., Pierce, H., Kunisaki, Y., Lacombe, J., Armstrong, S. A., Dührsen, U., & Frenette, P. S. (2014). Acute Myelogenous Leukemia-Induced Sympathetic Neuropathy Promotes Malignancy in an Altered Hematopoietic Stem Cell Niche. *Cell Stem Cell*, *15*(3), 365–375. https://doi.org/10.1016/j.stem.2014.06.020

Hatfield, K., Ryningen, A., Corbascio, M., & Bruserud, Ø. (2006). Microvascular endothelial cells increase proliferation and inhibit apoptosis of native human acute myelogenous leukemia blasts. *International Journal of Cancer*, *119*(10), 2313–2321. https://doi.org/10.1002/ijc.22180

Hato, L., Vizcay, A., Eguren, I., Pérez-Gracia, J. L., Rodríguez, J., Gállego Pérez-Larraya, J., Sarobe, P., Inogés, S., Díaz de Cerio, A. L., & Santisteban, M. (2024). Dendritic Cells in Cancer Immunology and Immunotherapy. *Cancers*, *16*(5), 981. https://doi.org/10.3390/cancers16050981

Hayakawa, F., Sugimoto, K., Harada, Y., Hashimoto, N., Ohi, N., Kurahashi, S., & Naoe, T. (2013). A novel STAT inhibitor, OPB-31121, has a significant antitumor effect on leukemia with STAT-addictive oncokinases. *Blood Cancer Journal*, *3*(11), e166-9. https://doi.org/10.1038/bcj.2013.63

Heazlewood, S. Y., Oteiza, A., Cao, H., & Nilsson, S. K. (2014). Analyzing hematopoietic stem cell homing, lodgment, and engraftment to better understand the bone marrow niche. *Annals of the New York Academy of Sciences*, *1310*(1), 119–128. https://doi.org/10.1111/nyas.12329

Heo, S. K., Noh, E. K., Kim, J. Y., Jeong, Y. K., Jo, J. C., Choi, Y., Koh, S. J., Baek, J. H., Min, Y. J., & Kim, H. (2017). Targeting c-KIT (CD117) by

dasatinib and radotinib promotes acute myeloid leukemia cell death. *Scientific Reports*, *7*(1). https://doi.org/10.1038/s41598-017-15492-5

Herceg, Z., & Wang, Z. Q. (2001). Functions of poly(ADP-ribose) polymerase (PARP) in DNA repair, genomic integrity and cell death. *Mutation Research*, *477*(1–2), 97–110. https://doi.org/10.1016/s0027-5107(01)00111-7

Hořínková, J., Šíma, M., & Slanař, O. (2019). Pharmacokinetics of Dasatinib. *Prague Medical Report*, *120*(2–3), 52–63. https://doi.org/10.14712/23362936.2019.10

Hörst, K., Kühn, C., Haferlach, C., Haferlach, T., & Khoury, J. D. (2024). Genetic studies in clonal haematopoiesis, myelodysplastic neoplasms and acute myeloid leukaemia – a practical guide to WHO-HAEM5. *Medizinische Genetik*, *36*(1), 21–29. https://doi.org/10.1515/medgen-2024-2010

Hou, D., Wang, B., You, R., Wang, X., Liu, J., Zhan, W., Chen, P., Qin, T., Zhang, X., & Huang, H. (2020). Stromal cells promote chemoresistance of acute myeloid leukemia cells via activation of the IL-6/STAT3/OXPHOS axis. *Annals of Translational Medicine*, *8*(21), 1346–1346. https://doi.org/10.21037/atm-20-3191

Hou, D., Zheng, X., Cai, D., You, R., Liu, J., Wang, X., Liao, X., Tan, M., Lin, L., Wang, J., Zhang, S., & Huang, H. (2023). Interleukin-6 Facilitates Acute Myeloid Leukemia Chemoresistance via Mitofusin 1-Mediated Mitochondrial Fusion. *Molecular Cancer Research*. https://doi.org/10.1158/1541-7786.MCR-23-0382

Houtenbos, I., Westers, T. M., Ossenkoppele, G. J., & van de Loosdrecht, A. A. (2006). Leukemia-derived dendritic cells: towards clinical vaccination protocols in acute myeloid leukemia. *Haematologica*, *91*(3), 348–355.

Hsu, P. C., Yang, C. T., Jablons, D. M., & You, L. (2020). The crosstalk between src and hippo/YAP signaling pathways in non-small cell lung cancer (NSCLC). In *Cancers* (Vol. 12, Issue 6). MDPI AG. https://doi.org/10.3390/cancers12061361

Huan, J., Hornick, N. I., Goloviznina, N. A., Kamimae- Lanning, A. N., David, L. L., Wilmarth, P. A., Mori, T., Chevillet, J. R., Narla, A., Roberts, C. T., Loriaux, M. M., Chang, B. H., & Kurre, P. (2015). Coordinate regulation of residual bone marrow function by paracrine trafficking of AML exosomes. *Leukemia*, *29*(12), 2285–2295. https://doi.org/10.1038/leu.2015.163

Huang, F., Guang, P., Li, F., Liu, X., Zhang, W., & Huang, W. (2020). AML, ALL, and CML classification and diagnosis based on bone marrow cell morphology combined with convolutional neural network: A STARD compliant diagnosis research. *Medicine*, *99*(45), e23154. https://doi.org/10.1097/MD.0000000000023154

Jacamo, R., Chen, Y., Wang, Z., Ma, W., Zhang, M., Spaeth, E. L., Wang, Y., Battula, V. L., Mak, P. Y., Schallmoser, K., Ruvolo, P., Schober, W. D., Shpall, E. J., Nguyen, M. H., Strunk, D., Bueso-Ramos, C. E., Konoplev, S., Davis, R. E., Konopleva, M., & Andreeff, M. (2014). Reciprocal leukemia-stroma VCAM-1/VLA-4-dependent activation of NF-κB mediates chemoresistance. *Blood*, *123*(17), 2691–2702. https://doi.org/10.1182/blood-2013-06-511527

Jaiswal, S., Fontanillas, P., Flannick, J., Manning, A., Grauman, P. V., Mar, B. G., Lindsley, R. C., Mermel, C. H., Burtt, N., Chavez, A., Higgins, J. M., Moltchanov, V., Kuo, F. C., Kluk, M. J., Henderson, B., Kinnunen, L., Koistinen, H. A., Ladenvall, C., Getz, G., … Ebert, B. L. (2014). Age-Related Clonal Hematopoiesis Associated with Adverse Outcomes. *New England Journal of Medicine*, *371*(26), 2488–2498. https://doi.org/10.1056/NEJMoa1408617

Kang, C. (2023). Olutasidenib: First Approval. *Drugs*, *83*(4), 341–346. https://doi.org/10.1007/s40265-023-01844-1

Karjalainen, R., Pemovska, T., Popa, M., Liu, M., Javarappa, K. K., Majumder, M. M., Yadav, B., Tamborero, D., Tang, J., Bychkov, D., Kontro, M., Parsons, A., Suvela, M., Mayoral Safont, M., Porkka, K., Aittokallio, T., Kallioniemi, O., McCormack, E., Gjertsen, B. T., … Heckman, C. A. (2017). JAK1/2 and BCL2 inhibitors synergize to counteract bone marrow stromal cell–induced protection of AML. *Blood*, *130*(6), 789–802. https://doi.org/10.1182/blood-2016-02-699363

Kaur, G., & Dufour, J. M. (2012). Cell lines. *Spermatogenesis*, *2*(1), 1–5. https://doi.org/10.4161/spmg.19885

Kelly, L. M., & Gilliland, D. G. (2002). Genetics of myeloid leukemias. *Annual Review of Genomics and Human Genetics*, *3*(1), 179–198. https://doi.org/10.1146/annurev.genom.3.032802.115046

Khoury, J. D., Solary, E., Abla, O., Akkari, Y., Alaggio, R., Apperley, J. F., Bejar, R., Berti, E., Busque, L., Chan, J. K. C., Chen, W., Chen, X., Chng, W. J., Choi, J. K., Colmenero, I., Coupland, S. E., Cross, N. C. P., De Jong, D., Elghetany, M. T., … Hochhaus, A. (2022). The 5th edition of the World Health Organization Classification of Haematolymphoid Tumours: Myeloid and Histiocytic/Dendritic Neoplasms. In *Leukemia* (Vol. 36, Issue 7, pp. 1703–1719). Springer Nature. https://doi.org/10.1038/s41375-022-01613-1

Kim, D. H., Byun, J. M., Shin, D.-Y., Kim, I., Yoon, S.-S., & Koh, Y. (2023). Concomitant ruxolitinib with cytarabine-based induction chemotherapy in secondary acute myeloid leukemia evolving from myeloproliferative neoplasm. *Blood Research*, *58*(3), 155–157. https://doi.org/10.5045/br.2023.2023136

Kim, J.-A., Shim, J.-S., Lee, G.-Y., Yim, H. W., Kim, T.-M., Kim, M., Leem, S.-H., Lee, J.-W., Min, C.-K., & Oh, I.-H. (2015). Microenvironmental Remodeling as a Parameter and Prognostic Factor of Heterogeneous Leukemogenesis in Acute Myelogenous Leukemia. *Cancer Research*, *75*(11), 2222–2231. https://doi.org/10.1158/0008-5472.CAN-14-3379

Kim, Y., Jekarl, D. W., Kim, J., Kwon, A., Choi, H., Lee, S., Kim, Y.-J., Kim, H.-J., Kim, Y., Oh, I.-H., & Kim, M. (2015). Genetic and epigenetic alterations of bone marrow stromal cells in myelodysplastic syndrome and acute myeloid leukemia patients. *Stem Cell Research*, *14*(2), 177–184. https://doi.org/10.1016/j.scr.2015.01.004

Kim, Y.-W., Koo, B.-K., Jeong, H.-W., Yoon, M.-J., Song, R., Shin, J., Jeong, D.-C., Kim, S.-H., & Kong, Y.-Y. (2008). Defective Notch activation in microenvironment leads to myeloproliferative disease. *Blood*, *112*(12), 4628–4638. https://doi.org/10.1182/blood-2008-03-148999

Kode, A., Manavalan, J. S., Mosialou, I., Bhagat, G., Rathinam, C. V., Luo, N., Khiabanian, H., Lee, A., Murty, V. V., Friedman, R., Brum, A., Park, D., Galili, N., Mukherjee, S., Teruya-Feldstein, J., Raza, A., Rabadan, R., Berman, E., & Kousteni, S. (2014). Leukaemogenesis induced by an activating β-catenin mutation in osteoblasts. *Nature*, *506*(7487), 240–244. https://doi.org/10.1038/nature12883

Kojima, K., McQueen, T., Chen, Y., Jacamo, R., Konopleva, M., Shinojima, N., Shpall, E., Huang, X., & Andreeff, M. (2011). p53 activation of mesenchymal stromal cells partially abrogates microenvironment-mediated resistance to FLT3 inhibition in AML through HIF-1α–mediated down-regulation of CXCL12. *Blood*, *118*(16), 4431–4439. https://doi.org/10.1182/blood-2011-02-334136

Kollet, O., Dar, A., Shivtiel, S., Kalinkovich, A., Lapid, K., Sztainberg, Y., Tesio, M., Samstein, R. M., Goichberg, P., Spiegel, A., Elson, A., & Lapidot, T.

(2006). Osteoclasts degrade endosteal components and promote mobilization of hematopoietic progenitor cells. *Nature Medicine*, *12*(6), 657–664. https://doi.org/10.1038/nm1417

Konig, H., Copland, M., Chu, S., Jove, R., Holyoake, T. L., & Bhatia, R. (2008). Effects of dasatinib on Src kinase activity and downstream intracellular signaling in primitive chronic myelogenous leukemia hematopoietic cells. *Cancer Research*, *68*(23), 9624–9633. https://doi.org/10.1158/0008-5472.CAN-08-1131

Konopleva, M., Konoplev, S., Hu, W., Zaritskey, A. Y., Afanasiev, B. V., & Andreeff, M. (2002). Stromal cells prevent apoptosis of AML cells by up-regulation of anti-apoptotic proteins. *Leukemia*, *16*(9), 1713–1724. https://doi.org/10.1038/sj.leu.2402608

Kumar, A., Taghi Khani, A., Sanchez Ortiz, A., & Swaminathan, S. (2022). GM-CSF: A Double-Edged Sword in Cancer Immunotherapy. *Frontiers in Immunology*, *13*. https://doi.org/10.3389/fimmu.2022.901277

Kumar, B., Garcia, M., Weng, L., Jung, X., Murakami, J. L., Hu, X., McDonald, T., Lin, A., Kumar, A. R., Digiusto, D. L., Stein, A. S., Pullarkat, V. A., Hui, S. K., Carlesso, N., Kuo, Y. H., Bhatia, R., Marcucci, G., & Chen, C. C. (2018). Acute myeloid leukemia transforms the bone marrow niche into a leukemia-permissive microenvironment through exosome secretion. *Leukemia*, *32*(3), 575–587. https://doi.org/10.1038/leu.2017.259

Kyurkchiev, D. (2014). Secretion of immunoregulatory cytokines by mesenchymal stem cells. *World Journal of Stem Cells*, *6*(5), 552. https://doi.org/10.4252/wjsc.v6.i5.552

Ladikou, E. E., Sivaloganathan, H., Pepper, A., & Chevassut, T. (2020). Acute Myeloid Leukaemia in Its Niche: the Bone Marrow Microenvironment in Acute Myeloid Leukaemia. *Current Oncology Reports*, *22*(3), 27. https://doi.org/10.1007/s11912-020-0885-0

Laing, A. (2021). *The role of the bone marrow microenvironment in response to Anti-CD33 treatment in childhood acute myeloid leukaemia*. University of Glasgow.

Laing, A., Elmarghany, A., Alghaith, A. A., Gouma, A., Stevens, T., Winton, A., Cassels, J., Clarke, C. J., Schwab, C., Harrison, C. J., Gibson, B., & Keeshan, K. (2025). Paediatric bone marrow mesenchymal stem cells support acute myeloid leukaemia cell survival and enhance chemoresistance via contact-independent mechanism. *British Journal of Haematology*, *206*(3), 858–863. https://doi.org/10.1111/bjh.19884

Lasry, A., Nadorp, B., Fornerod, M., Nicolet, D., Wu, H., Walker, C. J., Sun, Z., Witkowski, M. T., Tikhonova, A. N., Guillamot-Ruano, M., Cayanan, G., Yeaton, A., Robbins, G., Obeng, E. A., Tsirigos, A., Stone, R. M., Byrd, J. C., Pounds, S., Carroll, W. L., … Aifantis, I. (2023). Author Correction: An inflammatory state remodels the immune microenvironment and improves risk stratification in acute myeloid leukemia. *Nature Cancer*. https://doi.org/10.1038/s43018-023-00518-x

Levêque, D., Becker, G., Bilger, K., & Natarajan-Amé, S. (2020). Clinical Pharmacokinetics and Pharmacodynamics of Dasatinib. *Clinical Pharmacokinetics*, *59*(7), 849–856. https://doi.org/10.1007/s40262-020-00872-4

Lévesque, J.-P., Helwani, F. M., & Winkler, I. G. (2010). The endosteal 'osteoblastic' niche and its role in hematopoietic stem cell homing and mobilization. *Leukemia*, *24*(12), 1979–1992. https://doi.org/10.1038/leu.2010.214

Li, Y., Seet, C. S., Mack, R., Joshi, K., Runde, A. P., Hagen, P. A., Barton, K., Breslin, P., Kini, A., Ji, H. L., & Zhang, J. (2024). Distinct roles of hematopoietic cytokines in the regulation of leukemia stem cells in murine MLL-AF9 leukemia. *Stem Cell Reports*, *19*(1), 100–111. https://doi.org/10.1016/j.stemcr.2023.11.003

Livak, K. J., & Schmittgen, T. D. (2001). Analysis of Relative Gene Expression Data Using Real-Time Quantitative PCR and the 2−ΔΔCT Method. *Methods*, *25*(4), 402–408. https://doi.org/10.1006/meth.2001.1262

Long, X., Yu, Y., Perlaky, L., Man, T. K., & Redell, M. S. (2015). Stromal CYR61 confers resistance to mitoxantrone via spleen tyrosine kinase activation in human acute myeloid leukaemia. *British Journal of Haematology*, *170*(5), 704–718. https://doi.org/10.1111/bjh.13492

Lu, J., Dong, Q., Zhang, S., Feng, Y., Yang, J., & Zhao, L. (2023). Acute myeloid leukemia (AML)-derived mesenchymal stem cells induce chemoresistance and epithelial–mesenchymal transition-like program in AML through IL-6/JAK2/STAT3 signaling. *Cancer Science*. https://doi.org/10.1111/cas.15855

Luo, F., Barrett, Y. C., Yang, Z., Camuso, A., McGlinchey, K., Wen, M. L., Smykla, R., Fager, K., Wild, R., Palme, H., Galbraith, S., Blackwood-Chirchir, A., & Lee, F. Y. (2008). Identification and validation of phospho-SRC, a novel and potential pharmacodynamic biomarker for dasatinib (SPRYCEL™), a multi-targeted kinase inhibitor. *Cancer Chemotherapy and Pharmacology*, *62*(6), 1065–1074. https://doi.org/10.1007/s00280-008-0699-5

Lussana, F., Cattaneo, M., Rambaldi, A., & Squizzato, A. (2018). Ruxolitinib-associated infections: A systematic review and meta-analysis. *American Journal of Hematology*, *93*(3), 339–347. https://doi.org/10.1002/ajh.24976

Lyu, T., Wang, Y., Li, D., Yang, H., Qin, B., Zhang, W., Li, Z., Cheng, C., Zhang, B., Guo, R., & Song, Y. (2021). Exosomes from BM-MSCs promote acute myeloid leukemia cell proliferation, invasion and chemoresistance via upregulation of S100A4. *Experimental Hematology and Oncology*, *10*(1). https://doi.org/10.1186/s40164-021-00220-7

Mantovani, A., Marchesi, F., Malesci, A., Laghi, L., & Allavena, P. (2017). Tumour-associated macrophages as treatment targets in oncology. *Nature Reviews Clinical Oncology*, *14*(7), 399–416. https://doi.org/10.1038/nrclinonc.2016.217

Marcucci, G., Geyer, S., Laumann, K., Zhao, W., Bucci, D., Uy, G. L., Blum, W., Eisfeld, A.-K., Pardee, T. S., Wang, E. S., Stock, W., Kolitz, J. E., Kohlschmidt, J., Mrózek, K., Bloomfield, C. D., Stone, R. M., & Larson, R. A. (2020). Combination of dasatinib with chemotherapy in previously untreated core binding factor acute myeloid leukemia: CALGB 10801. *Blood Advances*, *4*(4), 696–705. https://doi.org/10.1182/bloodadvances.2019000492

Masamoto, Y., Arai, S., Sato, T., Kubota, N., Takamoto, I., Kadowaki, T., & Kurokawa, M. (2017). Adiponectin Enhances Quiescence Exit of Murine Hematopoietic Stem Cells and Hematopoietic Recovery Through mTORC1 Potentiation. *Stem Cells*, *35*(7), 1835–1848. https://doi.org/10.1002/stem.2640

Mascarenhas, J., & Hoffman, R. (2012). Ruxolitinib: The first FDA approved therapy for the treatment of myelofibrosis. *Clinical Cancer Research*, *18*(11), 3008–3014. https://doi.org/10.1158/1078-0432.CCR-11-3145

Mascarenhas, J. O., Rampal, R. K., Kosiorek, H. E., Bhave, R., Hexner, E., Wang, E. S., Gerds, A., Abboud, C. N., Kremyanskaya, M., Berenzon, D., Odenike, O., Farnoud, N., Krishnan, A., Weinberg, R. S., McGovern, E., Salama, M. E., Najfeld, V., Medina-Martinez, J. S., Arango Ossa, J. E., … Hoffman, R.

(2020). Phase 2 study of ruxolitinib and decitabine in patients with myeloproliferative neoplasm in accelerated and blast phase. *Blood Advances*, *4*(20), 5246–5256. https://doi.org/10.1182/bloodadvances.2020002119

Maslak, P. G., Dao, T., Bernal, Y., Chanel, S. M., Zhang, R., Frattini, M., Rosenblat, T., Jurcic, J. G., Brentjens, R. J., Arcila, M. E., Rampal, R., Park, J. H., Douer, D., Katz, L., Sarlis, N., Tallman, M. S., & Scheinberg, D. A. (2018). Phase 2 trial of a multivalent WT1 peptide vaccine (galinpepimut-S) in acute myeloid leukemia. *Blood Advances*, *2*(3), 224–234. https://doi.org/10.1182/bloodadvances.2017014175

Matozaki, S., Nakagawa, T., Kawaguchi, R., Aozaki, R., Tsutsumi, M., Murayama, T., Koizumi, T., Nishimura, R., Isobe, T., & Chihara, K. (1995). Establishment of a myeloid leukaemic cell line (SKNO-1) from a patient with t(8;21) who acquired monosomy 17 during disease progression. *British Journal of Haematology*, *89*(4), 805–811. https://doi.org/10.1111/j.1365-2141.1995.tb08418.x

McKinnell, Z., Karel, D., Tuerff, D., SH Abrahim, M., & Nassereddine, S. (2022). Acute Myeloid Leukemia Following Myeloproliferative Neoplasms: A Review of What We Know, What We Do Not Know, and Emerging Treatment Strategies. *Journal of Hematology*, *11*(6), 197–209. https://doi.org/10.14740/jh1042

Mei, Y., Ren, K., Liu, Y., Ma, A., Xia, Z., Han, X., Li, E., Tariq, H., Bao, H., Xie, X., Zou, C., Zhang, D., Li, Z., Dong, L., Verma, A., Lu, X., Abaza, Y., Altman, J. K., Sukhanova, M., … Ji, P. (2022). Bone marrow–confined IL-6 signaling mediates the progression of myelodysplastic syndromes to acute myeloid leukemia. *Journal of Clinical Investigation*, *132*(17). https://doi.org/10.1172/JCI152673

Méndez-Ferrer, S., Bonnet, D., Steensma, D. P., Hasserjian, R. P., Ghobrial, I. M., Gribben, J. G., Andreeff, M., & Krause, D. S. (2020). Bone marrow niches in haematological malignancies. In *Nature Reviews Cancer* (Vol. 20, Issue 5, pp. 285–298). Nature Research. https://doi.org/10.1038/s41568-020-0245-2

Miari, K. E., & Williams, M. T. S. (2024). Stromal bone marrow fibroblasts and mesenchymal stem cells support acute myeloid leukaemia cells and promote therapy resistance. In *British Journal of Pharmacology* (Vol. 181, Issue 2, pp. 216–237). John Wiley and Sons Inc. https://doi.org/10.1111/bph.16028

Montero, J. C., Seoane, S., Ocaña, A., & Pandiella, A. (2011). Inhibition of Src family kinases and receptor tyrosine kinases by dasatinib: Possible combinations in solid tumors. In *Clinical Cancer Research* (Vol. 17, Issue 17, pp. 5546–5552). https://doi.org/10.1158/1078-0432.CCR-10-2616

Morrison, S. J., & Scadden, D. T. (2014). The bone marrow niche for haematopoietic stem cells. *Nature*, *505*(7483), 327–334. https://doi.org/10.1038/nature12984

Mpakou, V. E., Kontsioti, F., Papageorgiou, S., Spathis, A., Kottaridi, C., Girkas, K., Karakitsos, P., Dimitriadis, G., Dervenoulas, I., & Pappa, V. (2013). Dasatinib inhibits proliferation and induces apoptosis in the KASUMI-1 cell line bearing the t(8;21)(q22;q22) and the N822K c-kit mutation. *Leukemia Research*, *37*(2), 175–182. https://doi.org/10.1016/j.leukres.2012.10.011

Mukherjee, S., & Sekeres, M. A. (2019). Novel Therapies in Acute Myeloid Leukemia. *Seminars in Oncology Nursing*, *35*(6), 150955. https://doi.org/10.1016/j.soncn.2019.150955

Naveiras, O., Nardi, V., Wenzel, P. L., Hauschka, P. V., Fahey, F., & Daley, G. Q. (2009). Bone-marrow adipocytes as negative regulators of the

haematopoietic microenvironment. *Nature*, *460*(7252), 259–263. https://doi.org/10.1038/nature08099

Negaard, H. F. S., Iversen, N., Bowitz-Lothe, I. M., Sandset, P. M., Steinsvik, B., Østenstad, B., & Iversen, P. O. (2009). Increased bone marrow microvascular density in haematological malignancies is associated with differential regulation of angiogenic factors. *Leukemia*, *23*(1), 162–169. https://doi.org/10.1038/leu.2008.255

Nekoukar, Z., Moghimi, M., & Salehifar, E. (2021). A narrative review on adverse effects of dasatinib with a focus on pharmacotherapy of dasatinib-induced pulmonary toxicities. *BLOOD RESEARCH*, *56*(4), 229–242. https://doi.org/10.5045/br.2021.2021117

Neoplasia, M. (2015). *Personalized medicine for AML ? Finding a diamond in the (mouse is) rough*. *116*(15), 4–6.

Nguyen, C. H., Schlerka, A., Grandits, A. M., Koller, E., van der Kouwe, E., Vassiliou, G. S., Staber, P. B., Heller, G., & Wieser, R. (2020). IL2RA Promotes Aggressiveness and Stem Cell–Related Properties of Acute Myeloid Leukemia. *Cancer Research*, *80*(20), 4527–4539. https://doi.org/10.1158/0008-5472.CAN-20-0531

Niu, J., Peng, D., & Liu, L. (2022). Drug Resistance Mechanisms of Acute Myeloid Leukemia Stem Cells. *Frontiers in Oncology*, *12*. https://doi.org/10.3389/fonc.2022.896426

Odero, M. D., Zeleznik-Le, N. J., Chinwalla, V., & Rowley, J. D. (2000). Cytogenetic and Molecular Analysis of the Acute Monocytic Leukemia Cell Line THP-1 With an MLL-AF9 Translocation. *Genes,Chromosomes & Cancer*, *29*, 333–338. https://doi.org/10.1002/1098-2264(2000)9999:9999

O'Reilly, E., Zeinabad, H. A., & Szegezdi, E. (2021). Hematopoietic versus leukemic stem cell quiescence: Challenges and therapeutic opportunities. *Blood Reviews*, *50*, 100850. https://doi.org/10.1016/j.blre.2021.100850

Ostanin, A. A., Petrovskii, Y. L., Shevela, E. Y., & Chernykh, E. R. (2011). *Multiplex Analysis of Cytokines, Chemokines, Growth Factors, MMP-9 and TIMP-1 Produced by Human Bone Marrow, Adipose Tissue, and Placental Mesenchymal Stromal Cells* (Issue 1).

Padró, T., Ruiz, S., Bieker, R., Bü, H., Steins, M., Kienast, J., Bü, T., Berdel, W. E., & Mesters, R. M. (2000). *Increased angiogenesis in the bone marrow of patients with acute myeloid leukemia*. 2637–2644. https://doi.org/https://doi.org/10.1182/blood.V95.8.2637

Papaemmanuil, E., Gerstung, M., Bullinger, L., Gaidzik, V. I., Paschka, P., Roberts, N. D., Potter, N. E., Heuser, M., Thol, F., Bolli, N., Gundem, G., Van Loo, P., Martincorena, I., Ganly, P., Mudie, L., McLaren, S., O'Meara, S., Raine, K., Jones, D. R., … Campbell, P. J. (2016). Genomic Classification and Prognosis in Acute Myeloid Leukemia. *New England Journal of Medicine*, *374*(23), 2209–2221. https://doi.org/10.1056/NEJMoa1516192

Paschka, P., Schlenk, R. F., Weber, D., Benner, A., Bullinger, L., Heuser, M., Gaidzik, V. I., Thol, F., Agrawal, M., Teleanu, V., Lübbert, M., Fiedler, W., Radsak, M., Krauter, J., Horst, H.-A., Greil, R., Mayer, K., Kündgen, A., Martens, U., … Döhner, H. (2018). Adding dasatinib to intensive treatment in core-binding factor acute myeloid leukemia—results of the AMLSG 11-08 trial. *Leukemia*, *32*(7), 1621–1630. https://doi.org/10.1038/s41375-018-0129-6

Patel, A., Agha, M., Raptis, A., Hou, J.-Z., Farah, R., Redner, R. L., Im, A., Dorritie, K. A., Sehgal, A., Rossetti, J., Saul, M., Normolle, D., Lontos, K., & Boyiadzis, M. (2021). Outcomes of Patients With Acute Myeloid Leukemia Who Relapse After 5 Years of Complete Remission. *Oncology Research*

Featuring Preclinical and Clinical Cancer Therapeutics, *28*(7), 811–814. https://doi.org/10.3727/096504020X15965357399750

Patt, H. M., & Quastler, H. (1963). Radiation effects on cell renewal and related systems. *Physiological Reviews*, *43*(3), 357–396. https://doi.org/10.1152/physrev.1963.43.3.357

Pelcovits, A., & Niroula, R. (2020). Acute Myeloid Leukemia: A Review. *Rhode Island Medical Journal (2013)*, *103*(3), 38–40. http://www.ncbi.nlm.nih.gov/pubmed/32236160

Peña-Martínez, P., Eriksson, M., Ramakrishnan, R., Chapellier, M., Högberg, C., Orsmark-Pietras, C., Richter, J., Andersson, A., Fioretos, T., & Järås, M. (2018). Interleukin 4 induces apoptosis of acute myeloid leukemia cells in a Stat6-dependent manner. *Leukemia*, *32*(3), 588–596. https://doi.org/10.1038/leu.2017.261

Pirillo, C., Birch, F., Tissot, F. S., Anton, S. G., Haltalli, M., Tini, V., Kong, I., Piot, C., Partridge, B., Pospori, C., Keeshan, K., Santamaria, S., Hawkins, E., Falini, B., Marra, A., Duarte, D., Lee, C. F., Roberts, E., & Lo Celso, C. (2022). Metalloproteinase inhibition reduces AML growth, prevents stem cell loss, and improves chemotherapy effectiveness. *Blood Advances*, *6*(10), 3126–3141. https://doi.org/10.1182/bloodadvances.2021004321

Przepiorka, D., Luo, L., Subramaniam, S., Qiu, J., Gudi, R., Cunningham, L. C., Nie, L., Leong, R., Ma, L., Sheth, C., Deisseroth, A., Goldberg, K. B., Blumenthal, G. M., & Pazdur, R. (2020). FDA Approval Summary: Ruxolitinib for Treatment of Steroid-Refractory Acute Graft-Versus-Host Disease. *The Oncologist*, *25*(2), e328–e334. https://doi.org/10.1634/theoncologist.2019-0627

Rai, K., Holland, J., Glidewell, O., Weinberg, V., Brunner, K., Obrecht, J., Preisler, H., Nawabi, I., Prager, D., Carey, R., Cooper, M., Haurani, F., Hutchison, J., Silver, R., Falkson, G., Wiernik, P., Hoagland, H., Bloomfield, C., James, G., … Kaan, S. (1981). Treatment of acute myelocytic leukemia: a study by cancer and leukemia group B. *Blood*, *58*(6), 1203–1212. https://doi.org/10.1182/blood.v58.6.1203.1203

Reusing, S. B., Vallera, D. A., Manser, A. R., Vatrin, T., Bhatia, S., Felices, M., Miller, J. S., Uhrberg, M., & Babor, F. (2021). CD16xCD33 Bispecific Killer Cell Engager (BiKE) as potential immunotherapeutic in pediatric patients with AML and biphenotypic ALL. *Cancer Immunology, Immunotherapy*, *70*(12), 3701–3708. https://doi.org/10.1007/s00262-021-03008-0

Roecklein, B. A., & Torok-Storb, B. (1995). Functionally distinct human marrow stromal cell lines immortalized by transduction with the human papilloma virus E6/E7 genes. *Blood*, *85*(4), 997–1005.

Rojek, A. E., McCormick, B. J., Cwykiel, J., Odetola, O., Abaza, Y., Nai, N., Foucar, C. E., Achar, R. K., Shallis, R. M., Bradshaw, D., Standridge, M., Kota, V., Murthy, G. S. G., Badar, T., & Patel, A. A. (2024). Real-world outcomes of intensive induction approaches in core binding factor acute myeloid leukemia. *EJHaem*, *5*(4), 728–737. https://doi.org/10.1002/jha2.981

Rountree, W., Lynch, H. E., Denny, T. N., Sempowski, G. D., & Macintyre, A. N. (2024). Sources of variability in Luminex bead-based cytokine assays: Evidence from twelve years of multi-site proficiency testing. *Journal of Immunological Methods*, *531*. https://doi.org/10.1016/j.jim.2024.113699

Rowe, J. M. (2022). The “7+3” regimen in acute myeloid leukemia. *Haematologica*, *107*(1), 3–3. https://doi.org/10.3324/haematol.2021.280161

Rupec, R. A., Jundt, F., Rebholz, B., Eckelt, B., Weindl, G., Herzinger, T., Flaig, M. J., Moosmann, S., Plewig, G., Dörken, B., Förster, I., Huss, R., & Pfeffer,

K. (2005). Stroma-Mediated Dysregulation of Myelopoiesis in Mice Lacking IκBα. *Immunity*, *22*(4), 479–491. https://doi.org/10.1016/j.immuni.2005.02.009

Ryningen, A., Wergeland, L., Glenjen, N., Gjertsen, B. T., & Bruserud, Ø. (2005). In vitro crosstalk between fibroblasts and native human acute myelogenous leukemia (AML) blasts via local cytokine networks results in increased proliferation and decreased apoptosis of AML cells as well as increased levels of proangiogenic Interleukin 8. *Leukemia Research*, *29*(2), 185–196. https://doi.org/10.1016/j.leukres.2004.06.008

Saadi, M. I., Ramzi, M., Hosseinzadeh, M., Ebrahimi, N., Owjfard, M., Abdolyousefi, E. N., Hesami, Z., Valibeigi, B., Zareei, N., Tavasolian, F., Haghighinejad, H., & Zare, A. (2021). Expression Levels of Il-6 and Il-18 in Acute Myeloid Leukemia and Its Relation with Response to Therapy and Acute GvHD After Bone Marrow Transplantation. *Indian Journal of Surgical Oncology*, *12*(3), 465–471. https://doi.org/10.1007/s13193-021-01358-w

Sadovskaya, A., Petinati, N., Drize, N., Smirnov, I., Pobeguts, O., Arapidi, G., Lagarkova, M., Vasilieva, A., Gavrilina, O., & Parovichnikova, E. (2023). PB1780: DIFFERENCES IN SECRETOME OF BONE MARROW MULTIPOTENT MESENCHYMAL STROMAL CELLS IN PATIENTS AT THE ONSET OF ACUTE MYELOID LEUKEMIA AND AFTER ACHIEVING REMISSION. *HemaSphere*, *7*(S3), e0433384. https://doi.org/10.1097/01.HS9.0000973976.04333.84

Sala-Torra, O., Hanna, C., Loken, M. R., Flowers, M. E. D., Maris, M., Ladne, P. A., Mason, J. R., Senitzer, D., Rodriguez, R., Forman, S. J., Deeg, H. J., & Radich, J. P. (2006). Evidence of Donor-Derived Hematologic Malignancies after Hematopoietic Stem Cell Transplantation. *Biology of Blood and Marrow Transplantation*, *12*(5), 511–517. https://doi.org/10.1016/j.bbmt.2006.01.006

Sanchez-Correa, B., Bergua, J. M., Campos, C., Gayoso, I., Arcos, M. J., Bañas, H., Morgado, S., Casado, J. G., Solana, R., & Tarazona, R. (2013). Cytokine profiles in acute myeloid leukemia patients at diagnosis: Survival is inversely correlated with IL-6 and directly correlated with IL-10 levels. *Cytokine*, *61*(3), 885–891. https://doi.org/10.1016/j.cyto.2012.12.023

Sansone, P., & Bromberg, J. (2012). Targeting the interleukin-6/Jak/stat pathway in human malignancies. *Journal of Clinical Oncology : Official Journal of the American Society of Clinical Oncology*, *30*(9), 1005–1014. https://doi.org/10.1200/JCO.2010.31.8907

Santamaría, C., Muntión, S., Rosón, B., Blanco, B., López-Villar, O., Carrancio, S., Sánchez-Guijo, F. M., Díez-Campelo, M., Alvarez-Fernández, S., Sarasquete, M. E., de las Rivas, J., González, M., San Miguel, J. F., & Del Cañizo, M. C. (2012). Impaired expression of DICER, DROSHA, SBDS and some microRNAs in mesenchymal stromal cells from myelodysplastic syndrome patients. *Haematologica*, *97*(8), 1218–1224. https://doi.org/10.3324/haematol.2011.054437

Schofield, R. (1978). The relationship between the spleen colony-forming cell and the haemopoietic stem cell. *Blood Cells*, *4*(1–2), 7–25.

Schweitzer, K. M., Dräger, A. M., van der Valk, P., Thijsen, S. F., Zevenbergen, A., Theijsmeijer, A. P., van der Schoot, C. E., & Langenhuijsen, M. M. (1996). Constitutive expression of E-selectin and vascular cell adhesion molecule-1 on endothelial cells of hematopoietic tissues. *The American Journal of Pathology*, *148*(1), 165–175.

Senapati, J., Daver, N. G., & Pemmaraju, N. (2022). Antibody-Drug Conjugates in Myeloid Leukemias. *The Cancer Journal*, *28*(6), 454–461. https://doi.org/10.1097/PPO.0000000000000635

Sendker, S., Reinhardt, D., & Niktoreh, N. (2021). Redirecting the immune microenvironment in acute myeloid leukemia. *Cancers*, *13*(6), 1–20. https://doi.org/10.3390/cancers13061423

Shafat, M. S., Gnaneswaran, B., Bowles, K. M., & Rushworth, S. A. (2017). The bone marrow microenvironment – Home of the leukemic blasts. *Blood Reviews*, *31*(5), 277–286. https://doi.org/10.1016/j.blre.2017.03.004

Shafat, M. S., Oellerich, T., Mohr, S., Robinson, S. D., Edwards, D. R., Marlein, C. R., Piddock, R. E., Fenech, M., Zaitseva, L., Abdul-Aziz, A., Turner, J., Watkins, J. A., Lawes, M., Bowles, K. M., & Rushworth, S. A. (2017). Leukemic blasts program bone marrow adipocytes to generate a protumoral microenvironment. *Blood*, *129*(10), 1320–1332. https://doi.org/10.1182/blood-2016-08-734798

Shah, N. P., Tran, C., Lee, F. Y., Chen, P., Norris, D., & Sawyers, C. L. (2004). Overriding Imatinib Resistance with a Novel ABL Kinase Inhibitor. *Science*, *305*(5682), 399–401. https://doi.org/10.1126/science.1099480

Shibuya, M., & Claesson-Welsh, L. (2006). Signal transduction by VEGF receptors in regulation of angiogenesis and lymphangiogenesis. *Experimental Cell Research*, *312*(5), 549–560. https://doi.org/10.1016/j.yexcr.2005.11.012

Shih, A. H., Jiang, Y., Meydan, C., Shank, K., Pandey, S., Barreyro, L., Antony-Debre, I., Viale, A., Socci, N., Sun, Y., Robertson, A., Cavatore, M., de Stanchina, E., Hricik, T., Rapaport, F., Woods, B., Wei, C., Hatlen, M., Baljevic, M., … Levine, R. L. (2015). Mutational Cooperativity Linked to Combinatorial Epigenetic Gain of Function in Acute Myeloid Leukemia. *Cancer Cell*, *27*(4), 502–515. https://doi.org/10.1016/j.ccell.2015.03.009

Short, N. J., Konopleva, M., Kadia, T. M., Borthakur, G., Ravandi, F., DiNardo, C. D., & Daver, N. (2020). Advances in the treatment of acute myeloid leukemia: New drugs and new challenges. *Cancer Discovery*, *10*(4), 506–525. https://doi.org/10.1158/2159-8290.CD-19-1011

Short, N. J., Rytting, M. E., & Cortes, J. E. (2018). Acute myeloid leukaemia. *The Lancet*, *392*(10147), 593–606. https://doi.org/10.1016/S0140-6736(18)31041-9

Sipkins, D. A., Wei, X., Wu, J. W., Runnels, J. M., Côté, D., Means, T. K., Luster, A. D., Scadden, D. T., & Lin, C. P. (2005). In vivo imaging of specialized bone marrow endothelial microdomains for tumour engraftment. *Nature*, *435*(7044), 969–973. https://doi.org/10.1038/nature03703

Skelding, K. A., Barry, D. L., Theron, D. Z., & Lincz, L. F. (2023). Bone Marrow Microenvironment as a Source of New Drug Targets for the Treatment of Acute Myeloid Leukaemia. In *International Journal of Molecular Sciences* (Vol. 24, Issue 1). MDPI. https://doi.org/10.3390/ijms24010563

Skopek, R., Palusińska, M., Kaczor-Keller, K., Pingwara, R., Papierniak-Wyglądała, A., Schenk, T., Lewicki, S., Zelent, A., & Szymański, Ł. (2023). Choosing the Right Cell Line for Acute Myeloid Leukemia (AML) Research. *International Journal of Molecular Sciences*, *24*(6), 5377. https://doi.org/10.3390/ijms24065377

Snaith, O., Poveda-Rogers, C., Laczko, D., Yang, G., & Morrissette, J. J. D. (2024). Cytogenetics and genomics of acute myeloid leukemia. In *Best Practice and Research: Clinical Haematology* (Vol. 37, Issue 1). Bailliere Tindall Ltd. https://doi.org/10.1016/j.beha.2023.101533

Song, Y., Chen, X., Huang, R., & Liu, J. (2023). Dysregulated YAP1/Hippo Pathway Contributes to Doxorubicin (ADM) Resistance in Acute Myeloid Leukemia (AML). *Current Pharmaceutical Biotechnology*, *24*(5), 676–685. https://doi.org/10.2174/1389201023666220617150346

Srinivasan, S. (2024). Dasatinib in core-binding factor acute myeloid leukemia: A promising therapeutic approach. *EJHaem*. https://doi.org/10.1002/jha2.994

Steensma, D. P., Bejar, R., Jaiswal, S., Lindsley, R. C., Sekeres, M. A., Hasserjian, R. P., & Ebert, B. L. (2015). Clonal hematopoiesis of indeterminate potential and its distinction from myelodysplastic syndromes. *Blood*, *126*(1), 9–16. https://doi.org/10.1182/blood-2015-03-631747

Stelmach, P., & Trumpp, A. (2023). Leukemic stem cells and therapy resistance in acute myeloid leukemia. *Haematologica*, *108*(2), 353–366. https://doi.org/10.3324/haematol.2022.280800

Stevens, A. M., Miller, J. M., Munoz, J. O., Gaikwad, A. S., & Redell, M. S. (2017). Interleukin-6 levels predict event-free survival in pediatric AML and suggest a mechanism of chemotherapy resistance. *Blood Advances*, *1*(18), 1387–1397. https://doi.org/10.1182/bloodadvances.2017007856

Suárez-Álvarez, B., López-Vázquez, A., & López-Larrea, C. (2012). *Mobilization and Homing of Hematopoietic Stem Cells* (pp. 152–170). https://doi.org/10.1007/978-1-4614-2098-9_11

Tabe, Y., Yamamoto, S., Saitoh, K., Sekihara, K., Monma, N., Ikeo, K., Mogushi, K., Shikami, M., Ruvolo, V., Ishizawa, J., Hail, N., Kazuno, S., Igarashi, M., Matsushita, H., Yamanaka, Y., Arai, H., Nagaoka, I., Miida, T., Hayashizaki, Y., … Andreeff, M. (2017). Bone Marrow Adipocytes Facilitate Fatty Acid Oxidation Activating AMPK and a Transcriptional Network Supporting Survival of Acute Monocytic Leukemia Cells. *Cancer Research*, *77*(6), 1453–1464. https://doi.org/10.1158/0008-5472.CAN-16-1645

Taga, T., Tomizawa, D., Takahashi, H., & Adachi, S. (2016). Acute myeloid leukemia in children: Current status and future directions. *Pediatrics International*, *58*(2), 71–80. https://doi.org/10.1111/ped.12865

Tang, L., Wu, J., Li, C.-G., Jiang, H.-W., Xu, M., Du, M., Yin, Z., Mei, H., & Hu, Y. (2020). Characterization of Immune Dysfunction and Identification of Prognostic Immune-Related Risk Factors in Acute Myeloid Leukemia. *Clinical Cancer Research*, *26*(7), 1763–1772. https://doi.org/10.1158/1078-0432.CCR-19-3003

Taniguchi, K., Wu, L. W., Grivennikov, S. I., De Jong, P. R., Lian, I., Yu, F. X., Wang, K., Ho, S. B., Boland, B. S., Chang, J. T., Sandborn, W. J., Hardiman, G., Raz, E., Maehara, Y., Yoshimura, A., Zucman-Rossi, J., Guan, K. L., & Karin, M. (2015). A gp130-Src-YAP module links inflammation to epithelial regeneration. *Nature*, *519*(7541), 57–62. https://doi.org/10.1038/nature14228

Tsimberidou, A. M., Estey, E., Wen, S., Pierce, S., Kantarjian, H., Albitar, M., & Kurzrock, R. (2008). The prognostic significance of cytokine levels in newly diagnosed acute myeloid leukemia and high-risk myelodysplastic syndromes. *Cancer*, *113*(7), 1605–1613. https://doi.org/10.1002/cncr.23785

Tsuchiya, S., Yamabe, M., Yamaguchi, Y., Kobayashi, Y., Konno, T., & Tada, K. (1980). Establishment and characterization of a human acute monocytic leukemia cell line (THP-1). *International Journal of Cancer*, *26*(2), 171–176. https://doi.org/10.1002/ijc.2910260208

Urs, A. P., Goda, C., & Kulkarni, R. (2024). Remodeling of the bone marrow microenvironment during acute myeloid leukemia progression. *Annals of Translational Medicine*, *12*(4), 63–63. https://doi.org/10.21037/atm-23-1824

Vago, L., & Gojo, I. (2020). Immune escape and immunotherapy of acute myeloid leukemia. *Journal of Clinical Investigation*, *130*(4), 1552–1564. https://doi.org/10.1172/JCI129204

Vanhooren, J., Dobbelaere, R., Derpoorter, C., Deneweth, L., Van Camp, L., Uyttebroeck, A., De Moerloose, B., & Lammens, T. (2023). CAR-T in the Treatment of Acute Myeloid Leukemia: Barriers and How to Overcome Them. *HemaSphere*, *7*(9), e937. https://doi.org/10.1097/HS9.0000000000000937

Vardiman, J. W., Harris, N. L., & Brunning, R. D. (2002). The World Health Organization (WHO) classification of the myeloid neoplasms. *Blood*, *100*(7), 2292–2302. https://doi.org/10.1182/blood-2002-04-1199

Vilaplana-Lopera, N., Cuminetti, V., Almaghrabi, R., Papatzikas, G., Rout, A. K., Jeeves, M., González, E., Alyahyawi, Y., Cunningham, A., Erdem, A., Schnütgen, F., Raghavan, M., Potluri, S., Cazier, J. B., Schuringa, J. J., Reed, M. A. C., Arranz, L., Günther, U. L., & Garcia, P. (2022). Crosstalk between AML and stromal cells triggers acetate secretion through the metabolic rewiring of stromal cells. *ELife*, *11*. https://doi.org/10.7554/eLife.75908

von der Heide, E. K., Neumann, M., Vosberg, S., James, A. R., Schroeder, M. P., Ortiz-Tanchez, J., Isaakidis, K., Schlee, C., Luther, M., Jöhrens, K., Anagnostopoulos, I., Mochmann, L. H., Nowak, D., Hofmann, W. K., Greif, P. A., & Baldus, C. D. (2017). Molecular alterations in bone marrow mesenchymal stromal cells derived from acute myeloid leukemia patients. *Leukemia*, *31*(5), 1069–1078. https://doi.org/10.1038/leu.2016.324

Walkley, C. R., Olsen, G. H., Dworkin, S., Fabb, S. A., Swann, J., McArthur, G. A., Westmoreland, S. V., Chambon, P., Scadden, D. T., & Purton, L. E. (2007). A Microenvironment-Induced Myeloproliferative Syndrome Caused by Retinoic Acid Receptor γ Deficiency. *Cell*, *129*(6), 1097–1110. https://doi.org/10.1016/j.cell.2007.05.014

Walkley, C. R., Shea, J. M., Sims, N. A., Purton, L. E., & Orkin, S. H. (2007). Rb Regulates Interactions between Hematopoietic Stem Cells and Their Bone Marrow Microenvironment. *Cell*, *129*(6), 1081–1095. https://doi.org/10.1016/j.cell.2007.03.055

Wang, A., & Zhong, H. (2018). Roles of the bone marrow niche in hematopoiesis, leukemogenesis, and chemotherapy resistance in acute myeloid leukemia. *Hematology*, *23*(10), 729–739. https://doi.org/10.1080/10245332.2018.1486064

Wang, B., Reville, P. K., Yassouf, M. Y., Jelloul, F. Z., Ly, C., Desai, P. N., Wang, Z., Borges, P., Veletic, I., Dasdemir, E., Burks, J. K., Tang, G., Guo, S., Garza, A. I., Nasnas, C., Vaughn, N. R., Baran, N., Deng, Q., Matthews, J., … Abbas, H. A. (2024). Comprehensive characterization of IFNγ signaling in acute myeloid leukemia reveals prognostic and therapeutic strategies. *Nature Communications*, *15*(1). https://doi.org/10.1038/s41467-024-45916-6

Wang, Y., Chen, H., Yu, J., Kang, W., & To, K. F. (2022). Recent insight into the role and therapeutic potential of YAP/TAZ in gastrointestinal cancers. In *Biochimica et Biophysica Acta - Reviews on Cancer* (Vol. 1877, Issue 5). Elsevier B.V. https://doi.org/10.1016/j.bbcan.2022.188787

Wang, Y., Chen, S., Yan, Z., & Pei, M. (2019). A prospect of cell immortalization combined with matrix microenvironmental optimization strategy for tissue engineering and regeneration. *Cell & Bioscience*, *9*(1), 7. https://doi.org/10.1186/s13578-018-0264-9

Wang, Y., Sun, X., Yuan, S., Hou, S., Guo, T., Chu, Y., Pang, T., Luo, H. R., Yuan, W., & Wang, X. (2020). Interleukin-1β inhibits normal hematopoietic expansion and promotes acute myeloid leukemia progression via the bone

marrow niche. *Cytotherapy*, *22*(3), 127–134. https://doi.org/10.1016/j.jcyt.2020.01.001

Weinberg, O. K., Porwit, A., Orazi, A., Hasserjian, R. P., Foucar, K., Duncavage, E. J., & Arber, D. A. (2023). The International Consensus Classification of acute myeloid leukemia. In *Virchows Archiv* (Vol. 482, Issue 1, pp. 27–37). Springer Science and Business Media Deutschland GmbH. https://doi.org/10.1007/s00428-022-03430-4

Winer, E. S., & Stone, R. M. (2019). Novel therapy in Acute myeloid leukemia (AML): moving toward targeted approaches. *Therapeutic Advances in Hematology*, *10*, 1–18. https://doi.org/10.1177/2040620719860645

Wu, Y., Li, Y., Gao, Y., Zhang, P., Jing, Q., Zhang, Y., Jin, W., Wang, Y., Du, J., & Wu, G. (2024). Immunotherapies of acute myeloid leukemia: Rationale, clinical evidence and perspective. In *Biomedicine and Pharmacotherapy* (Vol. 171). Elsevier Masson s.r.l. https://doi.org/10.1016/j.biopha.2024.116132

Xie, M., Lu, C., Wang, J., McLellan, M. D., Johnson, K. J., Wendl, M. C., McMichael, J. F., Schmidt, H. K., Yellapantula, V., Miller, C. A., Ozenberger, B. A., Welch, J. S., Link, D. C., Walter, M. J., Mardis, E. R., Dipersio, J. F., Chen, F., Wilson, R. K., Ley, T. J., & Ding, L. (2014). Age-related mutations associated with clonal hematopoietic expansion and malignancies. *Nature Medicine*, *20*(12), 1472–1478. https://doi.org/10.1038/nm.3733

Yamazaki, S., Ema, H., Karlsson, G., Yamaguchi, T., Miyoshi, H., Shioda, S., Taketo, M. M., Karlsson, S., Iwama, A., & Nakauchi, H. (2011). Nonmyelinating Schwann Cells Maintain Hematopoietic Stem Cell Hibernation in the Bone Marrow Niche. *Cell*, *147*(5), 1146–1158. https://doi.org/10.1016/j.cell.2011.09.053

Yanagisawa, K., Horiuchi, T., & Fujita, S. (1991). Establishment and characterization of a new human leukemia cell line derived from M4E0. *Blood*, *78*(2), 451–457.

Yao, Y., Li, F., Huang, J., Jin, J., & Wang, H. (2021). Leukemia stem cell-bone marrow microenvironment interplay in acute myeloid leukemia development. *Experimental Hematology & Oncology*, *10*(1), 39. https://doi.org/10.1186/s40164-021-00233-2

Young, A. L., Spencer Tong, R., Birmann, B. M., & Druley, T. E. (2019). Clonal hematopoiesis and risk of acute myeloid leukemia. *Haematologica*, *104*(12), 2410–2417. https://doi.org/10.3324/haematol.2018.215269

Yu, S., Ye, J., Wang, Y., Lu, T., Liu, Y., Liu, N., Zhang, J., Lu, F., Ma, D., Gale, R. P., & Ji, C. (2023). DNA damage to bone marrow stromal cells by antileukemia drugs induces chemoresistance in acute myeloid leukemia via paracrine FGF10–FGFR2 signaling. *Journal of Biological Chemistry*, *299*(1). https://doi.org/10.1016/j.jbc.2022.102787

Zambetti, N. A., Ping, Z., Chen, S., Kenswil, K. J. G., Mylona, M. A., Sanders, M. A., Hoogenboezem, R. M., Bindels, E. M. J., Adisty, M. N., Van Strien, P. M. H., van der Leije, C. S., Westers, T. M., Cremers, E. M. P., Milanese, C., Mastroberardino, P. G., van Leeuwen, J. P. T. M., van der Eerden, B. C. J., Touw, I. P., Kuijpers, T. W., … Raaijmakers, M. H. G. P. (2016). Mesenchymal Inflammation Drives Genotoxic Stress in Hematopoietic Stem Cells and Predicts Disease Evolution in Human Pre-leukemia. *Cell Stem Cell*, *19*(5), 613–627. https://doi.org/10.1016/j.stem.2016.08.021

Zeng, Z., Xi Shi, Y., Samudio, I. J., Wang, R.-Y., Ling, X., Frolova, O., Levis, M., Rubin, J. B., Negrin, R. R., Estey, E. H., Konoplev, S., Andreeff, M., & Konopleva, M. (2009). Targeting the leukemia microenvironment by CXCR4

inhibition overcomes resistance to kinase inhibitors and chemotherapy in AML. *Blood*, *113*(24), 6215–6224. https://doi.org/10.1182/blood-2008-05-158311

Zhai, Y., Zhang, J., Wang, H., Lu, W., Liu, S., Yu, Y., Weng, W., Ding, Z., Zhu, Q., & Shi, J. (2016). Growth differentiation factor 15 contributes to cancer-associated fibroblasts-mediated chemo-protection of AML cells. *Journal of Experimental & Clinical Cancer Research*, *35*(1), 147. https://doi.org/10.1186/s13046-016-0405-0

Zhang, B., Wang, Y., Zheng, G.-G., Ma, X.-T., Li, G., Zhang, F.-K., & Wu, K.-F. (2002). Clinical significance of IL-18 gene over-expression in AML. *Leukemia Research*, *26*(10), 887–892. https://doi.org/10.1016/S0145-2126(02)00025-5

Zhang, Y., Guo, H., Zhang, Z., Lu, W., Zhu, J., & Shi, J. (2022). IL-6 promotes chemoresistance via upregulating CD36 mediated fatty acids uptake in acute myeloid leukemia. *Experimental Cell Research*, *415*(1), 113112. https://doi.org/10.1016/j.yexcr.2022.113112

Zhou, B. O., Yu, H., Yue, R., Zhao, Z., Rios, J. J., Naveiras, O., & Morrison, S. J. (2017). Bone marrow adipocytes promote the regeneration of stem cells and haematopoiesis by secreting SCF. *Nature Cell Biology*, *19*(8), 891–903. https://doi.org/10.1038/ncb3570

Zhou, L. J., & Tedder, T. F. (1996). CD14+ blood monocytes can differentiate into functionally mature CD83+ dendritic cells. *Proceedings of the National Academy of Sciences*, *93*(6), 2588–2592. https://doi.org/10.1073/pnas.93.6.2588

Zhou, X., Li, Z., & Zhou, J. (2017). Tumor necrosis factor α in the onset and progression of leukemia. *Experimental Hematology*, *45*, 17–26. https://doi.org/10.1016/j.exphem.2016.10.005

Zimmer, S. N., Zhou, Q., Zhou, T., Cheng, Z., Abboud-Werner, S. L., Horn, D., Lecocke, M., White, R., Krivtsov, A. V, Armstrong, S. A., Kung, A. L., Livingston, D. M., & Rebel, V. I. (2011). Crebbp haploinsufficiency in mice alters the bone marrow microenvironment, leading to loss of stem cells and excessive myelopoiesis. *Blood*, *118*(1), 69–79. https://doi.org/10.1182/blood-2010-09-307942